# Mismatch Repair in *T. brucei*: Roles in protection against oxidative damage


## Tehseen Fatima Zeb

BSc, MSc


Submitted in fulfillment of the requirements for the Degree of

Doctor of Philosophy


Wellcome Centre for Molecular Parasitology and

Institute of Infection, Immunity and Inflammation

College of Medical Veterinary and Life Sciences,

University of Glasgow


**July, 2013**

# Abstract

Cells are continuously exposed to different intracellular and extracellular mutagens, which can damage several different molecules, including DNA. To ensure survival, cells have evolved various defence and repair mechanisms. Mismatch repair (MMR) is the mechanism that serves to repair mismatched bases in DNA that are missed by the proof reading activity of DNA polymerases. Besides this, MMR also corrects base mismatches formed by altered bases modified by certain chemical mutagens. Thus, MMR is important to avoid mutagenesis and maintain genome fidelity. MMR is a complex, highly conserved pathway that involves a range of proteins along with several accessory proteins.

In *T. brucei*, as in other eukaryotes, MMR core functions are carried out by bacterial MutS and MutL homologues, working as heterodimers: MSH2α (MSH2-MSH3) and MSH2β (MSH2-MSH6), and MLH1-PMS1, respectively. To date, only MSH2 and MLH1 function have been examined and only in bloodstream form (BSF) *T. brucei* cells. It was observed that MMR mutants are tolerant towards methylation damage, exhibit microsatellite instability and display elevated rates of homologous recombination between imperfectly matched DNA molecules. This confirmed the role of MMR in genome maintenance in BSF *T. brucei*. More recently, it was observed that BSF *MSH2* mutants were sensitive towards oxidative damage, though the same phenotype was not observed in *MLH1* mutants. This suggests that some aspect of the MMR machinery acts to protect BSF *T. brucei* cells against oxidative stress, but the machinery and mode of action is unknown.

In this study we have generated null mutants of *MSH2* and *MLH1* in procyclic form (PCF) *T. brucei* cells, and *MSH3* and *MSH6* mutants in BSF cells. Characterization of tolerance to DNA methylation damage and evaluating microsatellite stability shows that each gene acts in MMR in both the life cycle stages, with the exception of MSH3, where null mutants show no discernible phenotypes. Mutants were also analyzed for their action towards oxidative stress in both the life stages and, remarkably, we find life cycle stage differences, with *MSH2* mutants displaying hydrogen peroxide sensitivity and resistance in the BSF and PCF, respectively. The same phenotypes are not seen in *MLH1* mutants, and we show that resistance to hydrogen peroxide in PCF cells is due to adaptation during the loss of MSH2. We have also shown that PCF *MSH2*

mutants may show a decrease in microsatellite instability when subjected to oxidative stress. This leads to the hypothesis that there might be an unidentified system, apart from MMR, present in *T. brucei* PCF cells that works as a defence in response to oxidative stress and can assume greater prominence when MSH2 is lost. Although we have tried to explore various cellular processes that might contribute this activity, our results are inconclusive.

MSH2 and MLH1 have also been epitope tagged to explore the subcellular localization of these proteins and to ask if any changes in expression levels or changes in localisation are seen when subjected to oxidative stress. These preliminary data suggest that both factors are nuclear and cytoplasmic. We have also tried to ask if MSH2 and/or MLH1 co-localize with either MSH5 or MSH4, which are MutS-like factors that act in meiosis in other eukaryotes, but whose functions have not been explored in *T. brucei*. However, our attempts at this analysis have been unsuccessful.

# Table of Contents

# List of Tables

# List of Figures

# Acknowledgements

As my firm belief, I am extremely grateful to my Lord ALLAH Subhana wa Ta'ala for blessing me and making me capable by all means to fulfill the requirements of this honorable degree.

I would also like to express my gratitude to my supervisor Dr. Richard McCulloch not only for proposing an interesting topic but also his help, guidance and encouragement throughout the project. I cannot forget to admire his patience for allowing me to pester him endlessly. I surely could not have done it without his support.

I am also very obliged to have worked in such a friendly environment of Wellcome Trust Centre for Molecular Parasitology. I should also pay special thanks to Dr. Michal Swiderski and Dr. Lucio Marcello for their guidance and suggestions which have been very helpful in my understanding and success of the project. I could never forget the temptitious chocolate cake shared by Craig. I can always keep my calorie counter turned off for that one.

I am also gratified to Dow University of Health Sciences and Higher Education Commission of Pakistan for their sponsorship and certainly University of Glasgow for the support throughout the course of study.

I would delightfully like to dedicate my degree to my family for their endless moral support and more specifically to my parents, my husband and to the biggest contributor to my PhD. my son Ibraheem. I am sorry for my all four year long tantrums and I cannot thank you enough for the love, understanding and temperament. Papa, Ammi, Rizwan and Ibhi 'I LOVE YOU'.

# Author’s Declaration

I declare that this thesis and the results presented within are entirely my own work except where otherwise stated. No part of this thesis has been previously submitted for a degree at any university.

_____

# Tehseen Fatima Zeb

# Abbreviations

| | |
|---|---|
| polδ/β/κ | polymerases delta/beta/kappa |
| 5meC | 5-methyl cytosine |
| 6metG | 6-methyl guanine |
| 8-oxoG | 8-oxoguanine |
| A | Adenine |
| AGT | Alkyl guanine transferase |
| AOX | Alternative oxidase |
| AP | apurinic/apyrimidic |
| APE | AP endonuclease |
| APx | Ascorbate peroxidase |
| ATL | Alkyl transferase-like |
| ATM | Ataxia telangiectasia mutated |
| ATP | Adenosine triphosphate |
| ATR | ATM and Rad3 related |
| BER | Base excision repair |
| BES | Base excision repair |
| *BSD* | Blasticidine S hydrochloride |
| BSF | Bloodstream form |
| C | Cytosine |
| CPD | cyclobutane pyrimidine dimers |
| CPX | cytoplasmic TXNPx |
| CSA | Cockayne syndrome A |
| Dam | Deoxyadenyl methylase |
| DHA | Dehydroascorbate |
| DNA | Dexoy ribonuclic acid |
| DNA PK | DNA dependent protein kinase |
| dNTPv | Deoxyribonucleotide triphosphate |
| Drp | 5'deoxyribosephosphatse |
| DSB | Double stranded break |
| DTT | Dithiothritol |
| EndoIII | Endonuclease III |
| ES | Expression site |
| ESAG | Expression site associated genes |
| EXO | Exonuclease |
| FAM | 6-carboxy-fluorescine |
| FCS | Fecal bovine serum |
| G | Guanine |
| GGR | Global genome repair |
| GHKL | Gyrase,Hsp90,Histidine –Kinase, MutL |
| Glu | Glutamate |
| GPI8 | Glycosylphosphatidylinositol |

| | |
|---|---|
| GPX | Glutathione peroxidase |
| GTBP | GT- binding protein |
| $H_2O_2$ | hydrogen peroxide |
| HJ | Holliday junctionvsp |
| HR | Homologous recombination |
| IDLs | Insertion deletion loop |
| KO | Knock out |
| MBD | Mismatch binding domain |
| MES | Metacyclic expression site |
| MGMT | methyl guanine methyl transferase |
| MLH | Mut L homologue |
| MMH | MutM homologue |
| MMR | Mismatch repair |
| MNNG | *N* -methyl-*N'*-nitro-*N* -nitrosoguanidine |
| MPX | mitochondrial TXNPx |
| MSH | Mut S homologue |
| MYH | MutY homologues |
| Neo | Neomycin sulphate |
| NER | Nucleotide excision repair |
| NHEJ | Non-homologous end-joining |
| $O^{2-}$ | superoxide |
| $OH^-$ | hydroxyl radical |
| PBS | Phosphate buffer saline |
| PBST | PBS with 0.05 % Tween |
| PCF | Procyclic form |
| PCNA | Proliferating cell nuclear antigen |
| Phe | Phelnylalanine |
| Phleo | Phleomycin |
| PMS | Post meiotic segregation |
| polβ | Polymerase Beta |
| polε | polymerase epsilon |
| PUR | Puromycin dihydrochloride |
| RFC | Replication factor C |
| RNA | Ribonuclic acid |
| ROS | Reactive oxygen species |
| RPA | replication protein A |
| SDM-79 | Semi defined medium 79 |
| SOD | Superoxide dismutase |
| SSB | Single stranded break |
| T | Thiamine |

| | |
|---|---|
| T(SH)2 | Trypanothione |
| TAO | Trypanosomes alternative oxidase |
| TCR | Transcription coupled repair |
| TCRF | transcription-repair coupling factor |
| Tet | Tetracycline |
| TLS | Translesion synthesis |
| TR | Trypanothione reductase |
| TXN | Tryparedoxin |
| TXNPx | Tryparedoxin peroxidase |
| U | Uracil |
| UNG | Uracyl-DNA glycosylase |
| UTR | untranslated regions |
| UTR | Upstream region |
| UV | Ultra violet |
| VSG | Varient surface glycoprotein |
| VSP | Very short patch |
| XP A/C/F/G | Xeroderma Pigmentosum A/C/F/G |

# 1 General Introduction

## 1.1 Introduction

The term Kinetoplastida was first defined by Honigberg in 1963 to identify an order of flagellated eukaryotes (Honigberg 1963). Kinetoplastids get their name because of an extra-nuclear, dark Giemsa-staining mass found in the cell of these organisms. This was the first instance when extra-nuclear DNA was observed (Vickerman and Coombs 1999). It was originally believed that the kinetoplast was associated with the movement of the organisms, hence the name (kineto (Greek); movement). This misconception was due to the position of the kinetoplast, found near the basal body at the base of flagellum (Ploubidou et al. 1999). However, later it was shown that it is not involved in motility, but is a component of mitochondrion (Shapiro and Englund 1995). The size of the kinetoplast varies according to the species. The family Trypanosomatidae belongs to the order Kinetoplastida and contains a number of major parasite, including the ones which infect humans and mammals (Podlipaev 2001). The Trypanosomatidae are further classified into genera, which include *Leishmania*, *Typanosoma*, *Blastocrithidia*, *Crithidia*, *Endotrypanum*, *Herpetomonas*, *Leptomonas*, *Phytomonas*, and *Wallaceina*.

## 1.2 Trypanosomiasis

Of several species of *Trypanosoma*, *T. brucei* and *T. cruzi* are the ones that cause disease in humans. Collectively this disease is termed "Trypanosomiasis" (Barrett 2003;Simpson et al. 2006). Trypanosomiasis is further divided into two groups on the basis of the major geographical distribution of the causative species: American Trypanosomiasis (or Chagas' disease), which is caused by *T. cruzi*, and African Trypanosomiasis, caused by *T. brucei*. African trypanosomiasis is not limited to human infections, since *T. vivax* and *T. congolense* cause severe cattle disease, termed Nagana. Indeed, *T. brucei brucei*, a sub species of *T. brucei*, also causes Nagana in cattle and does not infect humans (Vanhamme et al. 2003).

### 1.2.1 The Parasite

Two sub-species of *T. brucei* are responsible for causing trypanosomiasis disease in humans, often called Human African Trypanosomiasis or Sleeping Sickness. These are *T. brucei gambiense* and *T. brucei rhodesiense*, which are differentiated from each other on the basis of their geographical distribution (Figure 1-1) and the course of the infection they cause. *T. b. rhodesiense* is mainly found in East Africa, while *T. b. gambiense* dominates in West and Central Africa (Pepin and Meda 2001). This geographical distribution is

determined by their respective vectors responsible for the spread of disease (Barrett 2003). *T. brucei* is spread between mammals by a fly generally termed the "tsetse". By biological classification this vector belongs to the genus *Glossina*. Different species are carriers of *T. b. gambiense* and *T. b. rhodesiense*, as outlined in Table 1-1 (biosci 2001;who vector 2009). In addition, the two pathogens are distinguished by their animal reservoirs, epidemiology and disease virulence (Barrett 2003) refer to Table 1-1.

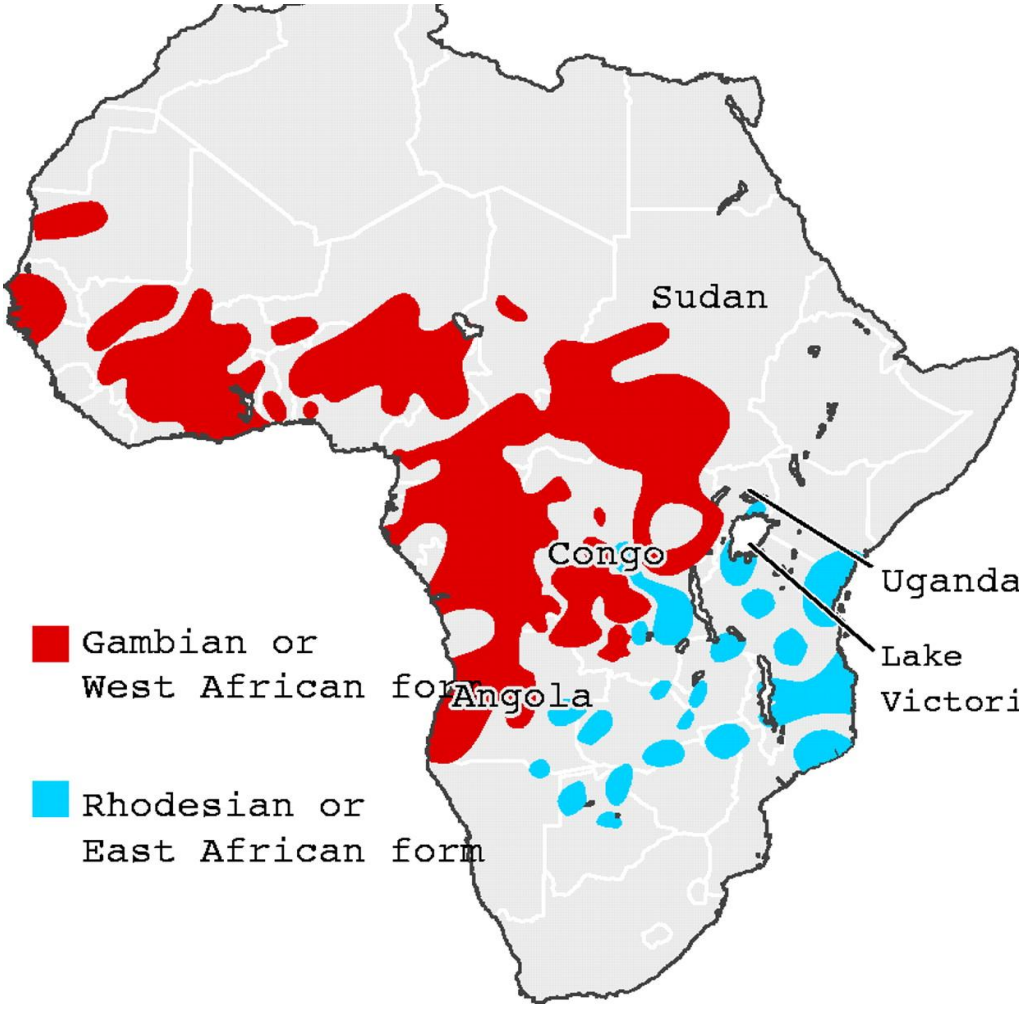


**Figure 1-1 Areas populated by Human African Trypanosomiasis.**

The regions of Africa in which *T. b. gambiense* dominates are shown in red (causing the Gambian or West African form of the disease), and the *T. b. rhodesiense* regions are shown in blue (causing the Rhodesian or East African form of the disease) Figure copied from (Lundkvist 2004).

**Table 1-1 Major differences in African trypanosomes**

| ATTRIBUTES | *T. b. rhodesiense* | *T. b. gambiense* |
|---|---|---|
| **Tsetse vector** | *G. moristans* | *G. palpalis* |
| **Ecology** | Dry bush, woodland | rain forest, rivers, lakes |
| **Transmission cycle** | Ungulate-fly-human | Human-fly-human |
| **Non-human reservoir** | Wild animals | Domestic animals |
| **Epidemiology** | Sporadic | Endemic |
| **Disease progression** | Acute | Chronic |
| **Parasitemia** | High | Low |

## 1.2.2 Biology of African Trypanosomes

### 1.2.2.1 Architecture of the parasite

Trypanosomes are unicellular protozoa with a single flagellum. Their overall cell architecture is typical of eukaryotes, but their subcellular structures display several novelties. All major organelles are clearly observed, including the nucleus, mitochondrion, endoplasmic reticulum, and Golgi apparatus. The pathogen does, however, exhibit certain unusual features, and many characteristic of this taxonomic order are highly diverged in the eukaryotic kingdom. These include, as shown in Figure 1-2:

- The presence of an organelle termed the glycosome, where glycolysis occurs (Opperdoes et al. 1977;Parsons 2004).

- Cytochromes dependent respiration does not occur in the long slender trypomastigotes in the mammalian bloodstream (see below); energy is mainly obtained from substrate level phosphorylation of glucose, whereas the tricarboxylic

acid (TCA) cycle and mitochondrial activity is needed in short stumpy trypomastigotes in the procyclic forms in the vector (Bush and Fernández 2001;Torri 1988).

- The flagellar pocket is a specialised site of 'feeding', which occurs through endocytosis in this location (Atrih 2005;Overath and Engstler 2004).

- A single flagellum is found that emerges from the basal body at the flagellar pocket, near the mitochondrion at the posterior end of the cell. It is made up of a typical flagellar axenome (Vaughan and Gull 2003) with microtubules in a 9+2 arrangement. This is a semirigid structure responsible for motality of the cell (Avidor-Reiss 2004;Bastin 1998;Pazour et al. 2005). The flagellum associates along the length of the cell until the anterior end and, in fact, emerges from the cell body, forming an undulating membrane (Heynaman 2007).

- A single elongated mitochondrion runs from the posterior to the anterior of the cell. In bloodstream form cells, the mitochondrion is a simple, tubular structure devoid of cristae. This reflects the absence of mitochondrial respiration during this life cycle stage, as energy generation is dependent on glycolytic reactions in the glycosome, due to large amount of glucose present in blood. Mitochondria develop cristae in procyclic form cells, reflecting active mitochondrial metabolism (Matthews 2005;Vickerman 1985).

- A cytoskeletal structure composed of sub-pellicular microtubules is found along the entire length of the parasite cell (Sant'Anna et al. 2005;Sherwin 1989). In this, the microtubules lie parallel to each other along the axis of the cell and are important to maintain the cell shape. They also work in conjunction with mitochondrial expansion subject to lifecyle-dependent morphological changes (Gull 2004;Sherwin 1989).

- In the mammal, the surface of the trypanosome cell is covered by a dense coat composed of $1x10^7$, 12-15 nm thick molecules of Variant Surface Glycoprotein (VSG) (Ferguson 1988;Vanhamme 2001) , which are linked to the cell membrane via GPI anchors (Englster 2007;Grunfelder et al. 2002). This thick VSG coat shields invariant surface epitopes of trypanosomes from the host immune response (Borst 2002). VSG coat is replaced by procyclin in the procyclic life stage in tsetse

fly (Matthews 1999;Roditi 1998) and is gained back at later stages in the fly salivary glands (Ginger 2002).

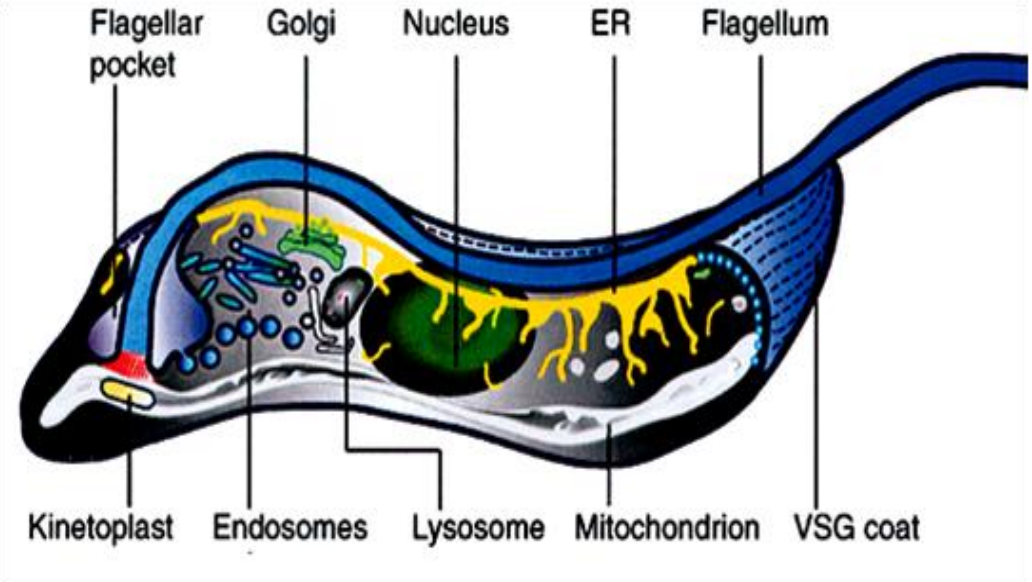


**Figure 1-2 Architecture of the African trypanosome.**

Cartoon model of a *T. brucei* bloodstream form parasite showing subcellular organelles. The parasite is covered with a dense coat of variant surface glycoprotein (VSG). A flagellum emerges from the flagellar pocket present at the posterior end and travels along the length of the cell. A single mitochondrion with kinetoplast is seen at the base of flagellar pocket. Endosomes, golgi apparatus and lysosome lie exclusively between flagellar pocket and nucleus. Figure copied from (Grunfelder 2003).

### 1.2.2.2 Life cycle of *T. brucei*

Trypanosomes are digenic parasites whose life cycle completion depends upon the transmission between vertebrate hosts by the tsetse fly vector. The parasite undergoes significant changes during its journey through the host and vector, resulting in different morphological forms, as summarized in Figure 1-3.

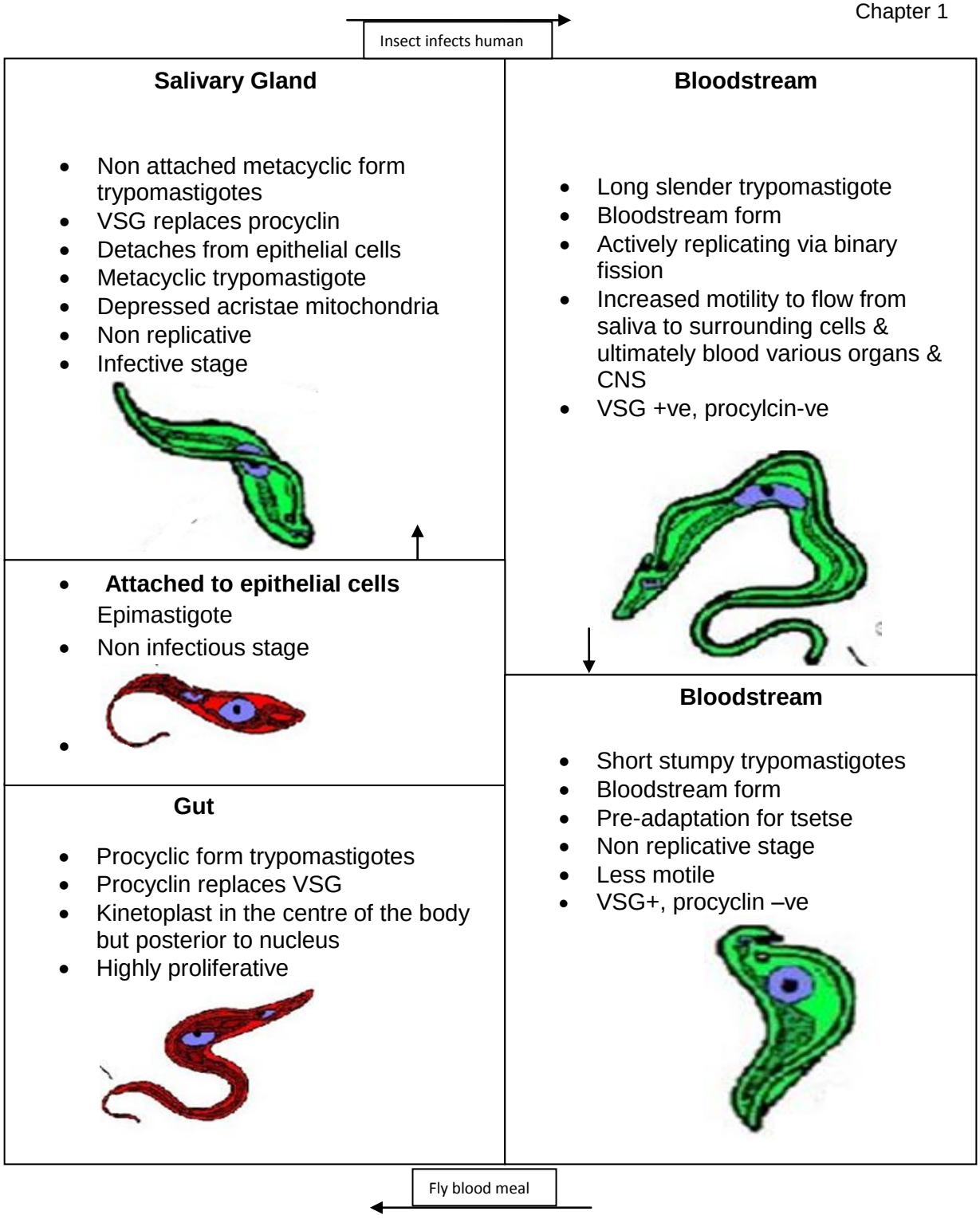


**Figure 1-3 Life cycle of *T. brucei.***

*T. brucei* is transmitted by the bite of a tsetse fly into the mammalian host, where the parasite multiplies as long slender VSG-expressing trypomastigote (bloodstream) forms in the bloodstream and lymph, with eventually transition to the CNS (Tetley 1985). Some of the bloodstream form (BSF) cells then differentiate into non-replicative short stumpy forms (Tetley 1987), which are ready to be taken up by the fly blood meal. At this stage they adapt themselves to their next life stage (Turner 1995), with enlarged mitochondria where energy production is by oxidative phosphorylation, rather than by the glycolysis of the long slender BSF cells. When the tsetse fly takes a blood meal, the short stumpy forms differentiate into replicative procyclic form (PCF) trypomastigotes in the tsetse midgut. These cells have a well-defined and functional mitochondrion, and the VSG coat is replaced with procyclin (Barry 2001;Roditi 1998). The PCF cells then migrate from the midgut and attach to epithelial cells of the fly salivary glands. Here, they are proliferative epimastigotes, which can detach from the epithelial cells and differentiate to infective metacyclic form trypomastigotes. This life cycle stage is non-replicative and pre-adapted for the mammal, with procyclin replaced by VSG (Ginger 2002). The parasites are then transmitted by the tsetse bite into

the new mammalian host, existing initially as metacyclic form cells but then differentiating into replicative long slender BSF cells, and thus completing the life cycle (Barry 1998). Figure adapted from (El Sayed 2000).

### 1.2.2.3 Genome of the African trypanosome.

The genome sequence of *T. brucei brucei*, strain TREU927, predicts a haploid genome of 36 Mb, encoding 12000 genes (El Sayed 2000) . However, the genome is divided into two parts (Ersfeld 1999;Riou 1969): kinetoplastid (mitochondrial) DNA, and nuclear DNA.

#### 1.2.2.3.1 Kinetoplastid DNA

The kinetoplast genome consists of maxi-circles and mini-circles (Klingbeil and Englund 2004), which occur in a concatenated mass within the mitochondrion. The maxi-circles (~50 copies /kinetoplast) contain genes that encode several of the mitochondrial proteins (Schnaufer et al. 2002;Sloof et al. 1992). Mini-circles (~10,000 copies /kinetoplast) are heterogeneous, rapidly evolving and function to encode short guide RNAs (Blum 1990;Estevez 1999). These guide RNAs serve in the post-transcriptional editing of certain transcripts formed from maxi-circles by the incorporation or deletion of uridines. Such RNA editing, which is not unique to the Kinetoplastida but the extent of its use is unparalleled, takes place in editosomes, which are multi-protein editing complexes (Madison-Antenucci 2002). Mini-circles do not encode any proteins and, because of being highly conserved among species, are used for parasite detection and distinguishing different isolates (Avila 1991).

#### 1.2.2.3.2 Nuclear DNA

The nuclear genome of *T. brucei* is made up of (Hertz-Fowler 2007) 11 diploid large chromosomes (1-6 Mbp in size; termed the megabase chromosomes),1-6 intermediate chromosomes (200-900 Kbp) and approximately 100 mini-chromosomes (around 50-100 Kbp) (Hertz-Fowler 2007). The megabase chromosomes encode most of the function of the cells, with many core conserved genes characteristic of eukaryotes. However, the genes on the megabase chromosomes are organized in a small number of polycistronic arrays that are each transcribed from single distant, poorly characterised RNA polymerase II promoter (Gilinger 2001;Imboden 1987). Genes that are differentially expressed through the life cycle can be adjacent to each other, and such gene expression control is regulated at the post-transcriptional level through differential RNA processing. All genes are converted

from the multigene pre-RNA to mature mRNA by coupled polyadenylation and trans-splicing, which causes the addition of a splice leader sequence that provides a 5' cap for the mRNA. mRNA stability and translation controls have been documented that can control gene expression levels (Clayton 2002;Mair et al. 2000).

Approximately 55% of the megabase chromosomes is assigend as sub-telomeres. Majority of this subtelomeric region is assigned to variant surface glycoprotein (*VSG*) or *VSG*-associated genes (Barry 2001;Hertz-Fowler 2007;Marcello 2007). In bloodstream form cells, antigenic variation of *VSG*s is used as a means of immune evasion (Barry 2001). Sequencing of the *T. brucei* genome revealed a huge *VSG* gene archive, made up of thousands of different *VSG* genes (Marcello 2007;Taylor and Rudenko 2006) with only one of these capable of being expressed at a time by RNA polymerase I (Gunzl 2003). Expression sites (ES) for *VSG*s are located in the subtelomers of intermediate and megabase chromosomes, and are classified on the basis of the two life stages in which VSG is expressed on parasite's surface. Metacyclic expression sites (MES) are used in metacyclic form life stages in the fly, while bloodstream expression sites (BES) are used during growth in the mammalian host. MES are monocistronic with a few repetitive sequences and are less recombinationally active than BES (Ersfeld 1999). BES are large polycistronic units that contain several ES-associated genes (ESAGs) (Pays 1994) with a *VSG* gene at the telomere-proximal end. As stated above, only one BES or MES is expressed in one cell at a time. VSG is expressed by the active expression site and immune response generated against that surface coat will kill the infecting trypanosomes. However, as replication is being carried out, there is a possibility that with each cell division some of the progenies will exchange transcription of the active expression site with a silent one, or change the *VSG* present at the active site; overall, such switching can occur at rates of $10^{-2}$ switches/cell/generation (Robinson 1999;Turner 1989). Parasites that have changed the VSG coat are not likely be detected by the existing antibodies. It takes several days to generate immune response against new trypanosome VSG coats. This time period gives the pathogen sufficient time to reproduce and increase infection numbers. Repetition of this process of antibody elimination and outgrowth of switched VSG variants prevents the extinction of the infecting trypanosomes, allowing chronic persistence of the parasites in the host (Barry 1979).

In minichromosomes, 90% of the sequence is composed of 177 bp repeat of unknown function (Weiden et al. 1991;Wickstead et al. 2004). In addition, the region between the telomeres and the 177 bp repeats contains a 74 bp GC-rich sequence separated by a 155 bp

AT-rich sequence (Delange 1983;Ersfeld 1999;Kipling 1995). Minichromosomes lack protein-coding genes except for *VSG*s at the sub-telomeric region of the chromosomes (Vanderploeg et al. 1984). The presence of these *VSG*s is striking and suggests these chromosomes evolved for host immune evasion, perhaps to expand the capacity of *VSG*s available for antigenic variation. Intermediate chromosomes range from 200-900 kb and are much like minichromosomes. However, they harbour silent VSG ESs. It is possible that they might also serve as a repository for *VSG*s or have evolved to increase the number of *VSG* ES (El Sayed 2000;Wickstead, Ersfeld, & Gull 2004).

## 1.3 DNA Damage

The Genomes are nature's repository, carrying all the information needed to generate and replicate a specific organism. Given this, any genome must be carefully protected from all sorts of damage, which could fatally alter the information within. However, damage is inevitable, and provides a fuel for evolution (in addition to errors during replication). Nonetheless, all cells contain efficient systems to limit damage, and to correct and repair any damage that is generated. The type and extent of damage that cells might suffer depends on the type of cell, the environment it occupies and its metabolic activity. In this introduction, I will not consider physical or mechanical damage to genomes, and concern ourselves with the biological or chemical damage that can be imposed onto the cell. I will also only consider DNA genomes. Damage to DNA genomes could be from exogenous sources: for instance, UV radiation causes pyrimidine dimers; γ or X ray radiation causes double-stranded or single-stranded breaks; and chemical mutagens, such as alkylation agents or oxidizing chemicals, can alter the base composition of DNA. DNA damage can also be caused endogenously, from cell sources, most notably from certain metabolic activities. An example of this includes free radicals produced during substrate level phosphorylation, which can damage a range of macromolecules, including DNA. DNA breaks can also be generated endogenously, for instance during replication stalling on specific DNA sequences or secondary structure, or by the action of endonucleases, such as during yeast mating type switching or meiotic exchange. Endogenous damage is also caused by the errors left during replication or base modifications caused by certain mutagens.

### 1.3.1 Response against DNA damage

Since DNA is vital for cell survival and reproduction, cells efficiently initiate different responses to any sort of damage. These act either by suppressing potential damage, for instance by cleansing any damaged dNTPs from the cellular pool, or by tolerance or repair of DNA lesions that are incorporated into the genome.

### 1.3.2 DNA damage checkpoints

DNA damage, if not repaired, can lead to genome instability and finally cell death. Therefore, it is essential for the cells to efficiently respond to DNA damage by coordinating DNA damage check points and repair pathways. In eukaryotes, this primarily requires the recruitment of ataxia telangiectasia mutated (ATM), Rad3 related (ATR) and DNA dependent protein (DNA PK) kinases. These three enzymes phosphorylate certain downstream factors that are involved in DNA repair (Su 2006).Mutations in ATM and ATR are associated with human syndromes, whereas mutations in DNA PK have been linked to immunodeficiency in mouse models (Smith 1999). ATM and ATR phosphorylate Chk2 and subsequently activate Chk1. Chk1 and Chk2 are kinases that further phosphorylate and activate p53, which activates p21 and arrests the cell cycle at G1 phase. Cell cycle arrest at the G1/S phase gives the cell a time window to repair DNA damage before the cell prepares to divide. Cell cycle might also be arrested at G2/M phase, which prevents the entry of damaged DNA into the daughter cell (Su 2006).Cell cycle arrest gives the cell the time to repair the damage, after which the cells exit the check point and cell cycle is resumed.

### 1.3.3 DNA damage tolerance

When damage afflicts DNA, cells frequently attempt to repair the damage, using several pathways depending on the nature and extent of damage (see below). However, in certain instances, cells live with the damage, inducing mutations. Examples of this can be considered to include somatic hypermutation and gene rearrangements during antibody generation, or genome rearrangements during immune evasion by pathogens such as *T. brucei*, where it assumed that the generation of lesions is tolerated and repaired inaccurately, as the changes they make are beneficial for survival (Friedberg 2005). Cells have also evolved mechanisms to bypass certain mutations, allowing replication to continue, in this case without repairing the lesion. Two pathways have been proposed for

this form of DNA damage tolerance: translesion synthesis (TLS) and template switching (Chang 2009).

Translesion synthesis involves the recruitment of DNA polymerases with low proofreading activity, allowing them to incorporate dNTPs opposite mutated bases. Examples of such polymerases are pol η and pol κ, which have bulky catalytic sites to allow access to DNA adducts, such as thymine dimers (Yagi 2005). Once these polymerases have performed the lesion bypass, they are normally again replaced by the higher fidelity replicative DNA polymerases, like pol ε and pol δ, and replication is carried forward (Chang 2009;McCulloch 2008).

Template switching is less well understood. It is presumed that the replication machinery switches from the template that it has been replicating to the newly synthesized strand of the sister duplex when certain lesions are encountered, such as those induced by UV radiation. This daughter strand, which is homologous to the error-containing strand, is now used to synthesize a new DNA strand and replication is continued (Chang 2009;Friedberg 2005).

## 1.4 DNA repair

Despite the potential for DNA damage tolerance, in most instances damage has to be repaired to maintain genome integrity and continue cellular processes in a conserved manner. Cells have evolved multiple mechanisms of DNA repair, which are activated depending on the mutagen and the lesion caused. These can be classified as line of defence, but this might not be always the case.

The mechanisms of repair can be classified as follows: (i) direct reversal of the base modification; (ii) excision of the DNA lesion by either base excision repair (BER), nucleotide excision repair (NER) or mismatch repair (MMR); (iii) repair of DNA strand breaks (single or double) by single-strand break repair, homologous recombination (HR) or non-homologous end-joining (NHEJ).

### 1.4.1 Direct reversal

UV-induced pyrimidine dimers and alkylation adducts can be repaired by direct reversal of the damage. This does not involve DNA incision and re-synthesis, but instead primarily functions by flipping out the damaged base into the active site of an enzyme where damage

is reversed (Daniels 2004;Torizawa 2004). One enzyme involved in direct repair is termed Photolyase, which repairs UV-induced pyrimidine dimers such as cyclobutane pyrimidine dimers (CPD) that, if left unrepaired, would block replication. Photolyases directly reverse the dimerization reaction by transferring an electron from $FADH^-$ to CPD (Payne et al. 1987;Sancar 2008). However, placental mammals lack photolyases and most of such damage is repaired by nucleotide excision repair (van der Horst 1999). Another enzyme of direct reversal is Alkyl guanine transferase (AGT), which repairs the damage induced by alkylating agents (Figure 1-4). The enzyme has conserved tyrosine and arginine residues present in its active site, which are responsible for flipping out alkylated bases from the DNA helix at which time the alkyl group is transferred from the DNA base to a cysteine residue, also present at the active site of the enzyme (Daniels 2004). Once the alkyl group is transferred, the enzyme becomes inactive and is then degraded (Lindahl 1982;Wiestler 1984). Alkyl transferase-like (ATL) is a protein that works in a similar way to AGT but does not have the conserved active site cysteine residue (Aramini 2010;Margison 2007). ATL binds to an alkylated base in the same manner as AGT but cannot transfer the alkyl group from the base. How they work in repair is not then fully understood (Aramini 2010;Morita 2008;Tubbs 2009), but it is thought that they work with NER. This differing mode of repair may be due to AGT and ATL having differences in their binding affinity: AGT preferentially binds to methylated groups, whereas ATL has higher affinity for larger adducts.

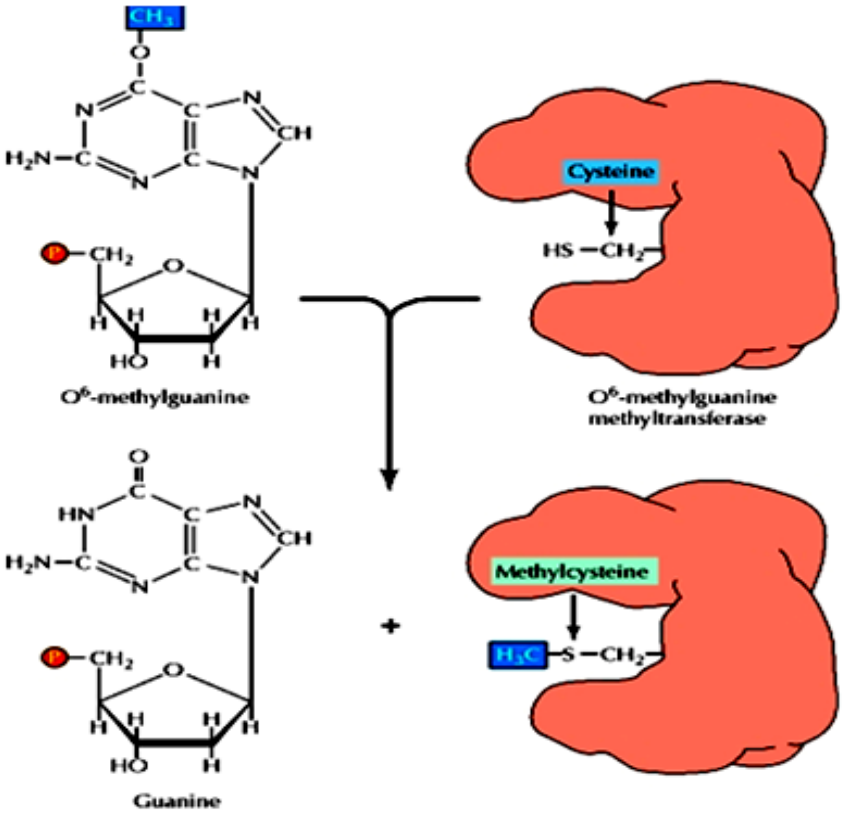


**Figure 1-4 Direct reversal by methyl guanine methyl transferase (MGMT).**

MGMT transfers the methyl group at the 6th carbon of guanine to a cysteine residue present at its active site and the damage is repaired. Figure copied from (Cooper 2000).

*T. brucei* and related kinetoplastids appear to possess direct repair pathways, since genes encoding a putative MGMT (methyl guanine methyl transferase) (Berriman 2005;El Sayed 2000) and a putative photolyase are present. In addition, kinetoplastids also encode a putative dioxygenase (AlkB, an iron-dependent dioxygenase) that may reverse the lesions 1-methyladenine and 3-methylcytosine in single-stranded DNA or RNA (Aravind 2001).

## 1.4.2 Base excision repair

Base excision repair (BER) is a widely used repair mechanism (Figure 1-5) that serves to repair DNA damage caused by deamination, apurination/apyrimidation, oxidation and alkylation (Gates 2009;Zharkov 2008). DNA glycosylases are the major recognition proteins involved in BER repair, with several different glycosylases encoded by most organisms that act on different adducts. For instance, deamination of cytosine forms uracil in DNA and repair of this is initiated by uracil DNA glycosylase (Pearl 2000), whereas oxidation of guanine forms 8-oxo guanine, whose repair is initiated by MutY/MYH (MutY

homologues) glycosylase (Michaels 1992;Ohtsubo 2000). DNA glycosylases are either mono-, bi- or tri-functional. Mono DNA glycosylases only break the N glycosidic bond between the base and sugar phosphate backbone and create an apurinic/apyrimidic (AP) site, whereas bi- and tri-DNA glycosylases have an additional downstream activity carried out by AP lyase or AP endonuclease (APE) activity (Fromme 2004). An AP site is targeted at the 5'end by AP endonuclease and generates 3'OH and 5'deoxyribosephosphatse (dRP) through a hydrolytic reaction. 5'dRP is removed by dRPase. An AP site is treated at the 3'end by AP lyase, which produces 3'phosphate and 5'phosphate. 3'phosphate is removed by 3'phosphoesterase. One nucleotide is generally left behind after AP site processing and is then repaired by DNA polymerase and sealed by DNA ligase. Damage can be repaired by incorporating a single nucleotide at the AP site, which is called as short patch BER and is mediated by DNA Polymerase Beta (DNA polβ). However, sometimes repair is performed by strand displacement of two or more bases; this is called long patch BER where DNA polymerases delta (DNA polδ) and DNA polymerase epsilon (DNA polε) perform more extensive DNA synthesis, producing a single-stranded 'flap' that removed by the FEN-1 endonuclease to allow ligation (Robertson 2009).

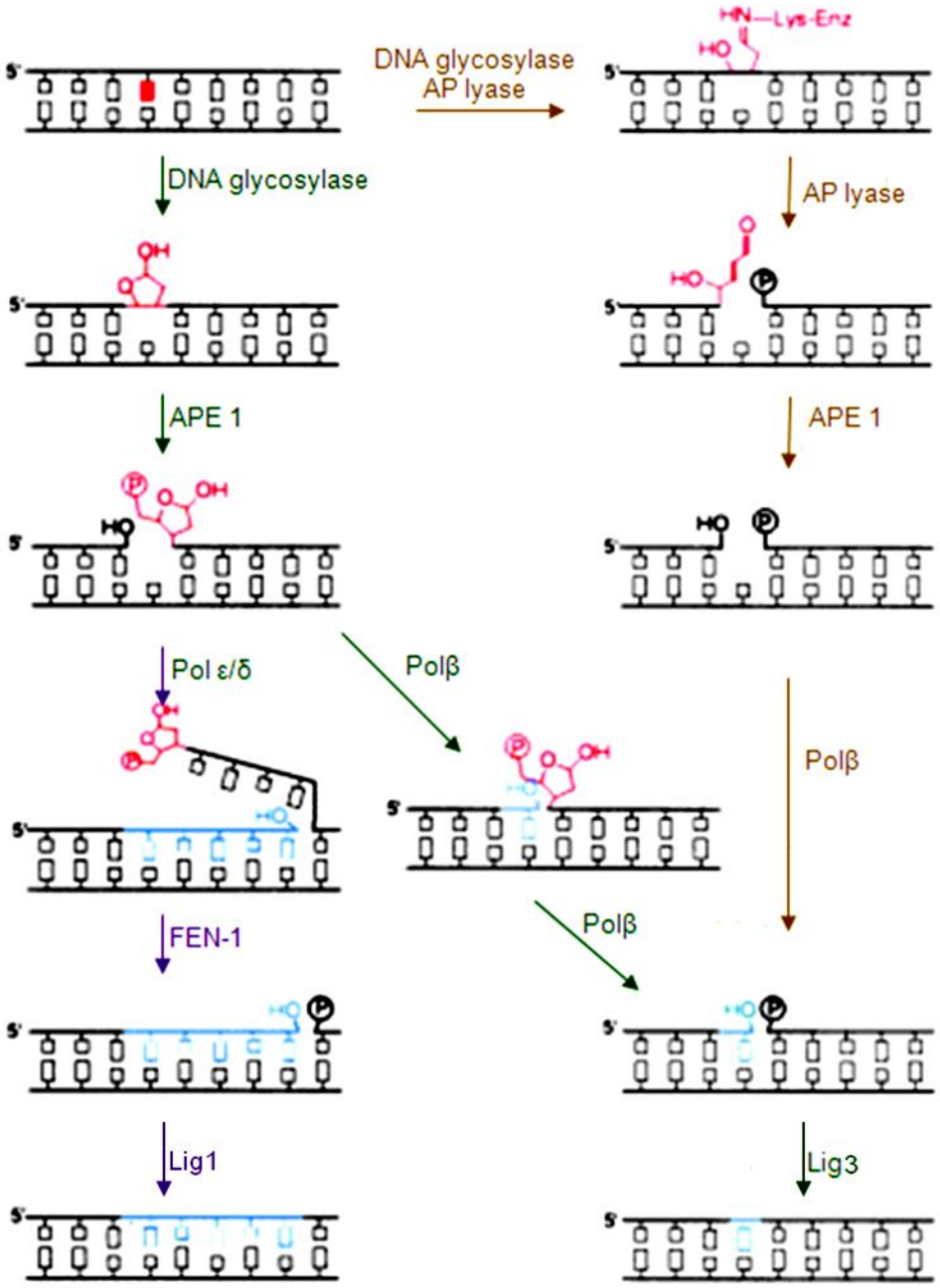


**Figure 1-5 Base excision repair (BER)**

Short patch BER is represented by green and brown arrows, whereas long patch BER is represented by purple arrows. The enzymes that catalyze each step are indicated beside their respective arrows. DNA glycosylases break the N-glycosidic bond and create an AP site, which is then targeted by either AP endonuclease (APE1; green arrows) or AP lyase (brown arrows). For the AP site targeted by APE1, the phosphodiesterase bond at the 5' end of the site is hydrolyzed. For an AP lyase-targeted AP site, the sugar phosphate backbone at the 3' end of the abasic site is hydrolysed. In short patch BER Polβ then incorporates a single nucleotide in the AP site and the nick is sealed by Ligase3 (Lig3). In Long patch BER, the AP site is targeted by APE1 and Polε/δ incorporate 2-6 nucleotides after the abasic site. This creates a single stranded flap, which is removed by Fen-1 endonuclease and the nick is sealed by Ligase1 (Lig1). Figure copied from (Scharer 2003).

In trypanosomatids, most of the BER enzymes have been characterized. However, since Lig3 of short patch BER appears not to be present, it cannot be said very clearly if both the

short patch and long patch BER pathways are present. The first BER enzyme characterized in trypanosomatids was Uracil-DNA glycosylase in *T. cruzi* (TcUNG), which removes a mispaired uracil (U), formed by the deamination of cytosine (C), paired against guanine (G) (Pena-Diaz 2004). It was found that TcUNG removes uracil by short patch BER. Also, it was reported that TcUNG is a functional homologue of *E. coli* and human UNG. Another important DNA glycosylase present in trypanosomatids is OGGI, the functional homologue of MutM, and is involved in the repair of oxidative lesions. OGG1 removes 8oxoG (see below) when paired against cytosine (C). Furtado and collegues have reported OGG1 being present in both the nucleus and mitochondrion of *T. cruzi* (Furtado 2012). Along with OGG1, homologues of MutT and MutY have also been annotated in *T. brucei* and related kinetoplastids (Tsuzuki 2007), and are thought to repair oxidative lesions. AP endonuclease 1 (APE1) has also been characterized in *T. cruzi* and *L. major* and it was shown that over expression of APE1 from *Leishmania* confers resistance against oxidative damage (Perez 1999). Among the BER polymerases, DNA polβ has been characterized in *T. brucei* and *T. cruzi* (Lopes 2008;Saxowsky 2003), where it was reported to be mitochondrial, while in higher eukaryotes it is localized in the nucleus (Foster 1976;Saxowsky 2003).

### 1.4.3 Nucleotide excision repair

Nucleotide excision repair (NER) is another highly conserved repair pathway present in both prokaryotes and eukaryotes (Sancar 2008;Vanhouten 1990). NER has a broad substrate specificity though is primarily responsible for catalysing the removal and repair of bulky adducts like UV-induced pyrimidine dimers or alkylation of DNA with larger alkyl groups (Truglio et al. 2006). Smaller lesions such as methylation damage, base mismatches or small insertion/deletion loops (IDLs) appear not to be good substrates for NER. NER has been sub-classified as two pathways: global genome repair (GGR), which involves repair throughout the genome, and transcriptional-coupled repair (TCR), which acts on lesions in transcribed regions of the genome that block movement of RNA polymerase (Scharer 2003). The general mechanism for NER is same for both the subpathways after the damage recognition step. In GGR (Figure 1-6) DNA lesions are first encountered by UvrA and B in prokaryotes and Xeroderma Pigmentosum C (XPC), XPA, TFIIH and replication protein A (RPA) in eukaryotes, which make a protein-DNA complex. In *Escherichia coli*, this complex further recruit UvrC, which incises at both sides of the DNA lesion a few nucleotides upstream and downstream of the lesion (Verhoeven 2000). In eukaryotes, two distinct endonuclease are recruited: XPG makes an

incision at 3' of the lesion and XPF/ERCC1 makes an incision 5' of the damage. In prokaryotes a distinct helicase, UvrD, unwinds and removes the incised nucleotide fragment, whereas in eukaryotes helicase activity is possessed by the TFIIH subunits, XPB and XPD (Evans 1997), and aided by XPA. PolI in prokaryotes, and in eukaryotes Polε and δ, synthesize a new strand and the gap is sealed by DNA ligase. TCR occurs in essentially the same way, though recognition of the lesion is distinct and the efficiency of repair may differ. In TCR repair is initiated by stalling of RNA polymerase on the transcribed strand, which initiates the recruitment of Cockayne syndrome A (CSA) and CSB protein in eukaryotes (Hanawalt 2002). In *E. coli* the transcription-repair coupling factor (TCRF) releases RNA polymerase and recruits NER enzymes (Selby 1993). In bacterial TCR, UvrA is directed more efficiently to the error-containing strand by TCRF because of the stalled polymerase. This contrast with GGR, where UvrA has to travel along the DNA and search for the damage.

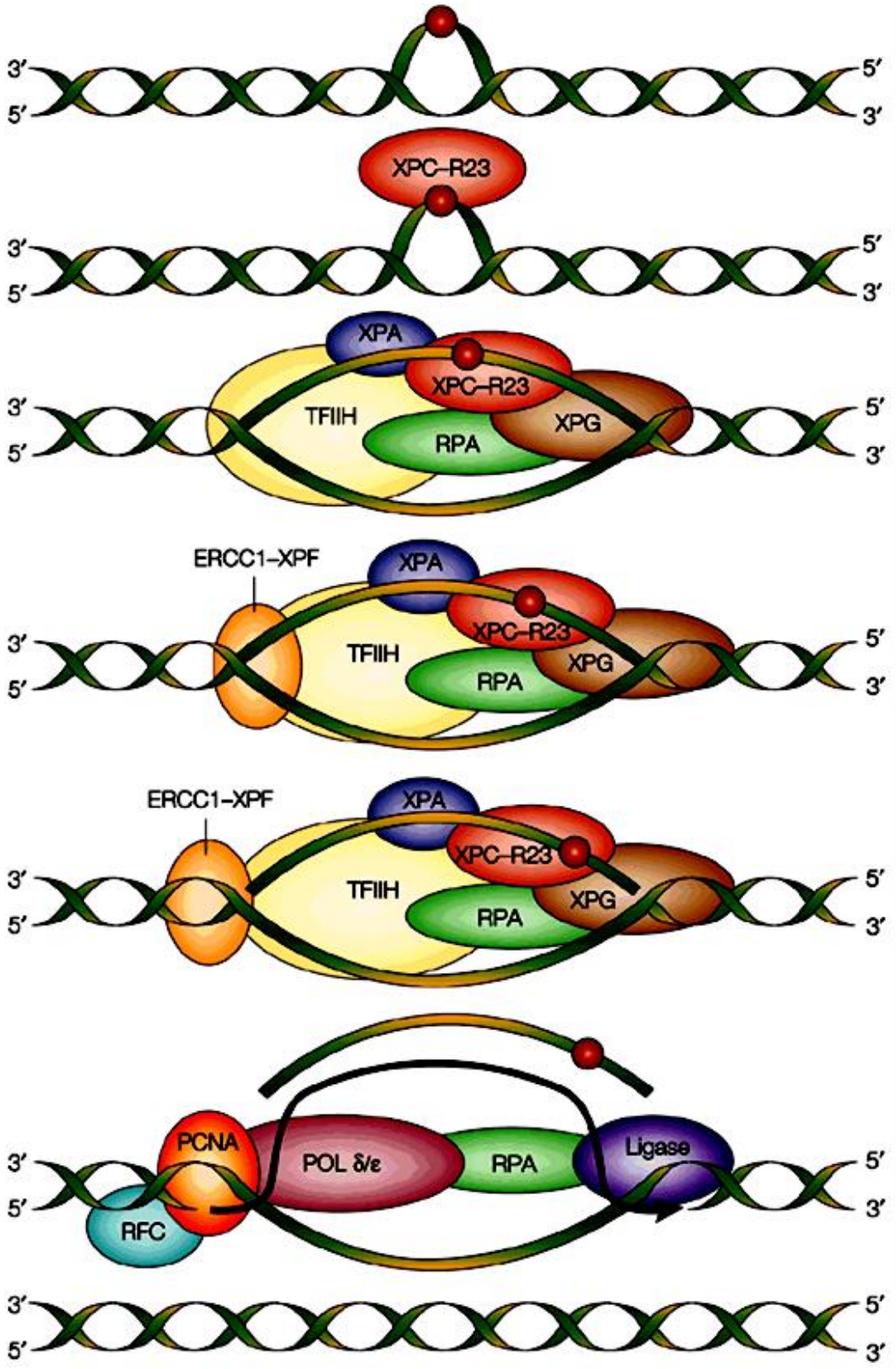


**Figure 1-6 Eukaryotic nucleotide excision repair**

A DNA lesion is detected by Xeroderma pigmentosum C (XPC) in global genome repair, followed by the recruitment of helicases XPA and TFIIH, along with replication protein A (RPA). These helicases break the hydrogen bond and form a bubble around the DNA lesion, which then recruits endonuclease XPG to incise at the 3' end, while XPF/ERCC1 incises at the 5' end. The Incised strand is removed and a new DNA strand is synthesized by DNA Polδ/ε and the nick is sealed by ligase. Figure copied from (Friedberg 2001).

Trypanosomatids contain most of the enzymes involved in eukaryotic NER (Aslett 2010). However, some of the proteins, most notably XPA and CSA, have not been annotated in genomes and no work has examined this repair reaction experimentally. Thus, there might be differences in the mechanisms of NER in *T. brucei* relative to other eukaryotes. It is presumed that TCR is predominant in these parasites, due to the unusual nature of polycistronic gene expression (Groisman 2006). If *T. brucei* is able to perform TCR in the absence of CSA, this might infer an adaptation of the machinery, perhaps with some alternate protein playing the role, though CSA in *T. brucei* might simply be highly diverged.

### 1.4.4 Non-homologous end-joining

Non-homologous end-joining (NHEJ) is one of the major pathways to repair double strand breaks (DSB) in eukaryotes (Smith 2003;Weterings and van Gent 2004) and some bacteria (Figure 1-7). It is a mechanism of direct joining of broken DNA ends, which requires proteins that recognize and bind to the exposed DNA ends and bring them together for ligation. A key factor is the Ku70/Ku80 heterodimer, which is involved in the initial recognition of the DSB ends and thus vital for the process to carry on.

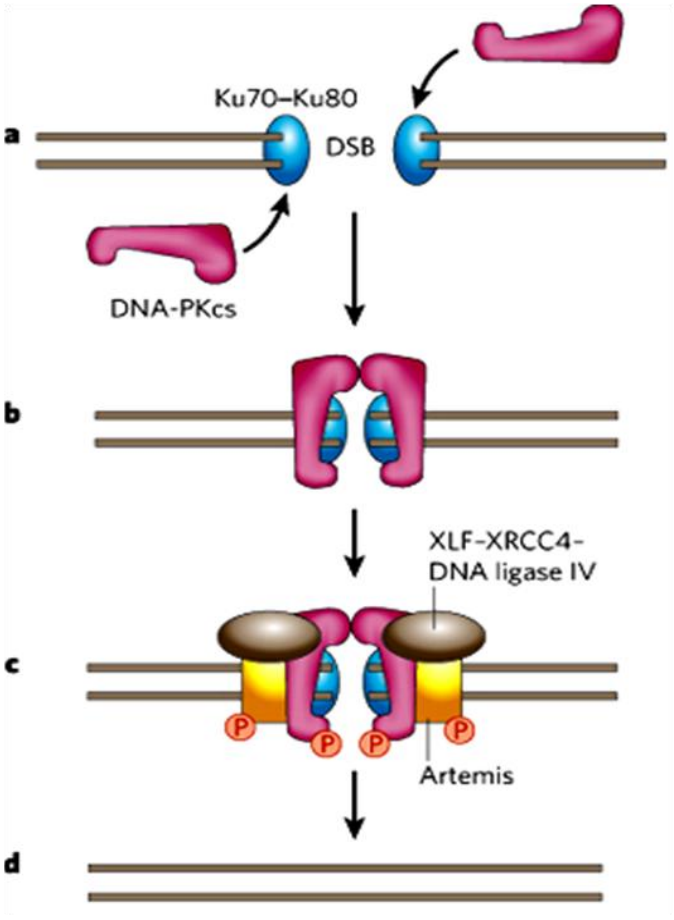

**Figure 1-7 Non-homologous end joining**

A DSB is identified by Ku70-Ku80, which in some eukaryotes interacts with the DNA-dependent kinase catalytic subunit (DNA-PKcs), bringing the two ends together and allowing ligation by XRCC4 and DNA ligase IV Figure copied from (Downs 2007).

Ku70 and Ku80 have been identified in *T. brucei* and shown to act in telomere maintenance (Conway 2002;Janzen 2004). However, DNA ligase IV and XRCC4, which together form an NHEJ-specific ligase, have not been detected in the genome sequence. This suggests that NHEJ in *T. brucei* and related trypanosomatids may function in variant form, or may even be absent (Burton 2007).

## 1.4.5 Homologous recombination

Homologous recombination (HR) is a process involving the exchange of sequence information between two homologous DNA molecules. HR is critical in repairing DNA double-stranded breaks (DSBs) (Li 2008b), and is a widely conserved process that broadly involves three main steps in the reaction (Figure 1-8). First is initiation, or presynapsis, which involves recognition and processing of the DNA break to reveal 3' single-stranded ends to which the key enzyme of HR, termed Rad51 in eukaryotes (Filippo 2008) RecA in bacteria and RadA in archaea, binds. Second is strand exchange or synapsis (Bugreev 2006), where Rad51 catalyses a search for sequence homology in an unbroken DNA molecule and then strand transfer from the broken end, which results in strand exchange intermediates, such as Holliday junctions. Finally, there is resolution or post-synapsis, where the strand exchange intermediates are resolved (Filippo 2008), allowing the strands to separate from each other and DSB repair to be completed with associated DNA synthesis and ligation.

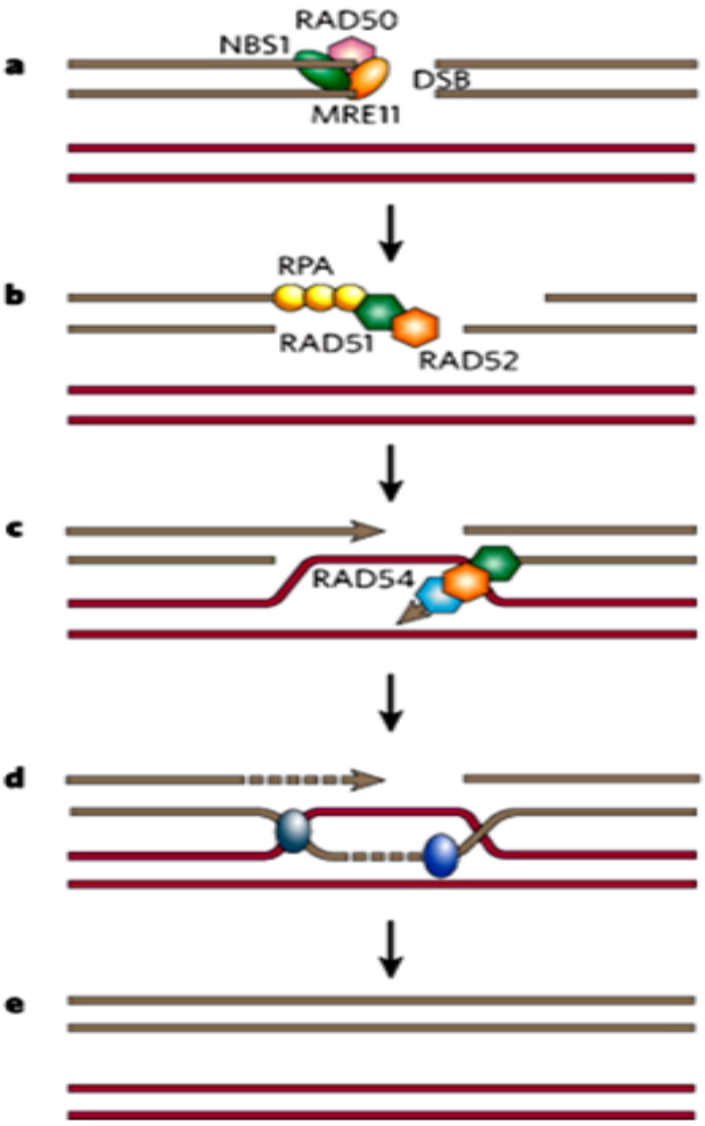


**Figure 1-8 Eukaryotic homologous recombination**

A DNA double strand break (DSB) is recognized by a complex of MRE11, RAD50 and NBS1, which contribute to the processing of the break to form single-stranded tails. The single-stranded DNA is stabilized by RPA, which is replaced by RAD51 in a reaction mediated RAD52 and other mediators (not shown). A nucleoprotein filament of RAD51 on the DNA then looks for homology in an unbroken DNA molecule and catalyses strand invasion and exchange, supported by RAD54, forming intermediates such as Holliday junctions. Resolution of such structures involves branch migration and then resolution by further factors, which are less well characterised in eukaryotes than in bacteria (not shown). Figure copied from (Downs 2007).

In *T. brucei* and related kinetoplastids most of the proteins involved in HR have been identified. Of the proteins involved in presynapsis, MRE11 mutants in *T. brucei* lead to compromised HR activity and genome instability (Robinson 2002;Tan 2002). Mutants in DMC1 and RAD51, the proteins involved in strand exchange, have also been made in *T. brucei*. It has been shown that absence of DMC1 does not impair HR activity (Proudfoot 2006), at least in bloodstream stage parasites, and this would be consistent with evidence that this factor's role is limited to meiotic HR, as in other eukaryotes; indeed, expression of

the protein appears to be limited to specific cells in the tsetse salivary glands (Peacock 2011), where *T. brucei* mating is thought to occur. In contrast, mutation of *RAD51* causes impaired HR in *T. brucei* and undermines the efficiency of antigenic variation (McCulloch 1999). A number of proteins that mediate RAD51 protein function have also been examined and shown to play roles in HR and antigenic variation. One of these is BRCA2, which interacts with Rad51, and whose mutation also results in genome instability (Hartley 2008;Oyola 2009). In addition, and a set of RAD51- related proteins have been examined, which are much less conserved amongst eukaryotes than Rad51 and are called "Rad51 paralogues" (Thacker 2005). Though these paralogues appear to function as recombination mediators, for instance in aiding the formation of the RAD51 nucleoprotein filament during recombination (Sung et al. 2003), their detailed roles in HR are less clearly defined than BRCA2 and it is not clear if they bind Rad51. *T. brucei* encodes four Rad51 paralogues that are all involved in DNA repair and HR, but only one appears to act in antigenic variation (Dobson 2011;Proudfoot 2006).

### 1.4.6 Mismatch repair

Mismatch repair (MMR) is a highly conserved biological pathway that acts to increase the fidelity of DNA polymerase-mediated replication 20-400 fold, thus enhancing the maintenance of genome integrity (Schaaper 1993). This is done by MMR identifying and correcting mispaired bases that do not follow the Watson and Crick base pairing model. Such base mismatches are repaired by two mechanisms. Very short patch (VSP) repair takes place during the stationary phase of cell growth and is thought to prevent 5meC to thymine mutations. All bacteria, higher eukaryotes and a few lower eukaryotes (like yeast and unicellular algae), use methylation at the $5^{th}$ Carbon of cytosine as a modification 'tag' for the recognition of certain DNA sequences for such processes as transcription control, protection from endonuclease activity and maintenance of chromosome structure (Ehrlich 1981). However, this increases the rate of 5meC-T mutation, since 5meC deaminates to form thymine, which then pairs with guanine in a T:G mismatch. Vsr is the key protein involved into VSP repair system, and acts by nicking the DNA exactly upstream of the mismatch. DNA polymerase then replaces the error-containing strand and the gap is sealed by ligase. Despite being a form of MMR, there is no enzymatic similarity between VSP MMR and the more predominant form of MMR, termed long patch MMR. Although loss of MSH2 or MLH1 results in reduced VSP repair (Bhagwat 2002), long patch MMR is often referred to as post-replicative MMR, since its role is mainly described as correcting the errors left behind after the proof reading activity of DNA polymerases. It is catalysed

by a number of multi-protein complexes and is highly conserved in living organisms (Bhagwat 2002;Modrich 2006). Long patch MMR is the main focus of this study and will be referred to from now on solely as MMR. Although MMR is mainly considered as a post replicative process, it has been shown to have a role in other pathways. One prominent function is in regulating homologous recombination between DNA strands that are <100% identical, thus creating a balance between genome integrity and allowing space for evolutionary variation (Bell 2003).

The best studied MMR pathways are those in of *E. coli* and *Saccharomyces cerevisiae.* Though conserved, slight variations are present between these two MMR systems. MMR employed by *E. coli* and other gram-negative bacteria is termed methyl-directed MMR. In contrast, nick-directed MMR is more widely used, being conserved in most eukaryotes and some prokaryotes, such as *T. thermophilus* and related mutH-less bacteria (explained below). Despite being slightly different in their mechanism, both pathways satisfy two basic requirements for MMR: they recognize single mismatched bases or insertion-deletion loops (IDLs), and they can direct the repair machinery to the nascent strand after replication (Jiricny 2006).

#### 1.4.6.1 Methyl-directed MMR

In *E. coli* and related gram-negative bacteria ~ 1.7-1.8% of adenine residues in the genome are modified to become $N^6$-methyl adenine by the enzyme deoxyadenyl methylase (Dam). Dam specifically recognizes GATC tetranucleotide sites and methylates adenine ~2-7 minutes after DNA replication. This time window is used by the MMR machinery to distinguish between fully methylated DNA and mismatch-containing, newly replicated hemi-methylated DNA (Langlerouault 1987;Modrich 1989). MutS is the first enzyme that acts in the MMR process and binds to DNA and recognizes mismatched bases (Figure 1-9). MutS then recruits MutL and, once this DNA-protein complex forms at the mismatched site, MutH is recruited. MutH is an endonuclease specific to the organisms that use methyl-directed MMR and creates a nick at the unmethylated GATC site (Ban 1998;Lee 2005). UvrD, a helicase, then unwinds the DNA spanning the mismatch (Dao 1998;Mechanic 2000). The unwound DNA is then targeted by one of the exonucleases (Exo VII, RecJ or ExoI) of the system to digest the DNA in either a 5'-3' or 3'-5' direction, depending on the position of nicked GATC site with respect to the mismatch (Burdett 2001;Jiricny 2006;Yamagata 2001). The gap is then re-synthesized by DNA polymerase and sealed by DNA ligase, allowing DNA replication to resume.

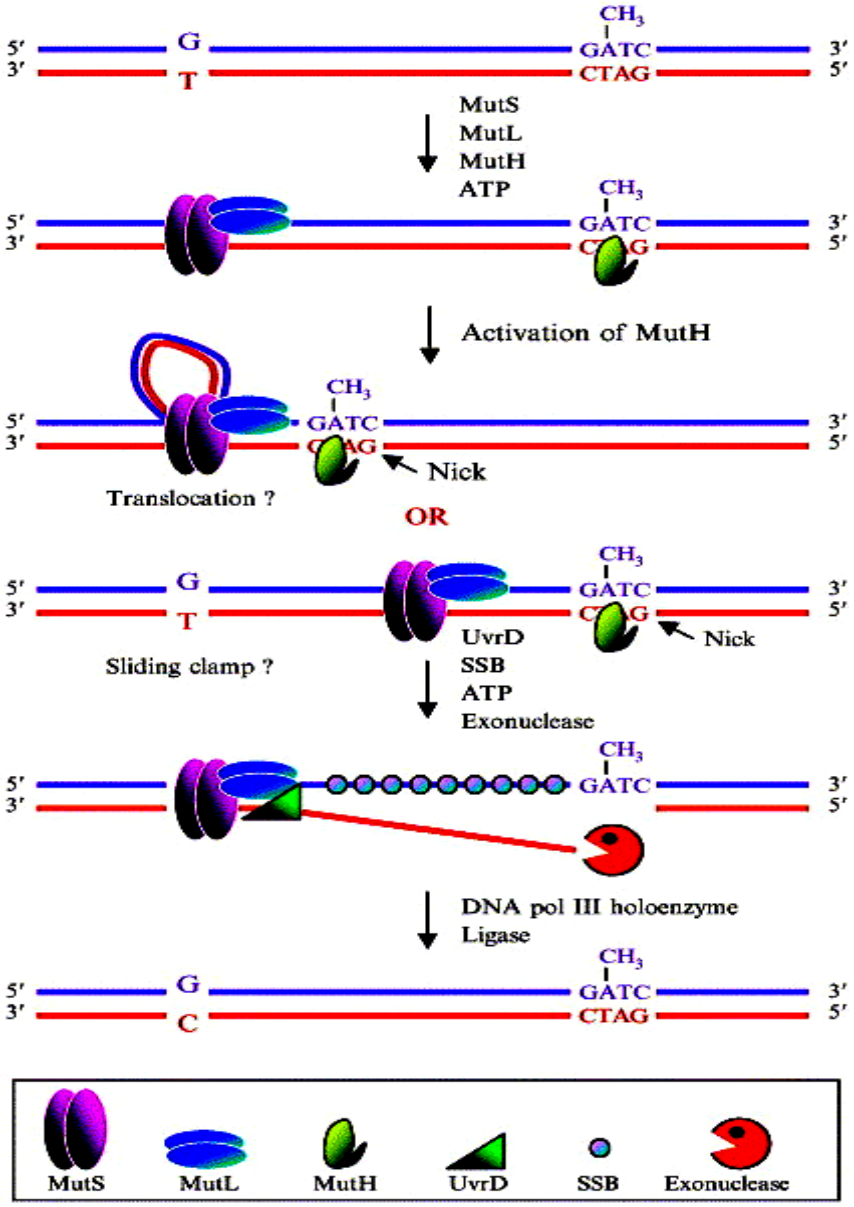


**Figure 1-9 Methyl-directed mismatch repair (MMR)**

A mispaired base in hemimethylated ($CH_3$) DNA is recognized by MutS, which then recruits MutL and MutH. MutH nicks the daughter strand at the hemimethylated GATC site followed by the helicase activity of UvrD helicase. DNA polymerase then re-synthesises the gap, which is further sealed by DNA ligase. Figure copied from (Joseph 2006).

### 1.4.6.2 Nick-directed MMR

In nick-directed MMR a strand discontinuity, rather than methylation, is used as a signal to direct MMR onto a specific strand. During DNA replication, strand breaks are present, either at the 3' end of the leading strand or at the 5' termini of okazaki fragments. This seems to prvide a signal for nick-directed MMR machinery to direct its activity onto the newly synthesized DNA strand (Kunkel 2005;Modrich 2006). The process is widely used by all eukaryotes and most prokaryotes that lack MutH, including several bacterial species.

The process is very similar in both prokaryotes and eukaryotes coding for nick-directed MMR. The only important difference between prokaryotes and eukaryotes is that MutS and MutL proteins used in prokaryotes work in the form of homodimers, like in prokaryotes featuring methyl-directed MMR, whereas in eukaryotes the related proteins act as heterodimers. In the absence of MutH, the endonuclease activity used in nick-directed MMR is accounted for by an endonuclease motif in the C-terminal of MutL that is not seen in MutL proteins in bacteria that use methyl-directed MMR. The same domain is found in MutL-related proteins in eukaryotes (Fukui 2008a). Thus, the molecular mechanism for nick-directed MMR is shared between eukaryotes and MutH-less bacteria. In the following text nick-directed MMR is used as a common term for eukaryotic organisms, and it is assumed to be the same for MutH-less bacteria, unless stated otherwise.

In eukaryotes, MutS homologues (named MSH), acting as heterodimers, compared with the MutS homodimers that acts in bacteria, bind to the DNA and identify mismatches on the nascent strand. Like in bacteria, MSH heterodimers then recruit MutL homologues (named MLH or PMS; post-meiotic segregation). As for MSH, MLH/PMS proteins act as heterodimers, distinct from bacterial MutL homodimers. The MSH-MLH/PMS protein complex then moves from the mismatch, away from the existing break (used as strand discrimination signal), and a nick is generated by the endonuclease activity of MLH1, rather than a MutH homologue, which is not present in eukaryotes. In this manner, the base mismatch is bracketed by an incision in the newly replicated DNA on either side. Helicases have not been reported in eukaryotic MMR so far. EXOI is the only exonuclease present in the system, which removes the error-containing strand (Dzantiev 2004;Fang 1993;Genschel 2002a), and the resulting gap is filled by DNA polymerase and sealed by DNA ligase.

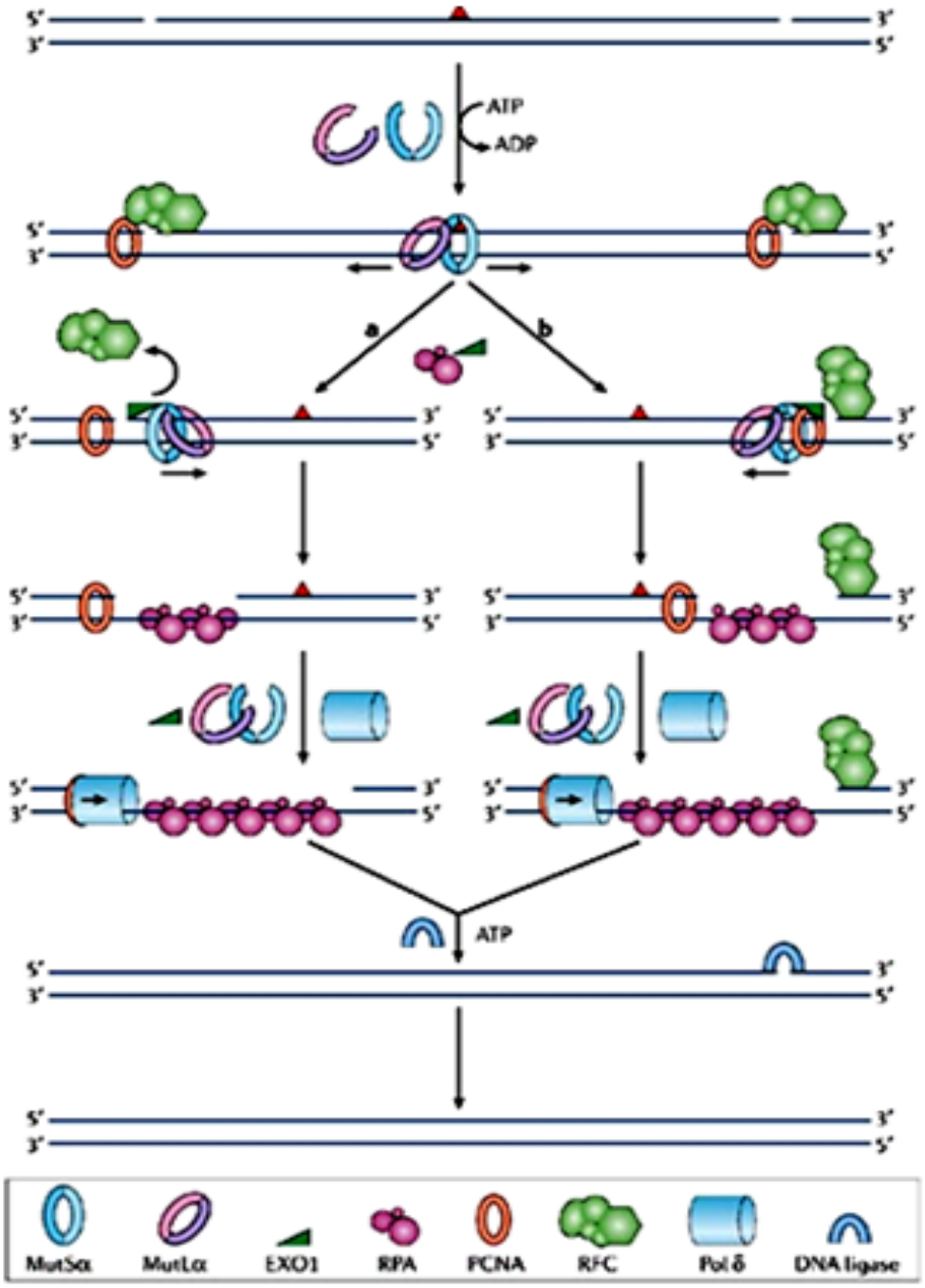


**Figure 1-10 Nick-directed mismatch repair (MMR)**

Pre-existing nicks serve as a point of entry for the MMR machinery to access DNA. Proliferating cellular nuclear antigen (PCNA) is loaded onto the 3' end of the strand break and Replication factor C (RFC) is loaded onto the 5' end. MutSα (aMSH heterodimer) is the first complex to be involved in the MMR reaction, recognising a mispaired base and then recruiting MutLα (an MLH/PMS heterodimer). From the mispaired base, the MutSα/MutLα complex moves away to catalyse repair. In 5'-3' directed MMR, RFC is displaced and EXO I removes the error-containing strand. In 3'-5' directed MMR, strand excision is facilitated by PCNA. In either case, single-stranded DNA is stabilized by RPA and the gap is resynthesized by DNA polymerase and sealed by DNA ligase. Figure copied from (Jiricny 2006).

### 1.4.6.3 Molecular insight into MMR

Given the relative complexity of MMR, several protein complexes and cofactors are involved. Of these, only MutS (MSH in eukaryotes), MutL (MLH/PMS in eukaryotes) and MutH are considered as the core components of MMR, with the rest of the factors involved accessory factors whose functions are not limited to MMR.

#### 1.4.6.3.1 Components of MMR

MMR is a highly conserved process in all prokaryotes and eukaryotes and, although slightly varying mechanisms are found (see above), the proteins involved share a high degree of homology. As mentioned previously, homologues of MutS and MutL in eukaryotes are termed MSH (MutS homologue) and MLH (MutL homologue) or PMS (post-meiotic segregation), respectively.

##### 1.4.6.3.1.1 MutS/MSH

This protein, also called the mismatch binding protein, is the first protein to bind to DNA and start the MMR reaction. By function, MutS is an ATPase that works in the form of a dimer. In bacteria MutS is a homodimer whereas in eukaryotes MSH proteins form a number of heterodimers (Figure 1-12) (Iyer 2006;Tachiki 2000;Takamatsu 1996). To date, seven MSH variants have been identified, MSH1 – MSH7. MSH1 was originally identified in *S. cerevisiae* as a functional homologue of MSH6 and is targeted to the mitochondrion, where it is involved in stability of the genome by counteracting instability induced by oxidation and promoting recombination (Kaniak 2009;Reenan 1992a;Reenan 1992b). MSH1 appears to have a limited phyletic distribution, being undetectable through sequence homology in vertebrates, insects, nematodes , or in *T. brucei* and related kinetoplastids. However, a more distant MutS-relative has been described in plants, corals and in *Toxoplasma* (Abdelnoor 2006;Garrison 2009) and shares the name MSH1, as it appears to perform similar functions. This unusual protein is a fusion of a MutS-like polypeptide to an endonuclease domain and, in plants, is targeted to both the mitochondrion and the plastid organelle, where it provides recombination and stress response functions. Of the remaining six MSH proteins, MSH2, MSH3, MSH6 and MSH7, which are homologues of MutSI in prokaryotes, have been shown to act in MMR (Eisen 1998;Johnson 1996;Marsischky 1996). In contrast, MSH4 and MSH5, homologues of MutSII in prokaryotes, appear always to be paired together in a heterodimers (Eisen 1998) and are involved in meiotic recombination (Hollingsworth 1995;Rossmacdonald 1994). To date, there has not been any

evidence of MSH4 and MSH5 being involved in repair. However, very recently MutSII in *Thermus thermophilus* has been shown to interact with MutS and MutL, and mutation of the *mutSII* gene resulted in increased mutagenesis after oxidative stress, though there is still no evidence that this is due to a role in MMR (Fukui 2011).

In most eukaryotes, MSH2 pairs with MSH3 or MSH6 to form two distinct heterodimers that act in MMR. In addition, in plants, a heterodimer forms between MSH2 and MSH7, which also is active in MMR (Culligan 2000). MSH2-MSH6 (MutSα) recognises 1-2 base mismatches and small IDLs of 1-3bp, whereas MSH2-MSH3 (MutSβ) recognises mismatches or IDLs of longer stretches of DNA (2-10 bp) (Acharya 1996;Genschel 1998;Habraken 1996). Thus, MutSα binds to mismatches preferentially compared with MutSβ, and this activity appears consistent with the fact that MSH6 levels are approximately 8-10 times higher than MSH3 (Drummond 1997;Genschel 1998;Iyer 2010), due to the greater abundance of simple mismatches. Plant MSH2-MSH7 (MSHγ) recognises almost the same DNA errors (single base mismatches) as recognised by MSH2-MSH6. However, for the systems where MSH7 is present, the two protein complexes were shown to have different binding affinities towards different base mismatches: whereas both MSH2-MSH6 and MSH2-MSH7 bind to G/T mismatches with equal efficiency, G/A,C/A,G/G and A/A are preferably recognised by MSH2-MSH7 whereas G/C and extranucleotide (+T) are preferred for MSH2-MSH6 binding (Culligan 2000;Wu 2003).

All MSH homologues share four conserved domains (Figure 1-13) (Bell et al. 2004;Obmolova 2000). Towards the C terminus of each is a helix-turn-helix motif, which is required for the dimerization of the proteins (Alani 1997;Lamers 2000;Obmolova 2000). Deletions or mutations in this region negatively affect ATP hydrolysis and cause loss of MMR activity, along with the loss of dimerization (Alani 1997;Aline 1985;Biswas 2001). Next to the helix-turn-helix motif is an ATP binding domain (Holland 1999), characteristic of the ABC ATPase superfamily and including Walker ATP binding motifs. Any mutation in this region does not affect the binding of protein to the DNA, but affects downstream processes (Alani 1997;Iaccarino 1998;Iaccarino 2000). The ATP domain also plays an important role in the conformational adaptations before and during MMR, including the translocation of the protein during the reaction (Blackwell 1998;Mendillo 2010). In the absence of DNA, the ATP binding domains of the two proteins that form the dimer are interlocked and clearly structured, whereas the rest of the protein appears less structured (Jiricny 2006). Although the two proteins of a dimer share sequence and structural homology, they have different affinity towards ADP and ATP binding (Antony

2003;Bjornson 2003;Martik 2004). Studies reveal that MSH6 has a high affinity towards ATP, whereas MSH2 binds preferentially to ADP. Thus, MutS dimers exist in ADP/ADP and ADP/ATP states, where ADP/ADP arises from hydrolysis of ATP at one of the subunits (Sixma 2001). States in which one or both of the ATP/ADP binding sites are empty are highly unstable.

A third conserved domain, towards the N terminus, is the middle domain (Obmolova 2000). Specific roles of this domain have not been described so far, but mutation in this region causes a loss of MMR activity (Wu 1994). At the N termini of MSH proteins that act in MMR is the mismatch binding domain (MBD), the fourth conserved region. This is the most conserved region in the proteins that form eukaryotic MutSα and MutSβ heterodimers, as well as in plant MSH7. The MBD is not conserved in MSH4 or MSH5 proteins in the eukaryotic MutSγ heterodimer, nor in MSH1 or in bacterial MutS II, providing the basis for the belief that these proteins are not involved in MMR. Within this domain is a highly conserved Phe-X-Glu motif (Malkov 1997) that is essential for the binding of MutS/MSH to the mismatch base and is present in MSH6 but not in MSH2 and MSH3 (Obmolova 2000). Alteration of either of these residues causes a dominant negative phenotype (Malkov 1997). The Glu amino acid residue forms a hydrogen bond with the N3 of mismatched pyrimidine, or N7 of mismatched purine (Natrajan 2003) and replacement of Glu with Aln or Gln results in loss of MMR activity. These data suggest that MSH6 is the key protein in the initiation of MMR on base mismatches, and it this part of the heterodimer, rather than MSH2, that is the recognition element. MSH3 shares some conserved residues with MSH6 around the Phe-X-Glu motif, but how MutSβ recognizes mismatches is still not resolved. In bacteria, although MutS is a homodimer and thus both the subunits share the same sequence, the protein acts as a functional and structural heterodimer, and only one of the two proteins binds to the DNA (Lamers 2000;Obmolova 2000;Warren 2007).

#### 1.4.6.3.1.2 MutL/MLH/PMS

MLH and PMS are the eukaryotic homologues of MutL proteins in the bacterial system (Figure 1-12). Like we see for MutS/MSH, bacterial MutL works as homodimer (Guarne 2004), whereas MLH and PMS proteins pair as heterodimers. These are termed MutLα (composed of MLH1-PMS2), MutLβ (MLH1-PMS1) (Raschle 1999), and MutLγ (MLH1-MLH3) (Harfe 2000a;Lipkin 2000;Nishant 2008). Of these three, MutLα is the most abundant in eukaryotic MMR and has been shown to widely interact with MutSα and

MutSβ. PMS2 of mammalian MutLβ is shown to be homologue of yeast PMS1, which does not code for PMS2. In mammalian systems, no role for MutLβ has been found in MMR. Also, in mammalian systems, the endonuclease activity of MutL homologues is present in PMS2 and MLH3 and has not been found in PMS1 (Cannavo 2007). MutLγ is also involved in MMR but is present in exceptionally low levels. Indeed, MutLγ is mainly involved in meiotic recombination and appears to work in MMR as a backup system (Cannavo 2007;Chen 2005;Wang 1999). In yeast a further homologue of MutL, MLH2, is found which pairs with MLH1 to form a MLH1-MLH2 heterodimer. *MLH2* mutants are shown to be resistant to DNA damaging agents like as cisplatin, and Wang et al have shown a role in correcting mismatches generated during meiotic recombination (Wang 1999).

Functionally, MutL (Figure 1-14) belongs to the GHKL (Gyrase,Hsp90,Histidine –Kinase, MutL) ATPase family, containing a conserved ATPase domain located at N terminus of the protein (Ban 1999;Dutta 2000), which is conserved in all the eukaryotic MLH and PMS homologues (see Figure 1-14). This domain plays an important role in conformation and regulation of the non-specific endonuclease activity that is found in MutL homologues from bacteria that lack MutH, and in some of the eukaryotic MutL homologues, including PMS2 and MLH3 in humans. This activity is found in a domain towards the C-termini of the protein and consists of a DQHA(X)2E(X)4E endonuclease motif associated with 2-4 smaller, more C-terminal motifs. Together, these motifs interact in the MutL 3D structure and form a $Zn^{++}$ ion binding catalytic site (Fukui 2008b;Kosinski 2008). If ATP is bound to the N terminal domain, the protein's conformation becomes more condensed and the nuclease activity of MutL is largely reduced (Fukui 2008b;Kadyrov 2006). Indeed, some work has suggested that ATP is only hydrolysed when the MutL heterodimers bind to the MutS heterodimers, accounting for the specific role of the endonuclease activity during MMR. However, ATP regulation may also depend on the concentration of MutL present in the system. At relatively high concentrations of MutL, and in the absence of MutS-mismatch complex, ATP stimulates rather than suppress the endonuclease activity of MLH1 (Mauris 2009).

The C termini of MutL homologue proteins contain, in addition to the endonuclease domain, a dimerization domain that shows relatively low levels of sequence homology but is conserved in both prokaryotes and eukaryotes (Lipkin 2000;Pang 1997). However, eukaryotic MLH homologues contain a relatively big interlink domain between C and N termini. In addition, MLH1 homologues specifically contain an additional conserved

domain at the extreme C-termini termed the carboxy terminal motif (Pang 1997). The exact role of this part of the protein has not been elucidated so far but deletion mutation in this region results in loss of MMR (Pang 1997).

#### 1.4.6.3.1.3 Accessory proteins

Further factors that are vital for successful MMR include replication factor C (RFC), proliferating cell nuclear antigen (PCNA), exonuclease I (EXOI), and replication protein A (RPA) (Genschel 2002b). RFC is a protein that is essential for loading PCNA onto the nicked strand, but no direct role of RFC in MMR has been demonstrated. On a pre-existing break, RFC loads PCNA at the 3' end of the break, while RFC itself is loaded onto the 5' end and is displaced by EXOI in 5' nicked MMR (Jiricny 2006).

PCNA is a ring shaped trimeric protein and coordinates different proteins in downstream reaction steps during MMR (Jonsson 1997;Kelman 1997;Warbrick 2000). PCNA is also important because MSH3 and MSH6 have specific PCNA binding domains (Kleczkowska 2001), and co-localize with PCNA during MMR (Kleczkowska 2001). Although PCNA is not required to load MSH/MutS onto DNA, but cannot execute endonuclease activity in the downstream event. It has been shown that PCNA is required not only to mediate the interaction between different proteins involved in MMR, but also between MMR, replication machinery and DNA. This providing an important role in strand discrimination (Maga 2003). Consistent with the information, it was observed that addition of PCNA to the complex consisting of MutSα, MutLα, ATP and mismatch containing DNA strand, results in the dislocation of MMR machinery away from the mismatch to recruit downstream factors (Bowers 2001)(see below). PCNA is also important in the 3'-5' exonuclease activity carried out by EXOI, since 3' directed MMR is completely abolished in the absence of PCNA, whereas in 5' directed MMR only 40-50% MMR activity is lost (Genschel 2003;Guo 2004;Jiricny 2006). EXOI is the only exonuclease present in MutH-less organisms with preferred 5'-3' activity (Genschel 2006;Kadyrov 2006). In *E. coli* and related organisms, exonuclease activity is carried out by EXOI (3'-5') and RecJ (5'-3') (Shimada 2010). RPA is an accessory protein in MMR that holds two very important functions. Firstly, it ensures that EXOI is removed from the system shortly after the mismatched base is removed from the duplex (Genschel 2009). Secondly, it also serves to stabilize the single stranded DNA until the new strand is synthesized by DNA polymerase (Jiricny 2006).

#### 1.4.6.3.2 MMR pathway: The molecular process

In the discussion below, MutS and homologues will simply be referred to as MutS, while MutL and homologues will be referred to as MutL, on the basis that the activities of the proteins are likely to be conserved. The process of MMR starts with binding of MutS to the DNA through a pre-existing break that could be either 3' or 5' to the mismatch (Harfe 2000b;Schofield 2001). If the protein binds to 5' nicked DNA, it first encounters RFC, which is displaced by MutS. In 3' directed MMR, MutS encounters PCNA (Jiricny 2006). As discussed earlier, MutS is an ATPase whose conformation and function are largely dependent on ATP binding. In the absence of DNA, the protein is highly unstructured. When MutS makes contact with DNA, ADP is exchanged with ATP. Upon ATP binding the protein changes conformation and wraps itself around the DNA, forming a sliding clamp (Jiricny 2000). ATP binding is also important because ATP-bound MutS has low affinity towards DNA, which helps in the translocation of MutS. Studies in *E. coli* show that when the MutS clamp passes through the DNA it bends the molecule by $60^{0}$ (Jiricny 2006;Kunkel 2005). However, when MutS encounters a mismatch, the DNA is bent and then unbent again (Wang 2003). At this conformation, the mismatched base flips out of the DNA helix, making a close interaction with the Phe-X-Glu residues in the protein (Wang 2003). This protein-DNA complex then recruits MutL. This binding hydrolyses ATP on MutL to ADP, activating the endonuclease activity (Kadyrov 2006;Kadyrov 2007). In *E. coli* and related gram negative organisms, which process methyl directed MMR, MutH is recruited to carry out the endonuclease activity which incises at hemimethylated GATC site. This hydrolysis of ATP dissociates the MutS-MutL ternary complex from the mismatch and perhaps forms a distinct sliding clamp that can travel along the DNA (Jiricny 2006).

Different models have been described to explain the activity of this MutS-MutL protein-protein complex after ATP hydrolysis by MutL in eukaryotes and Mut- less bacteria, and the recruitment of MutH in bacteria with methyl directed MMR. The "stationary" or "trans" model suggests that MutS-MutL remains at the site of a mismatch and a distal region of DNA is looped out to interact with MLH/MutH to create a nick (Jiricny 2006;Kunkel 2005). Although *in vivo* the *E. coli* MMR machinery can be seen to be moving (see below), this stationary model is supported by the observation that DNA can be incised at the distal end even if there is a physical barrier between the mismatch and excision initiation sites (Junop 2001). Another model is called the "cis" or "moving" model in which the clamp leaves the mismatch and travels along the DNA. Two explanations

have been presented so far regarding this model. A molecular switch model suggests that several MutS-ADP molecules are loaded onto DNA and move bidirectionally; when one encounters a mismatch, it exchanges ADP for ATP, moves away from the mismatch in the direction opposite to the pre-existing break and the MutS-ATP then recruits MutL and carries out the repair process (Fishel 1998;Gradia 1997;Gradia 1999;Jiang 2005). The active translocation model suggests the binding of a specific MutS at the mismatch, which recruits MutL and this MutS-MutL complex then slides away from the mismatch to initiate the downstream processes (Allen 1997;Blackwell 1998;Martik 2004).

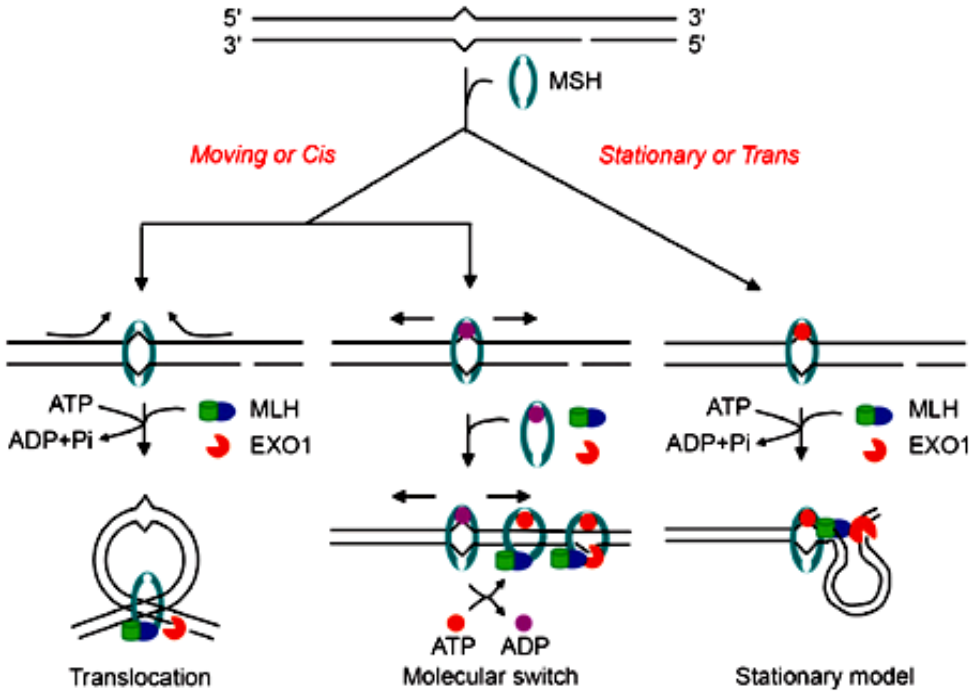


**Figure 1-11 Different models of MutS-MutL activity during MMR .**

After the initial recognition of a mismatch by MutS/MSH, MutL/MLH is recruited for its endonuclease activity. In the stationary/trans model, MutS/MSH-ATP recruits MutL/MLH at the site of the mismatch. A part of the DNA is bent to bring it closer to MutL/MLH, forming a loop and a second nick is generated by the MutL/MLH endonuclease activity. In the moving/cis model, MutS/MSH moves away from the site of the mismatch after initial recognition, and the endonuclease activity of MLH is employed out when the MutS/MSH-MutL-MLH protein-protein complex moves or forms at a distal end. Two explanations have been proposed for this. In the translocation model, ATP is hydrolysed at the site of MutS/MSH loading, which drives a MutS/MSH-MutL/MLH complex away from the mismatch (in direction opposite to a prexisting break) and a second nick is generated. In the molecular switch model, several MutS/MSH-ADP complexes are loaded onto the DNA and the one that encounters the DNA hydrolyses ADP to ATP. This slides the protein complex from the mismatch, at which point it recruits MutL/MLH and a second nick is produced. Figure copied from (Li 2008a).

Irrespective of the precise details of MutS and MutL mobility, in *E. coli* and several other bacteria MutH is responsible for incising the DNA at a semi-defined site away from the mismatch, while in eukaryotes and in bacteria lacking MutH MutL itself performs this

catalytic step. The mismatch is thus bracketed by a strand break at either side (Plotz 2006;Pluciennik 2010), and an exonuclease is then recruited. Several exonucleases are involved in bacterial MMR (Shimada 2010), whereas in eukaryotic MMR EXOI is the only exonuclease implicated so far (Jiricny 2006). EXOI activity is affected by MutS binding and the position of pre-existing strand break. For 5' nick-directed MMR, MutL incises at the 3' end (Pluciennik 2010). EXOI then enters the reaction at the 5' end, displacing RFC and removing the error-containing strand in 5'-3' direction until it reaches the second break at the 3' end (Genschel 2002;Kenji Fukui 2010). EXOI activity can also be seen when MutL is not present; here, EXOI digests the DNA in 5'-3' direction but in this case its activity is regulated by RPA, which ensures that EXOI is removed from the system shortly after the removal of the mismatched base (Genschel 2003;Genschel 2009). For 3' nick-directed MMR, MutL nicks the DNA 5' to the mismatched base. For such a reaction, EXOI can enter into the reaction through the nick generated by MutL and catalyze the reaction in a 5'-3' direction (Dzantiev 2004). However, though EXOI prefers 5'-3' exonuclease activity, it has been shown to be involved in 3'-5' reactions as well (Fang 1993). This activity is more complex and requires PCNA and RFC to trigger the reaction (Jiricny 2006). Downstream reactions are similar following both exonuclease reactions, and single-stranded DNA is stabilized by RPA and the excised strand is re-synthesized by DNA polymerase, allowing DNA replication to continue.

From the above, it is clear that the MMR machinery is very well characterized and extensive molecular details are known, from different model organisms, regarding the MMR reaction. However, there remain areas in which either little or nothing is known. For instance, no helicase has been reported in eukaryotic MMR. It could be that cells possess several helicases and MMR can use these non-specifically for its activity, or EXOI might bind to double-stranded DNA and possess helicase activity (Song 2010). Little work has characterised whether the proteins involved in MMR are subject to modifications that might affect their activity during the reaction, as is common in homologous recombination (see below). More broadly, though MMR is well known to repair base mismatches that arise during nuclear DNA replication, increasing evidence suggests that it has more broad roles, including sensing and responding to some damage (Campos 2011) and promoting genome rearrangements, such as during immune gene development (Chahwan 2011) or in triplet repeat instability in certain genetic conditions (Bourn 2009). How MMR acts in these processes is still being detailed. Finally, the potential role of MMR in mitochondrial DNA still needs detailing (Liu 2010). Do mitochondria possess their own repair machinery

that can conduct MMR, or can MMR components shuffle between the nucleus and mitochondria when needed?

### 1.4.6.4 Mismatch repair in *T. brucei*

Mismatch repair in *T. brucei* appears to follow all the rules of nick-directed MMR. Most, though not all, of the proteins identified as a part of eukaryotic MMR have been identified in *T. brucei* and related kinetoplastids (Figure 1-12). MSH2, MSH3 and MSH6 (originally termed as MSH8, due to its relatively truncated N-terminal, as discussed below) have each been identified as MutS homologues and implicated in MMR. In contrast, MLH1 and PMS1 are the only MutL homologues annotated so far as part of *T .brucei* MMR system. MSH4 and MSH5 are also present in *T. brucei* but their roles have not yet been characterized; though it might be presumed that they are involved in meiotic recombination, as in other eukaryotes.

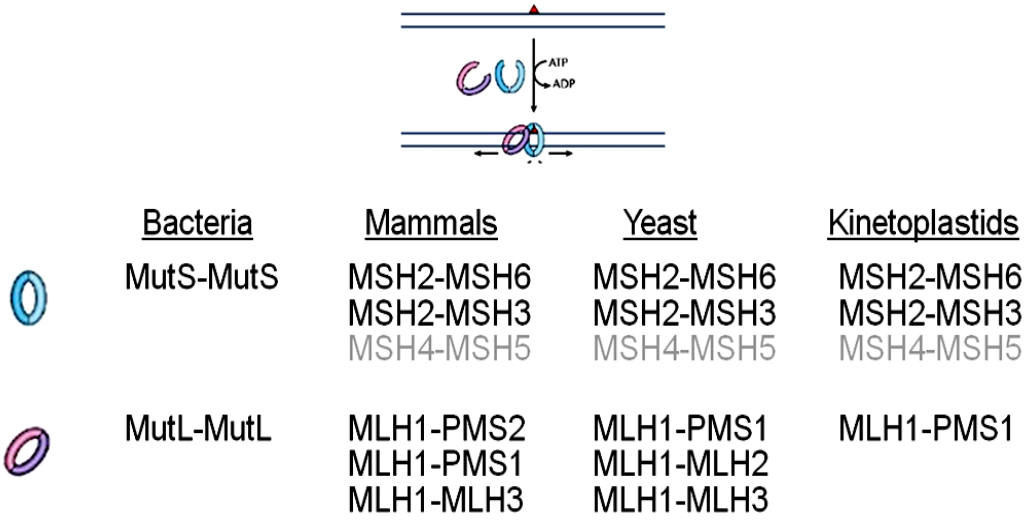


**Figure 1-12 Profile of MMR proteins present in various systems**

MMR proteins are present in bacteria in the form of homodimers of MutS and MutL. In eukaryotes, as represented here by yeast, mammals and kinetoplastids, MMR proteins work in the form of heterodimers. MSH (MutS homologue) heterodiemrs conserved in all the three systems are MSH2-MSH6 and MSH2-MSH3. MSH4-MSH5 has also been reported as a part of MutS family but their role is more pronounced during meiotic recombination. ThreeMLH (MutL homologue) heterodimers are conserved in mammals: MLH1-PMS1, MLH1-PMS2 and MLH1-MLH3. In yeast MLH heterodimers involved in MMR are MLH1-PMS1, MLH1-MLH2, MLH1-MLH3, whereas in kinetoplastids only one MLH heterodimer has been reported so far: MLH1-PMS1.

*T. brucei* MutS MMR homologues have all the four conserved domains identified in MutS homologues that are required for MMR activity (Bell, Harvey, Sims, & McCulloch 2004). Most variation is seen at the N-termini, within and around the MBD (mismatch binding domain) of MSH proteins. MSH6 from *T. brucei* is well conserved at its N-terminus, with

all the four important residues (Obmolova 2000) required for binding to mismatches and anchoring the protein onto the DNA, indicating the role of this protein in *T. brucei* MMR. However, despite being conserved at the mismatch binding residues, MSH6 from *T. brucei* has a truncated N-terminus (363 residues shorter as compared to *H. sapiens*). For this reason it was originally termed MSH8, as MSH7 proteins also have truncated N-termini with conserved MBDs. Moreover, the *T. brucei* genome had not been sequenced at that moment. However, since the completion of the sequencing of the T. brucei genome revealed no further MutS-like proteins and phylogenetic analysis shows that *T. brucei* MSH8 is most closely related to eukaryotic MSH6; it will be referred to here as MSH6. *T. brucei* MSH3 is shown to be partly conserved at the MBD with residues for anchoring the protein to DNA, but it does not have the residues for binding to mispaired sites. Although MSH3 is also truncated at its N-terminus, it pairs well with the rest of eukaryotic MSH3 proteins. *T. brucei* MSH2 is the least conserved within the mismatch interacting domain. consistent with the suggestion that eukaryotic MSH2 mainly coordinates downstream MMR processes and does not determine DNA binding. The *T. brucei* sequencing project identified MSH4 and MSH5 homologues (Berriman 2005). Multiple sequence alignments of these proteins have revealed that they lack N-terminal MBD domains and roles of these proteins have yet been described in MMR (Barnes 2006). No homologues of MSH1 have been identified in *T. brucei.*

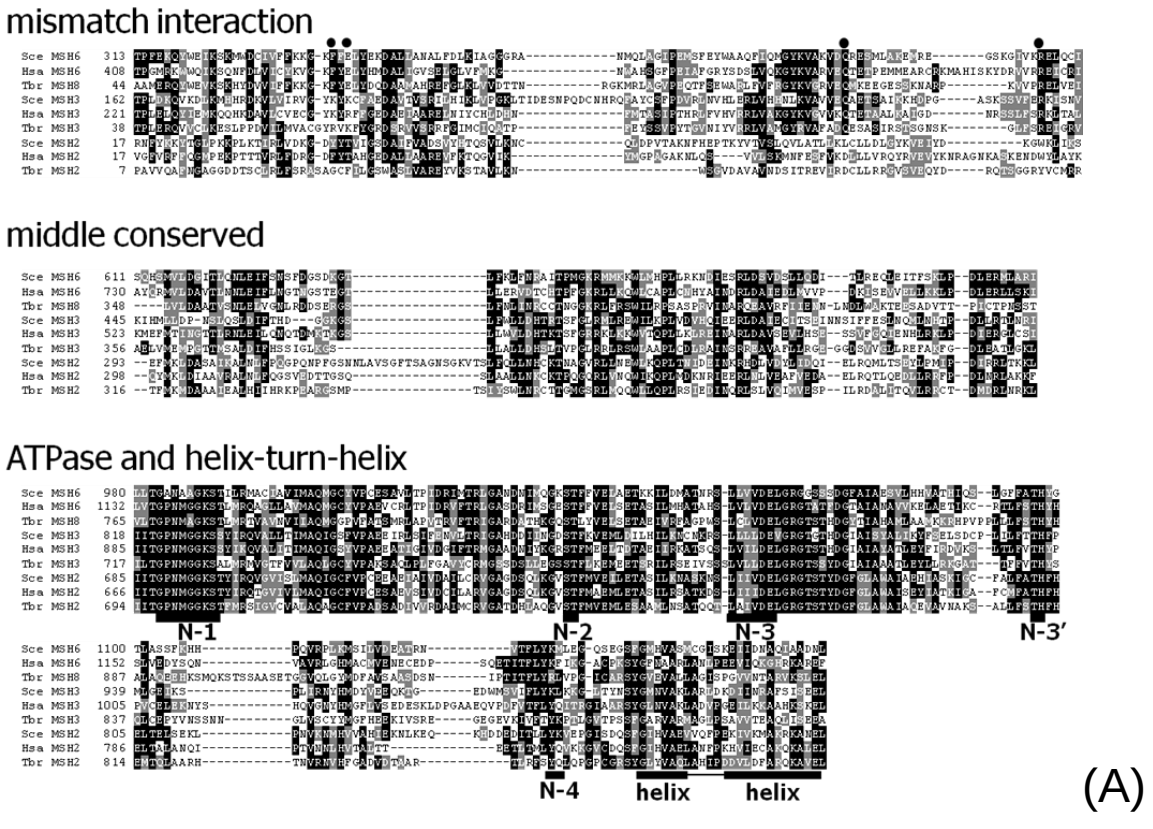


(A)

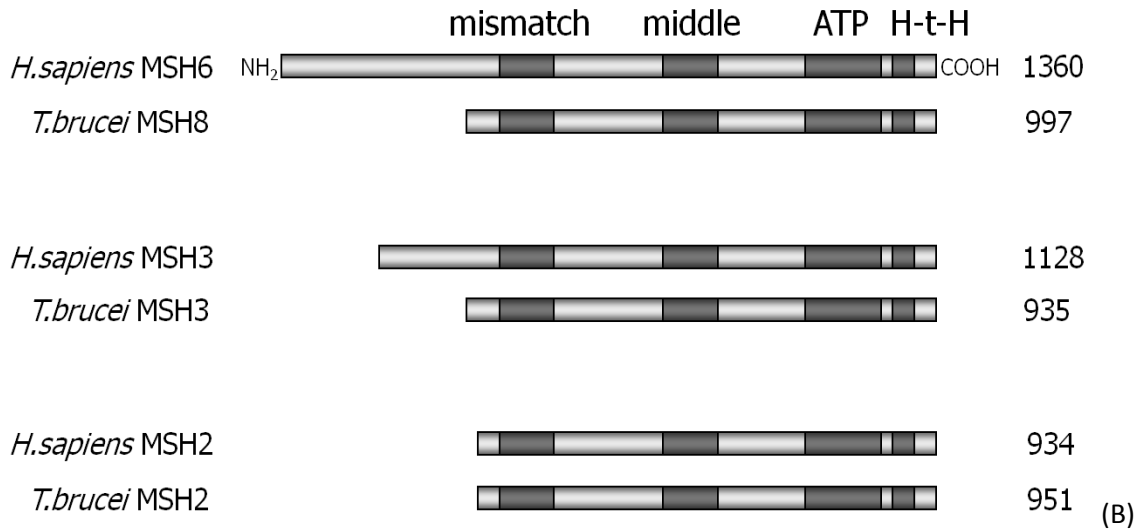


**Figure 1-13 Amino acid sequence alignment of *T. brucei* (Tbr) MSH proteins involved in MMR with homologues from *H. sapiens* (Hsa) and *S. cerevisiae* (Sce).**

(A) Residues that are identical in at least 30 % of protein sequences are shown in black, whereas residues that are conserved in at least 30% of protein are shown in grey. Circles in the mismatch binding domain refer to mismatch interaction and DNA binding residues, as described by (Obmolova 2000) in *Thermus aquatics*. Two helices and the turn forming the helix-turn-helix motif are labelled as two thick lines and a thin line, respectively. N1-N4 are the domains involved in ATPase activity. (B) Schematic representation of three MSH proteins involved in *T. brucei* MMR in comparison with *H. sapiens.* The respective sizes of the proteins are shown. Figure adapted from (Bell, Harvey, Sims, & McCulloch 2004).

Since only two MutL homologues have been identified in *T. brucei,* it is possible that MMR displays lesser complexity at later steps, though this has not been examined experimentally. PMS1 is the subunit of MutLα that has the endonuclease activity present at its C-terminal, and groups well with PMS1 from *S. cerevisiae* and PMS2 from *H. sapiens*. MLH1 has an additional extended conserved C-terminal domain, termed the carboxy C-terminal homology motif. No homologues of MLH2 and/or MLH3 of yeast and human origin have been found in *T. brucei*.

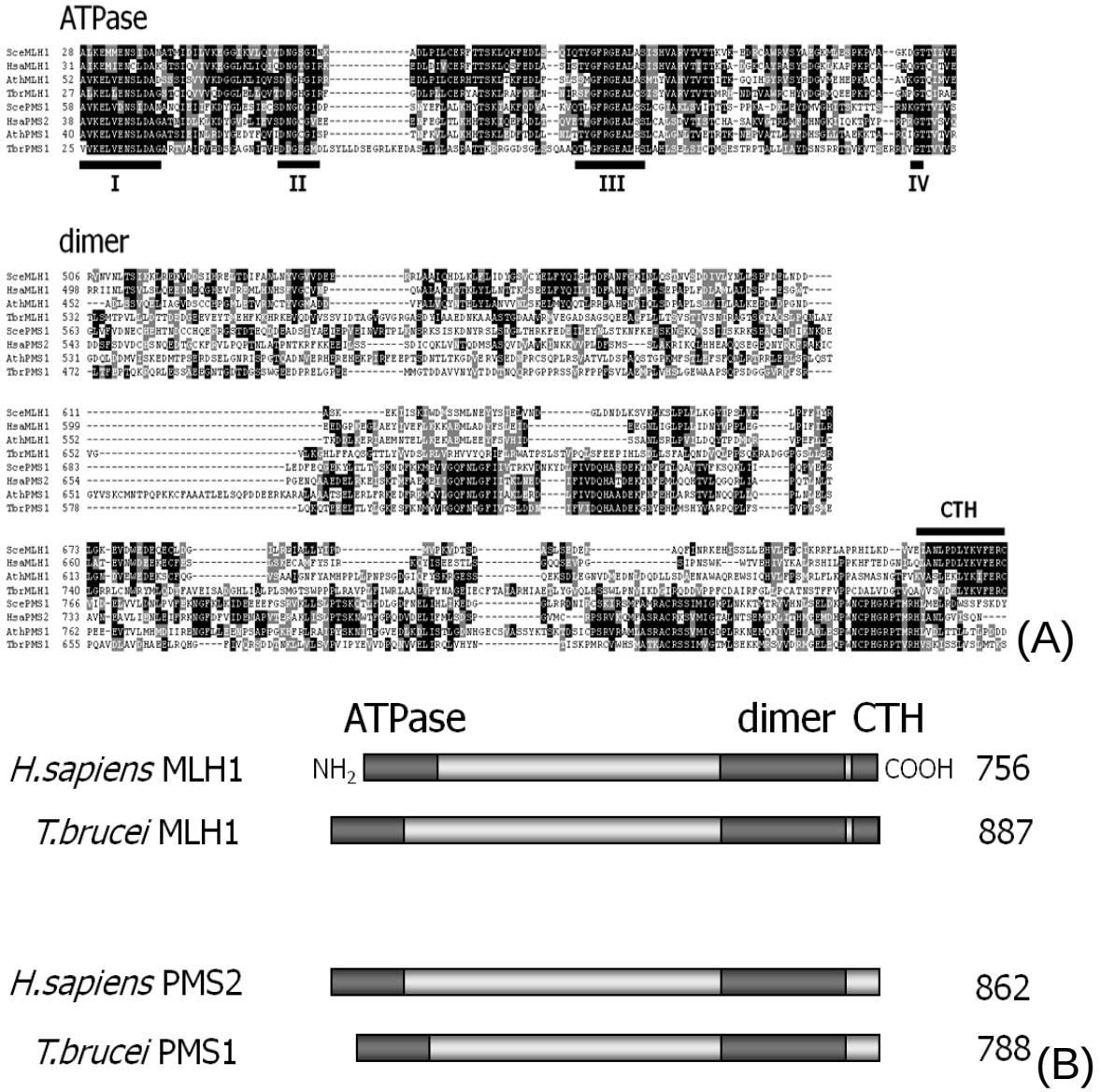


**Figure 1-14 Amino acid sequence alignment of *T. brucei* (Tbr) MLH proteins, involved in MMR, with *H. sapiens* (Has). *A. thaliana* (Ath) and *S. cerevisea* (Sce).**

(A)Residues that are identical in at least 30 % of protein sequences are shown in black where as residues that are conserved in at least 30% of protein are shown in grey. The underlined residues in ATPase domain are the ones required for ATP binding and hydrolysis where as CTH corresponds to carboxy terminal homology motif conserved in MLH1. (B) Schematic representation of two MLH proteins involved in *T. brucei* MMR in comparison with *H. sapiens.* Respective sizes of the proteins from two homologues are shown. Figure adapted from (Bell, Harvey, Sims, & McCulloch 2004).

Of the five genes predicted to be involved in *T. brucei* MMR, only *MSH2* and *MLH1* have been genetically characterized, and only in bloodstream form (BSF) parasites. Deletion of each of these genes to generate null mutants involved two rounds of gene deletion. During the study it was found that generation of heterozygous mutants for either of these genes do not show any phenotype of impaired MMR. Generation of null mutants for either of these genes showed no growth defect as compared with wild type BSF *T. brucei*. MMR null mutants were tested for resistance to alkylation damage in the presence of increasing

concentrations of MNNG (*N*-methyl-*N'*-nitro-*N*-nitrosoguanidine), and microsatellite instability was used as a indicator of loss of replication proofreading, each markers of MMR activity. Loss of MMR activity has been shown to confer tolerance to alkylation damage. Alkylating agents such as MNNG introduce a methyl group at the $6^{th}$ carbon of guanine, forming $O^6$ methylguanine. As described in Section 3.2.2.2, this mutated base has a tendency to base pair with thymine, thus creating a mismatch, which if left uncorrected results in GC-TA transition mutation (Griffin 1994). Since MMR can only correct the base mismatches by removing the newly incorporated base in the daughter strand, it removes thymine from the daughter strand, leaving the lesion in the template strand. DNA polymerase then incorporates a thymine opposite the methylated guanine and the process is repeated, eventually leading to persistent strand breaks. As in other eukaryotes, BSF *T. brucei msh2* and *mlh1* null mutants were found to display increased tolerance to MNNG (Bell, Harvey, Sims, & McCulloch 2004). Microsatellites are repetitive stretches of DNA that are prone to replicative slippage by forming IDLs (Sia 1997). This base slippage is recognized by the MMR machinery (Buermeyer 1999). Depending on the size of the loop, MutSα or MutSβ recognize the error (see section 1.4.6.3.1.1) and carry out the MMR repair process. In the absence of functional MMR, IDLs are left unrepaired and differences is the size of microsatellites can be observed by PCR-amplifying a specific microsatellite and comparing the sizes with respect to MMR proficient cells. Microsatellite instability in MMR-deficient *T. brucei* BSF mutants was analysed by cloning wild type, heterozygous and homozygous cells and, in 10 independent subclones, and PCR-amplifying a number of microsatellite loci (Bell, Harvey, Sims, & McCulloch 2004). It was observed that *msh2* and *mlh1*null mutants showed increased microsatellite instability of nearly all such loci (Bell, Harvey, Sims, & McCulloch 2004).

More recently, the contribution of MMR to the repair of oxidative damage has been examined. When cultured in the presence of increasing concentration of $H_2O_2$, only *msh2* null mutants were shown to be sensitive to oxidative damage, whereas *mlh1* mutants did not show any difference in phenotype when compared with MMR-proficient cells (Machado-Silva 2008). Damage caused by oxidative stress and the role of MMR in repair of oxidative damage is explained further in Section 1.4.7.

Finally, a role of MMR is also observed during *T. brucei* homologous recombination. Mismatches can arise during recombination of non-identical DNA strands. Such mismatches are recognized by MMR, which either corrects the base mismatch or might terminate the recombination process (Harfe 2000b). It was shown by J.S.Bell (Bell 2003)

that MMR-proficient cells have less transformation efficiency in constructs in which the sequences for genome targeting are less than 100% identical, and that this is alleviated in *msh2* null mutants, which showed relatively increased transformation efficiency. A role of MMR in homologous recombination was also shown in relation to the length and percentage homology of the strands involved in recombination (Barnes 2007). It has been documented that for sequences that are 100% identical both MMR-deficient and -proficient cells have similar recombination efficiency for constructs with targeting sequences that are up to 200 base pairs in length. However, for sequence lengths of 450 bp, *msh2* null mutants had a higher recombination efficiency compared with wild type and heterozygous mutants. Although these data confirm the role of MMR in homologous recombination, impaired MMR had no effect on VSG switching (Bell 2003). As detailed in Section 1.2.2.3.2, VSG switching by HR is a major source of antigenic variation, and the lack of involvement of MMR in this reaction remains unexplained.

### 1.4.7 Oxidative stress

In the sections above I have discussed the types of DNA damage caused by various exogenous and endogenous sources and the different mechanisms that cells possess to repair such damage. In this, I have emphasized that specific types of repair pathways are used to react to specific sorts of damage. However, this is not always the case. In certain instances, functional overlap can be seen between different pathways of repair and certain types of damage; for example, methylation damage can be repaired by direct repair and NER together or independently depending on the type of lesion (Mazon 2010). Similar to that, human cells defective in TCR-NER have been shown to lack the ability to remove the lesions caused by oxidative stress (Tuo 2003). This shows that, although BER and NER are independent pathways, they work in conjunction with each other at certain points (Scharer 2003). This has been further observed in yeast where MMR and NER have been shown to interact with each other in msh3 msh6 and mlh1 pms1 double mutants (Bertrand 1998). Here, I will discuss oxidative stress, which is an important damage that all cells face and provides a strong example of multiple mechanisms involved in repair, some overlapping. In addition, this type of damage and the contribution made to its repair by MMR is one aspect of study in this thesis.

Oxidative stress is a condition in which the levels of reactive oxygen species (ROS) in a cell require increases in the levels of cellular defence and repair mechanisms (Klaunig 1998). ROS are continuously produced by both intracellular and extracellular sources and

are the most predominant source of cellular damage, including to DNA (see below). ROS include superoxide ($O_2^-$), hydrogen peroxide ($H_2O_2$), hydroxyl radical ($OH^-$) and nascent oxygen ($O^-$). ROS are constantly produced during several metabolic processes, such as substrate level phosphorylation, oxidative phosphorylation and ATP production by the electron transport chain. In fact, ATP production by the electron transport chain is one of the major sources of ROS production that causes oxidative damage to mitochondrial DNA, resulting in various sorts of DNA lesions like oxidized bases, abasic sites and strand breaks. During mitochondrial respiration, 1-5% of oxygen is converted to $O_2^-$, which is then converted to $H_2O_2$ (Moller 2001) $H_2O_2$ can either be converted to $H_2O$ by catalase or, in presence of metal ions ($Fe^{+2}$, $Cu^{+2}$), it is reduced to highly reactive hydroxyl radicals (Moller 2001).

ROS damage a range of macromolecules, including proteins, lipids and nucleic acids. In lipids, unsaturated fatty acids are oxidized to lipid hydroperoxides, which are further reduced to non-reactive fatty acid alcohols or react with metals to form aldehydes. These aldehydes can then go on to damage DNA by forming different exocyclic adducts. One of these is ethano adducts that modify bases, such as ethanodeoxyadenosine. These modified bases are prone to base mismatches and give rise to transition mutations (De Bont 2004). ROS can also directly damage DNA, causing different sorts of DNA lesions (Esterbauer 1990), which are discussed below

#### 1.4.7.1 Oxidative DNA damage

Despite robust cellular defense and repair mechanisms, ROS account for $10^4$ DNA lesions/cell/day (Fraga 1990). In DNA, nucleotides are the prime subject of damage by oxidation, either due to damage to dNTPs in the nucleotide pool or within the DNA duplex. Approximately 20 different types of damage have been identified in response to oxidative stress (Slupphaug 2003); some of these that affect the bases within nucleotides are shown in Figure 1-15.

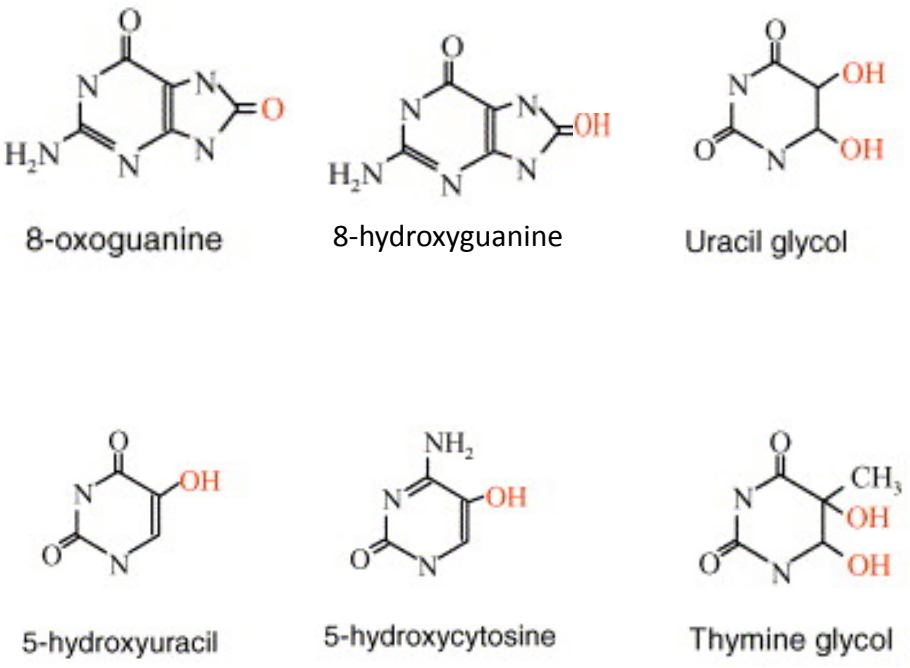


**Figure 1-15 Altered bases formed by reactive oxygen species (ROS).**

ROS react with a range of molecules to induce $O^-$ or $OH^-$ to generate base lesions. Altered bases are labeled respectively and reactive radicals responsible for the modification are indicated in red. Figure adapted from (De Bont 2004;Slupphaug 2003).

In pyrimidines, the 5, 6 double-bond is most vulnerable to oxidative damage. The most commonly oxidized pyrimidine variant is thymine glycol, which is formed indirectly by reactions with oxygen radicals. Reactive oxygen molecules first react with 5-methyl cytosine (5 meC) and oxidize the 5, 6 double bond. This forms an intermediate product, 5 meC glycol. This then deaminates to form thymine glycol. This adduct basepairs with A and cause GC-AT transition. Oxidation of 5 meC is a particular problem in organisms in which gene expression is regulated by 5 meC, causing elevated mutations in these loci (Slupphaug 2003). However, thymine glycol is a weak mutagen and when incorporated in the DNA helix blocks transcription (De Bont 2004).

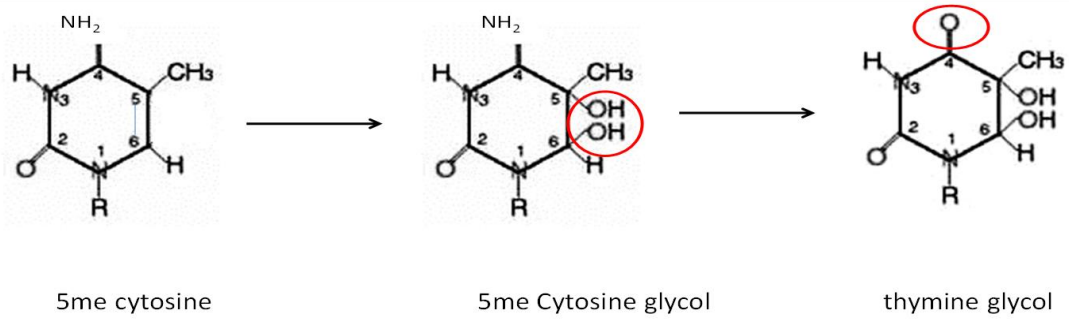


**Figure 1-16 Oxidation of 5 methyl (5me) cytosine.**

ROS oxidize the 5,6 double bond in 5me Cytosine and form 5me Cytosine glycol, which then further deaminates to form thymine glycol. Figure adapted from (Marnett 2001).

In purines, the most prevalent oxidized molecule is 8oxoguanine (8-oxoG), which is also the most stable oxidized molecule in the cell (Slupphaug, Kavli, & Krokan 2003). Of the reactive molecules, both $OH^-$ and $O^-$ react with $8^{th}$ carbon of guanine to form 8-hydroxyguanine and 8-oxoguanine. 8-oxoguanine can also be formed from 8-hydroxyguanine by the subsequent loss of an electron ($e^-$) and a proton ($H^+$).

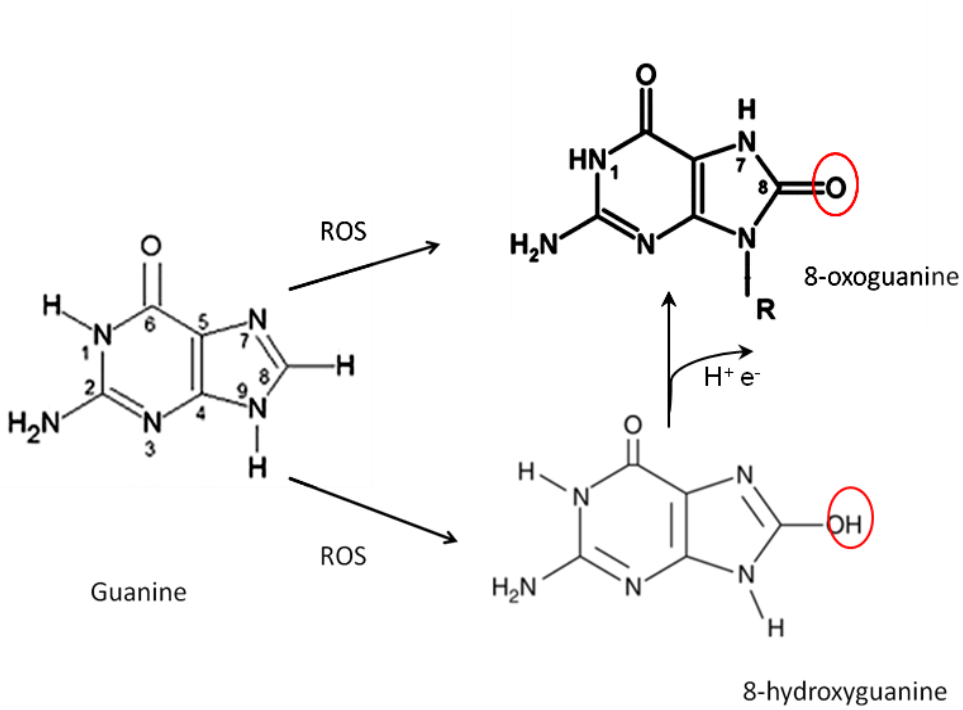


**Figure 1-17 Oxidative lesions of Guanine.**

$OH^-$ or $O^-$ (both types of reactive oxygen species; ROS) oxidize the $8^{th}$ carbon of Guanine to form either 8-oxoguanine or 8-hydroxyguanine.

8-oxoG is identical to guanine (G) in terms of base pairing in the anti conformation, forming a pair with cytosine (C). However, 8-oxoG can also rotate around its glycosidic bond (syn conformation) and base pair with both adenine (A) and cytosine (C) (Shibutani 1991). Thus, if G is oxidized in the template, DNA polymerase can incorporate A opposite to 8-oxoG, thus inducing a mutation in the genome. G oxidized in the dNTP pool can also be incorporated by DNA polymerase and again paired against A. In both the cases, GC-TA transversions are caused (Moriya 1993;Shibutani 1991;Wood 1990).

### 1.4.7.2 Repair of Oxidative damage

Since oxidative damage is one of the most predominant types of damage afflicting the cell, several routes of repair have evolved, which can work synchronously. Most of the damage is repaired before replication to avoid mutations being transmitted to progeny cells. However, if oxidative damage bypasses check points and is not corrected during DNA replication by the proofreading activity of replicative DNA polymerases, it can be repaired during the post replicative (G2) phase of the cell cycle. Here, the rate of repair of purine lesions is slower than pyrimidine lesions (Jaruga 1996). The repair systems involved are those discussed above (including BER and MMR), but here I highlight their specific modes of action in response to oxidative DNA damage, and discuss the mechanisms used for the protection, repair or bypass of such lesions.

Superoxide dismutase (SOD) serves as a primary line of defense against superoxide, quenching the reactive molecule and reducing it to oxygen and hydrogen peroxide molecules. SODs in mammals are found in the cytoplasm, nucleus and mitochondria and use two protons to convert superoxide to $O_2$ and $H_2O_2$, which is also a ROS. $H_2O_2$ is then further converted to $H_2O$ and $O_2$ by catalase (Slupphaug, Kavli, & Krokan 2003).

$$2\ O_2^- + 2H^+ \longrightarrow H_2O_2 + O_2$$

$$2\ H_2O_2 \longrightarrow 2H_2O + O_2$$

Further ROS detoxifying enzymes have been described, including alternative oxidase, pyruvate dehydrogenase, glutathione and peredoxin (Fang, Yang, & Wu 2002). Alternative oxidase (AOX) is a terminal oxidase present in the mitochondria, which transfers an electron to $O_2$, thus making it molecular oxygen (Colasante 2009;Maxwell 1999;Umbach 2005). Pyruvate dehydrogenase has been shown in *Streptococcus pneumoniae* to confer resistance to $H_2O_2$ by contributing to $H_2O_2$ resistant energy source (Pericone 2003).

Non-enzymatic compounds can also detoxify ROS, including Vitamin A, Vitamin C, Vitamin E, Vitamin B1, antioxidant amino acid (arginine) and polyphenols. Thiamine (Vit B1) has been thought to have ROS scavenging ability, though the process is poorly understood. Thiamine, when incorporated in the culture media of the cells, makes the cells comparatively resistant to $H_2O_2$. It is postulated that that thiamine added in the media may work in two ways. It can either quench $H_2O_2$ present in the media, and thus make it less available, or it can enter the cells and perform the defense intracellularly. It has been

observed in *Thermus thermophilus* that cell lines resistant to $H_2O_2$ express an elevated level of thiamine as compared with wild type (Fukui 2011;Tunc-Ozdemir 2009).

An important mechanism to counteract damage caused by 8-oxoG is the "*GO system*", components of which are present in most living organisms, but there is remarkable diversity in the presence or absence of individual components in eukaryotes (Jansson 2010). This system involves MutM/MMH and MutY/MYH acting as part of BER to specifically repair 8oxoG damage, and MutT/MTH acting to prevent such damage. MutT can be considered as a first line of defence, as it prevents genome damage rather than repairing it (Michaels 1992). MutT is a bacterial hydrolase that sanitizes the nucleotide pool by hydrolysing 8oxodGTP and 8oxoGTP to their respective monophosphates, thus making them unavailable to be incorporated into the DNA helix or into RNA, respectively (Maki 1992). MutT homologue (MTH) is the eukaryotic homologue of bacterial MutT. The two proteins were shown to functionally complement each other when human MTH was expressed in *E. coli MutT* mutants (Fujii 1999). Mammalian MTH mutants display increased GC- TA transversion (Egashira 2002) whereas *E. coli mutT* mutants show an increased AT-CG transversion (Tajiri 1995). Hydrolysis of oxidized guanine is important because some repair polymerases, such as DNA polβ, even more than high fidelity replicative DNA polymerases, can poorly discriminate between 8oxodGTP and dGTP. Indeed, these polymerases have a high preference for incorporating 8oxodGTP opposite A rather than C in the template (Miller 2000). As this increases the rate of mutation, the activity of MutT is yet more critical.

Some 8oxodGTP escapes MutT/MTH hydrolysis, and can be present in the nucleotide pool, becoming incorporated in the DNA helix during replication. This requires the presence of second line of defense which can remove 8oxoG from the genome. This is catalysed one of two DNA glycosylases. One is termed MutM in bacteria, and the same function is carried out by a structurally unrelated protein in eukaryotes termed MMH (MutM homologue) in mammals or Ogg1.in yeast. Remarkably, *A. thaliana* encodes homologues of both MutM and MMH/Ogg1 (Garcia-Ortiz 2001). These DNA glycosylases have high specificity for 8oxoG when paired against C, G, or T, but not against A (Bjoras 1997;Tchou 1991). They are bi-functional glycosylase/lyase enzymes that excises 8oxoG from the template strand (Bjoras 1997;Lu 2001;Tchou 1991) and their mutation results in elevated GC-TA transversion (Klungland 1999). In certain instances, repair of an 8oxoG: C lesion is not completed until the second round of replication. Here, dATP, instead of dCTP, is incorporated against 8oxoG in its *syn* conformation (see above). This calls for the

second DNA glycosylase that is active against 8oxoG, which is called MutY in bacteria and MYH (MutY homologue) in eukaryotes. MutY/MYH is an adenine glycosylase that removes A paired against 8oxoG (Ohtsubo 2000;Tsaiwu 1992).

The above describes the *GO system* that serves to prevent or repair 8oxoG lesion in DNA. Distinct from this, in *E. coli*, oxidized pyrimidines are recognized by endonucleaseIII (EndoIII) and EndoVIII. These are BER enzymes with broad range of oxidized pyrimidines as substrates (Cunningham 1997). Homologues of Endo-III have also been identified in yeast (Ntg1p and Ntg2p) (You 1999) and in mammals (designated as Nth1)(Asagoshi 2000).

While most oxidative lesions are repaired by BER and NER, MMR have also been found to be involved in repair of this damage. It was reported that oxidized bases are repaired more efficiently in coding regions of the yeast (Swanson 1999) and human genomes (Scharer 2003), thus suggesting a role of TCR in repair of oxidative DNA damage . A role for MMR has also been reported in the repair of 8oxoG lesions (DeWeese 1998;Mazurek 2002). Mismatch repair mainly serves to correct the oxidative lesions induced by 8-oxoG by identifying the potential mismatch formed by 8oxoG-A base pair. In addition, it has been shown that MutSα from humans binds to DNA duplexes containing 8oxoG:A, T or G pairs, but not 8oxoG:C (Mazurek 2002). It has been well observed that loss of MMR in bacterial system is directly attributed to increased accumulation of ROS. and thus increased mutagenesis (Sanders 2011). This is supported by the observation that there is an increased level of oxidative DNA damage in *msh2* null mutants in mouse embryonic fibroblasts (Colussi 2002). Finally, MSH2-MSH6 in mammals has been shown to interact with MYH and mediate 8oxoG excision (Gu 2002).

### 1.4.8 Response of *T. brucei* against oxidative damage

*T. brucei* are digenic parasites and subjected to different levels of both extracellular and intracellular oxidative stress throughout their life cycle. BSF cells are subjected to higher levels of oxygen when they divide extracellularly in mammalian host in the presence of molecular oxygen, which can be partially reduced to ROS like as $O^-$, $OH^-$ and $H_2O_2$. In procyclic form (PCF) parasites, cells are subjected more to intracellular oxidative stress due to active mitochondrial respiration. This may leave PCF cells with less capacity to entertain extracellular stress. Indeed, it was observed that PCF wild type cells are 10-30

fold more sensitive to $H_2O_2$ as compared with BSF parasites (Barnes 2006). The sensitivity of *T. cruzi*, a close relative of *T. brucei* and causative agent of American trypanosomiasis, towards oxidative stress by was examined by Furtado et al. who showed that parasites exposed to lower concentration (50 μM) of $H_2O_2$ encounter lesions in mitochondrial DNA which saturate at higher concentration (100 μM). However, no nuclear DNA lesions were observed at lower concentration of $H_2O_2$, while at higher concentrations of $H_2O_2$ nuclear DNA lesions increase proportionally to $H_2O_2$ concentration (Furtado 2012). During the study it was also observed that though nuclear DNA has more lesions, they were all repaired within first 24 hours of removal of mutagen; in contrast, the lower levels of lesions in mitochondrial DNA are not or poorly repaired.

As in other organisms, *T. brucei* cells are well equipped with both defence and repair mechanisms to firstly prevent the oxidative lesions or later repair the damage so caused. *T. brucei* possess a range of defence systems present to prevent the oxidative damage. *T. brucei* contain an alternative oxidase system as a terminal oxidase, trypanosomes alternative oxidase (TAO) (Fang and Beattie 2003). This is a mitochondrial protein and decreases ROS production by direct electron transfer and energy is released as heat. BSF *T. brucei* are unique in that they are the only organisms which only have TAO as means of terminal oxidase (Chaudhuri et al. 1995). Other organisms, including PCF *T. brucei*, contain an additional oxidase system, termed cytochrome C oxidase, which reduces the oxidative stress. Though in PCF form cells cytochrome C oxidase is expressed more abundantly as compared to TAO, in conditions of oxidative stress, TAO expression levels increase. It was also observed in *T. brucei* that when TAO is inhibited, concentrations of ROS increase with subsequent increase of an another enzyme iron superoxide dismutase (Fe-SOD) (Fang & Beattie 2003). SOD is an enzyme that converts superoxide anion to $H_2O_2$, which is then broken down $H_2O$ and $O_2$. It was also shown that SOD expression is more pronounced in PCF cells as compared to BSF, which may counteract increased ROS production in PCF due to mitochondrial metabolism (Vertommen 2008). In *T. cruzi*, TAO and cytochrome C oxidase are expressed throughout the life cycle and reduce the oxidative stress generated during mitochondrial respiration, though to my knowledge, extensive studies on role of TAO in *T. cruzi* have not been done. SOD has also been annotated in *T. cruzi* (Ismail 1997) though their role in protection against oxidative stress have not been studied.

Another important antioxidant enzyme found in *T. brucei* is tryparedoxin peroxidase (TXNPx). TXNPx are a part of trypanothione-dependent antioxidant defence system,

which works by the transfer of electron from NADH to trypanothione (T $(SH)_2$) via trypanothione reductase (TR). Reduced trypanothione then transfers the electron to tryparedoxin (TXN) or dehydroascorbate (DHA). TXN then reduces either of two peroxides (tryparedoxin peroxidase/2-Cys peroxidase (TXNPx) or non-selenium glutathione peroxidase;TbGPX), whereas DHA transfers the electrons to oxidized ascorbate peroxidase (APx). Peroxidases then reduce substrates such as $H_2O_2$ to $H_2O$ and $O_2$. In trypanosomes, two independent TXNPxs have been isolated: cytoplasmic TXNPx (TbCPX/ TRYP1) and mitochondrial TXNPx (TbMPX/ TRYP2). TbGPX I have also been localized in both the cytoplasm and mitochondria, though they could not be differentiated (Schlecker 2005). These are collectively termed TXNPx. Though this protein is also abundant in PCF parasites compared with BSF *T. brucei*, RNAi analysis have confirmed that TbCPX is essential for both life forms, whereas TbMPX is not essential, at least in the BSF, as tested by RNAi (Wilkinson 2003). Interestingly, it was found that when cultures are grown in the presence of tetracycline for long periods, the growth pattern of PCF RNAi induced cultures for both TbCPX and TbGPX I was independent of addition of tetracycline and growth was resumed (Schlecker 2005). In contrast, growth was not resumed in BSF RNA-induced cultures. This again highlights the importance of the redox system in PCF cells as compared with BSF parasites. The role of TXPNx has also been highlighted in *T. cruzi*, where it was observed that the parasite grow at a higher rate in the presence of non-cytotoxic levels of $H_2O_2$ (Finzi 2004). It was observed that parasites, when exposed to lower dose of oxidative stress, tend to be more resistant to the oxidative damage than cells exposed to a lethal dose. It was further shown that if cells are exposed to a sub lethal dose of $H_2O_2$ and then grown in the presence of a higher concentration of $H_2O_2$. They are more resistant to the damage compared with parasites directly grown in the presence of a higher dose of $H_2O_2$. Thus, at sublethal doses, parasite may increase the expression of proteins that it would need for defence against oxidative stress. Western blotting analysis has shown that levels of TcCPX levels increase in the course of acclimatization in the presence of lower doses of $H_2O_2$ (Finzi 2004). However, it was also shown that TcGPX has no substrate specificity towards $H_2O_2$, which is in contrast to *T. brucei* (Wilkinson 2000).

Despite the presence of robust defence mechanisms in trypanosomes, at some instances the presence of ROS increases the cells defence capacity and creates a condition termed as oxidative stress. A described earlier, ROS causes damages to a range of macromolecules, but in the context of this study I have discussed below only the repair systems in *T. brucei* and related trypanosomes recruited for the repair of oxidized DNA damage. BER and MMR are the pathways involved in the repair of oxidative DNA damage. Most of the

knowledge of repair against oxidative stress in trypanosomes has come from initial studies done in *T. cruzi* (Augusto-Pinto 2003). It was observed that MSH2 in different species of *T. cruzi* are present in the form of three different haplotypes (A,B and C). Different haplotypes of MSH2 were characterized on the basis of single nucleotide polymorphisms (SNPs) present towards the C-terminus in the ATPase domain and Helix-turn-Helix motif. It was observed that different haplotypes of MSH2 present in *T. cruzi* do not confer any microsatellite instability under physiological conditions. However, when subjected to $H_2O_2$, a different pattern of instability in microsatellite loci was seen in strains with different haplotypes of MSH2. This thus showed different levels of MMR efficiency in different MSH2 haplotypes-bearing strains of *T. cruz*i. It has also been shown that strains bearing MSH2 haplotypes with reduced MMR efficiency also accumulate higher levels of 8oxoG (Campos 2011). As described in Section 1.4.6.4, loss of MSH2 or MLH1 resulted in impaired MMR activity, as described by tolerance to alkylation damage and increased instability in microsatellite loci. Furthermore, it was observed that MSH2 from MMR machinery may be solely responsible for repair of oxidative damage. This was concluded on the basis of the observation that only *msh2* null mutants were sensitive towards oxidative damage when compared with wildtype cells and *mlh1* null mutants. This was further supported by experiments in which MSH2 expression was restored using protein from either *T. brucei* or *T. cruzi*. In these circumstances, the response towards oxidative damage was restored and was comparable to MMR-proficient wild type cells. However, re-expression of an *MSH2* gene from *T. cruzi* in *T. brucei* MSH2 null mutants did not restore MMR activity, as analyzed by alkylation tolerance and microsatellite instability assay (Machado-Silva 2008). A role for MSH2 in response to oxidative stress is also supported by the observation that *Tbmsh2* mutants under physiological conditions show an increase in akinetoplastid parasites, and the number of these akinetplastid parasites increase in the presence of $H_2O_2$ (Campos 2011).

Other than MMR, repair of oxidative DNA damage is also widely carried out by the BER pathway (see Section 1.4.7.2) or more specifically the "*GO system*" of BER. Genes of the proteins involved in GO system have been annotated in trypanosomes (Aslett 2010). However, their role in protection against oxidative stress has to date only been studied in *T. cruzi.* An orthologue of 8-oxoguanine glycosylase (Ogg1) has been characterized for its role in repair of oxidative DNA damage. As described in Sections 1.4.2 and 1.4.7.2, Ogg1/MMH is a eukaryotic homologue of bacterial MutM and removes 8-oxoG lesions, creating an abasic site which is processed by further enzymes involved in BER. However, over expression of TcOGG1, though resulting in reduced 8-oxoG levels in the nucleus and

mitochondria, makes the cells sensitive towards oxidative damage as compared with control parasites expressing normal levels of the protein (Furtado 2012).

## 1.5 Aims of thesis

Based on the understanding of the various mechanisms for the efficient repair of DNA lesions caused by reactive oxygen species (ROS) in other organisms, and the relatively incomplete picture of this in *T. brucei*, we wanted to further investigate the role of MMR in this process, and in particular in PCF *T. brucei* in the presence of oxidative stress. . The specific questions addressed in this thesis are:

1. **What role does MMR play in protection against oxidative damage**?

   The part of the study mainly asked if it is possible to generate null mutants for *MSH2* and *MLH1* in PCF *T. brucei*. Although MMR mutants have been generated in BSF parasites, all attempts to generate null mutants in *T. cruzi* have so far failed. Secondly, we wished to extend the characterization of the role of *T. brucei* MMR in protection against oxidative stress and ask if any differences in activity were seen between PCF and BSF *T. brucei.*

2. **Where does the MMR machinery localize**?

   Independent epitope-tagged lines of MSH2 and MLH1 were generated in both BSF and PCF *T. brucei* and use to localize the proteins by immunofloursence. We also asked if localization or expression of the MMR proteins is altered when subjected to stress.

3. **What is the role of other MMR proteins, apart from MSH2 and MLH1, in response to DNA damage?**

   In this part of the study, we attempted to characterize the functions of MSH3 and MSH6 in MMMR and to ask if the play a role in protection against oxidative DNA damage in BSF *T. brucei*.

4. **What are other factors work in support of, or in conjunction with, MMR**?

During this part of the study we have tried to identify any potential candidates that might aid in protection against oxidative DNA damage in the absence of functional MMR.

# 2 Materials and Methods

# 2.1 Trypanosome strains, cell culture and transformation

## 2.1.1 *T. brucei brucei* strains

*Trypanosoma brucei* cells of strain Lister 427 MITat1.2 were primarily used for studying both bloodstream form (BSF) and procyclic form (PCF) trypanosomes. For assay comparison between different strains, TREU 927 *T. brucei* were occasionally used and DNA from other strains examined, where indicated. *T. brucei* PCF strain pLew29-pLew13 and BSF pLew90-pLew13 were used for RNA interference (RNAi) studies and are derived from Lister 427.

## 2.1.2 Cell Culture of trypanosomes

### 2.1.2.1 Procyclic form cell culture

PCF *T. brucei* were cultured *in vitro* at 27 °C in the semi-defined medium SDM-79 (recipe given below)(Brun 1992), supplemented with 10% v/v heat-inactivated foetal bovine serum (FCS-SIGMA) and 0.2% v/v haemin (diluted from a 2.5 $mg.ml^{-1}$ stock in 0.2 M NAOH (GIBCO). PCF cells were diluted routinely to maintain their cell density between 5 x $10^5$-1 x $10^7$$cells.ml^{-1}$(which is referred to herein as log phase).

**SDM 79 Recipe (5L)**

| | |
|---|---|
| One sachet SDM 79 | Cat# 07490916N,Gibco |
| Sodium bicarbonate | 24 mM |
| Distilled water | added to 5L |
| pH (adjusted with 5 M NaOH) | 7.3 |

### 2.1.2.2 Bloodstream form cell culture

BSF *T. brucei* were cultured *in vitro* at 37°C, 5% $CO_2$. Cultures were grown in HMI-9 (Hirumi and Hirumi 1994)(recipe below) medium supplemented with 20 % v/v FCS and 5 ml of Penicillin and Streptomycin (10,000 $\mu g/ml^{-1}$ Cat# 15140, Gibco). BSF cultures were maintained at a density of 1x$10^5$-2x$10^6$ $cells.ml^{-1}$(log phase).

**HMI-9 Recipe (5L)**

| | |
|---|---|
| One sachet HMI-9 powder | Cat #07490915N, Gibco |
| Sodium bicarbonate | 36 mM |
| B-mercaptoethanol (Sigma) | 1.4% |
| Distilled water | added to 5 L |

## 2.1.3 Cryopreservation of *T. brucei*

Aliquots of trypanosomes were stored by cryopreservation. BSF and PCF parasites were grown to 5 x $10^5$ cells.ml$^{-1}$ and 1x$10^7$ cells.ml$^{-1}$, respectively, and 10% glycerol was added to the cultures and 1ml aliquoted in cryo-vials with unique stabilate numbers. Vials were wrapped in cotton wool and placed at -80 $^0$C overnight. Next day they were transferred to liquid nitrogen tanks and their position with their respective stabilate numbers were recorded electronically. Stabilates were recovered by thawing them at room temperature and then transferring to 5 ml of appropriate media. No drugs were added initially and cultures were grown for 2-3 days. During the next dilution of the culture, drugs were added, as appropriate to the antibiotic resistance of the cells.

## 2.1.4 Transformation of *T. brucei*

### 2.1.4.1 Transformation of procyclic form *T. brucei*

2.5 x $10^7$ cells at a density of 5 x $10^6$ cells.ml$^{-1}$ were used per transformation. Cells were centrifuged at 600 *g* for 10 min at room temperature. The supernatant was stored and the cell pellet was resuspended in 0.5 ml of ice-cold electroporation buffer, termed Zimmerman medium (ZMnoG) (Table 2-1). 5-10 µg of linearized DNA (prepared as described below), in a maximum volume of 10 µl, was added to the resuspended cells and mixed gently. A no DNA control was also conducted by preparing the cells in the same way and not adding the DNA. The mixture was transferred to electroporation cuvettes (BioRad Cat # 165-2088) and 1.5 kV of current was applied to two pulse at 25 µF capacitance using BioRad Gene Pulser II. The cells were then transferred to 10 ml of SDM-79 medium and incubated overnight at 27 $^0$C. After overnight recovery, 200 µl and 2

ml of recovered cells were diluted in 20 ml conditioned medium and plated in 96 well plates (175 µl per well) with appropriate antibiotics (general concentrations given in (Table 2-2). Conditioned medium was prepared by combining 10% v/v FCS, 15% v/v pre-conditioned medium (medium collected as supernatant when the cells were pelleted) and 75% SDM-79. Cells were allowed to grow for 10-14 days. After 10 days, wells were examined for densely growing cells and compared with the control plate. Clones were selected when all cells in the control plate were dead and a few wells had densely growing cells in the cells with DNA transformation. Clones selected were diluted initially into 2 ml of SDM-79 without any drug and then grown in 10 ml of the media with drug for at least 5 generations before being used for any further experiments. The same procedure was used for all PCF cells transformation except for variation in the concentrations of antibiotics, which that depended on the drug resistance gene used for selection of clones and the gene being targeted (discussed in the Results).

**Table 2-1 Zimmerman medium (ZMnoG) Recipe**

| Chemicals | Stock conc. | Working conc. |
|---|---|---|
| **NaCl** | 1 M | 132 mM |
| **KCL** | 1 M | 8 mM |
| **Disodium hydrogen orthophosphate** | 1 M | 8 mM |
| **Potassium dihydrogen orthophosphate** | 1 M | 1.5 mM |
| **Magnesium acetate** | 1 M | 1.5 mM |
| **Calcium acetate** | 1 M | 90 µM |

### 2.1.4.2 Transformation of bloodstream form *T. brucei*

AMAXA Nucleofactor kit (Amaxa Biosystems, Cat# VPA-1002) was used for transformation of BSF cells. Cultures were grown to a density of 1 x $10^6$ cells.ml$^{-1}$ and ~ 4x$10^7$ cells were used per transformation. Cultures were centrifuged at 800 *g* for 10 minutes at room temperature and pellets were resuspended in 100 µl nucleofactor solution (provided with the kit) and mixed with 5-10 µg of linearized DNA in a maximum volume of 15 µl of sterile water. Samples were put into electroplated cuvettes provided with the kit and electroporated according to manufacturer's protocol, optimised for Human T-cells.

Cells were then added to 30 ml of HMI-9 media without any drugs and plated into 24 well plate (1 ml per well). 20 ml media was then added to the 6 ml of culture that remained and plated into a second plate (1ml per well). The plates were incubated overnight at 37 $^{0}$C for recovery. Following recovery, 1 ml of HMI-9 with double concentration of appropriate selective antibiotics was added to each well and the plates incubated again for 5-7 days. No DNA controls were conducted by the same procedure, but without addition of DNA. Antibiotic-resistant clones were selected when none of the wells of the control plate had any densely growing cells. Clones selected were the grown in 5 ml of HMI-9 with no drug and then cultured for at least 5 generations in the presence of antibiotics before to be used into any experiments.

**Table 2-2 General concentrations of antibiotics used for selection of transformant clones**

| Antibiotics | Stock conc. | Working Dilution | |
|---|---|---|---|
| | | PCF | BSF |
| **Blasticidin** | 10 mg.ml$^{-1}$ | 10 µg.ml$^{-1}$ | 10 µg.ml$^{-1}$ |
| **Puromycin** | 10 mg.ml$^{-1}$ | 1 µg.ml$^{-1}$ | 1 µg.ml$^{-1}$ |
| **Phleomycin** | 20 mg.ml$^{-1}$ | 2.5 µg.ml$^{-1}$ | 2.5 µg.ml$^{-1}$ |
| **Neomycin/G4l8** | 50 mg.ml$^{-1}$ | 15 µg.ml$^{-1}$ | 5 µg.ml$^{-1}$ |
| **Hygromycin** | 50 mg.ml$^{-1}$ | 50 µg.ml$^{-1}$ | 10 µg.ml$^{-1}$ |
| **Tetracycline** | 2 mg.ml$^{-1}$ | 2 µg.ml$^{-1}$ | 2 µg.ml$^{-1}$ |

## 2.2 Standard Molecular Biology Techniques

### 2.2.1 Primer design

GeneDB (http://www.genedb.org/Homepage/Tbruceibrucei927) was referred to in order to retrieve DNA sequences of genes of interest. Primer design and appropriate restriction sites were identified by using the CLC® software. Restriction recognition sites were added to the 5' end of the primers. 3 further additional nucleotides were added at the 5' end of the restriction sites. All primers were designed to have a GC clamp at 3' end. Primers were synthesized by Eurofins MWG Operon® (Germany). A list of the all the primers used is given in Table 2-4.

## 2.2.2 DNA Isolation

Genomic DNA from parasites was isolated using the DNAse Easy Blood and Tissue kit from Qiagen (Cat# 69506) following the manufacturer's protocol. Plasmid DNA from *E. coli* was isolated using the Miniprep kit from Qiagen (Cat# 27106). DNA was also isolated from agarose, as per the requirement of certain experiments, using the Qiagen Gel extraction kit (Cat# 28706).

## 2.2.3 PCR purification

To concentrate and to purify DNA from a solution, the Qiagen PCR Purification kit (Cat# 28106) was used following manufacturer's protocol. DNA was eluted into sterile distilled water in 50-30 µl to get concentrated DNA.

## 2.2.4 DNA quantification

DNA was quantified, when required, using Thermo Scientific Nanodrop 1000 Spectophotometer according to manufacturer's protocol.

## 2.2.5 Polymerase Chain Reaction (PCR)

*T. brucei* genomic DNA was PCR-amplified from TREU 927 , for instance to PCR-amplify the 3'UTR, 5'UTR or ORF of chosen genes, when generating constructs using high-fidelity Herculase enzyme (NEB). In contrast in diagnostic PCR, for instance to check transformants, PCR-amplification used Taq Polymerase (NEB). All PCRs were performed in 40 µl reactions using the buffers provided with the enzyme at the dilution detailed by the manufacturer, as shown below.

**Table 2-3 PCR reaction components**

| | Stock conc. | Working Conc. |
|---|---|---|
| **Substrate DNA** | | 100 ng |
| **dNTP mix** | 10 mM | 150 µM |
| **Forward Primer** | 10 mM | 0.5 mM |
| **Reverse Primer** | 10 mM | 0.5 mM |
| **Buffer** | 10x | 1x |
| **Taq/Herculase** | | 1.5 U |

| | | |
|---|---|---|
| **$H_2O$** | | Up to 40 µl |

Standard PCR conditions were: Denaturation at 94 $^0$C for 3 minutes, followed by 30 cycles of denaturation at 94 $^0$C for 30 seconds, primer annealing at 55 $^0$C for 40 seconds and elongation at 72 $^0$C (60 seconds/kb). A final elongation was performed at 72 $^0$C for 10 minutes. Where conditions varied from this, it is indicated in the Results. Samples were stored at 4 $^0$C until they were run on agarose gel to check for PCR- amplification.

## 2.2.6 Agarose Gel Electrophoresis.

DNA samples were visualized on 1% agarose (unless stated otherwise) in 1 x Tris Acetate EDTA buffer (40 mM Tris-HCL, 1 mM EDTA pH 8, 0.11% Acetic acid). Sybersafe (10,000x; Invitrogen, Cat# S33102) was added at 5 µl per 100 ml of gel to visualize double-stranded DNA. Gels were run in MupidOne® Advance gel electrophoresis tank, typcially at 100 V for 30 minutes with 1 kb ladder (NEB, Cat# N3232)or 1kb plus ladder (Invitrogen, Cat# 10787-018) run in parallel to compare the sizes. DNA was visualized under a UV transilluminator (Bio Rad) and photographed using QuantityOne® software.

## 2.2.7 Restriction Digestion

Restriction digestion reactions were typically performed in 20 µl using 1x reaction buffer (provided as appropriate for the enzyme, NEB) and 1 µl of enzymes (10,000-20,000 Units $ml^{-1}$). 5 µg of DNA was digested at a temperature optimal for the enzyme activity for 30 mins-1 hr. These reaction conditions were followed if checking for the confirmation of a restriction site or a specific size of digested product. For linearizing DNA to be used for transformation, ~30-50 µg DNA was digested in a 500 µl reaction volume and reagents scaled to correct concentration. In addition, the digests were incubated for longer times (5 hrs- overnight), depending on the activity of enzyme, at specified temperatures.

## 2.2.8 DNA Ligation

DNA ligation was performed in 20 µl reactions containing 2 µl of 10 x reaction buffer, 1U of T4-DNA ligase (NEB ),100 ng of vector and enough water was added to make up the volume to 20µl. Insert to be ligated to vector was added at 3:1 insert to vector molar ratio. Reactions were incubated either for 4 hrs at 16 $^0$C or overnight on the bench at room temperature.

## 2.2.9 Bacterial Transformation

Transformation was either done to clone the ligation mixes for new constructs or to generate further DNA from existing plasmid DNA mini-prep. To clone a ligation mix, 10 µl of the mix was transformed into 150 µl of *E. coli* DH5α chemically competent cells (NEB), whereas to clone plasmid DNA, 2 µl of DNA was mixed to the 50 µl of *E. coli* DH5α chemically competent cells (NEB). The DNA added was mixed gently and incubated on ice for 30 minutes. The mixture was then heat shocked at 42 $^{0}$C for 40 seconds and immediately put on ice for 5 minutes. 700 µl of SOC was added to cells and then incubated at 37 $^{0}$C in a shaking incubator for 1 hr. After recovery, cells were briefly centrifuged at 6000 *g* for 1 minute. 500 µl of supernatant was removed and the pellet was resuspended in the remaining liquid. If cloning a ligation mix, all the cells were plated on antibiotic selective agar plates. For cloning plasmid DNA, 50 µl of cells were cultured on plates. For both, LB agar (tryptone 10 g.L$^{-1}$, Yeast extract 5 g.L$^{-1}$, NaCl 10 g.L$^{-1}$, Agar agar 15 g.L$^{-1}$) plates, supplemented with 100 µg.ml$^{-1}$ ampicillin (Sigma) were used. Plates were placed overnight at 37 $^{0}$C incubator.

## 2.2.10 Colony PCR and Plasmid Retrieval

For colony PCR, single colonies were picked aseptically and inoculated into 20 µl sterile water. PCR was done in the same way as described in Section 2.2.5 with the only difference being that 7µl of inoculated culture was used in place of DNA and the volume of water was adjusted accordingly. After PCR, samples were analyzed by agarose gel electrophoresis, as described in Section 2.2.6. and 3-5 positive clones were inoculated in 5 ml of LB broth supplemented with 100 µg.ml$^{-1}$ ampicillin. Cultures were grown overnight at 37 $^{0}$C in a shaking incubator. The following day, 750 µl of the culture was aliquoted in a sterile eppendorf, mixed with 750 µl 100% sterile Glycerol and stored at -80 $^{0}$C. Plasmid DNA was isolated from the 4 ml culture as described in Section 2.2.2. DNA samples were checked on agarose gels and sent to Eurofins MWG DNA sequencing services to validate the sequence (using primers appropriate for the constructs). Sequenced samples were analysed by aligning them with the referenced sequence retrieved from databases, as described in Section 2.2.1, using CLC® software. Glycerol stocks of the respective clones confirmed by sequencing were labelled and stored at -80 $^{0}$C for future use. To grow the cultures from glycerol stock, tiny amount of culture was scraped and inoculated in 5 ml LB broth with 100 µg.ml$^{-1}$ ampicillin. Cultures were grown overnight at 37 $^{0}$C in a shaking overnight and plasmid DNA isolated as described in Section 2.2.2.

## 2.2.11 RNA Isolation and cDNA synthesis

Total RNA from *T. brucei* was isolated from 4 x $10^7$ cells (cell densities being 1 x $10^7$cells. $ml^{-1}$ for PCF cells and 2x$10^6$cells.$ml^{-1}$ for BSF cells). Total RNA purification kit was used from QIAGEN (Cat#74104). Extra care was taken to avoid RNAse contamination: pipettes and the bench top were wiped with RNAse wipes (Ambion, Cat# 9786, 9788) and filter tips were used. To ensure complete DNAase digestion, samples were treated on the column with RNAse free DNAse as per the manufacturer's instructions.Qiagen DNAase kit (RNAase free- DNAase kit, Cat#79254) was used for on column DNA digest. RNA isolated was PCR-amplified with any housekeeping gene primers, as described in Section 2.2.5, to check for any contaminating DNA. If samples were contaminated with DNA, samples were treated again with RNAse free DNAse, as detailed by manufacturer, with prolonged incubation with DNAse for 1 hr at room temperature.

cDNA was synthesized using High Capacity RNA-cDNA master mix (Applied Biosystems, Cat# 4390777) according to manufacturer's instructions. 500 ng – 1 µg of total RNA was used per reaction. After cDNA was synthesized samples were PCR-amplified again, as described in Section 2.2.5 with the exception of using 1µl of cDNA in place of DNA, for any housekeeping gene to estimate the product quantities and amplification efficiency.

## 2.2.12 Real-Time PCR

To quantify the levels of mRNA, primers were designed using the Primer Express® Software (Applied Biosystems). A List of the QRT-PCR primers is given in Table 2-4. SYBR® Green PCR master mix from Applied Biosystems (Cat# 4367659) was used for PCR-amplification in 96 well plates. For each reaction, PCR was set up as follows: 12.5 µl SYBER Green master mix, 1 µl of each primer (10 mM stock), 1 µl cDNA and 9.5 µl of sterile water. All samples were PCR-amplified in quadruplicate for every gene along with *GPI8* as endogenous control. For every primer set, master mix was made depending on the number of samples to be analyzed for expression. PCR conditions used were 1 cycle each of 50 $^0$C for 2 minutes and 95 $^0$C for 10 minutes, followed by 40 cycles of 95 $^0$C for 15 seconds and 1 cycle of 60 $^0$C for 1 minute. Data was collected at the final stage and expression levels of specific genes were determined by the quantitative expression plot generated by the Applied Biosystem software (7500 system SDS software version 1.4.0.25).

# 2.3 Protein analysis

## 2.3.1 Western Blotting

### 2.3.1.1 Preparation of whole cell extracts

$10^8$ cells were grown at the density of 2 x $10^7$ cells.ml$^{-1}$ for PCF and 2 x $10^6$ cells.ml$^{-1}$ for BSF. Cells were pelleted by centrifuging them at 1000 *g* for 10 minutes at room temperature. Supernatant was removed and the pellet was resuspended in 100 µl protein loading buffer (50 mM Tris-HCL pH 6.8, 2% SDS, 10% Glycerol, 12.5 mM EDTA and 0.02% Bromophenol blue) and 200 mM Dithiothritol (DTT, Sigma). Samples were boiled at 100 $^0$C on a heat block before loading on an acrylamide gel.

### 2.3.1.2 Sodium dodecyl Sulfate-Polyacrlamide gel electrophoresis (SDS-PAGE)

Samples were loaded onto pre-cast 10% polyacrylamide gel (Invitrogen, Cat# NP0301) 20 µl preheated sample was loaded per lane along with sharp pre-stained protein ladder (Invitrogen, Cat# LC5800) in a parallel lane. Samples were separated at 200 V for 55 minutes in MOPS electrophoresis buffer (Invitrogen). After electrophoresis samples were transferred to nitrocellulose membrane for immunoblotting.

### 2.3.1.3 Immunoblotting

Protein samples resolved by SDS-PAGE were transferred to nitrocellulose membrane (GE Healthcare) at 100 V for 80 minutes. Samples were transferred using transfer buffer (25 Mm Tris base, 192 mM Glycine and 20% methanol). After transfer, blots were blocked for 1 hr with PBST (PBS with 0.05% Tween) containing 5% w/v powdered milk (semi skimmed Marvel). Primary antibody was diluted in block solution (PBST containing 5% w/v powdered milk) in dilution specific to each antibody. After 1 hour, block solution was removed and blots were incubated in 10 ml diluted primary antibody for 1 hour-overnight. After incubation, primary antibody was removed and blots were washed 3 times with PBST to remove any unbound antibody. Blots were then incubated for 1 hr in HRP-conjugated secondary antibody in 1:5000 dilutions in block solution. Blots were again washed three times with PBST. Excess PBST was removed by touching the corners of the membrane with a tissue and detected by incubating for 5 minutes in dark with enhanced chemiluminescence (Piercenet, Cat# 34078) and exposing to X-ray film (KODAK). Film was developed using KODAK Ex-OMAT system.

## 2.3.2 Sub-cellular fractionation

To localize a specific protein in a specific compartment of cell, subcellular fractionation was used. Fractionation was carried out as explained by Zeiner et al (Zeiner et al. 2003). Briefly, $5x10^8$ cells, at $1x10^7$cells.ml$^{-1}$ density for PCF or $2x10^6$cells.ml$^{-1}$ density for BSF, were centrifuged at 1000 *g* for 20 minutes at 4 $^0$C. Pellets were washed twice in 5 ml buffer A (recipe given below) and then resuspended in 1 ml buffer A. 200 µl was removed as whole extract (fraction 1). In the remaining 0.8 ml cell suspension Nonidet P-40 was added to 0.2% v/v and passed three times through a 26 gauge needle. Lysate was then centrifuged at 16000 *g* for 10 minutes at 4 $^0$C. Supernatant was collected as the cytoplasmic fraction (fraction 2). The pellet was then spun twice at 16000 *g* for 5 minutes each to remove any contaminating cytoplasmic proteins and was then resuspended in 500 µl buffer A. Pellet was then passed through the 26 gauge needle 16 times and centrifuged at 16000 g for 10 minutes at 4$^0$C. Supernatant was collected in a fresh tube (fraction 3). Pellet was rinsed in 0.5 ml buffer A without resuspending the pellet and then resuspended in 0.5 ml buffer A, generating nuclear fraction (fraction 4). All fractions were stored at -80 $^0$C until analyzed by western blotting as described in Section 2.3.1. As a control to check if fractionation was successful, protein markers specific for each fraction were used. Sheep anti- OPB antiserum (gifted by Jeremy Mottram lab; 1:2000 dilution), rabbit anti-NOG antiserum (gifted by Marilyn Parsons; 1:5000 dilution) and rat anti-POLβ antiserum (gifted from Paul Englund; 1:5000 dilution) were used to confirm fractionation of cytoplasmic, nuclear and mitochondrial fractions respectively.

### Buffer A

| Chemicals | Stock conc. | Working conc. |
|---|---|---|
| **Sucrose** | 1 M | 150 mM |
| **KCL** | 100 mM | 20 mM |
| **$MgCl_2$** | 100 mM | 3 mM |
| **HEPES-KOH pH 7.9** | 100 mM | 20 mM |
| **Dithiothritol** | 1 M | 1 mM |
| **Complete Protease inhibitor (Roche, Cat# 10787-018)** | 50 x | 1x |

## 2.3.3 Co-Immunoprecipitation (Co-IP)

Co-IP was performed to check for interaction between two proteins. *T. brucei* clones in which two different proteins were tagged by different epitopes were used to check if these two proteins together form a complex. Non-tagged cells and clones with only one protein tagged were used as control. Cells were grown to their log phase and a total of $10^9$ cells were used per sample. Cultures were centrifuged at 1000 *g* and pellets were store at -80 $^0$C until ready to use. The whole procedure was done either on ice or in the cold room at 4 $^0$C.

### 2.3.3.1 Preparing magnetic beads

Goat anti-mouse IgG coated magnetic beads (Invitrogen – M280) were used for immunoprecipitation. 50 µl of beads were aliquoted in 2 ml eppendorff tubes and 1 ml of block solution (PBS with 0.5% BSA) was added. The solution was mixed thoroughly and tubes were placed on a magnetic rack. Beads were collected and the supernatant was removed with a pipette. This step was repeated three times and the beads were resuspended in 125 µl block solution. 5 µg of antiserum specific to epitope was added and incubated overnight at 4 $^0$C on a rotor. The following day, the beads were washed again with block solution to remove any unbound antibody and finally resuspended in 50 µl of block solution.

### 2.3.3.2 Lysis of whole cells

2 ml of whole cell extract buffer (recipe given below) was added to the cell pellets. Samples were mixed thoroughly and incubated at 4 $^0$C for 2 hours. Cell extracts were then transferred to a fresh 2 ml eppendorf and centrifuged at 15000 *g* for 30 minutes at 4$^0$C.

### 2.3.3.3 Immunoprecipitation

After centrifugation, 50 µl of supernatant was aliquoted in a fresh tube which served as the input sample for western blotting. The remaining supernatant was then added to the prepared beads (see Section 2.3.3.1) and incubated for 2 hours at 4 $^0$C on a rotor. Tubes were then placed on magnetic rack, the supernatant was collected in a fresh tube and stored at -80 $^0$C. This served as ‘flow through’ for western blotting.

### 2.3.3.4 Washing

Beads were completely resuspended in 1 ml ice cold wash buffer (recipe given below) and liquid was collected by placing the beads on magnetic rack. This step was repeated 7 times. Beads were then resuspended in 1 ml TE wash buffer (see recipe below) and centrifuged at 1000 *g* for 3 minutes at 4 $^{0}$C. Residual TE buffer was discarded.

### 2.3.3.5 Elution

200 µl elution buffer (recipe given below) was added to the beads and incubated at 65 $^{0}$C (in a heat block) for 30 minutes, vortexing every 2-5 minutes. Beads were then centrifuged for 1 minute at 16000g at room temperature. Supernatant was collected and stored at -80 $^{0}$C to serve as eluate in western blotting.

To check if the two proteins interact western blotting was performed as described in section 2.3.1.

**Whole Cell Extract Buffer (WCE) – Stored at 4ºC ❄**

| Chemicals | Stock solution | Working conc. |
|---|---|---|
| **Hepes pH 7.55** | 1 M | 50 mM |
| **NaCl** | 1 M | 100 mM |
| **EDTA pH=8.0** | 0.5 M | 1 mM |
| **EGTA** | 0.5 M | 1 mM |
| **Glycerol** | 50% | 10% |
| **Triton X-100** | 10% | 1% |
| **complete protease inhibitor** | 50x | 1 tablet / 5 ml |

**Wash Buffer– Store at 4ºC ❄**

| Chemicals | Stock solution | Working conc. |
|---|---|---|
| **Hepes pH=7.55** | 1 M | 50 mM |
| **LiCl** | 1 M | 100 mM |
| **EDTA pH=8.0** | 0.5 M | 1 mM |
| **EGTA pH=8.0** | 0.5 M | 1 mM |
| **Na deoxycolate** | 10% | 0.7% |
| **NP40** | 10% | 1% |
| **complete protease inhibitor** | 50x | 1 tablet / 5 ml |

**TE wash Buffer**

| Chemicals | Stock solution | Working conc. |
|---|---|---|
| **Tris pH=8.0** | 1 M | 10 mM |
| **EDTA pH=8.0** | 0.5 M | 1 mM |
| **NaCl** | 1 M | 50 mM |

**Elution Buffer**

| Chemicals | Stock solution | Working conc. |
|---|---|---|
| **Tris pH=8.0** | 1 M | 50 mM |
| **EDTA pH=8.0** | 0.5 M | 10 mM |
| **SDS** | 10% | 1% |

## 2.4 Slide Microscopy

To visualize cells under the microscope, $10^6$ *T. brucei* cells were centrifuged at 800 *g* for 10 minutes at room temperature. Cell pellet was washed twice with PBS and resuspended in 50 µl PBS. Samples were then spread on pre cleaned glass slides (Manzel-glaser) and allowed to air dry. When completely dried, the slides were fixed in chilled methanol for 1 hour- overnight. Excess methanol was then removed and slides were washed twice with PBS. The slides were now ready to be stained appropriate to the experiment.

### 2.4.1 4, 6-Diamidino-2-phenylindole (DAPI) Staining

*T. brucei* cells air dried and fixed on slides (above) were mounted with DAPI with vectasheild (Vector labs, Cat# H-1200) to stain the DNA in order to visualise the nucleus and kinetoplast. A drop of DAPI was added to the slides and covered with cover slip. Slides were sealed with clear nail varnish and examined under UV light on a Zeiss Axioplan microscope. Images were captured using Hamamatsu ORCA-ER digital camera and Openlab software was used for analyzing the images.

### 2.4.2 Immunofloursence Assay (IFA)

Fixed slides were blocked for 1 hour with 2% FCS diluted in filtered PBS. Blocked slides were then incubated for 1 hour in 200µl primary antibody diluted in block solution (PBS with 2% FCS). After 1 hour, the slides were washed three times with block solution and then incubated for 1 hour with 200 µl Alexaflour® 594 conjugated secondary antibody diluted in block solution (Millipore, Cat# A11003). Slides were placed in the dark to avoid bleaching of antibody. Slides were again washed with filtered PBS, mounted with DAPI as described in Section 2.4.1 and visualized under respective filters to visual the labelled antibodies using Zeiss Axioplan microscope. Images were captured using Hamamatsu ORCA-ER digital camera and analyzed by Openlab Software.

## 2.5 Generation and analysis of genetically-modified *T. brucei*

### 2.5.1 Generation of mismatch repair knock out cell lines

Knock out constructs were generated by PCR-amplifying the 5' and 3' UTRs from genomic DNA. Primers were designed as described in Section 2.2.1. DNA was PCR-amplified from *T. brucei* TREU 927 genomic DNA using Herculase polymerase as explained in section 2.2.5. The UTRs were cloned into pBluescript II KS and separated by antibiotic resistance gene, flanked by 230 bp of β-α tubulin and 330 bp of α-β tubulin processing signals. Plasmids were then cloned into *E. coli* as described in section 2.2.9. To generate KO mutants in *T. brucei* plasmid was extracted from cloned *E. coli* as described in section 2.2.2 then linearized by digesting with appropriate restriction enzymes of which the recognition sequences are present in the Forward primer of 5'UTR and reverse primer of 3' UTR (see respective results chapters). Digested DNA was then cleaned by PCR purification (refer to section 2.2.3) and then cloned into *T. brucei* (as described in 2.1.4).

#### 2.5.1.1 Genotypic analysis of knock out clones

Different sets of primers were designed to PCR-amplify various regions of the mutated genomic DNA. Primers were used in a combination to PCR-amplify the regions of genomic DNA along with the region of integrated plasmid DNA to check the correct integration of the plasmid. A different set of internal primers was used complementary to the ORF of the gene to ensure the loss of gene.

Along with PCR, Clones were also confirmed by RNA analysis of the knock out lines. RNA was extracted from wild type and knock out cell lines and cDNA was made as explained in 2.2.11. cDNA was amplified with the primers complementary to ORF to check for the presence and thus expression of gene.

#### 2.5.1.2 Phenotypic analysis of knock out lines

##### 2.5.1.2.1 *In vitro* growth analysis

Growth rate was measured of knock out cell lines and compared with wild type to check if the absence of gene imposes any growth defect in parasite. PCF cultures were inoculated in 10 ml cultures at density of 5 x $10^5$ cells.ml$^{-1}$ and BSF cultures were inoculated in 15 ml at density of 1x$10^5$cells.ml$^{-1}$. Samples were counted every 24 hours for 72 hours using a haemocytometer (Bright-line, Sigma).

##### 2.5.1.2.2 Measuring cell survival in the presence of DNA damaging agents

Cultures were setup at a starting density as explained in 2.5.1.2.1. Different concentrations of $H_2O_2$ (VWR Cat #23619-297) and N-methyl-N'-nitro-N-nitrosoguanidine (MNNG) (Tokyo chemical industry Ltd, Cat# M0527) were added to the culture to measure the survival of knockout mutants in the presence of damage and compared with wild type. Survival was monitored in the presence of 3 different concentrations of DNA damaging agents and experiment was done in triplicate. Cultures were counted every 24 hours up to 72 hours and graph of the respective cell densities was plotted to analyze the effect.

To analyse the effect of $H_2O_2$ care was taken that cultures used for the study are in their mid log phase as it was observed that if cultures used in the study were post log phase they expressed a different and non-reproducible growth phenotype. Furthermore, $H_2O_2$ used was no more than 6 months old when opened for the first time and a fresh dilution was

prepared every time. $H_2O_2$ stock was 30% and it was serially diluted in 1 ml SDM-79 to 1 M and 100 mM and 1 mM for PCF growth curves and 1 ml HMI-9 to 1 M and 10 mM for BSF growth curves, before $H_2O_2$ was added in respective cultures.

1 M MNNG stock was prepared in 100% DMSO and 1 ml aliquots were stored at 4 $^0$C. When used for growth curves, serial dilutions were prepared in PBS as 10 mM and 1mM before respective volumes were added to the cultures. MNNG being highly carcinogenic, care was taken to use double gloves when making the dilutions.

Effect of MNNG on BSF cells was monitored by the Alamar Blue assay. This assay uses Resazurin (Sigma), generally named as Alamar blue, which is colorimetric dye which changes its colour by the activity of metabolising cells (O'Brien 2000). Intensity of change in colour is a measure of cell growth. 200 µl of $1x10^5$cells.ml$^{-1}$ cultures were plated on polystyrene 96 well plates (Nunc, Cat # 136101) in the presence of media containing doubling dilutions of MNNG from 400 µM to 0.39 µM. After 48 hours, 20 µl of Resazurin (12.5 mg in 100 ml PBS) was added to the wells. Cultures were allowed to grow for another 24 hours and then florescence was measured using luminescence spectrometer (LS 55, Perkin Elmer) (R+ñz et al. 1997) at an emission wavelength of 590 nm. IC50 values (*i.e.*, drug concentrations causing death of 50% of the cells) were then calculated using Prism (GraphPad). Each experiment was carried out in triplicate.

#### 2.5.1.2.3 Microsatellite instability

PCF wild type and knockout mutants were sub-cloned to obtain 10 independent clonal populations growing form each cell line. To do this, the cultures were diluted as 200-50 cells/96 well plate and grown in the presence of conditioned SDM 79 (75% SDM 79, 10%FCS and 15% pre-conditioned media). Several attempts were done to subclone PCF cultures however they did not grow proportional to the number of cells plated on the 96 well plates. Therefore, for every cell line to be subcloned, three plates were set up. Cultures grown for 15 days before the clones were selected. BSF wild type and knockout mutants were plated as 15 and 30 cells/96 well plate and cultures were grown for 5 days before the clones were selected. 10 independent clones were selected and grown for 10 generations in respective medium before DNA was extracted. PCF were grown in 10 ml SDM-79 where as BSF were grown in 25 ml HMI-9. Genomic DNA of each clone was then PCR-amplified with JS2 microsatellite complementary primers as described in section 2.2.5. Samples were resolved for 50 minutes at 100 V by gel electrophoresis as detailed in

section 2.2.6 but 3% low gelling temperature agarose (Sigma, Cat# A4018) was used to resolve the samples.

## 2.5.2 Generation of RNAi lines

RNAi plasmid for a specific gene was generated by ligating a region of ORF of the gene of interest into the cloning site of RNAi vector (vector pZJM obtained from L.Marcello (WTCMP, University of Glasgow)). Vector uses two tetracycline inducible T7 promoters that express a specific gene (of which the ORF has been ligated to the vector) along with phleomycin drug resistance gene as selection for cloning. Vector is linearized by *Not I* and transformed into BSF and PCF cell line specific for RNAi analysis (refer to Section 2.1.1). The constructs integrate into the ribosomal locus of *T. brucei* genome and expression of dsRNA is induced by the addition of tetracycline to the medium. dsRNA is degraded by the RNAi machinery of the cell and expression levels of the target gene are reduced.

Effect of RNAi on mutant clones were analysed in two ways. First the difference in doubling time of RNAi clones were measured upon induction with tetracycline and compared with the non induced RNAi lines. Secondly, RNA was isolated from the induced and non induced RNAi lines, cDNA was made and changes in expression levels were measured by Real Time PCR.

## 2.5.3 Epitope tagging of *T. brucei*

Proteins were C-terminally tagged with either 12 repeats of the Myc epitope or 6 repeats of the HA. Primers were generated against a region of ORF just before the STOP codon. The region was selected to have a unique restriction enzyme recognition site within the ORF fragment that could be used to linearize the DNA. Gene fragments were cloned into *HindIII* and *XbaI* restriction site in either 12 myc plasmid (pISRPIbsd-12myc or 6-HA plasmid (TbMCM-HA gifted by C.Tiengwe (Tiengwe 2012).12myc construct was, linearized by *BmgBI* and transformed into heterozygous knockout mutants to check for the expression levels of the proteins and to localize it in cellular compartments. 6-HA constructs were linearized by either *BsmI* or *BsgI* (see results) and transformed into heterozygous 12 myc tagged knockout clones. Transformation and selection of clones was done as explained in section 2.1.4.

#### 2.5.3.1 Analyzing the tagged protein

Clones were checked if tagging of proteins has interfered with the functionality of the protein. Clones were checked for the presence and integration of the construct was checked by PCR. Functionality of the tagged proteins by measuring the cell survival in presence of DNA damaging agents and comparing to wild type and knockout mutants (see section 2.5.1.2.2).

#### 2.5.3.2 Localization of tagged protein

Tagged proteins were localized using the commercially available antibodies against the epitope tags. Two approaches were used to localize the protein in specific cell compartment: subcellular fractionation (section 2.3.2 ) and IFA (Section 2.4.2). Cell lines with both HA epitope and Myc tag epitope were co-immunoprecipitated as described in Section 2.3.3.

**Table 2-4 List of oligos used in the study**

| PRIMERS | SEQUENCE |
|---|---|
| **FOR KNOCK OUTS** | |
| **MSH2 GENE** | |
| MSH2 5'A-*EcoRI* (F) | 5'--GTGAATTCGCACAGATGTGGAATGAGGG--3' |
| MSH2 5'B-*HindIII* (R) | 5'--CCAAGCTTGTTAACTTGCTGACTACACACCCG--3' |
| MSH2 3'A-*HindIII* (F) | 5'-GGAAGCTTGATATCTGGTGGAGGTGTGAGAAGG-3' |
| MSH2 3'B-*XhoI* (R) | 5' --AACTCGAGCGAGGTACTGAAGTAAGG--3' |
| MSH2 (F) | 5'--AGTCCAGGAGAAAACAGCGC--3' |
| MSH2 (R) | 5'--CCGTTTGCGTTTGTAGCT--3' |
| MSH2-int. (F) | 5'--ACGTCAACGTACGATGGATTCG--3' |
| MSH2-int. (R) | 5'--CACCTCCACCAATGACG--3' |
| MSH2 D2 | 5'--GGAGCATTGGTGTTTGTGTCG--3' |
| **MLH1 GENE** | |
| MLH1 5'A-*EcoRI* (F) | 5' --GGGAATTCTCTTAGATATGGGTATGC--3' |
| MLH1 5'B-*XbaI* (R) | 5'--GGTCTAGAAAATGTGTGAAAGAGCGG--3' |
| MLH1 3'A-*XbaI* (F) | 5'-GGTCTAGAGATATCCTCTTCTTTCTGTCGTGG-3' |
| MLH1 3'B-*XhoI* (R) | 5'--AACTCGAGAGGAAACAAGCCACAAACACGCCG--3' |
| MLH1 (F) | 5'--TTTGTCTGGTGGCAATCG--3' |
| MLH1 (R) | 5'--TCGCTGTCTCCTGTTGAAAGG--3' |
| MLH1-int. (F) | 5'--ATAACAAGGCGGCTGCATCG--3' |
| MLH1-int. (R) | 5'--AACGCTCGAAGACCTTGTACAGC--3' |
| *MLH1* D6 (R) | 5'--CCAGCAACACTACCATCG--3' |
| *MLH1* U1 (F) | 5'--GCATTCAGGTGGTTGTTCAGG--3' |
| **MSH3 GENE** | |
| MSH3-5'A-*SacI* (F) | 5'--CATGAGCTCCTACGGGAAAATTTAGCAAGGG--3' |

| | |
|---|---|
| MSH3-5'B-*NotI* (R) | 5'--CATGCGGCCGCACGGCGGCGTTTGCTCATTTTGC--3' |
| MSH3-3'A-*PacI* (F) | 5'--CATTTAATTAAGAAGTCGAGTCGAATGTGTGACC--3' |
| MSH3-3'B-*XhoI* (R) | 5'--CATCTCGAGCACACACACACTACTACTACGAGAGG--3' |
| MSH3 out (F) | 5'--ACGTGTAGATGGAAAACG--3' |
| MSH3 int. (R) | 5'--GAGTTGCTTGAATGCACATTATCC--3' |
| MSH3 D3 (F) | 5'--CTTCTCAGTTTCGTCACG--3' |
| MSH3 U4 (R) | 5'--ATTACCAACTCAGCCACC--3' |
| **MSH8 GENE** | |
| MSH8-5'A-*SacI* (F) | 5'--CATGAGCTCCGTGTATGTATCGGGTACACCC--3' |
| MSH8-5'B-*NotI* (R) | 5'--CATGCGGCCGCAGGATACCAAGGGTCAGATCTCC--3' |
| MSH8-3'A-*PacI* (F) | 5'--CATTTAATTAAGTGACGCCTTTACCAATGAGTCC--3' |
| MSH8-3'B-*XhoI* (R) | 5'--CATCTCGAGTCTTTGCTTATCCCTCCTGCCG--3' |
| MSH8 out (F) | 5'--TTCTTAGGTATTACCGAAGG--3' |
| MSH6 int. (R) | 5'--TTCAACCCGAACTCACGGTGAGC--3' |
| MSH8 D3 (F) | 5'--CAGTGGTGTCGCTACTTGC--3' |
| *MSH8* U1 (R) | 5'--GGTAGAGAAGAGTAGAAGGG--3' |
| **RAD51 GENE** | |
| RAD51-*HindIII* (F) | 5'--AAGCTTATGAACACTCGCACCAAAAATAAG--3' |
| RAD51-*XBAI* (R) | 5'--TCTAGAGTCCCTAACGTCTCCCACACC --3' |
| **FOR TAGGING** | |
| MSH2-INT.-*HindIII* (F) | 5'--CCCAAGCTTACGTCAACGTACGATGGATTCG--3' |
| MSH2-INT.-*XbaI* (R) | 5'--CCCTCTAGACACCTCCACCAATGACG--3' |
| MSH2-U12 (F) | 5'-ACCTTGCGCAAGGAGTTTCTACC-3' |
| MLH1-INT.-*HINDIII* (F) | 5'--CCCAAGCTTATAACAAGGCGGCTGCATCG--3' |
| MLH1-INT.-*XBAI* (R) | 5'--CCCTCTAGAAACGCTCGAAGACCTTGTACAGC--3' |
| MLH1-U12 (F) | 5'-GTTCTGTAATAGATACCGCAGGG-3' |
| 12 MYC (R) | 5'--AATGACGAACGGGAAATGCC--3' |
| **Co-IP** | |
| MSH5 *HindIII* (R) | 5'--CATAAGCTTGACTGCCTAATAGGTTTTGC--3' |
| MSH5 *XbaI* (R) | 5'--TCTAGAAACACACTCACTGGTCATCACG--3' |
| MSH4 *HindIII* (R) | 5'--AACAAGCTTCGAACAATATTTGCGACGC--3' |
| MSH4 *XbaI* (R) | 5'--TCTAGACTCAGTAGAGGAACCGCATGG--3' |
| **MSI** | |
| JS-2A (F) | 5'--GATTGGCGCAACAACTTTCACATACG--3' |
| JS-2B (R) | 5'--CCCTTTCTTCCTTGGCCATTGTTTTACTAT--3' |
| JS2 A FAM (F) | 5'FAM--GATTGGCGCAACAACTTTCACATACG--3' |

| | |
|---|---|
| K DNA MS FAM (F) | 5'FAM--GTTGCATTTAGAAATAAAAAAGTAG--3' |
| K DNA MS (R) | 5'--GGAAAAAATAATGGGGGGTTTGG--3' |
| VSG 221 (F) | 5'--ATGCCTTCCAATCAGGAGGC--3' |
| VSG 221 (F) | 5'--TGTATCGGCGACAACTGCAG--3' |
| IJ 15 (F) | 5'--GTTAGGTTACGCAAGTCAGT--3' |
| IJ 15 (R) | 5'--GAAACACTCAGTTCCACACC--3' |
| 5L5 (F) | 5'--GTACGTGGTTAACCACAACCTACT--3' |
| 5L5 (R) | 5'--GGAAACTGCTTAAACTTGCGTGAG--3' |
| 2/5 (F) | 5'--ATGGCGTGTATCACATTCGTGATG--3' |
| 2/5 (R) | 5'--CCGTTGGCATTAGGCACAAGTA--3' |
| 18 (F) | 5'--TGTGAGAATGGTACTCACGCGCTG--3' |
| 18 (R) | 5'--CAAGCTTAGCACACAATTCCTGTG--3' |
| **Drug genes** | |
| BSD (F) | 5'--ATGGCCAAGCCTTTGTCTC--3' |
| BSD (R) | 5'--TTAGCCCTCCCACACATAACC--3' |
| PUR A (F) | 5'--TACGAGCGGCTCGGCTTCACCGTCACC--3' |
| PUR B (R) | 5'--TGTGGCGCGTGGCGGGGTAGTCGGC--3' |
| Phleo (F) | 5'--GTGGCTACTGTATTCTTCTTG--3' |
| Phleo (F) | 5'--GTTTCAGGTGCGTCTTTCTTTG--3' |
| **QRT-PCR** | |
| TbCPX (F) | 5'--CGACTTCACGTTTGTGTGCCCCACTGA--3' |
| TbCPX (R) | 5'--TTGGGGATCAATGATGAAAAGACCGCGG--3' |
| TbOGG1 (F) | 5'-TCGGGAACACCTCCATTCC-3' |
| TbOGG1 (R) | 5'-GCTCTGGGTTTTGGCTATCG-3' |
| TbDinB (F) | 5'--GCAGAGTTTGCTCGCATCAG--3' |
| TbDinB ® | 5--CAATAGTGTGGGCATAGCACGAT--3' |
| TbGPI8 (F) | 5'--TCTGAACCCGCGCACTTC--3' |
| TbGPI8 (R) | 5'--CCACTCACGGACTGCGTTT--3' |
| **RNAi** | |
| MSH2 RNAi (F) | 5'--TGCCGGTGGCGATGATA--3' |
| MSH2 RNAi (R) | 5'--AACAGCCAGCCGATGCA--3' |
| MLH1 RNAi (F) | 5'--TTTTGGTGATCTCCCATTGCT--3' |
| MLH1 RNAi (R) | 5'--TCAGTTCATCAAAAGCGCGTAA--3' |

Forward and reverse primers are indicated as (F) and (R) respectively. Restriction sites, if any, were added at the 5' end of the primer and are underlined.

# 3 Role of MSH2 and MLH1 in response to oxidative damage in PCF *T. brucei*

## 3.1 Introduction to mismatch repair in *T. brucei*

Proteins involved in *T. brucei* mismatch repair (MMR) were first characterized by J.S.Bell (Bell 2004). *T. brucei* encodes five MutS homologues, of which three possess all the four conserved domains identified in such proteins that are required for MMR activity; see Sections 1.4.6.3.1.1 and 1.4.6.4. The *T. brucei* MutS homologues were originally called MSH2, MSH3 and MSH8, as they were most homologous in sequence to MSH2, MSH4 and MSH6 proteins in other eukaryotes. MSH8 was so named because the genome had not been sequenced and the predicted protein is small relative to eukaryotic MSH6 orthologues, meaning that it was possible a further MutS protein, most like MSH6, may be revealed. However, no such gene was revealed by genome sequence (Berriman et al. 2005) and MSH8 can now be considered to be the *T. brucei* MSH6 orthologue. *T. brucei* MSH2 is the least conserved in the mismatch interacting domain, also called the mismatch binding domain (Bell 2004;Obmolova 2000) present towards the N terminus. This would be consistent with the other proteins (MSH6 and MSH3) doing the job of recognising mismatches while forming two distinct heterodimers with MSH2, which would then coordinate downstream processes. This central role of MSH2 would suggest a conventional eukaryotic MutS homologue organisation in *T. brucei*, though it has not been tested experimentally.

Only two MutL homologues have been described in *T. brucei*, with both possessing the key conserved domains so far described in MutL homologues; see Sections 1.4.6.3.1.2 and 1.4.6.4. This number of MutL homologues would suggest that *T. brucei* encodes only a single, putative MutLα –like heterodimer. The likely function of the two proteins has been inferred from sequence homology, though not tested experimentally. PMS1 is the likely subunit of the putative MutLα that has the endonuclease activity, based on the conservation of this domain present at its C-terminus. MLH1 has an extended, conserved C-terminal domain that is seen in other MLH1 proteins, termed the carboxy terminal homology motif (Pang, Prolla, & Liskay 1997).

Of the five genes proposed to be involved in *T. brucei* MMR, only *MSH2* and *MLH1* have been further characterized to date, and this work has been limited to genetic analysis in bloodstream form (BSF) parasites. *T. brucei* MSH2 (Tb927.10.11020) is 2856 bp in length and positioned at chromosome 10, whereas MLH1 (Tb427.08.6840) is 2664 bp in length and positioned at chromosome 8. Deletion of either of these genes revealed their contribution to the presence of functional nuclear MMR in *T. brucei*, since homozygous (-

/-) mutants were found to display increased tolerance to the alkylation N-methyl-N'-nitro-N-nitrosoguanidine (MNNG) and increased rates of nuclear microsatellite sequence changes (microsatellite instability) (Bell 2004). Both these phenotypes have been associated with non-functional MMR in other eukaryotes (Dewind 1995;Sinicrope 2012;Svrcek 2010). In addition to this, the efficiency of recombination has been analysed in *msh2-/-* BSF mutants relative to MMR functional cells and it has been shown that recombination between imperfectly homologous DNA molecules is more efficient when MSH2 is absent (Barnes & McCulloch 2007;Bell 2003), at least when the DNA molecules are rather long (Datta et al. 1996;Selva et al. 1995;Barnes 2007). This is consistent with MMR constraining *T. brucei* recombination to occur only between well-matched DNA sequences, as has been seen in other eukaryotes and bacteria (Datta 1996;Selva 1995).

Several further studies on MMR in both *T. brucei* and *T. cruzi* have prompted the part of my project described in this chapter, where I have tried to generate and characterize MMR mutants in procyclic form (PCF) *T. brucei,* and to elucidate the role of MSH2 and MLH1 in protection of *T. brucei* against oxidative damage. Different strains of *T. cruzi* have been shown to display sequence polymorphisms in *MSH2*, which could be mapped to the different lineages of this parasite that have been described (Augusto-Pinto 2003). Remarkably, the same study showed that the different *T. cruzi* strains display differing levels of microsatellite instability after growth in hydrogen peroxide ($H_2O_2$) and differing levels of tolerance to cisplatin, each phenotype suggestive of varying basal levels of MMR activity, perhaps related to the MSH2 polymorphisms. In *T. brucei*, *MSH2* sequences from a number of isolates derived of *T. b. brucei, T. b. gambiense* and *T. b. rhodesiense* sub-species show much lower levels of sequence change compared with those seen in *T. cruzi* (Barnes 2006). Nonetheless, PCF cells of these different *T. brucei* isolates appeared to display variations in sensitivity to MNNG, methyl methane sulphonate and $H_2O_2$ (Barnes 2006). However, whether this can be explained by differing MMR levels has not been demonstrated. To assess the relationship between MMR and oxidative damage, suggested by the work of Augusto-Pinto et al (2003) in *T. cruzi*, the sensitivities of BSF *T. brucei msh2*-/- and *mlh1*-/- mutants to $H_2O_2$ were tested, revealing that loss of MSH2, but not of MLH1, rendered the parasites sensitive to this oxidative stress (Machado-Silva 2008). When *T. cruzi* MSH2 protein was expressed in the *msh2*-/- mutant cells, it was capable of complementing the $H_2O_2$ sensitivity phenotype (to a similar extent to re-expression of *T. brucei* MSH2) but was unable to complement the MNNG tolerance defect. These data appear to suggest that MSH2 acts distinctly from MLH1 in the *T. brucei* response to oxidative stress and raises the question of whether such a role involves MMR, or any

MMR component other than MSH2. The most recent study in this area, by Campos et al (2011), has built on these findings, revealing further complexities in the contribution of MSH2 to oxidative stress. This work showed that *MSH2* heterozygous *(*+/-) mutants in *T. cruzi* display increased accumulation of 8-oxoG after $H_2O_2$ treatment relative to wild type cells. Furthermore, the 8-oxoG DNA damage was seen to be more abundant in the kinetoplast than in the nucleus, which appears consistent with the finding that *T. brucei msh2-/-* mutants display increased loss of kinetoplast DNA relative to wild type cells before and after $H_2O_2$ treatment. These data may suggest a mitochondrial function for MSH2, which had not previously been detected, though direct evidence for this is lacking.

Given the above work, it was decided to attempt to generate *MSH2* and *MLH1* mutants in *T. brucei* PCF cells. PCF cells not only inhabit a different environment compared to BSF cells, they also have modified intracellular metabolism. The most pronounced difference in metabolism is the presence of an extensively functioning mitochondrion in PCF cells, relative to the more truncated mitochondrial metabolism in BSF cells {Colasante, 2009 223 /id}. In PCF cells more energy is thus produced in the mitochondrion. This most likely leads to increased production of reactive oxygen species (ROS), which are mainly produced in mitochondria as a by-product of oxidative phosphorylation. As discussed previously (Section 1.4.7.1), ROS are a pronounced source of DNA mismatches, and MMR is one of the key mechanisms to repair this lesion and other damage ROS cause. Given this increased production of ROS in PCF cells, leading to increased oxidative DNA damage (along with the other deleterious effects of oxidative stress), it may be hypothesised that the role that MSH2, and perhaps MMR, plays in responding to this damage assumes a more crucial role in PCF *T. brucei* cells relative to BSF cells. Indeed, it is possible that such a role may be essential, questioning whether or not MMR, or specifically MSH2, mutants would be viable in *T. brucei* PCF cells, as they are in the BSF. Indeed, *msh2-/-* mutants have to date not been successfully generated in *T. cruzi,* where even the loss of a single allele in *MSH2*+/- cells results in observable sensitivity to $H_2O_2$ (Campos 2011 ). It is also of relevance to note the observation that wild type *T. brucei* PCF cells are ~30 fold more sensitive to $H_2O_2$ (Barnes 2006) than BSF cells (Barnes 2006;Machado-Silva et al. 2008). This may be because of the greater use of mitochondrial respiration in PCF cells, but may also be a consequence of differences in the culture media in which the two life cycle stages are grown.

# 3.2 Results

## 3.2.1 Generation of *MSH2* and *MLH1* null mutants

### 3.2.1.1 Strategy for the generation of knock out mutants

In order to attempt to make null mutants of *MSH2* and *MLH1* in PCF *T. brucei*, constructs for homologous recombination-based genome integration that had been generated previously for the BSF mutants were used (Bell 2004; Figure 3-1). Briefly, the constructs were made using primers designed to PCR-amplify 5' and 3' untranslated regions (UTRs) immediately flanking the ORF of the genes. These served as recombination substrates for homologous integration into the genome and were cloned into pBluescriptSKII using the restriction sites at the ends of the primers (as shown in Figure 3-1). Between these flanks, drug resistance cassettes were then cloned that carried genes encoding resistance to the antibiotics blasticidin (*BSD*) or puromycin (*PUR*); in each case these ORFs were further flanked by tubulin processing signals that allow trans-splicing and polyadenylation to generate mature mRNAs. For introduction into the parasites, linear products containing the knockout cassettes were produced using *Xho*I and *Not*I restriction digestion. If the 5' and 3' UTRs are used as sequences of homology then integration results in the ORF being replaced by the drug resistance cassette. Since the cassettes do not contain any promoter sequence, *T. brucei* expresses the integrated drug resistance genes using the endogenous promoter of the replaced *MSH2* or *MLH1* gene. Note that one drawback of these constructs is that tubulin sequences are positioned 5' and 3' of the *BSD* and *PUR* genes, and it is possible that these elements may guide integration of the antibiotic resistance genes into tubulin, rather than into the MMR genes based on the expected UTRs.

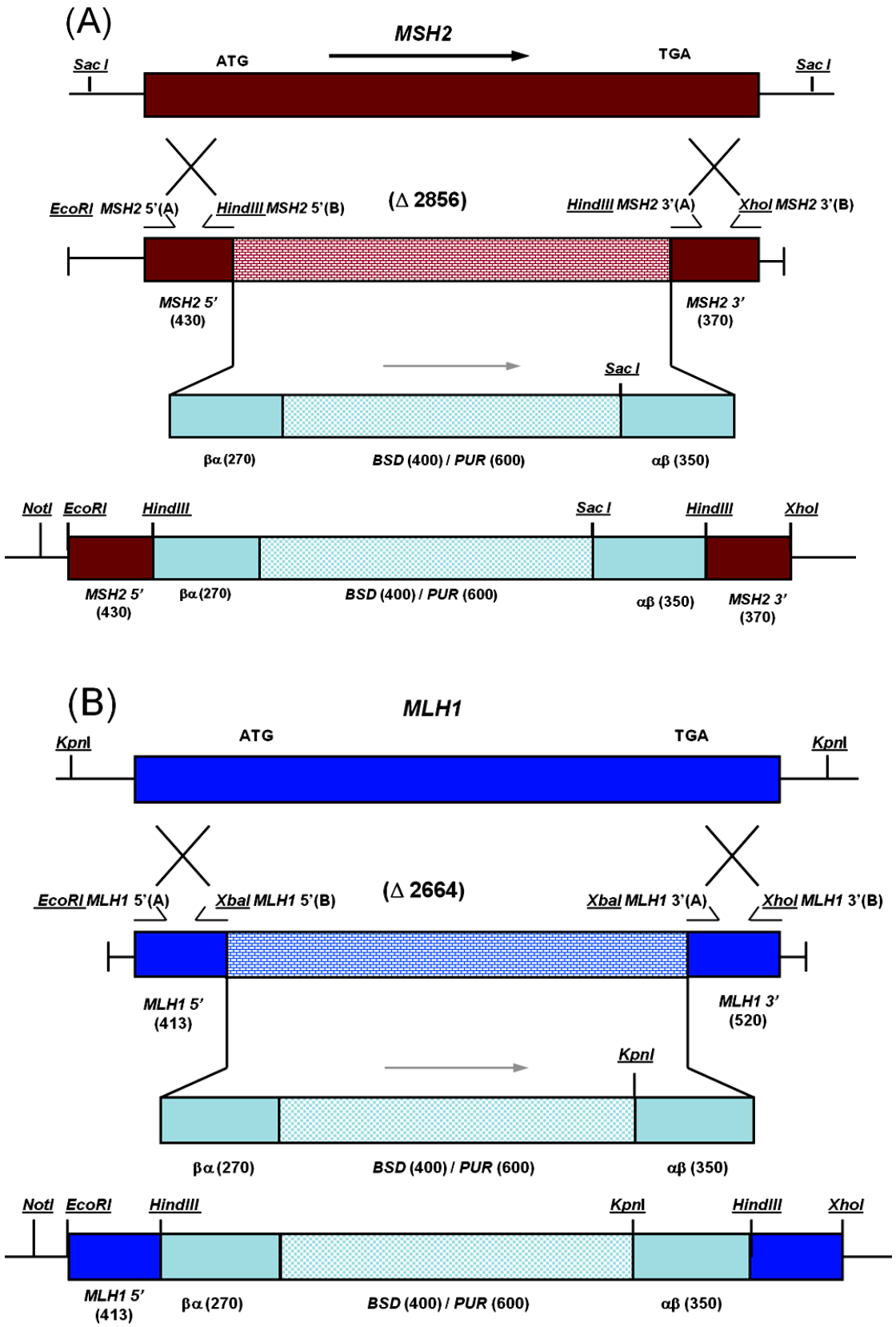


**Figure 3-1 Constructs for the generation of *MSH2* and *MLH1* mutants.**

*MSH2* (A) and *MLH1* (B) loci are indicated as coloured boxes (red and blue, respectively). 5' and 3' UTR regions used for integration of knockout constructs are indicated (crosses) and the primers used to PCR-amplify these flanking regions are shown by corresponding arrows; the size of amplified product (in bp) is denoted in brackets. Two constructs were generated for each gene, where the ORF is replaced (the deleted sequence size is indicated) with either blasticidin (*BSD*) or puromycin (*PUR*) ORFs flanked by β-α tubulin sequences (sizes indicated). Upon transformation

into *T. brucei*, ORF is replaced by the resistance cassettes and the expected arrangement of the mutated loci is shown.

#### 3.2.1.2 Transformation of wild type Lister 427 PCF *T. brucei* and generation of *MSH2* and *MLH1* mutants

PCF cells of the *T. brucei* Lister 427 strain were grown to a density of $1x10^7$ cells.ml$^{-1}$ and ~$2.5x10^7$ cells were used per transformation, which was performed using 5 μg of *Xho*I and *Not*I-digested knockout constructs (Section 3.2.1.1). For transformation, plasmid DNA was produced from *E. coli* using Qiagen miniprep (as described in Section 2.2.2) and then linearized with *XhoI* and *NotI (EcoRI* present at 5'A primer cannot be used as the tubulin region also contains *EcoRI* sites, so *NotI* was used instead as it is present in PBSKII upstream to the 5'UTR). Digested DNA was purified using the PCR purification kit (Qiagen; see Section 2.2.3) and eluted in 30 μl. Parasites were transformed with 5 μg DNA as described in Section 2.1.4.1. For each transformation a control was done with no template DNA. Parasites were allowed to recover from transformation by growth overnight in non-selective medium, and were then cloned in media containing the appropriate antibiotic. Two independent putative *MSH2* and *MLH1* heterozygous (+/-) cell lines were first generated, one using the *BSD* construct (blasticidin was added at 10 μg.ml$^{-1}$) and the other using the *PUR* construct (puromycin added at 1 μg.ml$^{-1}$). For each gene, and for each construct, three antibiotic transformants from each transformation were selected and integration of the constructs confirmed by PCR using the primers as used in Figure 3-2 and Figure 3-3, respectively (data not shown). Doubling times of the three putative *MSH2* and *MLH1* mutants were calculated by diluting them to 5 x $10^5$ cells.ml$^{-1}$ and counting densities every 24 hrs to determine if any clones grew differently from others derived from the same transformation; no growth differences were obvious either between the clones generated, whether *BSD* or *PUR* integrations, for *MSH2* or *MLH1* (data not shown).

To attempt to generate null mutants, one of the three putative +/- clones for each of *MSH2* and *MLH1* was selected for further analysis. In each case, the basticidin resistant clones were selected and transformed with the *PUR* resistance cassettes. In order to attempt to recover homozygous (-/-) mutants, the transformed cells were selected in media containing both the drugs, using 10 μg.ml$^{-1}$ of blasticidin and 1 μg.ml$^{-1}$ of puromycin. Generation of homozygous mutants took a couple of attempts using different concentrations of selective drug (Table 3-1, and data not shown). 3 initial attempts failed to recover any null mutant transformants, giving the thought that it might not be possible to generate null mutants.

However, after a further attempt, several clones were collected that were resistant to both drugs and yielded mutants (see below).

**Table 3-1 Summary of attempts made to generate MSH2 and MLH1 KO mutants.**

| Attempts | Cells transformed | DRUGS (µg.ml$^{-1}$) | | DILUTION | No. of clones recovered | Clones Analysed |
|---|---|---|---|---|---|---|
| | | BSD | PUR | | | |
| 1 | 2.5 x 10 | 5 | 1 | 50 µl/20 ml , 1 ml/20 ml | 0/96 | - |
| 2 | 2.5 x 10 | - | 1 | 200 µl/20 ml , 2 ml/20 ml | 40/96 | 6 (none +ve) |
| 3 | 2.5 x 10 | 2.5 | 0.2 | 200 µl/20 ml , 2 ml/20 ml | 96/96 | - |
| 4 | 3.5 x 10 | 10 | 1 | All cells transformed were plated by serial dilution | 20/96 | 6 (All +ve) |

After outgrowth from the transformation, the putative mutants were grown initially on half the drug concentration and then the drug concentration was gradually increased to 10 µg.ml$^{-1}$ basticidin and 1 µg.ml$^{-1}$ puromycin. However, after further couple of generations, mutants started to grow on drugs with no apparent growth defect. Cultures were grown on drugs for further 10 generations before genomic DNA was made and PCR was used to analyse the transformants, as described in Section 2.2.5.

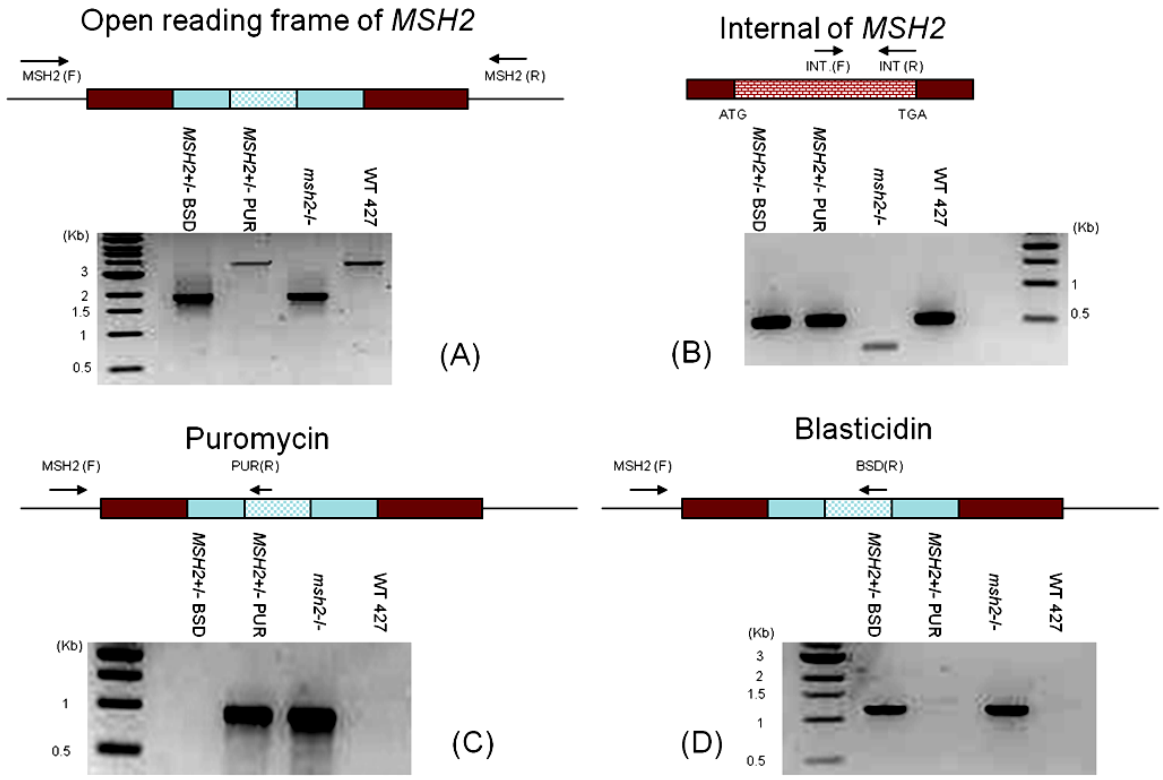


**Figure 3-2 PCR analysis of *MSH2* mutants.**

Different sets of primers were designed for PCR to distinguish between wild type (WT 427), *MSH2+/-BSD*, *MSH2+/-PUR* and *msh2-/-* cells. In all cases arrows denote what regions of the wild type or mutated loci are recognised by the different primers, which are labelled. (A) Primers MSH2 (F) and MSH2 (R) were designed upstream to the recombining 5' and 3' UTRs in the knockout constructs, testing for PCR-amplification of the intact *MSH2* ORF or the mutated loci in which *BSD* or *PUR* had integrated. (B) MSH2 int (F) and MSH2 int (R) primers were used to attempt to PCR-amplify an internal ~500 bp region of the *MSH2* ORF. (C) To test for integration of the puromycin resistance cassette into *MSH2*, PCR is shown with the primers MSH2 (F) and PUR (R), which bind to sequence upstream to the 5' UTR flank and within the PUR gene, respectively. (D) To test for integration of the blasticidin resistance cassette into *MSH2*, PCR is shown with the primers MSH2 (F) and BSD (R), which bind to sequence upstream to the 5' UTR flank and within the BSD gene, respectively. In all gels size markers are shown and their sizes are indicated.

In order to test for the loss of the *MSH2* or *MLH1* ORF in blasticidin and puromycin-resistant transformants, and to thus determine if they are null (knockout) mutants, PCR was performed on genomic DNA using several sets of primers. Primers were designed not only to test for the replacement of the ORF with the resistance cassettes, but also the expected orientation of the integrated constructs. Analysis of the putative *msh2*-/- mutants is shown in Figure 3-2. For all the reactions, DNA from wild type (untransformed) Lister 427 cells, and from the *MH2+/- BSD* and *MSH2+/-PUR* cells, was PCR-amplified in comparison with the putative *msh2* -/- mutants. The PCR analysis shows that in the *MSH2*+/- mutants it is possible to PCR-amplify a product of the predicted size for the expected antibiotic resistance cassettes, while in the putative *msh2*-/- mutants both antibiotic cassettes could be PCR-amplified; in contrast, no PCR product was generated from the wild type cells

(Figure 3-2 C and D). In each case the forward primer used was specific to sequence outside the recombining region (upstream of the UTR flanks), whereas the reverse primer used was specific to the drug resistance gene. The *BSD* resistance cassette was PCR-amplified using a reverse primer specific to the 3' end of the BSD ORF. A product of ~1.1 kb was PCR-amplified only in *MSH2+/-BSD* and *msh2-/-* samples, which is the size expected (1156 bp). For the *PUR* resistance cassette, which is difficult to PCR-amplify due to high GC content, the reverse primer was designed to be complementary to the region closer to the 5' end of the ORF so that it needs only to PCR-amplify a small part of rather than the whole gene. PCR products of ~0.8 kb were observed in the *MSH2+/-PUR* and *msh2-/-* cells (the expected size was 856 bp).

To ask if the *MSH2* ORF was present, Figure 3-2 A shows an attempt to PCR-amplify the ORF with primers that flank the UTRs used in the constructs, while Figure 3-2 B shows an attempt to PCR a 500 bp fragment within the ORF. In the *MSH2*+/- *BSD* mutant and in the putative *msh2-/-* mutant, PCR-amplification by the primers outside the recombining region generated a product smaller in size than seen from the wild type cells or from the *MSH2*+/- *PUR* mutants. The size of the smaller band (~1.9 kb) is consistent with that expected (1950 bp) for the loci generated when the *BSD* resistance cassette replaces the ORF (PCR product 3.786 kb). Though the wild type allele should be present in the *MSH2+/- BSD* mutants, no PCR-amplification of this size was seen, possibly because the smaller size of the PCR-product from the mutant copy is preferred for amplification. In contrast, in *MSH2+/-PUR* mutant, PCR product is only seen from the wild type allele (3.786 kb), with the expected product from the PUR-mutated allele (2150 bp) not seen. This is likely due to the *PUR* ORF being rich in GC content, and thus the wild type copy is preferentially PCR-amplified. These observations most likely explain why in the putative *msh2 -/-* cells only a product from the *BSD*-mutated allele is PCR-amplified, despite the fact that Figure 3-2 C shows that the *PUR*-mutated allele is present. PCR with the flanking primers cannot, however, determine if the *MSH2* ORF is absent in the putative *msh2 -/-* cells. However, Figure 3-2 B shows that primers binding to the internal region of the *MSH2* ORF do not PCR-amplify a product of the expected size from *msh2 -/-* DNA, whereas a product of ~500 bp was PCR- amplified from the *MSH2+/- BSD*, *MSH2+/-PUR* and wild type cells. Taken together, the above PCR analysis confirms that the *BSD* and *PUR* constructs have integrated as expected, and that the *MSH2* ORF appears to have been removed in the putative *msh2-/-* mutants, suggesting that *MSH2* knockout (null) mutants were successfully made in PCF cells of *T. brucei* .

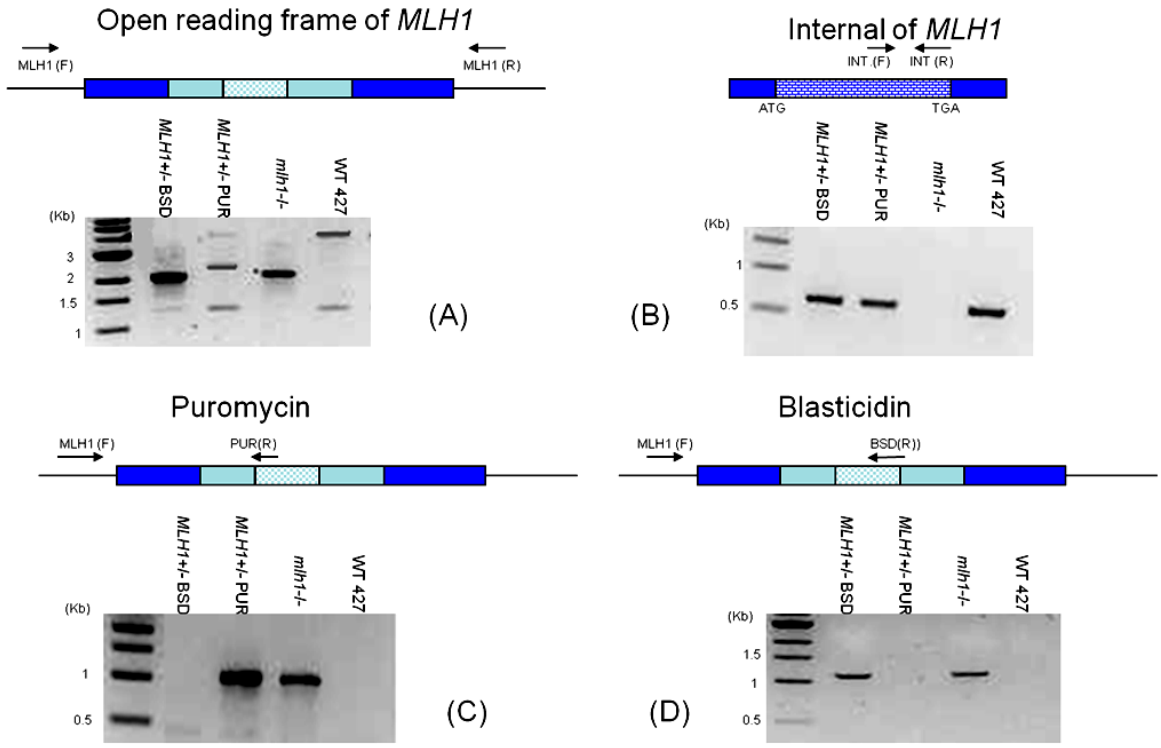


**Figure 3-3 PCR analysis of *MLH1* mutants.**

Different sets of primers were designed for PCR to distinguish between wild type (WT 427), *MLH1+/-BSD*, *MLH1+/-PUR* and *mlh1-/-* cells. In all cases arrows denote what regions of the wild type or mutated loci are recognised by the different primers, which are labelled. (A) Primers MLH1 (F) and MLH1 (R) were designed upstream to the recombining 5' and 3' UTRs in the knockout constructs, testing for PCR-amplification of the intact *MSH2* ORF or the mutated loci in which *BSD* or *PUR* had integrated. (B) MLH1 int (F) and MLH1 int (R) primers were used to attempt to PCR-amplify an internal ~900 bp region of the *MLH1* ORF. (C) To test for integration of the puromycin resistance cassette into *MLH1*, PCR is shown with the primers MLH1 (F) and PUR (R), which bind to sequence upstream to the 5' UTR flank and within the PUR gene, respectively. (D) To test for integration of the blasticidin resistance cassette into *MSH2*, PCR is shown with the primers MLH1 (F) and BSD (R), which bind to sequence upstream to the 5' UTR flank and within the BSD gene, respectively. In all gels size markers are shown and their sizes are indicated.

Figure 3-3 shows equivalent PCR analysis to that described above for *MSH2*, but this time directed towards testing for the generation of *mlh1-/-* null mutants. Figure 3-3 A and B show attempts to PCR-amplify the *MLH1* ORF in wild type, *MLH1+/-BSD*, *MLH1+/-PUR* and putative *mlh1-/-* cells. Using flanking primers to the knockout cassettes, a PCR product of ~3.7 kb was PCR-amplified from wild type and *MLH1+/-PUR* genomic DNA, consistent with the expected size of the un-mutated allele (3715 bp). In addition, a further band of ~ 2.1 kb was generated from the *MLH1+/-PUR* DNA, which is consistent with the size of the allele when *PUR* replaces the *MLH1* ORF (2271 bp). Although also it is expected that the *MLH1* ORF should PCR-amplify from the *MLH1+/-BSD* cells, only a band of ~1.9 kb was seen, of the size expected for the *BSD*-mutated allele (2071bp). Loss of the *MLH1* ORF in the putative null mutants is confirmed by the PCR of an ORF-internal fragment, where a product of ~900 bp was seen in all cell lines except *mlh1-/-*. Figure 3-3

C and D show PCR analysis that confirmed the correct integration of the drug resistance cassettes. The forward primer used was specific to upstream of the ORF, whereas the reverse primer was specific to the drug resistance gene (refer to Figure 3-3 C and D). To confirm the presence of the blasticidin resistance cassette, the reverse primer was designed to the 3' region of the *BSD* ORF. A ~1.1 kb PCR product was amplified from *MLH1+/-BSD* and *mlh1-/-* , consistent with the expected size (1153 bp) of the mutated allele. The reverse primer for PUR was close to the 5' of the ORF so that it does not PCR-amplify whole of the puromycin gene, as it is rich in GC content and thus sometimes get difficult to PCR-amplify. A specific 0.9 kb band was observed in *MLH1+/-PUR* and *mlh1-/-* cells, compared with the expected product of 853 bp. These data suggest that an *mlh1*-/- null mutant has been generated in PCF Lister 427 *T. brucei*.

The above genomic DNA PCRs confirm the loss of ORF and replacement with respective resistance cassettes for both the MMR genes. To further ensure that gene is not being expressed in the null mutants, reverse transcriptase PCR was performed. Total RNA samples were prepared from wild type cells and from +/- and -/- mutants and were first checked for the presence of any contaminating genomic DNA by performing PCR amplification with primers recognising *RAD51*, a gene that should be unaffected by the MMR mutation events; this is shown in Figure 3-4 A. The RNA samples were then reverse transcribed to make cDNA using high capacity RNA-to-cDNA master mix (Applied Biosystems, see Section 2.2.10) and the resulting cDNA PCR-amplified with primers recognising *RAD51* as a control to check for the conversion of RNA to cDNA in all the samples; this is shown in Figure 3-4 B and in each case where PCR-amplification was expected to occur a band of the expected size (1122 bp) was seen. Having performed these controls, the cDNA samples were then PCR-amplified with primers binding specifically to the ORF of either *MSH2* or *MLH1*, as shown in Figure 3-4 C and 3-4D, respectively.

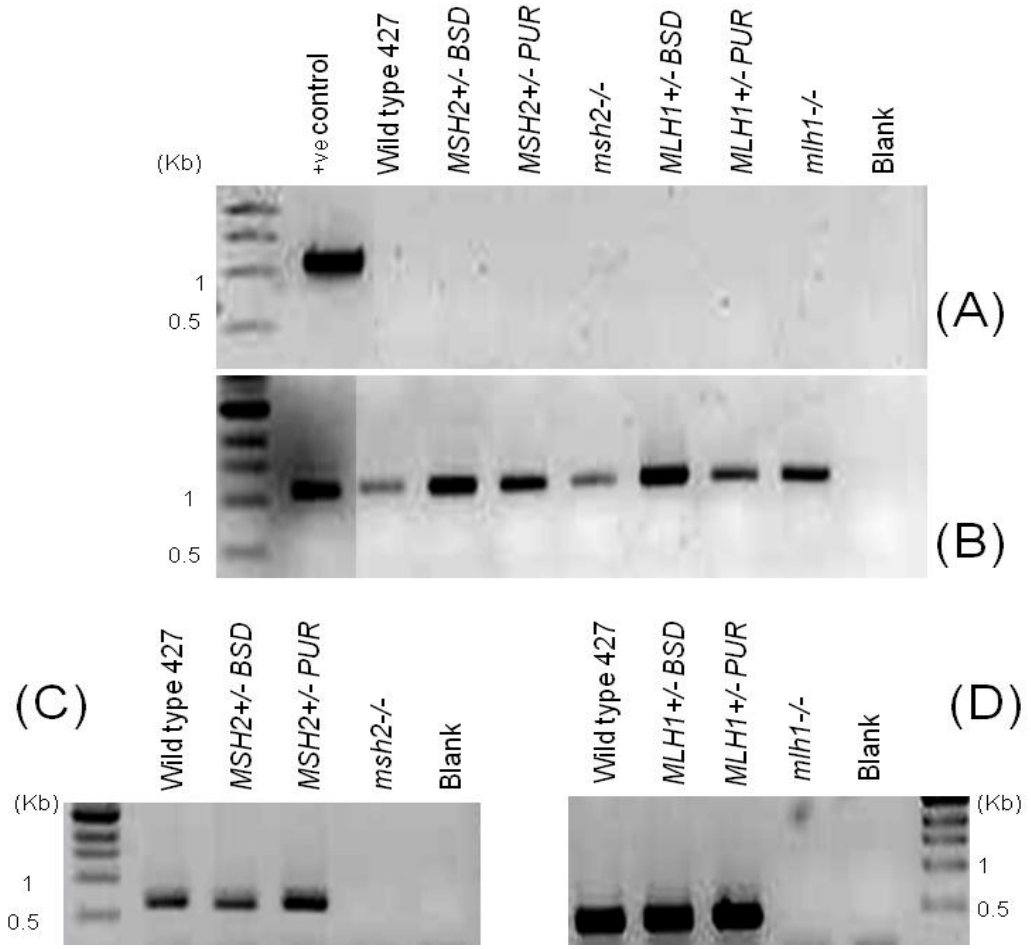


**Figure 3-4 RT-PCR analysis of PCF MMR mutants.**

Agarose gels are shown of reverse transcriptase (RT) PCRs to check for loss of mRNA in procyclic form *T. brucei* MMR knockout mutants (labelled -/-), compared with wild type cells and heterozygous (+/-) mutants (A) PCR is shown from RNA samples of wild type and mutants PCR-amplified with *RAD51* primers (RAD 51 (F) and RAD 51 (R)); genomic DNA from wild type *T. brucei* was used as a positive control for the reaction, and blank is a control PCR with water as template. (B) *RAD51*PCR is shown from cDNA generated from the RNA used from the samples shown in A .(C) PCR is shown using cDNA from wild type and *MSH2* mutants and primers MSH2-D2 (F) and MSH2-int (R). (D) PCR is shown using cDNA from *MLH1* mutants and primers MLH1-U1 (F) and MLH1-D6 (R). In all gels markers are shown and selected sizes indicated.

This reverse transcriptase PCR analysis demonstrates that each MMR null mutant has lost the expression of mRNA of the expected gene, while mRNA for both *MSH2* and *MLH1* could be detected from wild type cells and from heterozygous mutants that preceded the generation of the -/- mutants; for *MSH2* a PCR-product of 730 bp was expected and for *MLH1* a product of 471 bp.

## 3.2.2 Phenotypic analysis of mismatch repair activity in the MMR mutants

In order to test whether the loss of *MSH2* and *MLH1* results in MMR deficiency in PCF *T. brucei* in the same manner as described previously in BSF cells, the two -/- mutants were

assayed for a number of phenotypes before the role of the gene products in response to oxidative stress was analysed. For all the phenotypic analysis described below, cultures were grown on their respective drugs, as used for the selection of transformants, for at least 3 days before assays were performed. During the analysis none of the cell lines were grown on antibiotics to ensure that any effect observed was only due to the loss of the gene and of the mutagen, if applied, and was not due to alterations to growth due to antibiotic selection.

#### 3.2.2.1 *In vitro* growth analysis

The population doubling time of wild type and MMR mutants was first analysed to determine if mutation of *MSH2* or *MLH1* causes any gross defects in the growth of PCF cells. *MSH2* and *MLH1* mutants in BSF cells do not show any such defect (Bell et al. 2004). This is also required to allow any such defect, if present, to be taken into account when performing further assays. As the three *MSH2*+/- and three *MLH1*+/- clones appeared equivalent to each other by growth analysis and by the PCR (data not shown), the following cell lines were compared in the analysis below: wild type Lister 427, *MSH2+/-(MSH2::BSD), msh2-/- (MSH2::BSD::PUR), MLH1+/-(MLH1::BSD)* and *mlh1-/-(MLH1::BSD::PUR).*

To compare *in vitro* growth rates, 5 ml cultures were inoculated at a cell density of 5 x $10^5$cells.ml$^{-1}$ and cell densities were counted using a haemocytometer (Bright-line, Sigma) at 24, 48 and 72 hours subsequently. Three replicates of this analysis were performed. These data are graphed in Figure 3-5, and doubling times for all the cell lines were calculated and are presented in Table 3-2.

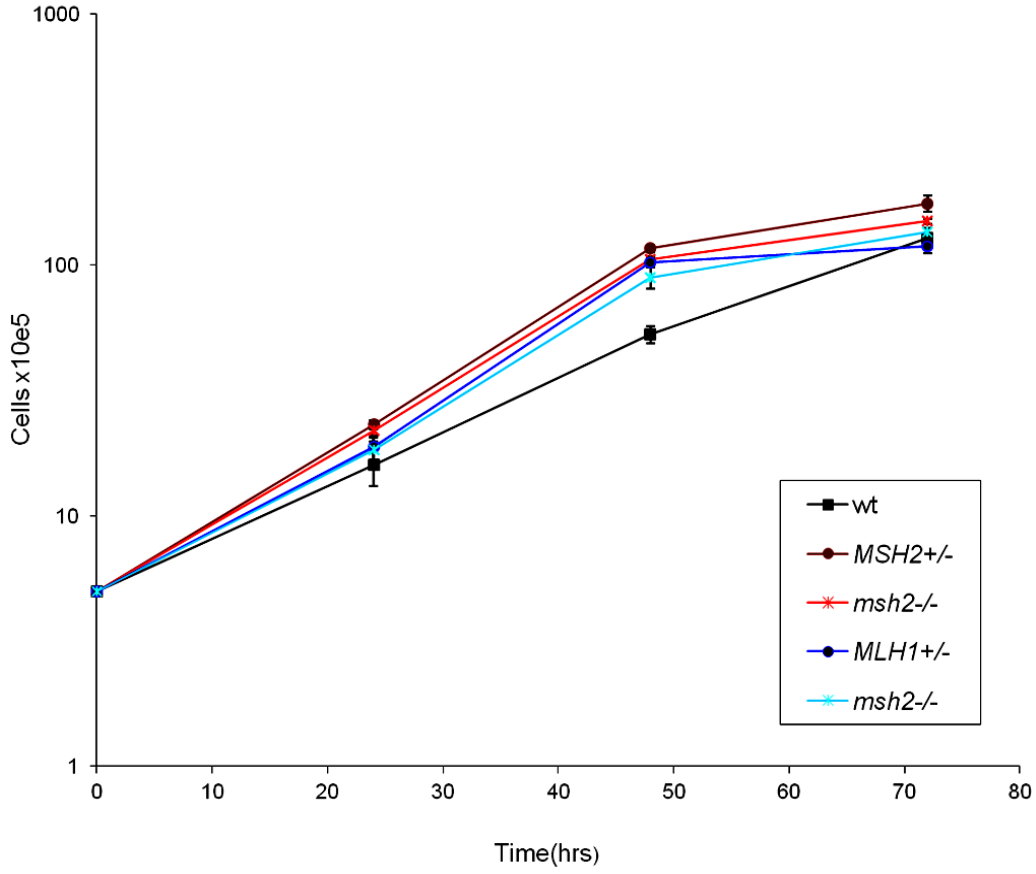


**Figure 3-5 Growth curve of *T. brucei* PCF wild type cells and MMR mutants.**

PCF wild type, *MSH2*+/-, *msh2-/-*, *MLH1*+/-, and *mlh1-/-* cells were inoculated at a density of $5x10^5$ cells.$ml^{-1}$ in 5 ml of media and cell densities counted at 24 hour intervals over a period of 72 hours using haemocytometer. Values show the mean cell densities at each time point, and vertical bars denote standard deviation from three replicates.

**Table 3-2 Population doubling time of wild type PCF *T. brucei* and MMR mutants *in vitro***

| Cell line | | | | | |
|---|---|---|---|---|---|
| | WT | *MSH2+/-* | *msh2-/-* | *MLH1+/-* | *mlh1-/-* |
| Doubling time | 15.49 | 14.13 | 14.8 | 15.89 | 15.24 |

From the growth curve shown in Figure 3-5 and the calculated population doubling times shown in Table 3-2, it is evident that deletion of either one or both the alleles of *MSH2* or *MLH1* had no detectable effect on growth. Thus, MMR mutation does not cause any clear increase or decrease in growth rate, similar to what is seen in BSF cells (Bell 2004). Although the mutants seem from the graphical data to grow somewhat more quickly in comparison to the wild type cells, this could be because mutants were recently cloned whereas the wild type cells were not.

### 3.2.2.2 Tolerance to alkylation damage

Alkylating agents generate DNA adducts by covalent interaction of alkyl groups with DNA. Alkylating mutagens frequently introduce alkyl group to Guanine (G), which covalently binds to 6$^{th}$ carbon of guanine molecule forming O$^6$-alkylG (Warren 2006). Several different alkylating agents introduce different alkyl groups, which can be repaired by several repair pathways. As discussed in Section 1.4.1, alkylated bases are most frequently repaired by a direct repair mechanism involving alkyl guanine transferase (AGT). However, NER and MMR are two alternate pathways that are shown to be involved in repair of alkylation damage if AGT is either less abundant or cells are under alkylation stress (Aquilina 1998). NER is involved in the repair of bulky alkyl adducts, such as O$^6$-propylG, whereas MMR is important in the repair of smaller adducts such as O$^6$-methylG (Mazon 2010).

O$^6$-methylG, though not very abundant in cells, induces both mutagenesis and cytotoxicity. O$^6$-methylG can pair with either cytosine (C) or thymine (T) during replication and thus introduce G:C-T:A transition mutations (Warren 2006). Provided O$^6$-Mg is methylated in the nucleotide pool and incorporated in the daughter strand during replication, MutSα recognizes O$^6$-mG-T lesions and efficiently repairs it. However, MMR could not repair the lesion if O$^6$-mG is in the template and T is paired opposite to O$^6$-mG. In this case, O$^6$-mG-T mismatch is recognized by MMR but not repaired (Duckett 1996;Griffin 1994). This activity of MMR is best explained by a 'futile cycle'. Since O$^6$-mG is present in the template, MMR excises the misincorporated T. However, upon DNA resynthesis O$^6$-mG is likely to pair with C or T again (Figure 3-6), which would lead to repeated cycles of MMR. This results in unpaired O$^6$-mG and subsequently DNA breaks followed by cell death (Aquilina 1999;Bell, Harvey, Sims, & McCulloch 2004;Claij 2002;D'Atri 1998;Griffin 1994;Karran 1994;Toft 1999). This process is avoided in MMR-deficient cells, which allow continuing replication with the mutated base. This phenomenon is termed as 'Methylation tolerance' and is a character of impaired MMR machinery (Claij 2002;Dewind 1995;Karran 1982). Resistance to increased cellular levels of alkylating agents has been termed as a marker phenotype of MMR mutants and has been observed in several organisms, including BSF *T. brucei* (Bell 2004), mouse cells (Dewind 1995;Karran 1994) *E. coli* (Karran 1982) and human cells (Claij 2002;Karran 1994).

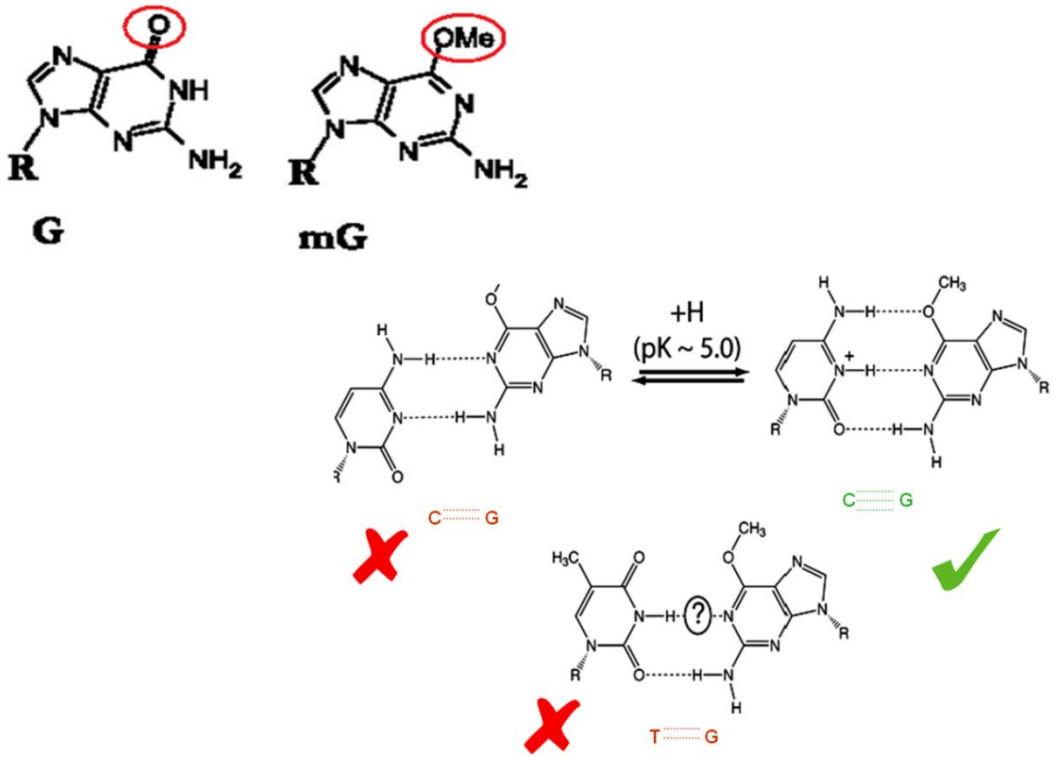


**Figure 3-6 DNA lesions caused by MNNG.**

Upon DNA methylation, MNNG causes $CH_3$ to be added to the oxygen (O) at 6$^{th}$ carbon of Guanine (G) and forms 6 methyl guanine ($O^6$-methylG; meG). $O^6$-methylG can base pair with cytosine(C) with a normal triple hydrogen bond, or aberrantly with double hydrogen bond. Alternatively, it can aberrantly pair with thiamine (T), resulting in transition mutation or can result in cytotoxicity if acted upon by MMR. Figure adapted from (Warren, Forsberg, & Beese 2006).

The methylating agent used for this study is *N*-Methyl-*N'*-Nitro-*N*-Nitrosoguanidine (MNNG), which promotes the formation of $O^6$-methylG (Zhang 2000). Previous work, using a clonal survival assay, has shown that BSF *T. brucei msh2*-/- and *mlh1*-/- cells display greater survival when grown in the presence of MNNG than wild type cells (Bell 2004). Here, sensitivity to MNNG was first assayed by measuring the metabolism of Alamar Blue (Resazurin), which has been used as an indicator of cell growth in several *T. brucei* studies (Barnes 2006;Dobson 2011). Alamar Blue is a blue, non-flourescent dye and redox indicator, which is reduced in growing, metabolising cells into the pink, fluorescent compound Resofurin (O'Brien 2000). The extent of conversion can be measured with a spectrometer and has been shown to correlate with the number of proliferating cells in culture. PCF wild type Lister 427, *MSH2* +/-, *msh2*-/-, *MLH1* +/- and *mlh* -/- cells were examined, as well as wild type TREU 927 PCF, a distinct strain of *T. b. brucei* to Lister 427 cells. PCF cultures were grown from a starting density of 5 x $10^5$.ml$^{-1}$ in media containing doubling dilutions of MNNG from 400 µM to 0.39 µM, in 96-well tissue culture plates (200 µl of cell culture per well). After 48 hours, 20 µl of Alamar Blue was added to each well and fluorescence measured after a further 24 hours of growth.

Fluorescence was measured by a luminescence spectrometer (LS 55, Perkin Elmer) at an emission wavelength of 590 nm. Fluorescence was then plotted relative to the MNNG concentration and IC50 values (drug concentrations causing death of 50% of the cells) were then calculated using Prism (GraphPad). Each experiment was carried out in triplicate. The IC50 values are shown in Figure 3-7.

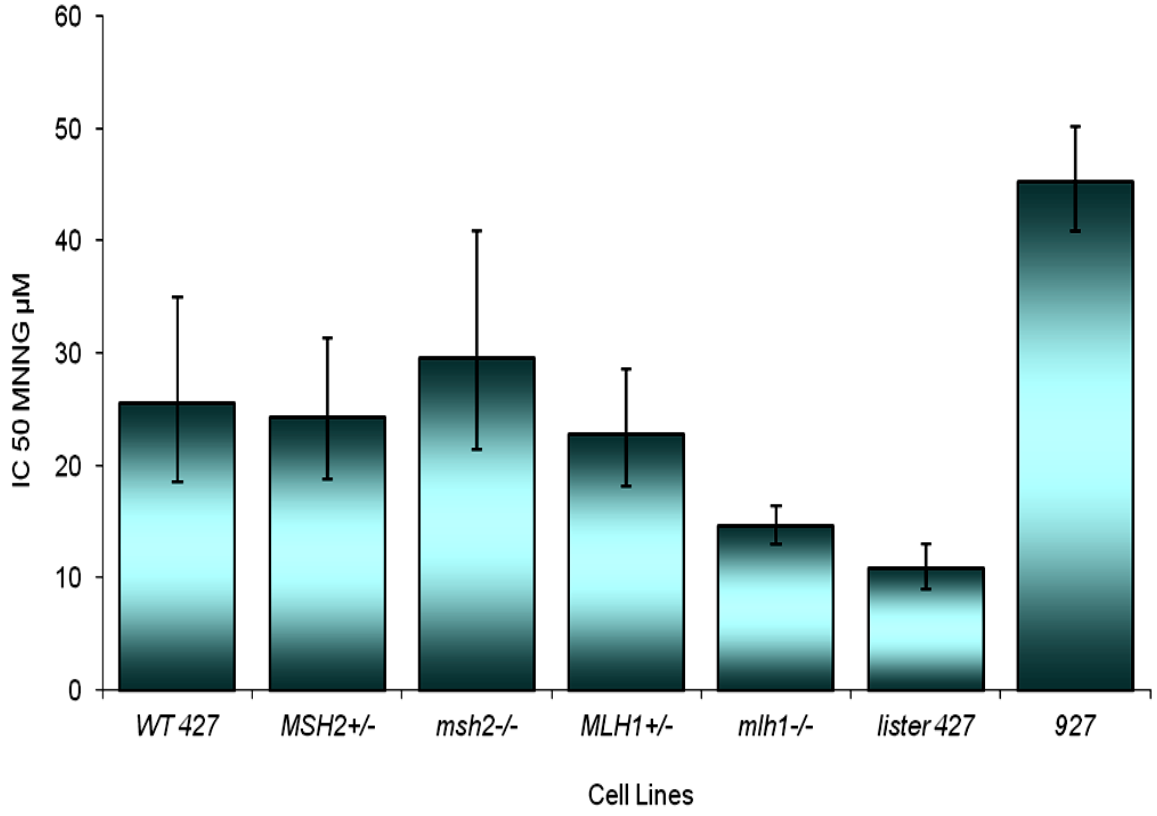


**Figure 3-7 IC50 values of *T. brucei* PCF MMR mutants grown in MNNG and assayed by Alamar Blue.**

The conversion of Alamar blue to fluorescent Resofurin was used to determine the sensitivity of the PCF *T. brucei* wild type (WT) and MMR mutants towards MNNG. IC50 values of Lister 427 WT, *MSH2+/-, msh2-/-, MLH1+/-* and *mlh1-/-* cells, and of WT TREU 927 cells, is shown. IC50 values are the mean of three experiments and vertical bars indicate standard deviation. Cells were grown from a starting density of $5x10^5$ cells.$ml^{-1}$ n the presence of doubling dilutions of MNNG (from 0.39 µM-400 µM) in fluorscence- readable 96 well plates. After 48 hrs Alamar Blue was added to each well and fluorescence measured after a further 24 hours of growth.

These data are surprising and do not fit to what might be expected for MMR deficient cells. Firstly, an increased tolerance, and hence greater IC50 value, towards the alkylating agent was expected for the *msh2-/-* and *mlh1-/-* mutants relative to the wild type cells and the +/- cells. Instead, the Alamar blue data suggest no clear change in the *msh2-/-* mutants, and the *mlh1-/-* mutants appear more sensitive to MNNG. Secondly, different apparent IC50 values were observed for two distinct stocks of wildtype PCF cells each thought to be of strain Lister427, and these also differed from the IC50 value of the TREU927 cells.

To try and understand this, the effect of MNNG on BSF MMR mutants was also tested using the Alamar blue assay (Figure 3-8), as described in Section 2.5.1.2.2. Alkylation tolerance of MMR mutants in *T. brucei* BSF cells has been examined before, although with a different strategy: cells were grown in media containing MNNG at concentrations of 0, 0.25 $\mu g.ml^{-1}$, 0.5 $\mu g.ml^{-1}$, 0.75 $\mu g.ml^{-1}$ and 1 $\mu g.ml^{-1}$ and the effect on survival monitored by measuring the number of clones that grew out after limiting dilution (Bell et al. 2004). Here, using the Alamar blue assay appeared to confirm these findings, since the *msh2-/-* and *mlh1-/-* mutants displayed IC50 values approximately 10- and 8-fold, respectively, higher than wild type. Although the *msh2-/-* mutants appeared more resistant to MNNG than *mlh1-/-* mutants, it is not clear that this was significant, and it was not observed in the clonal survival assay (Bell et al. 2004). Another difference that was seen consistently is that the BSF *MSH2*+/- cells were more tolerant of MNNG than either the wild type cells or *MLH1*+/- mutants, which appeared equivalent to wild type. Moreover, when MSH2 was re-expressed in the *msh2*-/- mutants, these too displayed MNNG tolerance, to levels equivalent to the *MSH2*+/- cells (no MLH re-expressers are available to conduct this comparison). This is again consistent with the clonal survival assay as suggests that loss of one allele of *MSH2*, but not of *MLH1*, impairs MMR function.

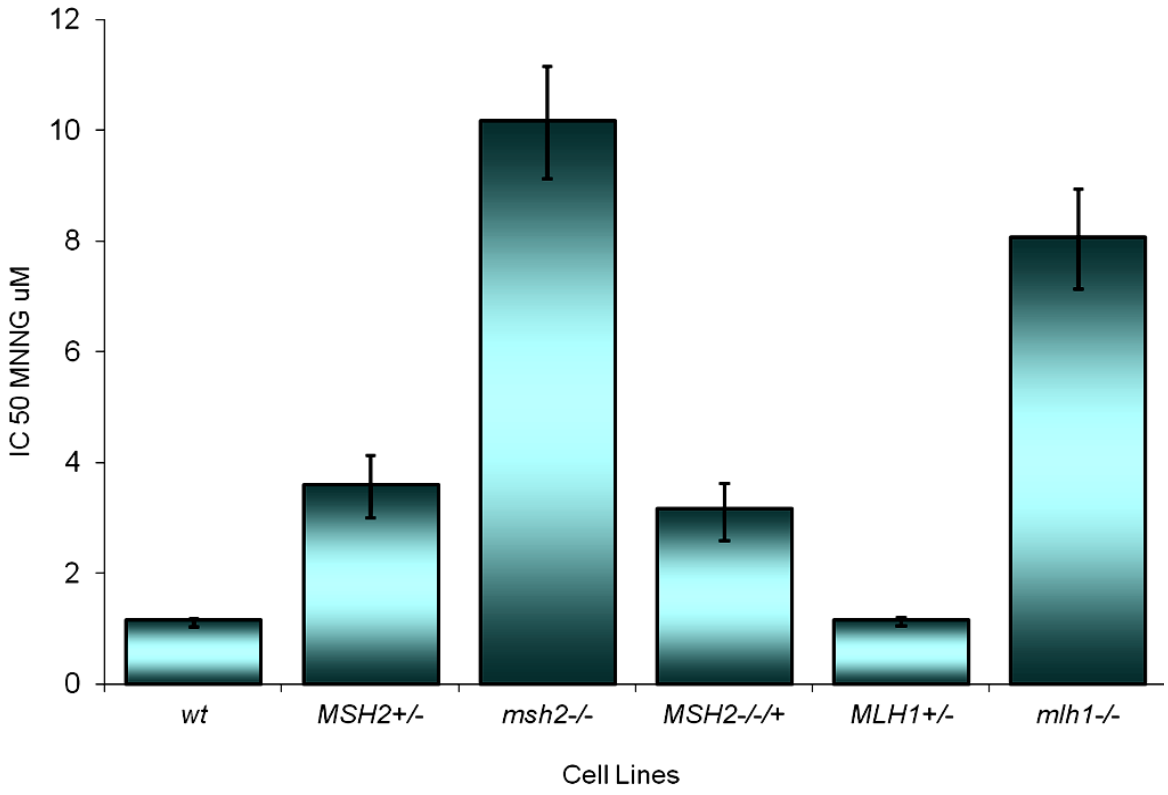


**Figure 3-8 IC50 values of *T. brucei* BSF MMR mutants grown in MNNG and assayed by Alamar Blue.**

The conversion of Alamar blue to fluorescent Resazurin was used to determine the sensitivity of the BSF *T. brucei* wild type (WT) and MMR mutants towards MNNG. IC50 values of Lister 427 WT,

*MSH2+/-*, *msh2-/-*,*MSH2-/-/+*, *MLH1+/-* and *mlh1-/-* cells, is shown. IC50 values are the mean of three experiments and vertical bars indicate standard deviation. Cells were grown from a starting density of 5 x $10^5$ cells.$ml^{-1}$ n the presence of doubling dilutions of MNNG (from 0.39 µM-400 µM) in fluorscence- readable 96 well plates. After 48 hrs Alamar Blue was added to each well and fluorescence measured after a further 24 hours of growth.

The above data suggest that, for reasons that are unclear, the Alamar blue assay is inappropriate for testing MNNG sensitivity of PCF cells, despite being effective for BSF cells. Therefore, MNNG sensitivity was next checked by a survival curve assay in the presence of varying concentration of MNNG. Because the cloning efficiency of PCF cells in 96 well plates is more variable than BSF cells, wild type cells and the *MSH2* and *MLH1* +/- and -/- mutants were seeded at density of 5x$10^5$ cells.$ml^{-1}$ in 10 ml cultures and grown in the presence of 0, 2.5, 5 and 7.5 µM MNNG. Cell density was then counted every 24 hours for 72 hours. These data are shown in Figure 3-9, where percent survival is calculated from the concentration of each cell line at the three concentrations of MNNG relative to the control without MNNG, where the cell concentration is taken as 100%. Similar counts were done with higher concentrations of MNNG (10 and 20 µM), but here the extent of cell killing was so great that these data were excluded.

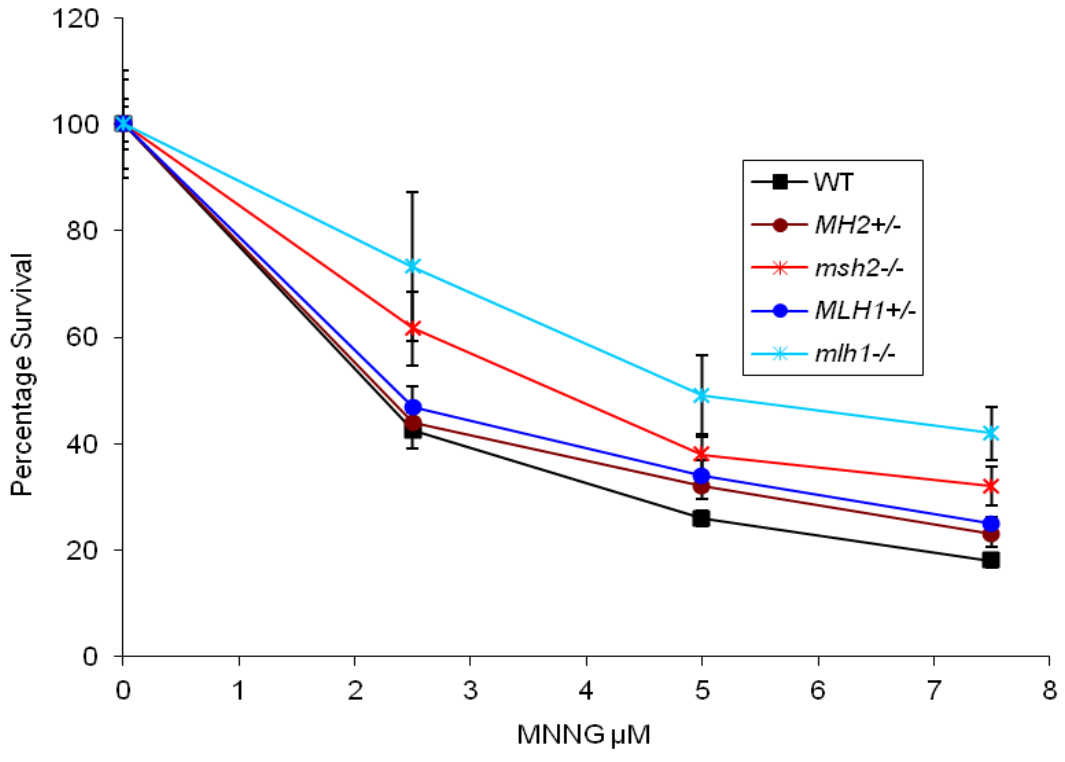


(A)

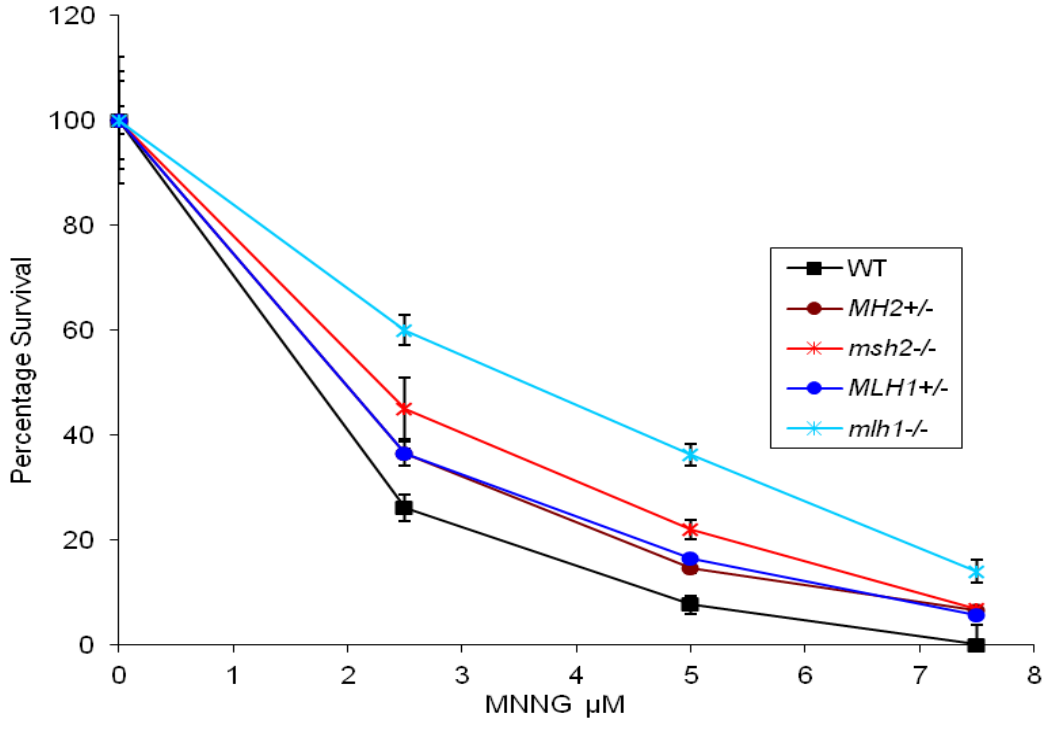


(B)

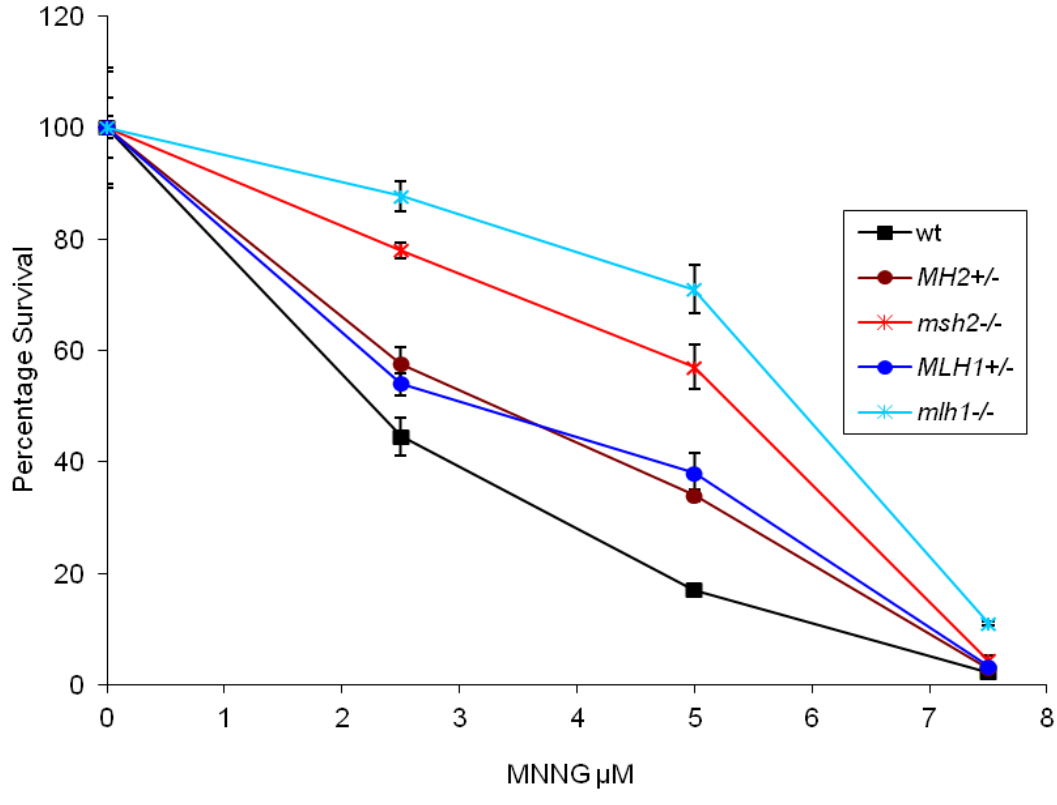


(C)

**Figure 3-9 Percentage survival of *T. brucei* PCF wild type and MMR mutants at various concentration of MNNG.**

Wild type, *MSH2*+/-, *msh2-/-*, *MLH1*+/- and *mlh1-/- T. brucei* cells were diluted to $5.10^5$ cells.ml$^{-1}$ in SDM-79 culture media containing 0, 2.5 µM, 5 µM or 7.5 µM MNNG. Cell densities were measured (A) 24 hours, (B) 48 hours and (C) 72 hours subsequently and are shown as a percentage of the

density of each cell line in the absence of MNNG (taken as 100 %). Each value is the mean of three experiments, and vertical bars depict standard deviation.

These data reveal tolerance of the PCF MMR mutants to MNNG methylation compared to wild type cells, which was not detected by the Alamar blue assay. Although all the cells show a decrease in survival in MNNG, the *mlh1*-/- mutants can be seen to be the most resistant to killing; the *msh2*-/- mutants are also resistant but to a lesser extent. Even at 24 hours the extent of growth impairment in the *mlh1*-/- cells appeared detectably less than that seen in all other cells at all concentrations of MNNG, and the elevated survival of these cells was even greater at 48 and 72 hrs. In contrast, the *msh2*-/- mutants were only clearly detectably more resistant to MNNG than the wild type cells and heterozygous mutants after 72 hours growth and at 2.5 and 5 μM MNNG; at earlier time points the -/- mutants were detectably more resistant than wild type cells, but this difference was less marked compared with the +/- cells. This seems to be because the PCF heterozygous mutants display some tolerance to MNNG: though at 24 hours the extent of cell death in these cells was not clearly distinguishable from wild type, at 48 and 72 hours they showed noticeably greater survival at 2.5 and 5 μM MNNG; at the highest concentration the extent of cell deaths was so severe that such effects were not seen.

Taken together, these data are consistent with MSH2 and MLH1 acting to attempt to repair methylation damage caused by MNNG, and acting through MMR to have the same deleterious effects on survival seen in other organisms. In contrast to BSF *T. brucei* mutants, where only *MSH2*+/- cells displayed MNNG tolerance, both heterozygous PCF MMR mutants appeared to show this effect. In addition, in the PCF cells the *mlh1-/-* cells were more resistant to MNNG than the *msh2*-/- cells, which were not observed in the BSF. This may suggests MLH1 has a more prominent role in protection against methylation damage in this life cycle stage. This, however, needs further analysis. Nonetheless, the results validate that MMR mutants have been made in *T. brucei* PCF cells are phenotypically MMR-deficient.

#### 3.2.2.3 Microsatellite instability

Microsatellites are stretches of DNA composed of several repetitive elements, usually one to six nucleotides long (Beckmann 1992). Such microsatellites are conserved within a species and are often used as a tool for genotyping. However, because of their repetitive nature they are more susceptible to replication errors, resulting in insertion and deletion of

repeat units (Ellegren 2000;Sia 1997;Strauss 1999). This is termed microsatellite instability (MSI). Such replication errors by DNA polymerases are normally corrected by MMR, thus preventing MSI. However, in conditions in which MMR is deficient, MSI rates are increased, as seen in BSF *T. brucei msh2*-/- and *mlh1*-/- cells (Bell 2004).

To investigate whether MSH2 and MLH1 are involved the repair of slipped replication intermediates in PCF *T. brucei*, the stability of a naturally occurring microsatellite loci, JS2, was compared in wild-type cells and *MSH2* +/-, *msh2-/-* , *MLH1* +/- and *mlh1-/-* mutants. To do this, each cell line was cloned by diluting to 200, 100 and 50 cells per 96 well plate and allowed to grow out to viable populations over 10-14 days. The efficiency of such cloning was very low (6-20 clones per plate), and the number of wells that grew out was not proportional to the number of cells plated (data not shown). Ten clones were therefore selected from all the plates, used to inoculate a 10 ml culture and grown to maximum cell density (approximately another 10 generations; see Section 2.5.1.2.3) and genomic DNA was isolated (see Section 2.2.2).

The JS-2 microsatellite has been mapped to Chromosome IV, and is composed of GT-dinucleotide repeats (Hope 1999). The JS-2 locus was amplified by PCR using the primers JS-2A and JS-2B from the DNA of each of the 10 sub clones of WT, *MSH2+/-*, *msh2-/-*, *MLH1+/-* and *mlh1-/-* cells. PCR was performed using the protocol detailed in Section 2.2.5 and the resulting PCR products were separated by electrophoresis on 3% low melting agarose gel (see Section 2.5.1.2.3); samples we were run at 100V for 50 minutes. The results of this work are shown in Figure 3-10.

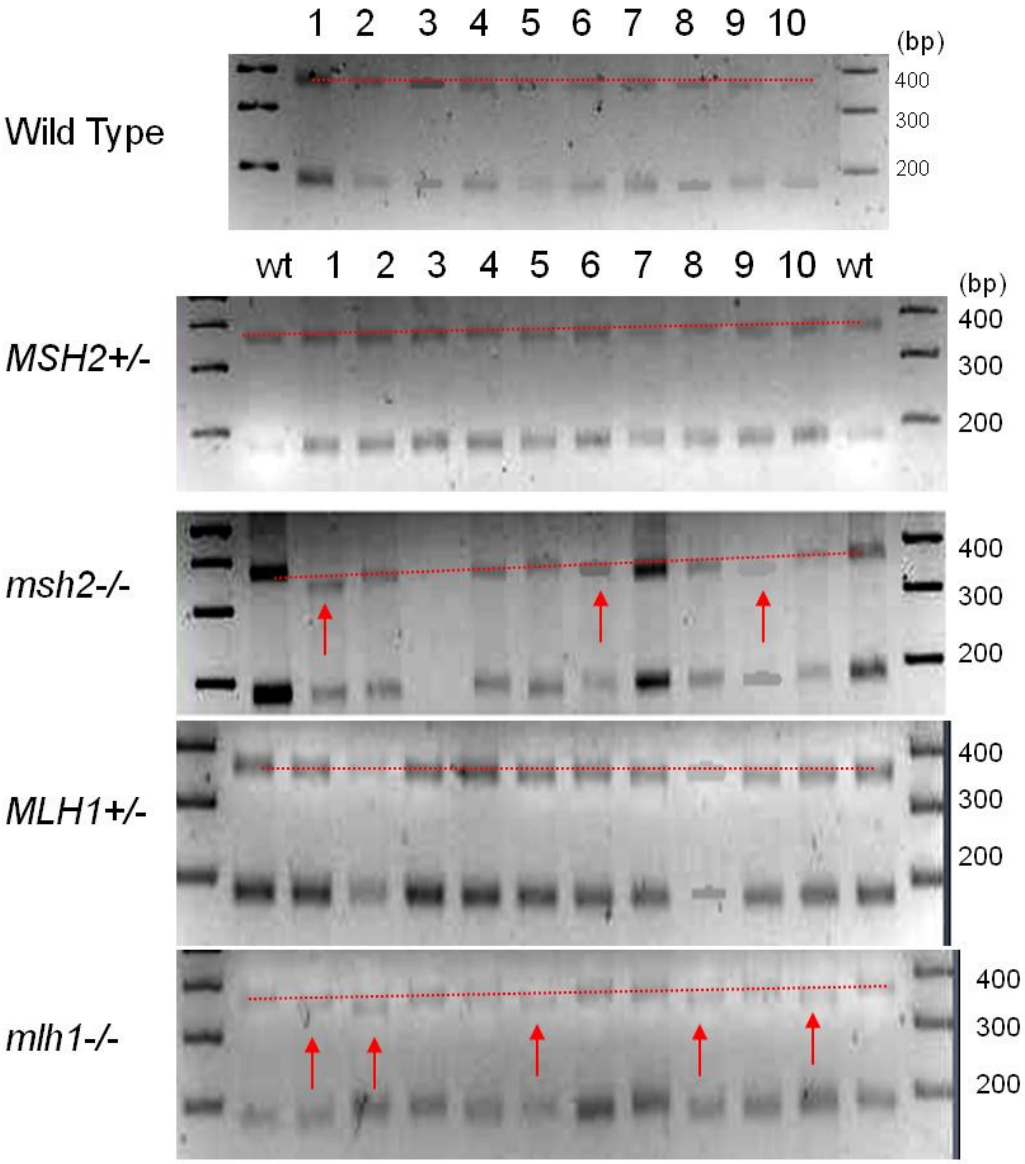


**Figure 3-10 Analysis of JS2 microsatellite instability in *T. brucei* PCF wild type and MMR mutants.**

JS2 locus was amplified from 10 clones each from WT, *MSH2+/-*, *msh2-/-*, *MLH1+/-*, *mlh1-/-* using primers JS2A and JS2B. PCR product was separated on 3% agarose gel at 100 V for 50 minutes. For a better comparison between wild type and mutants, PCR product from one of the wild type sub clones was also added in the first and last lane parallel to the mutants. Clones that show a difference in size relative to WT are indicated by an arrow; size markers are shown.

It is evident that the JS-2 locus is stable in the wild-type cells, since two PCR products of equivalent length (approximately ~350 bp and ~180 bp) were generated in all ten clones (Figure 3-10). The same finding was seen for both the *MSH2*+/- and *MLH1*+/- clones, indicating that loss of one allele does not impede MMR of replication errors at this locus. In contrast to this stability, a number of clones from both the *msh2-/-* and *mlh1-/-* mutants exhibited change in sizes of the amplified PCR product. In all cases, this appeared most apparent in the bigger allele, though some indication of non-uniformity in size of the PCR

products from the smaller allele was perhaps detectable. Taken together, these data provide an indication of MSI specifically in the homozygous mutants, consistent with a role in MMR in PCF *T. brucei*.

A potential complication emerged at this point from these data, which is seen in the presence of two different allele sizes for the JS-2 locus. JS-2 PCR-amplification with the same primers has been previously reported from BSF Lister 427 *T. brucei*, revealing a PCR product of ~320-340 bp, suggesting the two alleles in this strain are essentially indistinguishable in size (Bell 2004). To most accurately compare the role of MSH2 and MLH1 in BSF and PCF cells, we wished to generate mutants in the same strain, and assumed that the PCF cells we used were also Lister 427. The data here raise the possibility that one or other of these strains may not in fact be Lister 427.

To try and ensure that the BSF and PCF cells are from the same lineage, two approaches were taken. Firstly, we tried to differentiate the existing BSF putative Lister 427 MMR mutants and wildtype to PCF cells *in vitro* (data not shown). To do this, we followed different two protocols based on sodium citrate and cis aconitate addition (Brun 1981) and cAMP (Breidbach 2002). The experiment as described by Bun and Schoenenberger was repeated 4 times with slight modifications with respect to suggestions made by Mark Carrington and Miguel Navarro (personel communications). The major differences between the four repeats were that after overnight incubation of BSF *T. brucei* with the metabolites (sodium citrate and cis-aconitate), cells were be diluted at 1:5 in DTM +20% FBS (fetal bovine serum), 2:5 in SDM79 + metabolites, 2:5 in SDM79 +20 % FBS, or 2:5 in SDM79 + 10% PCM (pre-conditioned media) + metabolites. A second protocol based on cAMP addition was followed as described by Sterverding *et al.* (Breidbach 2002). However, in all cases when morphologically PCF- looking cultures were seen and transferred to SDM-79, PCM or DTM medium, they grew and divided for approximately a week and then the cultures ‘collapsed’ as the cells ceased being able to divide. This was not due to the MMR mutations, as it was seen also in the wild type controls, though the basis for this is unclear. Unfortunately, healthy dividing cells are needed for the phenotypic analysis above, so this experimental option was not viable.

The second approach that was adopted was to attempt to confirm that strains that we have been using are, indeed, Lister427. For this, we PCR-amplified several different microsatellites, which are used to use as markers to distinguish different strains. Genomic DNA of BSF and PCF cells thought to be wild type Lister 427 were taken from different

research groups in the WTCMP, and compared with the PCF cells analysed in this study. In addition, BSF cells were taken from the repository of J.S.Bell (Bell 2002), who had previously analysed MMR mutants in Lister427. Finally, genomic DNA from wild type TREU927 cells were also analysed to provide comparisons with microsatellites expected to be a different size from Lister 427. These data are discussed below.

#### 3.2.2.3.1 Confirmation of strain

Firstly, genomic DNA from wild type, putative Lister427 PCF cells (used here) and BSF cells (J.S.Bell), as well as from wild type TREU927 was PCR-amplified with primers VSG221 (F) and VSG221(R) that recognise *VSG221*. *VSG221* encodes a variant surface glycoprotein and is present in single copy in the strain MITat1.2 (the expected Lister427 strain for both the PCF and BSF studies) (Hertz-Fowler 2008), and thus provides a characteristic marker.

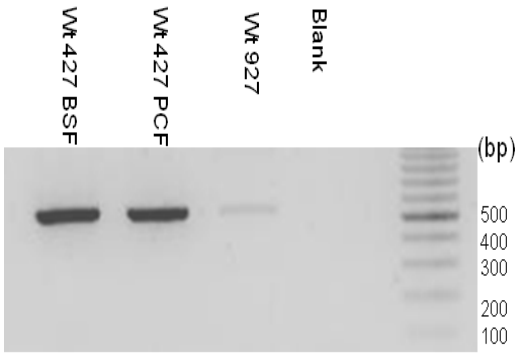


**Figure 3-11 PCR of *VSG221* in both procyclic and bloodstream form wild type *T. brucei*.**

Genomic DNA from wildtype (wt) Lister427 bloodstream form (BSF) and procyclic form (PCF) cells, and from wildtype TREU927 PCF cells, was used to PCR-amplify part of the gene *VSG221*. PCR products were run on an 3% agarose gel; size markers (in bp) are shown.

PCR-amplification of a product of the size expected for *VSG221* was generated from the PCF and BSF Lister 427DNA (Figure 3-11), suggesting each contains this gene. However, a faint band of the same sizes as that seen in the Lister427 samples was also generated from wild type TREU927 DNA. Comparing the intensities of PCR-amplification may suggest this is a non-specific amplification, or a possible contamination from neighbouring wells, but this is not clearly capable of determining the identity of the strains.

Since amplification of the microsatellite JS-2 has shown differences in putative Lister427 BSF and PCF cells, several other microsatellites were next PCR-amplified. Six

microsatellites were PCR-amplified from different chromosomes; these microsatellites have been tested previously for genetic mapping and are routinely used for the confirmation of strains in such studies (MacLean et al. 2004;MacLeod 2005). Putative Lister427 wild type and MMR mutants were analysed, as well as PCF wild type Lister 427 from other sources. For all the PCRs, DNA from wild type TREU927 was used as a control to see if these microsatellites can differentiate between different strains. PCR of JS-2 is shown in Figure 3-12 A. This shows that both alleles are significantly longer in all the putative Lister427 cells than the larger JS-2 allele in TREU927/4, which is 177 bp in length (containing 47 GT-dinucleotide repeat units). The data also reveal the difference in allele organisation between the putative BSF and PCF Lister 427 cells, and shows that PCF Lister 427 strains from a number of labs have the same organisation as the strain used in this study.

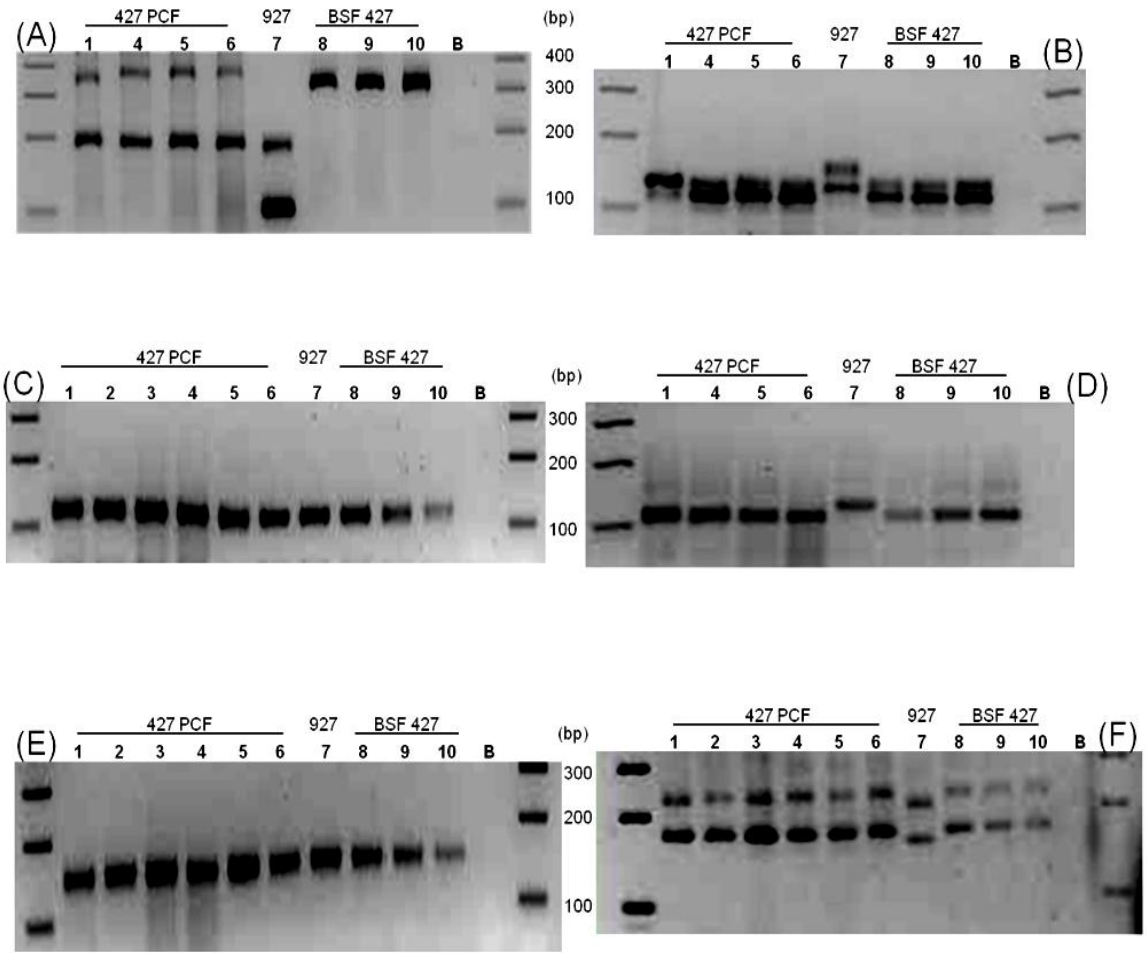


**Figure 3-12 Confirmation of *T. brucei* strains by PCR-amplification of different microsatellites.**

All gels show PCR products generated for different microsatellites. Genomic DNA substrate in the lanes are indicated as follows: 1- wild type Lister 427 PCF (gift from L.Morrison), 2- wild type Lister427 PCF (gift from M.Barrett), 3- wild type Lister427 PCF (gift from S.Mary), 4- wild type PCF Lister427 (this study), 5- *msh2-/-* Lister427 PCF (this study), 6- *mlh1-/-* Lister427 PCF (this study), 7- wild type TREU927 PCF, 8- wild type Lister 427 BSF (J.S.Bell), 9-*msh2-/-* Lister427 BSF (J.S.Bell), 10- *mlh1-/-* Lister427 BSF (J.S.Bell). PCR amplification of the following primers is shown:

(A)Microsatellite JS-2 (chromosome IV), using primers JS2 A, JS2 B; (B) Microsatellite IJ 15 (chromosome III), using primers IJ15 A, IJ15 B; (C) microsatellite 5L5 (chromosome III), using 5L5 A, 5L5 B; (D) microsatellite 2/5 (chromosome II), using primers 2/5 A, 2/5 B; (E) microsatellite PLC (chromosome II), using primers PLC A, PLC B; and (F) microsatellite 18 (chromosome I), using primers 18 A, 18 B. In all cases amplicons were resolved in a 3% agarose gel; B indicates PCR using water as a control substrate, and markers (bp) are shown.

Combining the results of the six microsatellites tested a difference between BSF and PCF Lister 427 was seen only in the JS-2 locus. Of the other five microsatellites, 5L5 and PLC did not differentiate between Lister427 and TREU927 and hence cannot be taken as markers for identification of these strains. In contrast, IJ-15, 2/5 and 18 showed very clear differences between Lister427 and TREU927. These three markers show that all the Lister 427 BSF cells and PCF cells share alleles of indistinguishable sizes, as no changes in these product sizes were seen. This suggests that the PCF cells used in this study and the previous BSF cells are of a common origin. A possible explanation of the different sizes of JS-2 between these life cycle stages could be that these have been separated in culture and animal for a long time and this microsatellite is uniquely prone to variation; thus, by the passage of time mutations might have occurred leading to heterozygous alleles. However, differences in sizes of the PCR product in some clones of the *MSH2* and *MLH1* homozygous mutants suggests that the MMR machinery is not compromised, and hence leads to mutations, in the wild type cells.

### 3.2.3 Role of MMR in protection towards oxidative stress

Oxidative stress, its causes and possible effects have already been discussed in Section 1.4.7. The most common lesion caused, both within DNA and in the cellular dNTP pool, by the oxidizing agent $H_2O_2$ (and by naturally occurring oxidative damage in cells) is 7,8-dihydro-8-oxoguanine, commonly abbreviated to 8-oxoG (Slupphaug 2003;Wiseman 1996). In DNA, this base is highly mutagenic as it pairs equally efficiently with A or C, causing GC - TA transversions.

Possible roles of MMR have been well defined in response to oxidative stress. It has been demonstrated that *msh2-/-* mutants in mammals show an elevated level of $H_2O_2$-induced 8oxoG in DNA (Colussi 2002). This is further supported by the fact that MutSα preferentially binds to 8oxoG-T and 8oxoG-A, but not with 8oxoG-C, in mammalian cells (Mazurek 2002). If a cell has an efficient MMR system it would correct such a mispaired base every time the cell divides. However, in mismatch-deficient cells this mis-incorporation of bases might eventually result in mutagenesis and/or cell death.

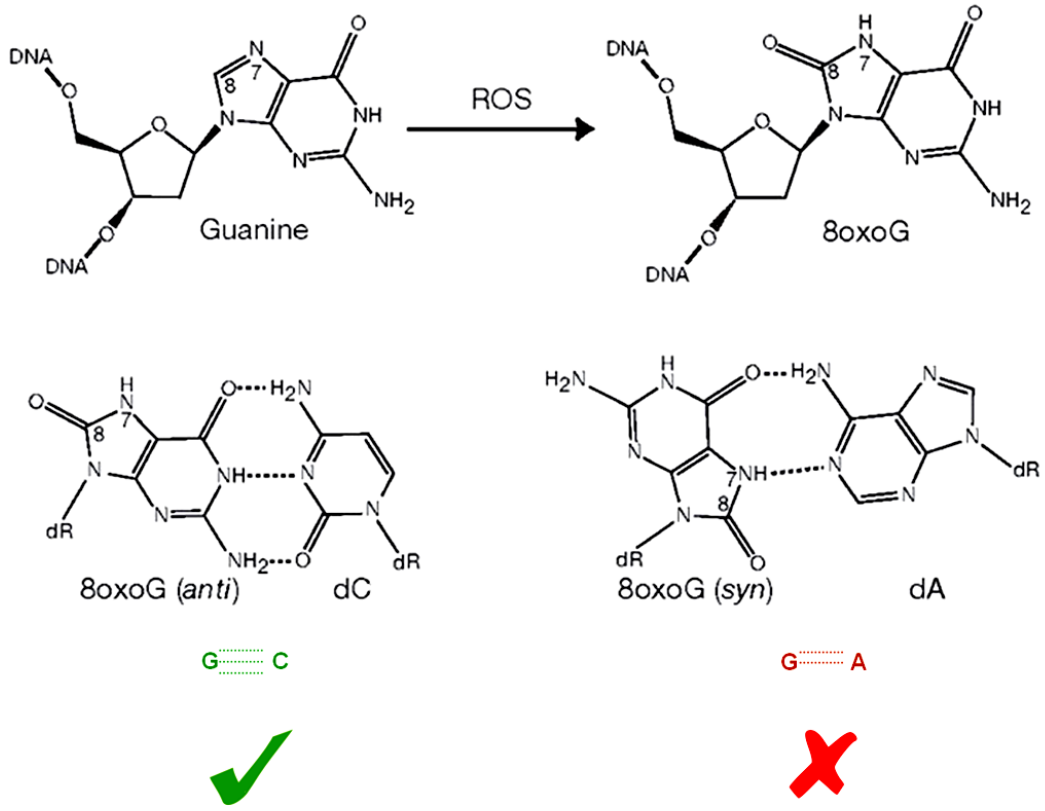


**Figure 3-13 Base mismatches caused by 8oxoG.**

Upon oxidation, Guanine (G) is converted to 8oxoG, which can either base pair with Cytosine (C) in its anti conformation ( ✔ ) or can pair with adenine (A) in its syn form (✖). Figure adapted from (Hsu 2004).

Similar phenotypes have already been characterised in *T. brucei* BSF MMR mutants and in *T. cruzi MSH2* heterozygous mutants (Campos 2011;Augusto-Pinto 2003;Machado-Silva, 2008). Having now successfully generated *MSH2* and *MLH1* null mutants in PCF *T. brucei*, we sought to extend this analysis to this life cycle stage. To test for $H_2O_2$ sensitivity wild type cells and the *MSH2* and *MLH1* +/- and -/- mutants were seeded at density of $5x10^5$ cells.ml$^{-1}$ in 10 ml cultures and grown in the presence of varying concentrations of $H_2O_2$: 10, 20 and 40 µM. A control with no $H_2O_2$ was also set up in the same way, and cell densities were counted at 24, 48 and 72 hrs. As for the MNNG analysis (Section 3.2.2.2, Figure 3-9), cell counts in the absence of $H_2O_2$ were taken as 100% and the survival of each cell in the varying concentrations of $H_2O_2$ calculated as a percentage of that from the cell counts. These data are shown in Figure 3-14.

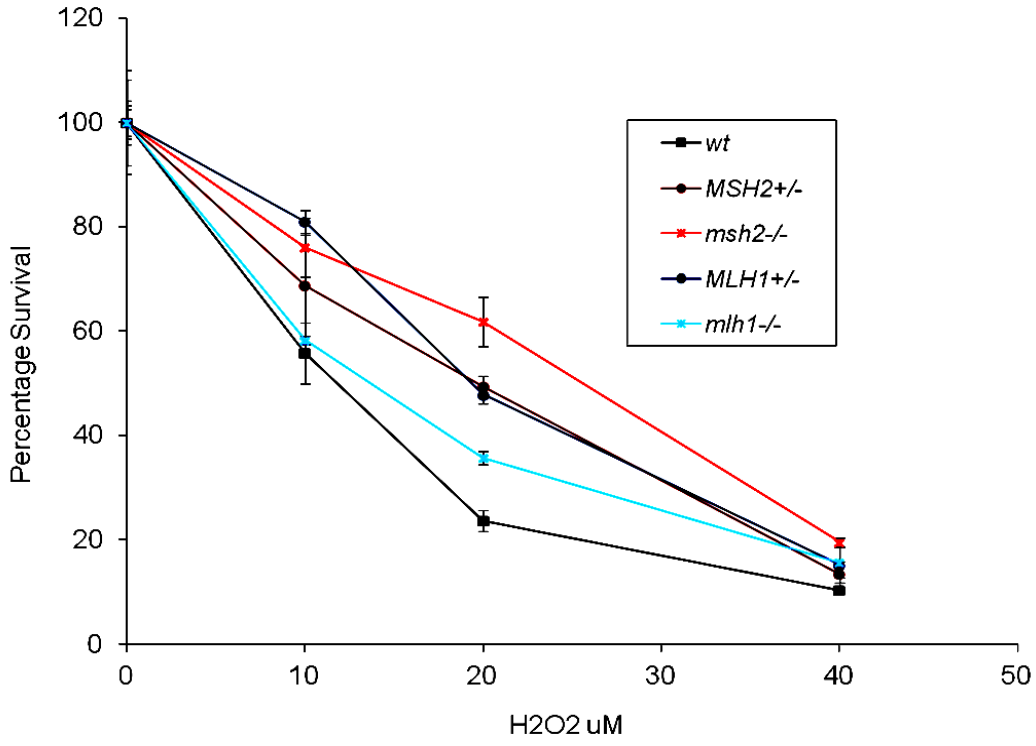
120
100
80
60
40
20
0
Percentage Survival
0
10
20
30
40
50
H2O2 uM
wt
MSH2+/-
msh2-/-
MLH1+/-
mlh1-/-

(A)

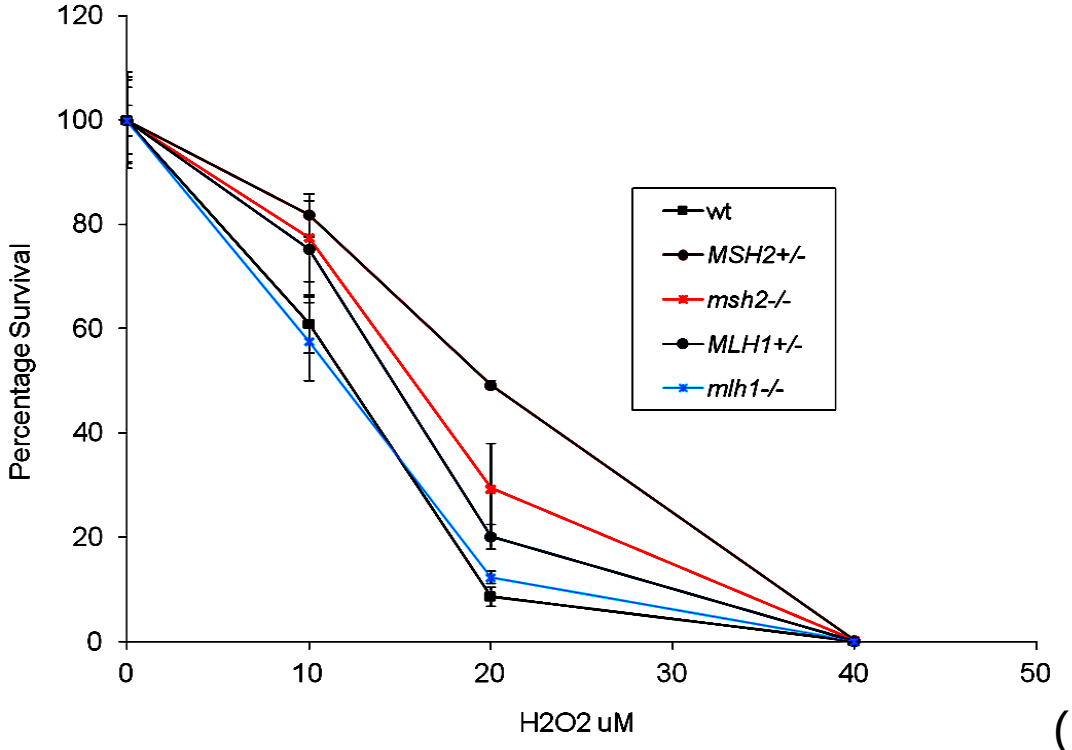
120
100
80
60
40
20
0
Percentage Survival
0
10
20
30
40
50
H2O2 uM
wt
MSH2+/-
msh2-/-
MLH1+/-
mlh1-/-

(B)

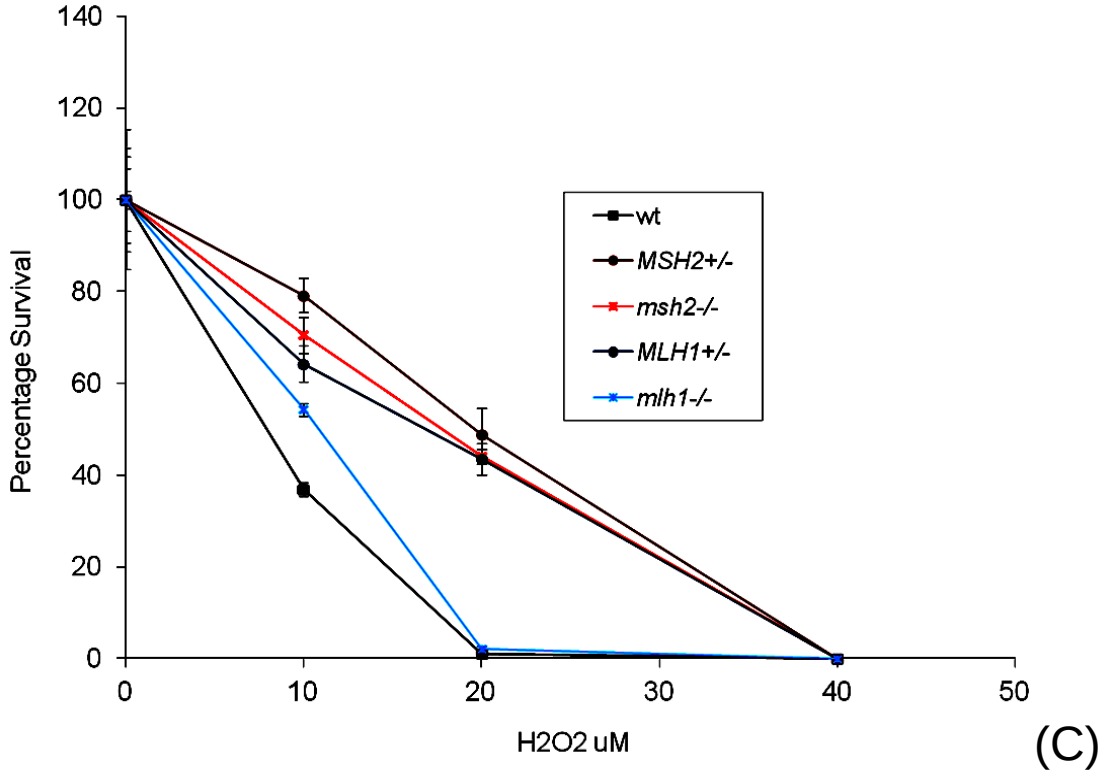


**Figure 3-14 Percentage survival of *T. brucei* PCF wild type and MMR mutants at various concentration of $H_2O_2$.**

Wild type, *MSH2*+/-, *msh2-/-*, *MLH1*+/- and *mlh1-/- T. brucei* cells were diluted to $5x10^5$ cells.$ml^{-1}$ in SDM-79 culture media containing 0, 10 , 20 or 40 µM $H_2O_2$. Cell densities were measured (A) 24 hours, (B) 48 hours and (C) 72 hours subsequently and are shown as a percentage of the density of each cell line in the absence of $H_2O_2$ (taken as 100 %). Each value is the mean of three experiments, and vertical bars depict standard deviation.

A striking contrast in the phenotypes of the PCF and BSF MMR mutants was revealed by this analysis. First, in contrast to in the BSF, where loss of *MSH2* results in sensitivity to $H_2O_2$ (Bell 2004), loss of the same gene caused resistance to $H_2O_2$ in the PCF cells. This appears to be seen not simply when both alleles are lost, but also when one allele is mutated. After 24 hrs, when subjected to 20 µM $H_2O_2$, the *msh2*-/- cells showed most resistance of all cells, though the *MSH2*+/- cells were clearly more resistant than the wild type. At 10 µM the difference between the +/- and -/- cells was less marked, though both were more resistant than wildtype, while at 40 µM the survival of the mutants and wild type was so low (10-20%) that they could not be distinguished. Note that this is consistent with the greater sensitivity of PCF cells compared with BSF cells (Barnes 2006;Machado-Silva 2008) where wild type cells show this level of survival only at 300 µM $H_2O_2$ (see below). At 48 hrs and 72 hrs, the resistance of the *MSH2*+/- and *msh2*-/- cells relative to wild type was still seen, but here it appears that loss of a single allele rendered the cells more resistant than loss of both alleles.

The second finding is that mutation of *MLH1* did not have the same effect as that of *MSH2*. No clear difference in the effect of $H_2O_2$ on cell survival was seen between wild type cells and *mlh1-/-* mutants after 24 hrs, 48 or 72 hrs growth, suggesting that the null mutant is neither more resistant nor more sensitive to oxidative stress. Indeed, there was a clear difference in survival between the *mlh1*-/- and *msh2*-/- cells throughout the analysis, consistent with the separation of function of these two MMR components that was seen in the BSF cells (Bell 2004). However, the loss of a single allele in the *MLH1*+/- cells did appear to cause increased resistance, which was most clearly seen at 24 and 72 hrs. They extent of this was not as great as that seen in the *MSH2*+/- mutants and was more comparable with the *msh2*-/- mutants.

Taking the data as a whole, the phenotypic trend appears to be the loss of a single allele of each gene caused increased resistance to $H_2O_2$ when compared with the wild type cells, though this was more marked for *MSH2*. After loss of both alleles, the *msh2*-/- cells remained more resistant, which is contradictory to what has been observed in BSF cells, where *msh2*-/- mutants are more sensitive to $H_2O_2$ as compared with wild type cells and *mlh1*-/- mutants (Machado-Silva 2008). Loss of both *MLH1* alleles in the *mlh1*-/- mutants reverted the small increased resistance of the *MLH1*+/- mutants such that the nulls were indistinguishable from wild type cells. There was some variability in the data between 24 and 72 hours, though the resistance patterns were always seen. The reason for this variability could be that at 24 hours the cells are in a 'pre- log' phase of growth, while at 72 hrs the cells are in 'post-log' phase and hence the effect of $H_2O_2$ may vary with the growth. Also, $H_2O_2$ is a very unstable compound, meaning its effects show variability and perhaps most clearly once the cells have begun growing rapidly. Therefore, the characteristic phenotypes of the mutants may be most clearly seen at 48 hrs in the log phase of growth.

#### 3.2.3.1 Microsatellite instability of *T. brucei* PCF MMR mutants in the presence of $H_2O_2$

The resistant phenotypes of the PCF MMR mutants is response to oxidative stress might be explained by activation of an unidentified repair or protection system during the mutation of the genes. This would suggest some adaptation during the mutation process, perhaps rendering the cells generally resistant to oxidative damage. To attempt to ask if there might be a system present that can work in place of, or in support of, non-functional MMR, we tested for MSI of MMR mutants in the absence or presence of 20 μM $H_2O_2$. Wild type cells and *MSH2+/-, msh2-/-, MLH1+/- and mlh1-/-* mutants were grown to log phase and then

diluted to $5x10^5$ cells.$ml^{-1}$. The cultures were then grown in the absence or presence of 20 μM $H_2O_2$ for 48 hours. After 48 hours, the cultures were counted and cloned in 96 well plates, as described in Sections 3.2.2.3 and 2.5.1.2.3. DNA was then extracted and PCR of the JS-2 microsatellite performed for each clone. This was first examined by gel electrophoresis (Figure 3-15).

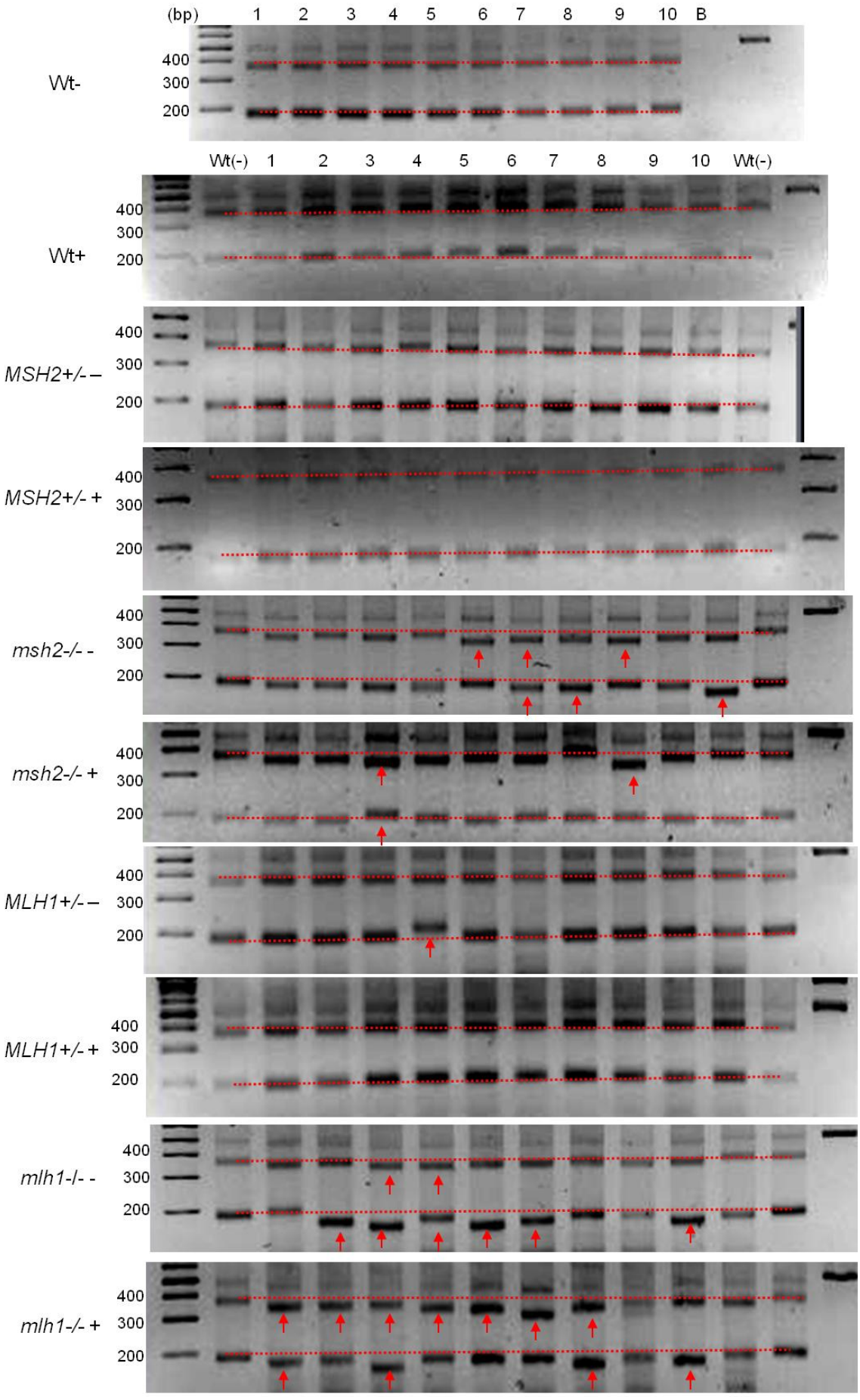


**Figure 3-15 Analysis of JS2 microsatellite instability in *T. brucei* PCF MMR mutants in the presence of 20 μM $H_2O_2$.**

WT, *MSH2+/-, msh2-/-, MLH1+/-,* and *mlh1-/-* cells were grown in the absence (-) and presence (+) of 20 μM $H_2O_2$ for 48 hours. The JS2 locus was amplified from 10 clones from each cell line using primers JS2A and JS2B and PCR products were separated on 3% agarose gel. PCR product from one of the wild type sub clones was also added in the first and last lane parallel to the mutants. Clones that show a difference in size relative to WT are indicated by an arrow; size markers are shown.

To try and gain a better understanding of the different sizes of the PCR-amplified JS-2 microsatellite, the samples were also analysed by Genescan (Bell, Harvey, Sims, & McCulloch 2004;Schuelke 2000). This is a highly sensitive technique that can distinguish between PCR products with a size difference of only1 bp. Genescan is a fluorescent-based technique, which uses one fluorescently labelled primer. The PCR products are separated by acrylamide-urea gel electrophoresis, with labelled size standards added in each track. The PCR products are analyzed by a DNA sequencer, which reads the fluorescence in the PCR-amplified product by comparing them with the size standards, revealing the detailed size of the PCR product. The system also takes into account potential errors made by Taq polymerase, for instance where several smaller products are generated, by taking the most prominent labelled molecule as representing the size of the PCR product. In this study a 5' FAM (6-carboxy-fluorescine) labelled version of the JS2A forward primer was used in the PCR reactions. PCR conditions were kept the same as described in Section 3.2.2.3, with the exception that care was taken to protect the samples from light during and after PCR. PCR products were run on a 3% agarose gel to check for amplification and also to determine the abundance of the products. The samples were then diluted at 1:100 for faint bands and 1:250 for stronger bands and then sent to the University of Dundee Genescan service for analysis. The results were obtained from in the form of electropherograms and sizes of the inferred products with respect to peak height. These data are shown in Figure 3-16, which displays the averages sizes of the larger and smaller alleles of the JS-2 microsatellite in the clones from the different cells, and shows the variation is size that was seen.

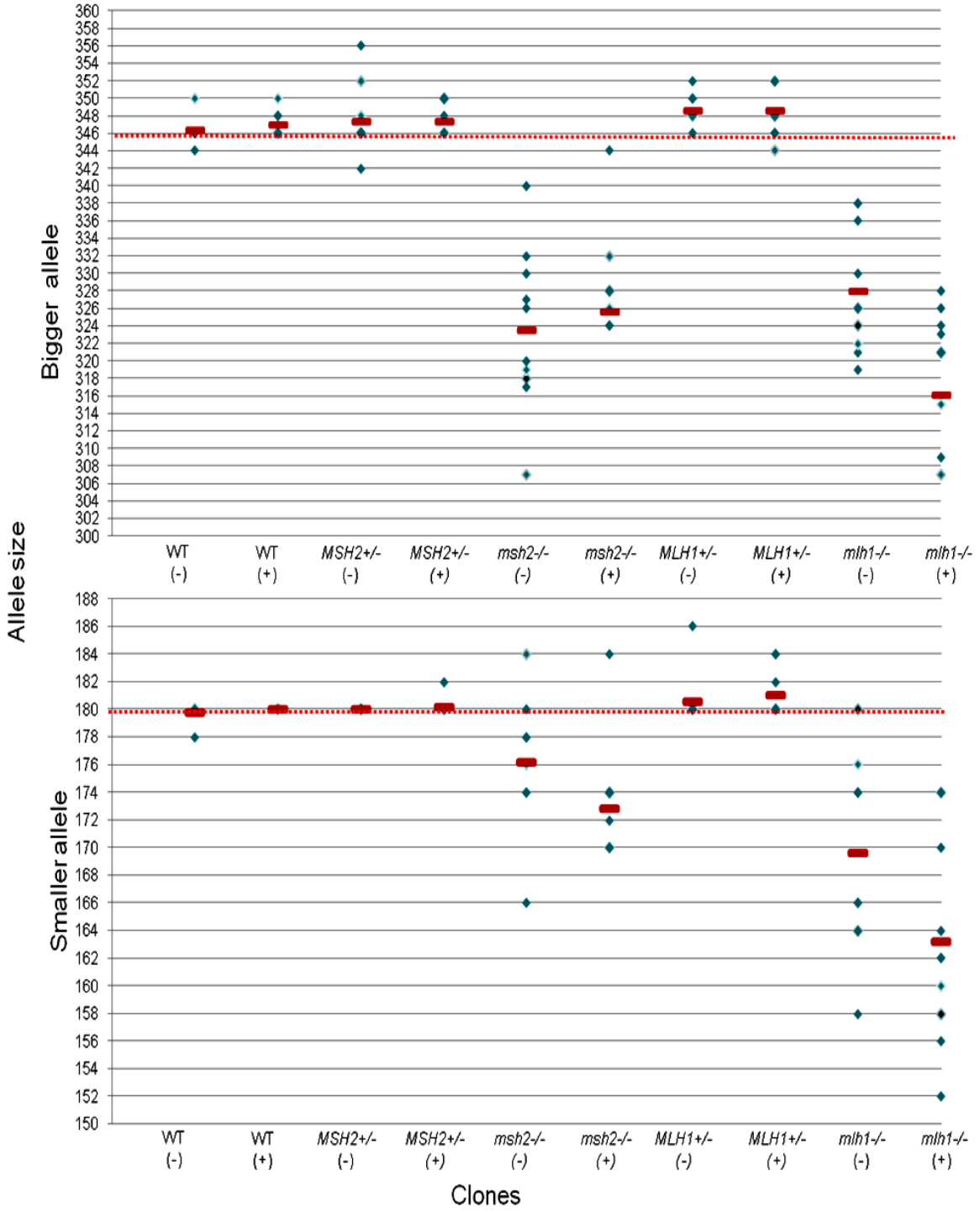


**Figure 3-16 MSI analysis of *T. brucei* PCF MMR mutants through Genescan analysis.**

Genomic DNA from multiple clones of non treated (-) and 20 μM $H_2O_2$ treated (+) wild type, *MSH2+/, msh2-/-, MLH1+/-* and *mlh1-/-* cells were PCR-amplified with 5' FAM labelled forward primer 5' FAM JS2 A (F) and unlabelled JS2 B (R). FAM labelled PCR products, along with ROX 500 labelled size standards, were loaded on polyacrylamide-urea gel for electrophoresis. Results are obtained in the form of electropherograms where allele size in bp refers to the size of the peak. Peaks were analyzed using Peak scanner software from Applied Biosystems v1.0. The average sizes of both the larger and smaller alleles of the JS-2 microsatellite locus was then inferred from the subclones from each cell type, and were plotted using scatter plot. Red bar indicate the average size of the alleles in each cell line and the dotted line indicates the expected size of JS2 alleles.

Results from the gel electrophoresis and the Genescan analysis of the JS-2 microsatellite in *T. brucei* PCF wild type and MMR mutants in the presence or absence of $H_2O_2$ may suggest that oxidative damage increases instability in this locus in the *mlh1-/-* cells but not in the *msh2-/-* cells. The wild type and heterozygous mutants seemed consistent in the two allele sizes in all the clones, which suggests lack of MSI, even after $H_2O_2$ treatment; some variation was detected in the size of, in particular, the bigger allele by the Genescan analysis, although this was markedly less than was seen in either of the null mutants. In the *mlh1-/-* mutants both the number of clones that showed MSI, and the extent of this size variation, appeared to increase after the addition of $H_2O_2$. From the gels, 2 and 6, respectively, of the larger and smaller alleles displayed detectable changes in size amongst the 10 clones examined in the absence of $H_2O_2$ treatment, in contrast with 7 and 4 of the 10 clones after treatment. Moreover, the average size of both the alleles was smaller after $H_2O_2$ treatment, suggesting greater loss of repeats. The same trend was not as clear in the *msh2-/-* mutants, which showed greater resistance to oxidative stress in the growth curve. Here, 3 each of the larger and smaller alleles displayed changes in size amongst the 10 clones examined in the absence of $H_2O_2$ treatment (detected by gel electrophoresis), in contrast with 2 and 1 of the 10 clones after treatment. For the larger allele, there was no evidence from the Genescan for increased loss of the repeats after $H_2O_2$ treatment, as was seen in the *mlh1-/-* cells that was seen. However, this data is not reflected in the smaller allele, which did seem to show a smaller average length after oxidative stress.

In concluding, the MSI analysis suggests that the *msh2-/-* mutants show a slight increase in genetic stability in presence of $H_2O_2$, whereas *mlh1-/-* mutants show a more pronounced increase in instability. This appears to reflect the survival curves, where *msh2-/-* mutants are more resistant to $H_2O_2$ than *mlh1-/-* mutants. This may suggest a broader adaptation to resistance to $H_2O_2$. However, since $H_2O_2$ effects the cells in several different ways, genetic instability may not be the only reason than can be attributed to the cells being sensitive or resistant to damage.

The above study examines MSI in the nuclear genome. In order to ask if the loss of MMR genes had a differential effect on genetic stability in the nucleus and kinetoplast genomes, MSI was also tested in the kinetoplast DNA (kDNA). Since kDNA is a more repetitive genome than the nuclear genome, it was hard to find a microsatellite and design primers for specific PCR-amplification. However, a repeat composed of 7 copies of the sequence AAAAC was identified, and the primers kDNA-FAM(F) and kDNA(R) were designed

(Figure 3-17), not only for specific PCR-amplification but also to give a PCR product that was of sufficient size to analysed on an agarose gel.


**Figure 3-17 Sequence of a microsatellite in *T. brucei* kDNA.**

A Microsatellite locus in kDNA is shown that contains 7 repeats of AAAAC (as shown in red). The Microsatellite was PCR-amplified using the forward, FAM-labelled primer kDNA-FAM(F) and reverse primer kDNA(R). Arrows denote the sequence and position of respective primers.

The samples analysed above for JS-2 MSI (Figure 3-15) were then PCR-amplified with these kDNA microsatellite primers, using PCR conditions as in Section 2.2.5. The resulting PCR products were resolved on a 3% low melting agarose gel (Figure 3-18). All samples showed a band size of 400 bp, which correlated well with the expected product of 411 bp. No difference in the size of the PCR- amplified product was seen in any clone, including the *msh2*-/- and *mlh1*-/- null mutants, in the presence or absence of $H_2O_2$. To test further for instability in this kDNA repeat, the samples were also tested by Genescan analysis in the laboratory of Carlos Machado (Federal University of Minas Gerais, Brazil) and, again, no size changes were seen in any of the clones (data not shown).

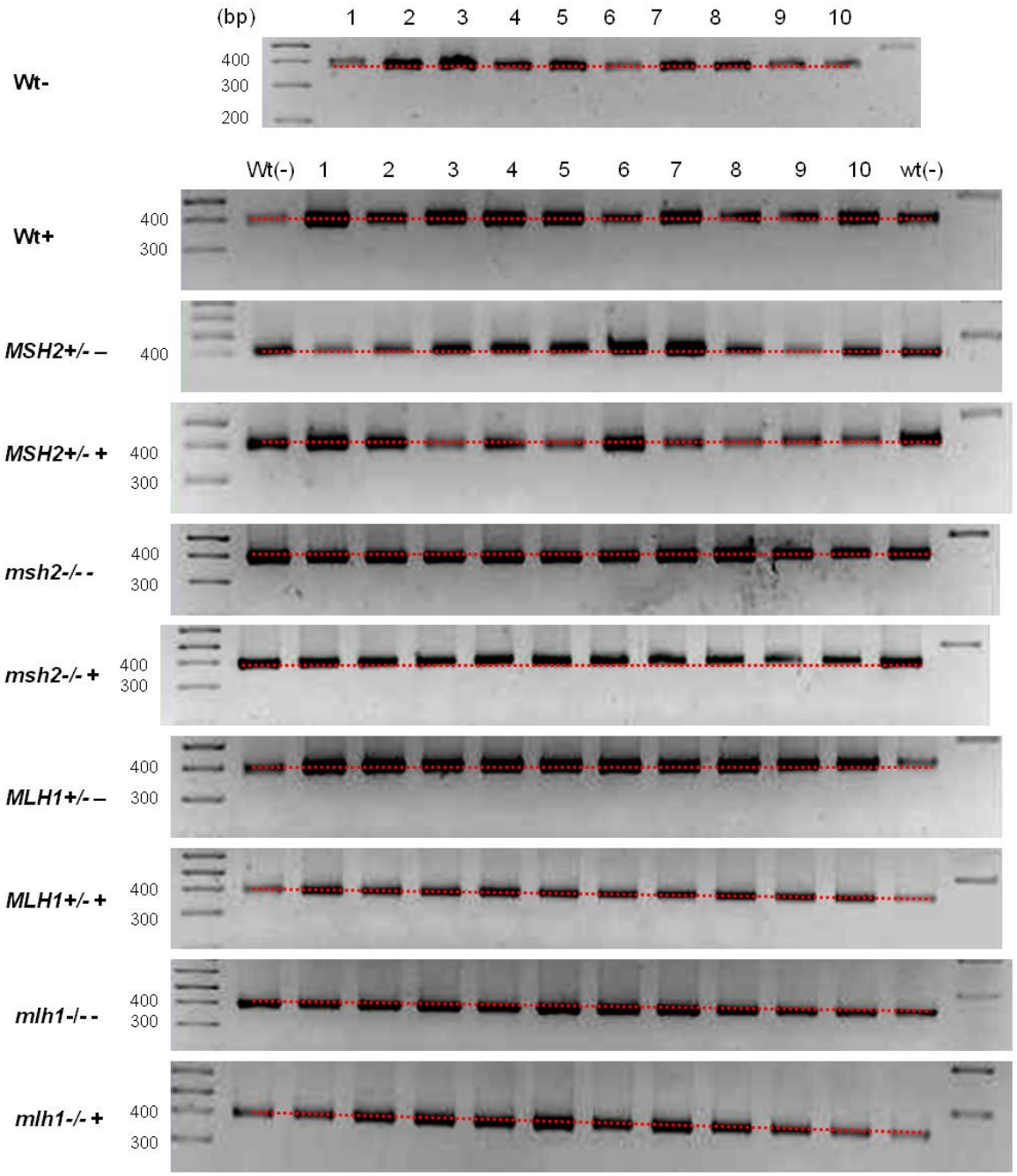


**Figure 3-18. Testing for kDNA microsatellite instability in *T. brucei* PCF MMR mutants in the presence of 20 µM $H_2O_2$.**

WT, *MSH2+/-*, *msh2-/-*, *MLH1+/-*, and *mlh1-/-* cells were grown in the absence (-) and presence (+) of 20µM $H_2O_2$ for 48 hours. kDNA microsatellite locus was amplified from 10 clones from each cell line using primers kDNA-FAM(F) and kDNA(R) and PCR products were separated on 3% agarose gel. PCR product from one of the wild type sub clones was also added in the first and last lane parallel to the mutants. Clones that show a difference in size relative to WT are indicated by an arrow; size markers are shown.

## 3.2.4 Generation of *T. brucei* PCF MSH2 re-expresser cells.

Based on the above results we wished to test further the hypothesis that some adaptation had occurred during the generation of the *msh2* mutants that led to increased resistance to oxidative stress. To do this a gene re-expression strategy was used. One copy of *MSH2* was

reinserted into the *msh2-/-* mutants to make *MSH2-/-/+* cells, and attempts were made to compare the phenotypes with the wild type, *MSH2+/-* and *msh2-/-* cells that preceded this cell line

### 3.2.4.1 Strategy for the generation of MSH2 re-expresser cells

This strategy relies upon, following transformation and recombination, a cassette containing *MSH2* that integrates and replaces either of the *BSD* or *PUR* resistance cassette in the mutated *msh2-/-* locus (Figure 3-19). Briefly, this construct (Bell 2004) was generated using a 4.5 kb region containing the *MSH2* gene that was digested from a lambda *T. brucei* genomic DNA clone using *EcoRI* restriction sites. The 4.5 kb fragment was cloned into pBluescript SK II, followed by cloning a phleomycin resistant cassette downstream of the 3' UTR of the *MSH2* gene. For transformation into *T. brucei* PCF *msh2-/-* mutants, linear DNA was produced from the construct using *HindIII* restriction digestion.

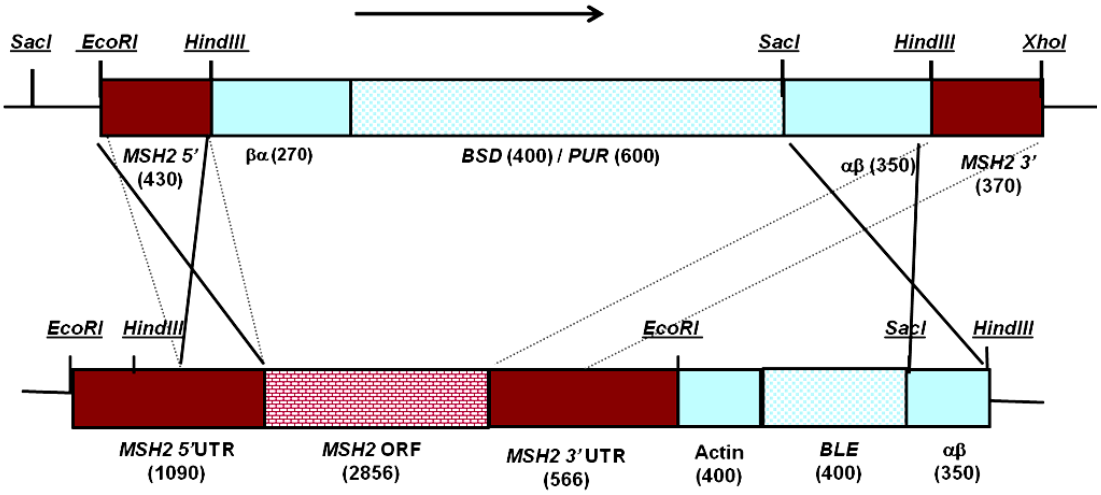


**Figure 3-19 Construct designed for generation of *MSH2* re-expresser cells.**

3' and 5' UTRs of *MSH2* are indicated by red block boxes; the *MSH2* ORF is indicated by a red checked box. Actin and tubulin processing signals are indicated by blue blocks, whereas the phleomycin resistance (*BLE*) gene in the construct is indicated by a blue checked box, as are the *BSD* and *PUR* ORFs within the mutated *msh2-/-* locus. Dotted lines indicate the relationship between the *MSH2* UTRs in the construct and genome, and crossed lines show the regions for recombination leading to integration of the *MSH2* gene and *BLE* cassette. Restriction sites used for generation of the construct are labelled and sizes of annotated fragments are written in brackets. Upon successful integration, an ~5 kb construct containing the *MSH2* ORF and *BLE* resistance cassette replaces either of the *BSD* or *PUR* resistance cassettes in the *msh2-/-* mutants and generates *MSH2-/-/+* re-expresser cells.

### 3.2.4.2 Transformation of PCF *msh2-/-* mutants with re-expresser construct

*T. brucei* PCF *msh2-/-* cells were grown to a density of $1x10^7$cells.ml$^{-1}$ in the presence of 10 µg.ml$^{-1}$ blasticidin and 1 µg.ml$^{-1}$puromycin. $2.5x10^7$ cells were used for transformation. Plasmid DNA was extracted from *E. coli* cells using Qiagen miniprep kit (see Section 2.2.2) and was linearized using *Hin*dIII. ~5 µg of linearized DNA was used per transformation. Parasites were transformed as described in Section 2.1.4.1 and clones were selected in the presence of 2.5 µg.ml$^{-1}$ phleomycin. Cells were incubated for 10-15 days until 3 independent clones were collected. Transformants selected were then cultured in 10 ml and grown for 5 generations in the presence of 2.5 µg.ml$^{-1}$ phleomycin before genomic DNA was made and confirmatory PCRs were done as described in Section 2.2.5.

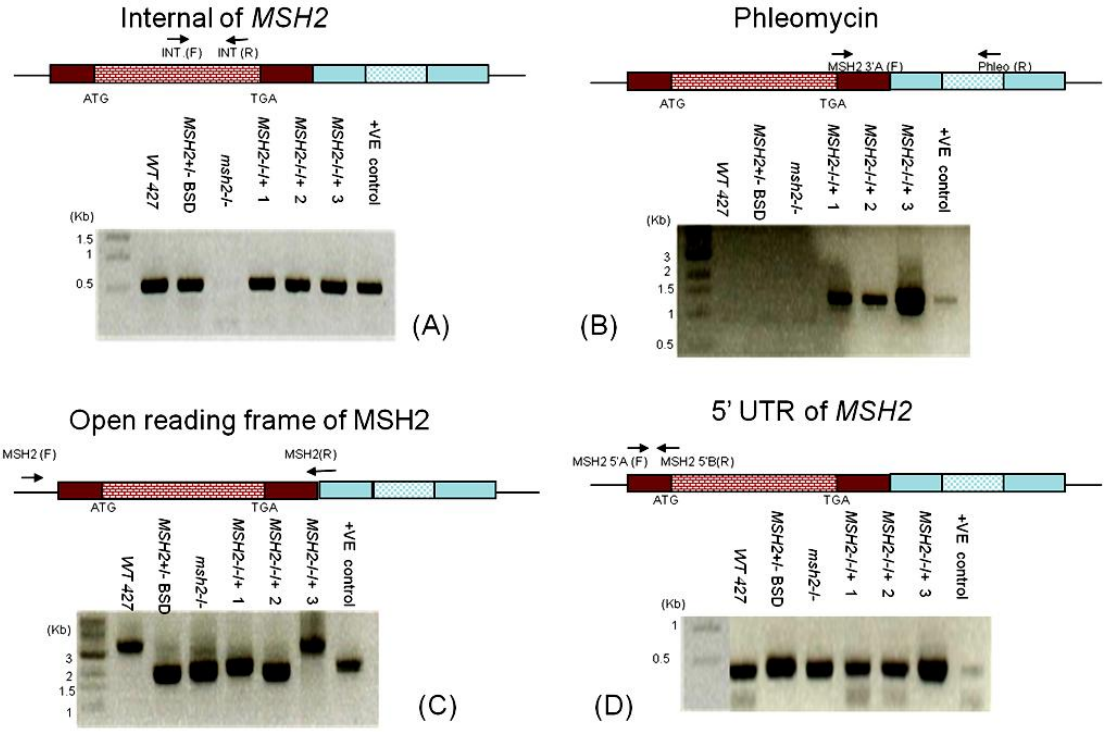


**Figure 3-20 PCR analysis of *T. brucei* PCF *MSH2-/-/+* re-expressers.**

Three putative PCF *MSH2-/-/+* clones (1-3) were analyzed by PCR to check for re-integration of the *MSH2* ORF in the *msh2-/-* cells; wild type, *MSH2+/- and msh2-/-* PCF cells were also examined, as well as *T. brucei* BSF *MSH2-/-/+* cells (made by J.Bell (Bell 2002)) as a positive control, as these were generated by the same strategy. PCR products are shown after separation on 1% agarose gel; size markers are indicated, and in the diagrams above the gels arrows depict the location of primers used. (A) DNA samples were PCR- amplified for a 500 bp region of the *MSH2* ORF using primers MSH2 int (F), MSH2 int (R). (B) PCR to check for correct linkage between *MSH2* and *Phleo*, using forward primer MSH2 3'A, specific to the 5' end of the 3' UTR, and reverse primer Phleo (R), specific to the phleomycin drug resistance gene (BLE). (C) The complete *MSH2* locus was PCR-amplified with forward primer MSH2 (F), specific to the sequence upstream of the 5'UTR, and MSH2 (R), which is complementary to the 3' UTR. (D) The 5'UTR of MSH2 was PCR-amplified with primers MSH2 5'A and MSH2 5'B.

In order to test whether or not *MSH2* had correctly re-integrated into the *msh2*-/- mutants, a number of PCRs were run (Figure 3-20). These results confirm that the construct containing the *MSH2* ORF and *BLE* drug resistance cassette has integrated and restored an *MSH2* gene copy, generating *MSH2-/-/+* cells. The *MSH2* 5'UTR was first PCR-amplified to confirm the presence of amplifiable DNA in all the test samples, including the three *MSH2*-/-/+ clones selected (Figure 3-20 D). Re-integration of *MSH2* was confirmed by PCR-amplifying an internal region of the gene's ORF using primers MSH2 int (F) and MSH2 int.(R), which generated a 500 bp product in wild type, *MSH2+/-* and *MSH2-/-/+* cells, but not in the *msh2*-/- null mutants (Figure 3-20 A). Only in the *MSH2-/-/+* cells could the *BLE* gene be PCR-amplified (Figure 3-20 B), of the product size 1366 bp. Although the parasites had been growing on drugs PCR was designed to confirm that the cassette remained connected with the 3' UTR of the *MSH2* gene. In attempt to PCR-amplify the complete *MSH2* ORF, only in one of the three *MSH2-/-/+* clones was a product of the expected size (3.76 kb) generated (Figure 3-20 C); however, the same was seen in BSF *MSH2-/-/+* cells generated previously (Bell 2002) and in the PCF *MSH2+/-* cells, suggesting this is due to preferential amplification of the smaller resistance gene-disrupted *msh2::PUR* or *msh2::BSD* alleles.

Growth analysis of the three *MSH2-/-/+* clones was next performed, which showed that there was no obvious growth difference between the clones (data not shown). Thus, one of these three clones was selected for further characterization.

## 3.2.5 Phenotypic analysis of MSH2 re-expressers

### 3.2.5.1 *In vitro* growth analysis of MSH2 re-expressers

Growth and doubling times of the *MSH2-/-/+ (MSH2::BLE)* cells was first measured and compared with wild type, *MSH2+/-* and *msh2-/-* cells to check for if any growth differences were observed. For all the growth analysis and other growth related experiments (see below), cultures were grown in the presence of their respective drugs for at least 3 days but during analysis none of the cells were grown on any drugs apart from any mutagen, if tested. For the growth and doubling time analysis wild type, *MSH2+/-*, *msh2-/-* and *MSH2-/-/+* cells were grown to log phase and then diluted to a density of 5x $10^5$cells.ml$^{-1}$ in 10 ml of SDM-79 media and incubated at 27 $^0$C. Cell densities were counted every 24 hours over a period of 72 hours (Figure 3-21 and Table 3-3).

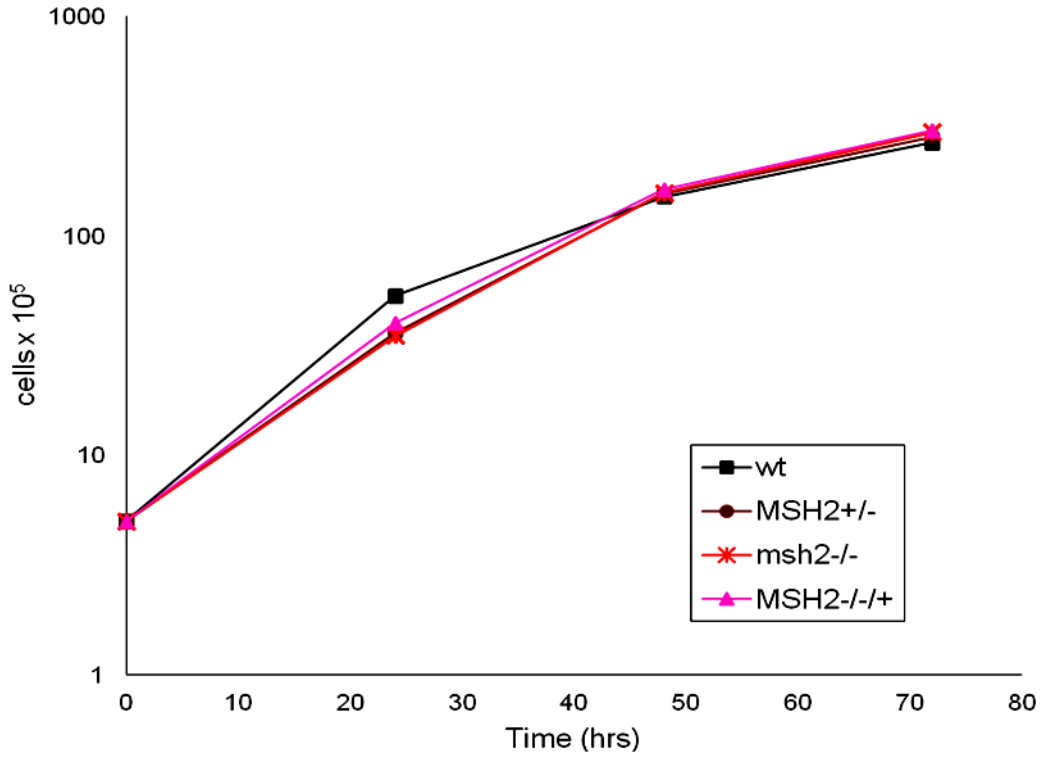


**Figure 3-21 Growth curve of *T. brucei* PCF wild type cells and *MSH2* mutants.**

PCF wild type, *MSH2*+/-, *msh2-/- and MSH2-/-/+* cells were inoculated at a density of $5x10^5$ cells.ml$^{-1}$ in 5 ml of media and cell densities counted at 24 hour intervals over a period of 72 hours using haemocytometer. Values show the mean cell densities at each time point, and vertical bars denote standard deviation from three replicates.

**Table 3-3 Doubling time of *T. brucei* PCF wild type and *MSH2* mutants.**

| CELL LINE | | | | |
|---|---|---|---|---|
| | **WT 427** | ***MSH2+/-*** | ***msh2-/-*** | **MSH2-/-/+** |
| **Doubling time** | 12.67 | 12.46 | 12.32 | 12.27 |

Both the *in vitro* growth curve and the extrapolated doubling times very clearly show that there is no difference in growth phenotypes between the wild type cells, the *MSH2* mutants and the re-expresser.

### 3.2.5.2 Alkylation tolerance of *MSH2* re-expressers.

As discussed in Section 3.2.2.2, a characteristic phenotype of MMR mutants is resistance to alkylation damage, including MNNG. To examine the response of the MSH2 re-expresser cells towards alkylation damage, wild type, *MSH2*+/-, *msh2*-/- and *MSH2*-/-/+ cells were grown in the presence of increasing concentration of MNNG and the relative

survival determined as described in Section 3.2.2.2. The results of this analysis are shown in Figure 3-22.

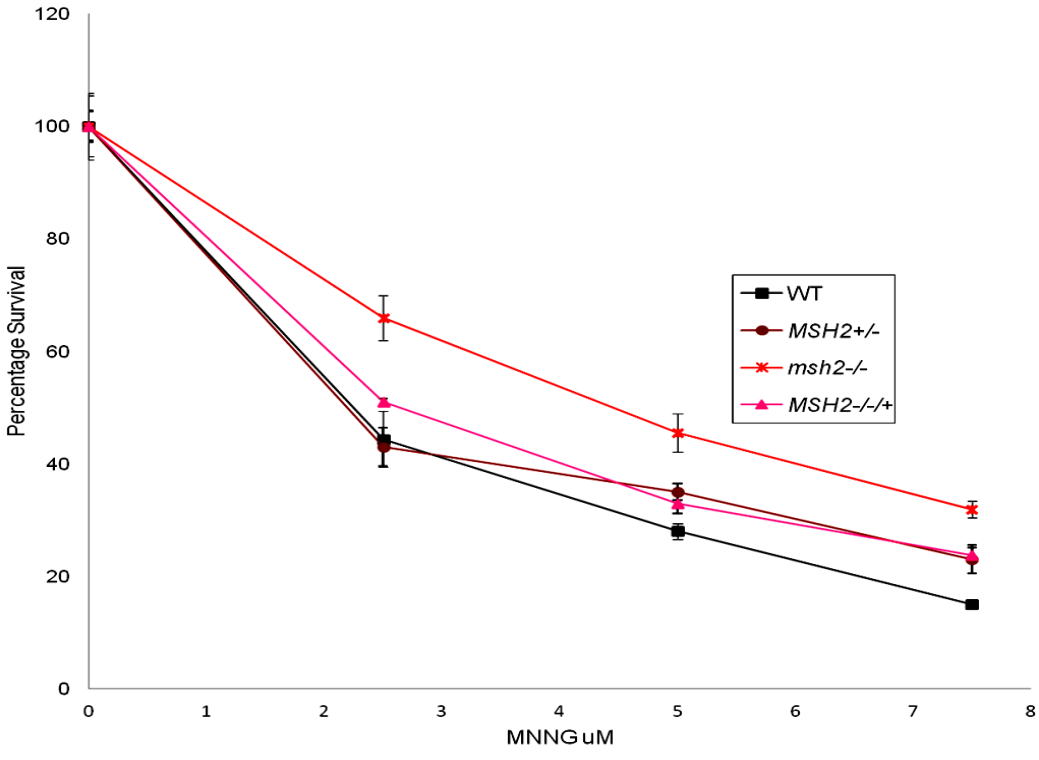


(A)

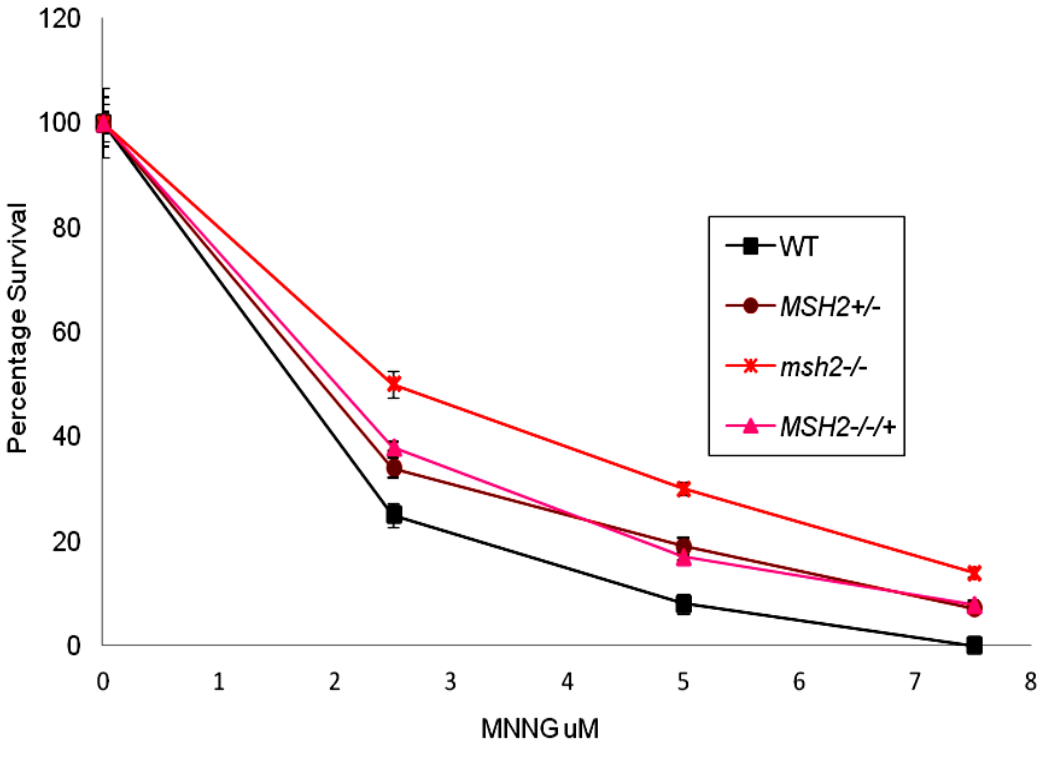


(B)

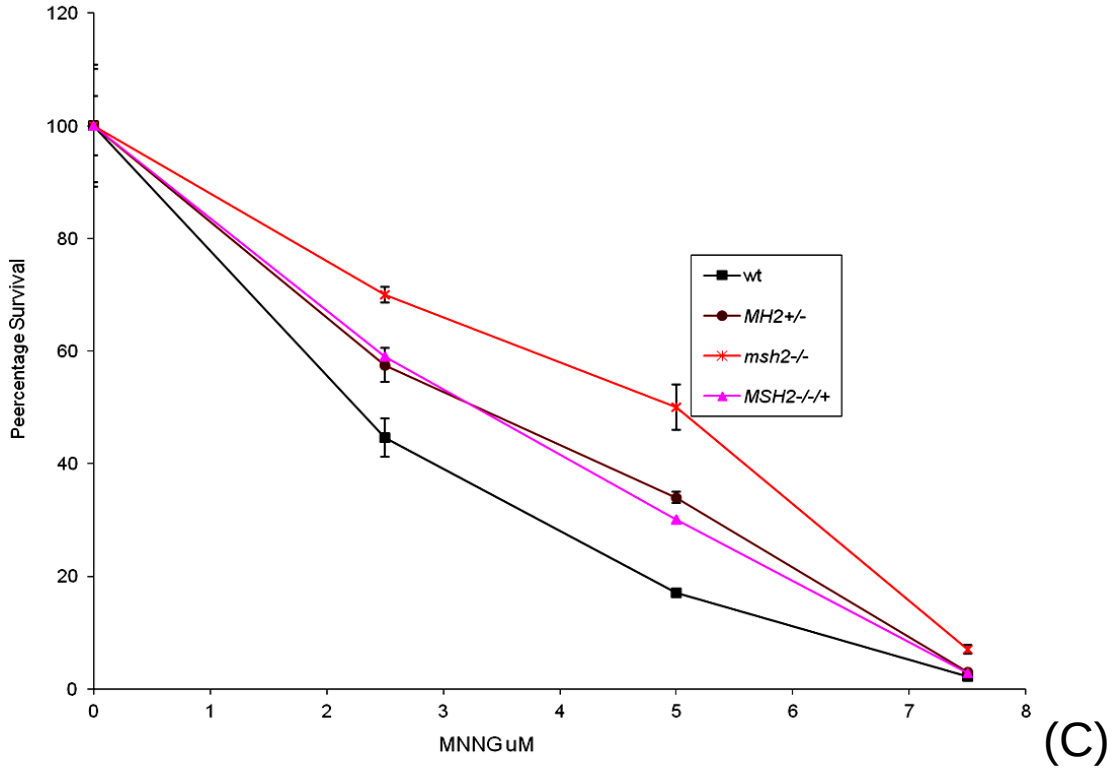


**Figure 3-22 Percentage survival of *T. brucei* PCF wild type and *MSH2* mutants at various concentration of MNNG.**

Wild type, *MSH2*+/-, *MSH2*-/-/+ and *msh2*-/- *T. brucei* cells were diluted to $5x10^5$ cells.$ml^{-1}$ in SDM-79 culture media containing 0, 2.5, 5 or 7.5 µM MNNG. Cell densities were measured (A) 24 hours, (B) 48 hours and (C) 72 hours subsequently and are shown as a percentage of the density of each cell line in the absence of MNNG (taken as 100 %). Each value is the mean of three experiments, and vertical bars depict standard deviation.

The relative survival of the wild type, *MSH2*+/- and *msh2*-/- cells in this independently preformed experiment confirm what was observed previously (Section 3.2.2.2), in that the loss of one and then two alleles of *MSH2* caused progressively greater resistance to MNNG. When compared with these cells, the percentage survival of the *MSH2*-/-/+ re-expressers clearly overlapped with the *MSH2*+/- cells at nearly all MNNG concentrations and at each time point, and was distinct from the wild type and *msh2*-/- cells. This indicates that the *MSH2* gene has been successfully re-introduced and re-expressed, and that the cells are phenotypically heterozygous for *MSH2*, suggesting a single copy of the gene has been integrated.

### 3.2.5.3 *In vitro* growth of MSH2 re-expressers in response to oxidative stress

The survival curves in the presence of MNNG confirmed that the *MSH2*-/-/+ cells have restored expression of, most likely, one gene copy of *MSH2*. We next attempted to examine the survival of the MSH2 re-expressers in the presence of $H_2O_2$ in order to test the hypothesis that an adaption has occurred in the generation of the *msh2*-/- mutants rendering

them resistant to oxidative stress. This was done by comparing the survival of the re-expresser cells in the presence of increase concentrations of $H_2O_2$ with wild type, *MSH2+/-* and *msh2-/-* mutants. Experimental conditions were set up as described in Section 3.2.3. The results are shown in Figure 3-23.

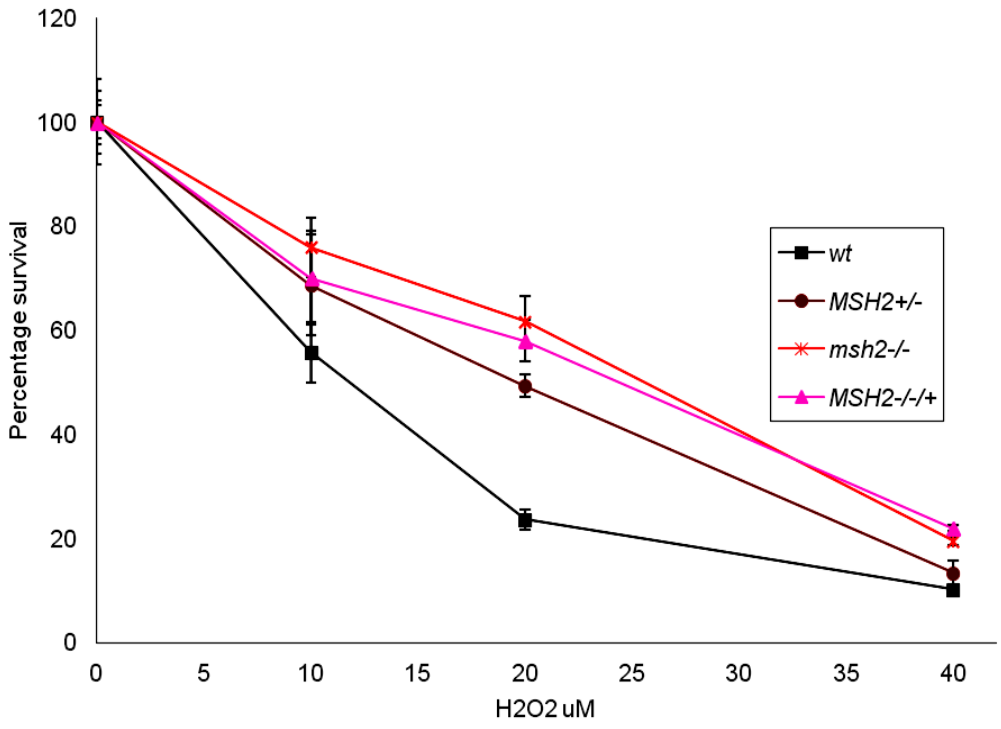


(A)

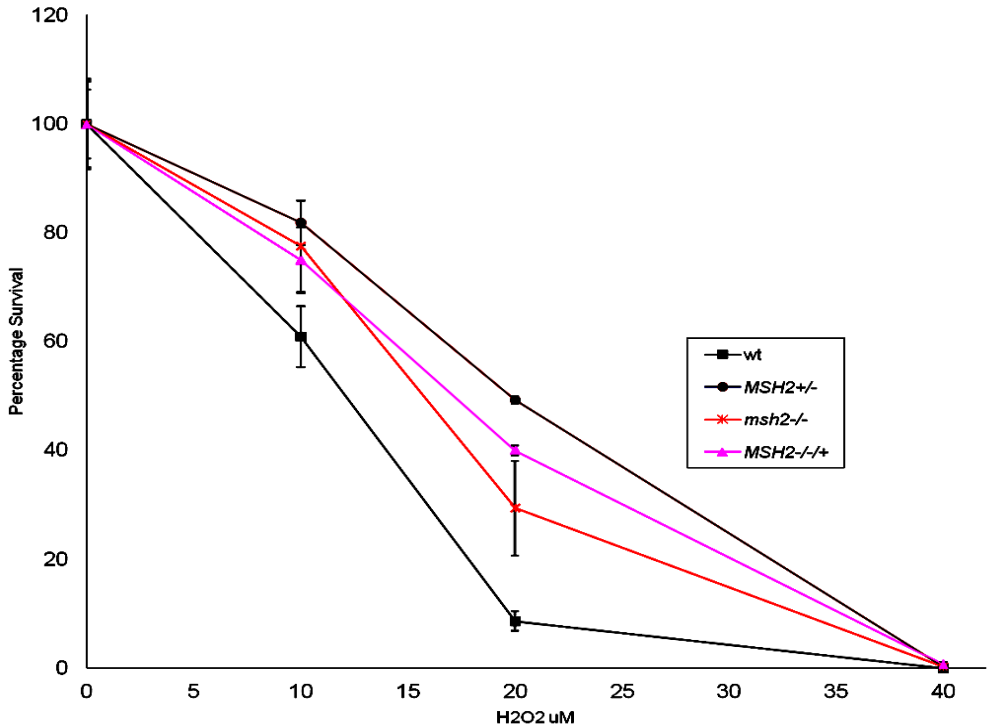


(B)

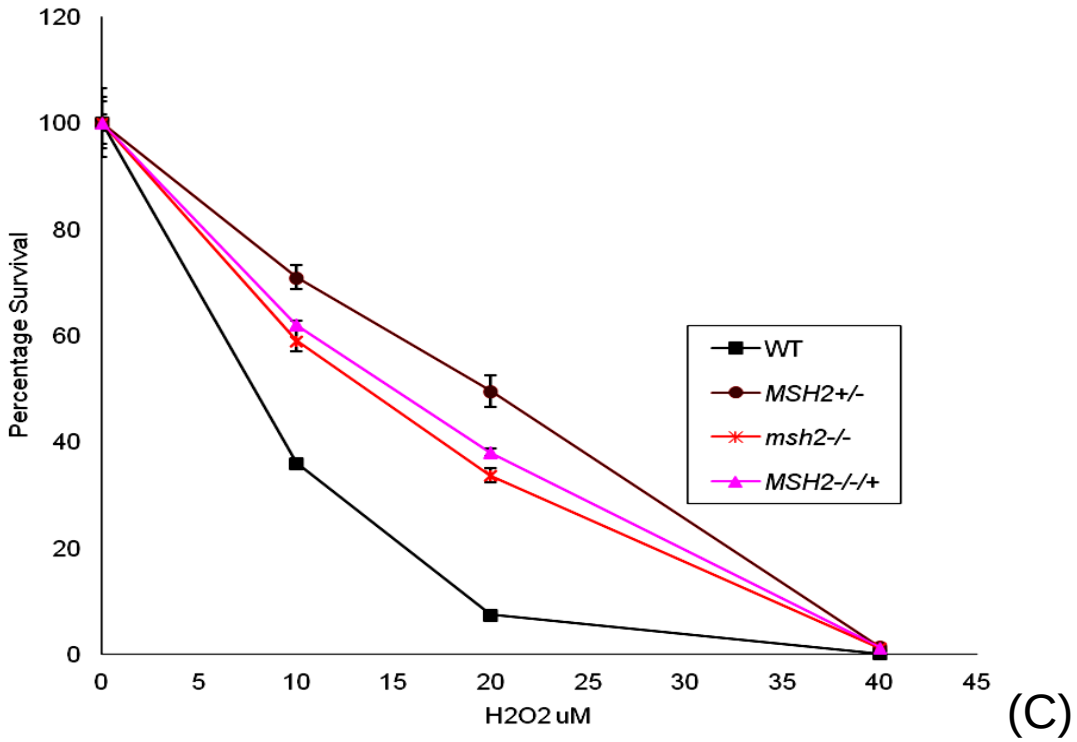


**Figure 3-23 Percentage survival of *T. brucei* PCF wild type and *MSH2* mutants at various concentration of $H_2O_2$.**

Wild type, *MSH2*+/-, *MSH2*-/-/+ and *msh2*-/- *T. brucei* cells were diluted to $5x10^5$ cells.ml$^{-1}$ in SDM-79 culture media containing 0, 10, 20 or 40 µM $H_2O_2$. Cell densities were measured (A) 24 hours, (B) 48 hours and (C) 72 hours subsequently and are shown as a percentage of the density of each cell line in the absence of $H_2O_2$ (taken as 100%). Each value is the mean of three experiments, and vertical bars depict standard deviation.

The resistance patterns of the *MSH2*+/- and *msh2*-/- cells with respect to wild type cells remains the same in this experiment as that performed previously (Figure 3-14), which shows the reproducibility of *T. brucei* PCF wild type and *MSH2* mutants' survival in the presence of $H_2O_2$ as a source of oxidative stress. However, in contrast to the equivalence in MNNG tolerance seen for the *MSH2*+/- and *MSH2*-/-/+ cells, a strikingly distinct phenotype was seen when grown in the presence of $H_2O_2$. Here, the *MSH2*-/-/+ cells were phenotypically distinct from the *MSH2*+/- cells at nearly all concentrations of $H_2O_2$ and at each of the three time points examined. In fact, the *MSH2*-/-/+ cells' survival closely overlapped with the *msh2*-/- mutants after 72 hrs growth in $H_2O_2$, and was closer to the null mutants at the earlier time points. The only exception to this trend is at 24 hours at 10 µM $H_2O_2$, where the *MSH2*-/-/+ cells has almost the same percentage survival as the *MSH2*+/-. Another data point which is different is at 48 hours at 20 µM $H_2O_2$, where the *MSH2*-/-/+ cells have a percentage survival of 40 %, different from both *msh2*-/- (30%) and *MSH2*+/- (50%). Thus, we cannot confidently say that the *MSH2*-/-/+ cells have an $H_2O_2$ resistance phenotype exactly like that of *msh2*-/-, but it is certainly different from

*MSH2*+/-. This appears consistent with the suggestion that unknown adaptations have occurred in the generation of the *MSH2* mutants, most likely to cope with the loss of MSH2's role in the response to oxidative damage. Such changes could have been selected either during the course of the transformations or during the growth of the *MSH2*+/- and *msh2*-/- mutants.

### 3.2.5.4 Microsatellite instability of MSH2 re-expressers

We next tested for the presence or absence of MSI in the *T. brucei* PCF MSH2 re-expressers, in order to test if the putative adaptation had any effect on genetic stability. To do this, the cells were grown in the absence and presence of 20 μM $H_2O_2$ for 48 hours and then cloned in 96 well plates as detailed in Section 3.2.3.1. Genomic DNA was then prepared and PCR used to amplify the JS-2 locus (Figure 3-24).

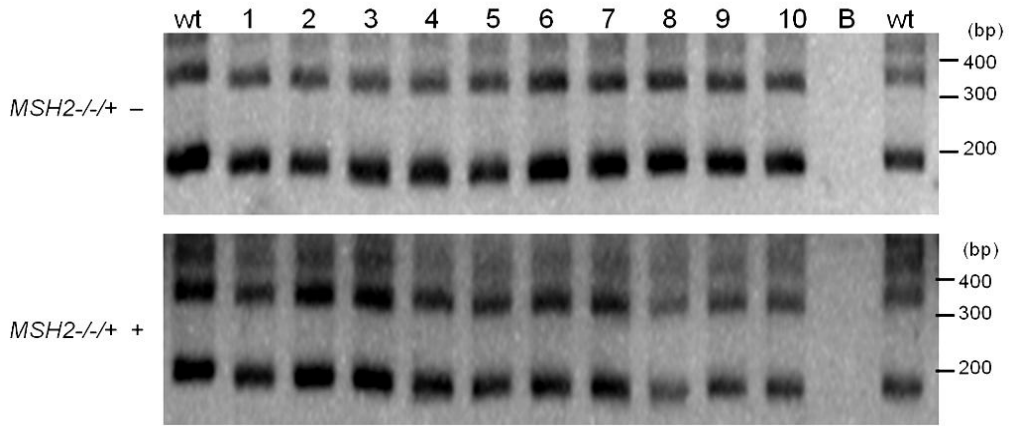


**Figure 3-24 Testing for microsatellite instability in *T. brucei* PCF MSH2 re-expressers.**

*MSH2-/-/+* cells were grown in the absence (-) and presence (+) of 20 μM $H_2O_2$ for 48 hours. JS2 locus was PCR-amplified from 10 clones using primers JS2A and JS2B and PCR products were separated on 3% agarose gel. PCR product from one of the wild type sub clones was also added in the first and last lane parallel to the mutants. Clones that show a difference in size relative to WT are indicated by an arrow; size markers are shown.

PCR analysis of the JS-2 microsatellite in the *MSH2* re-expressers grown in either the presence or absence of $H_2O_2$ revealed no changes in allele size, showing that no clones displayed MSI. This finding is like the alkylation tolerance phenotype, where the *MSH2*-/-/+ cells are phenotypically the same as the *MSH2*+/- cells and have reverted the loss of MMR seen in the *msh2*-/- mutants. Thus, if adaptation has occurred, this does not have an influence on MSH2's contribution to MMR in genome stability.

### 3.2.6 Survival of *T. brucei* BSF MMR mutants in the presence of $H_2O_2$

*T. brucei* BSF MMR mutants have already been analyzed in the presence of increasing concentrations of $H_2O_2$ (Machado-Silva et al. 2008). We repeated and extended these experiments for two reasons. Firstly, only *MSH2+/-* and *msh2-/-* cells have been analyzed before and no results have been reported for *MSH2-/-/+* mutants in BSF. Thus, we cannot say if the lack of complementation in the oxidative stress response when re-expressing MSH2 in the PCF *msh2-/-* mutants is lifecycle stage-dependent. This we predict to be the case, as the PCF and BSF MSH2 mutants have contrasting phenotypes in response towards oxidative stress, where the BSF *msh2-/-* mutants are more sensitive to $H_2O_2$. This would infer that MSH2 has a less critical function in this life cycle stage and its loss does not necessitate the adaptation that we propose. *MSH2-/-/+* cells had been previously made by J.S Bell (Bell 2002) and have been confirmed to have restored one gene copy of MSH2 by testing for MNNG tolerance (Bell 2004). Secondly, previously it was reported that *mlh1 -/-* mutants do not show any phenotypic sensitivity in the presence of $H_2O_2$ (Machado-Silva 2008), though over a rather limited range of concentrations (50 and 100 μM $H_2O_2$).

To test the effect of $H_2O_2$, wild type, *MSH2+/-* (1 μg.ml$^{-1}$ puromycin), *msh2-/-* (0.5 μg.ml$^{-1}$ puromycin, 10 μg.ml$^{-1}$ blasticidin), *MSH2-/-/+* (2.5 μg.ml$^{-1}$ phleomycin) *MLH1+/-* (1μg.ml$^{-1}$ puromycin), and *mlh1-/-* (0.5 μg.ml$^{-1}$ puromycin, 10μg.ml$^{-1}$ blasticidin) cells were grown to their log phase. The cultures were then diluted to 1 x $10^5$cells.ml$^{-1}$ in 20 ml HMI-9 without antibiotics. $H_2O_2$ was added to the culture media to a concentration of 0, 100, 200 or 300 μM and the cultures were incubated at 37 $^0$C, 5% $CO_2$. All cultures were setup in duplicate and cells counted 48 hours and 72 hours subsequently. These data are shown in Figure 3-25.

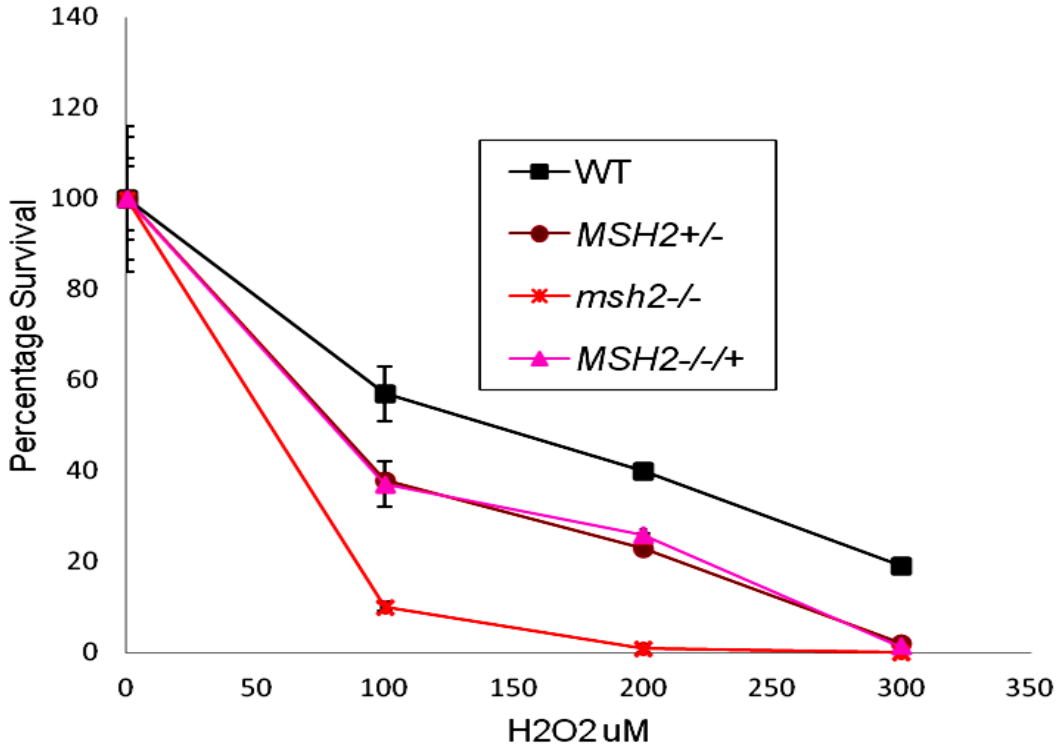
140
120
100
80
60
40
20
0
Percentage Survival
0
50
100
150
200
250
300
350
H2O2 uM
WT
MSH2+/-
msh2-/-
MSH2-/-/+

(A)

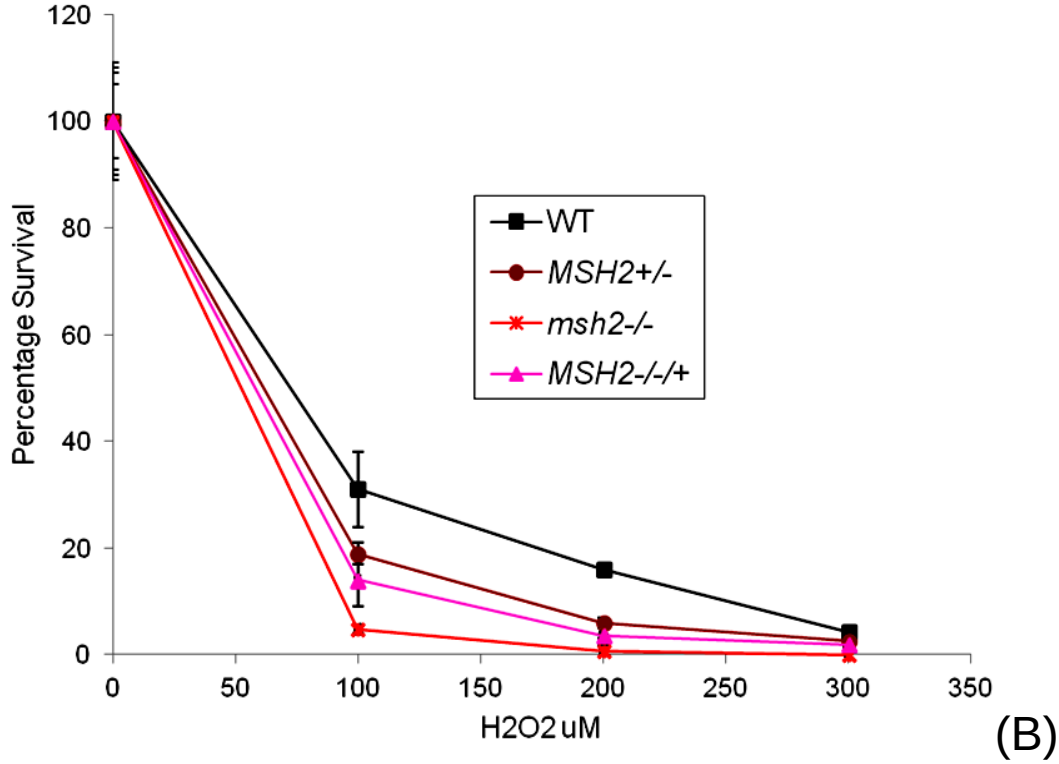
120
100
80
60
40
20
0
Percentage Survival
0
50
100
150
200
250
300
350
H2O2 uM
WT
MSH2+/-
msh2-/-
MSH2-/-/+

(B)

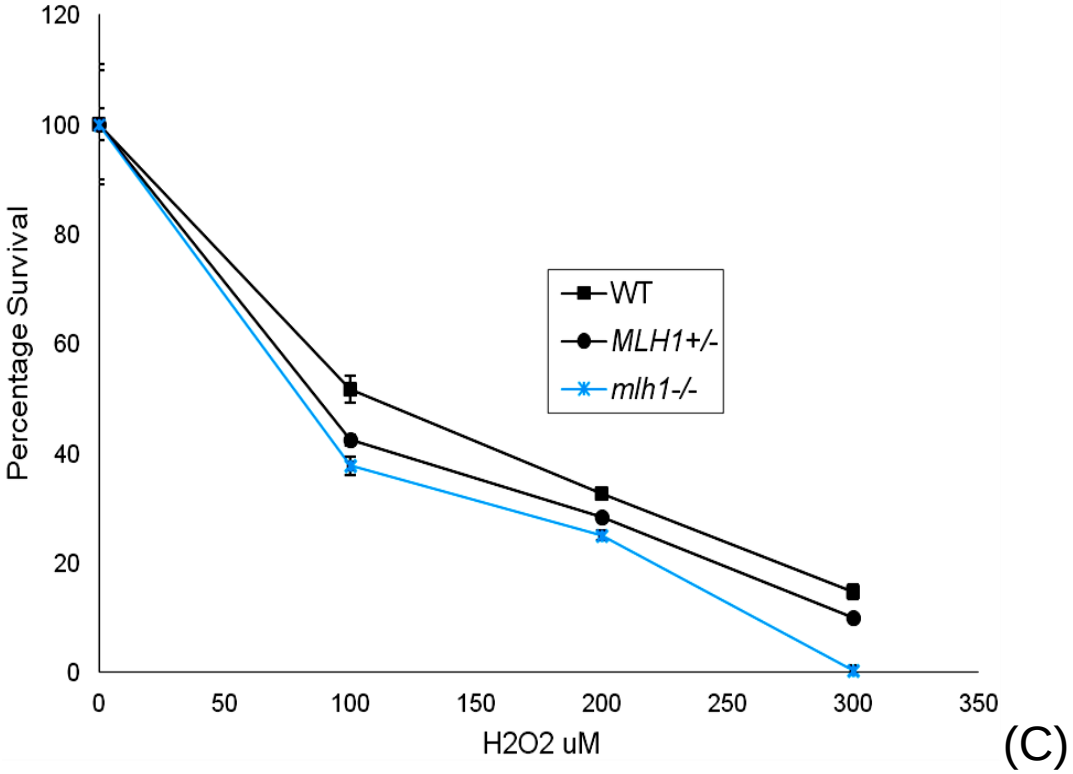


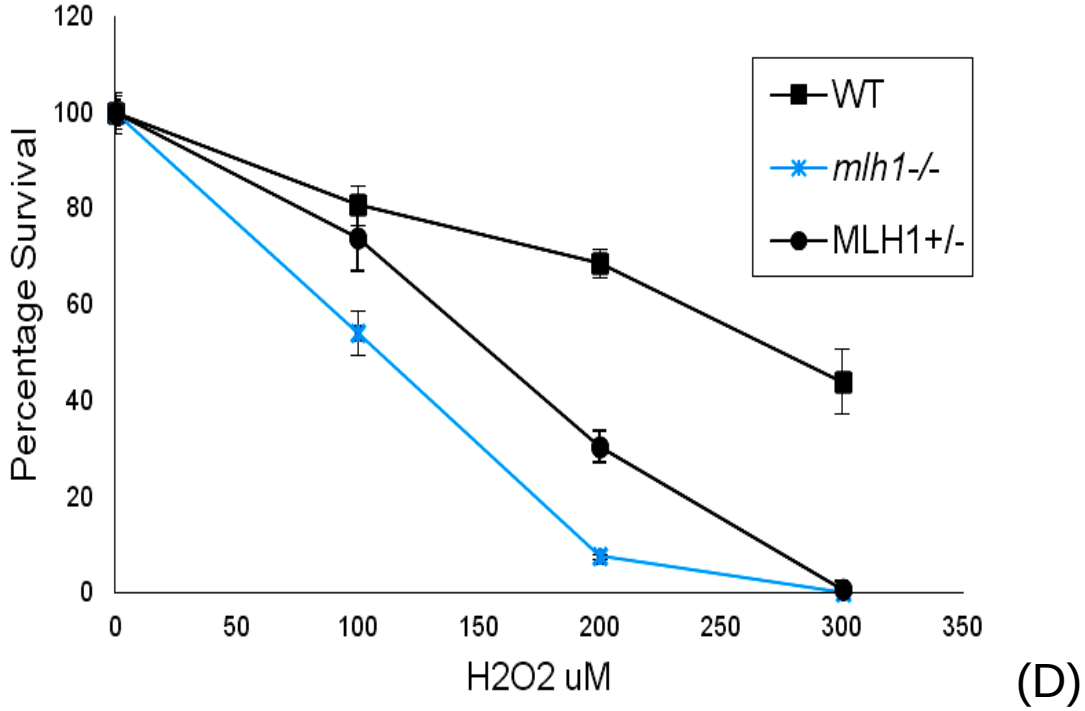


**Figure 3-25 Percentage survival of *T. brucei* BSF wild type, *MSH2* and *MLH1* mutants at various concentration of $H_2O_2$.**

Wild type, *MSH2*+/-, *MSH2*-/-/+, *msh2*-/-, *MLH1*+/- and *mlh1*-/- *T. brucei* cells were diluted to 1x$10^5$ cells.$ml^{-1}$ in HMI-9 culture media containing 0, 100, 200 or 300 μM $H_2O_2$. Two independent experiments were setup where cell densities of wild type and *MSH2* mutants were measured (A) 48 hours, (B) 72 hours. Cell densities of wild type and *MLH1* mutants were measured at (C) 48 hours and (D) 72 hours. Cell counts are shown as a percentage of the density of each cell line in the

absence of $H_2O_2$ (taken as 100%). Each value is the mean of two experiments, and vertical bars depict standard deviation.

The results from this experiment demonstrates that the *MSH2-/-/+* cells in BSF *T. brucei* are phenotypically more like the *MSH2+/-* heterozygous mutants in response towards $H_2O_2$ (Figure 3-25 A-B). At 48 hours, the *MSH2-/-/+* cells' survival curve overlapped with the *MSH2+/-* mutant's curve and was clearly distinct from the *msh2-/-* mutants. At 72 hours, although the *MSH2-/-/+* cells appeared slightly more sensitive than the *MSH2+/-* mutants, their percentage survival was closer to the *MSH2+/-* mutants than the *msh2-/-* mutants. At each time point, the *MSH2+/-* and *MSH2-/-/+* cells were more sensitive to $H_2O_2$ than the wild type cells, suggesting that a single allele of *MSH2* provides insufficient MSH2 protein for its role in oxidative repair. These data contrast with that seen in PCF *T. brucei*, where re-expression of MSH2 in an *msh2-/-* mutant does not revert the altered cell response to $H_2O_2$.

This analysis also suggests that *MLH1*mutants, when grown at high concentrations of $H_2O_2$, show some sensitivity to oxidative damage (Figure 3-25 C-D), which contrasts with previous reports (Machado-Silva 2008). Reduced survival of the *mlh1-/-* cells relative to wild type was not clear after 48 hrs, though appeared more pronounced at 72 hours. Some caution must be taken in this interpretation, however, as the extent of the cell killing in the wild type cells is less than expected in this experiment at this time point (compare Figure 3-25 B and D). This is most likely due to variability in the effects of $H_2O_2$ in culture, as have been discussed before, and suggests this needs further verification. Nonetheless, these data confirm that the *msh2-/-* cells display greater sensitivity to $H_2O_2$ than *mlh1-/-* cells, especially at lower concentrations, confirming a differential contribution of the two MMR proteins to oxidative damage repair.

## 3.3 Discussion

The MMR repair system is a widely studied process involved in the maintenance of genome stability, and has been previously characterized in *T. brucei* and *T. cruzi* (Bell 2004;Machado-Silva 2008). This chapter sought to compare the function of MMR in two life cycle stage of *T. brucei* in the response to oxidative stress, since it had been shown that loss of MSH2, but not MLH1, renders BSF *T. brucei* sensitive to $H_2O_2$. Our initial hypothesis was, in fact, that it would not be possible to make *MSH2* null mutants in PCF *T. brucei* cells. In part this was because attempts to date to make null mutants for *MSH2* in *T. cruzi* have failed and heterozygous mutants show a strong phenotype of increased sensitivity to $H_2O_2$ (Campos et al. 2011). In addition, it was clear that PCF cells are at least 10-fold more sensitive to $H_2O_2$ than BSF cells. This hypothesis was incorrect, since all the results clearly demonstrate that both *MSH2* and *MLH1* null mutants were successfully made in *T. brucei* PCF parasites. However, during initial attempts to make the null mutants, we were unable to get antibiotic resistant clones, which appeared consistent with the possibility that both MSH2 and MLH1 might be essential. At this point, the heterozygous mutants were characterized for their doubling time and survival in the presence of MNNG (data not shown) to ask if they showed any phenotypes, as has been seen for *MSH2*+/- cells in *T. cruzi*. However, no differences were observed relative to wild type cells and, since the MMR mutants had been successfully made in BSF *T. brucei*, we tried several approaches, including selecting the parasites in various reduced antibiotic concentrations during growth prior to transformation and after transformation during cloning by serial dilutions. After several attempts, double resistant clones for both *MSH2* and *MLH1* were recovered, though the efficiency of cloning was very low, as detailed in Table 3-1. In addition, the clones selected initially grew poorly in media containing the selective antibiotics and had to be maintained at a higher cell density (~$2x10^6$ cells.$ml^{-1}$) than the wild type cells of this strain, which could be routinely diluted to $5x10^5$ cells.$ml^{-1}$. These putative mutant clones were diluted every day for about 1 week, at which time they started to grow in SDM-79 in the presence of the drugs with no difference in doubling time relative to wild type cells. These observations may be consistent with selection of adaptive changes during the loss of the MMR genes, though may simply reflect inappropriate levels of antibiotic selection. Since no control transformations were run in parallel it is not possible to draw conclusions.

Once verified by genotypic analysis, the PCF MMR mutants were analyzed by phenotypic analysis for the loss of the respective genes. When analyzing the alkylation tolerance in the

PCF MMR mutants, all the MMR mutants were shown to be resistant to MNNG damage, with null mutants being more resistant than heterozygous mutants, which were also more resistant than wild type cells. This is a characteristic phenotype of impaired MMR machinery. Throughout the survival curve analysis, *mlh1-/-* mutants were found to be the most resistant of all the clones, which was not seen in BSF MMR mutants, both in previous analysis (Bell 2004), and in the Alamar blue approach used for analysis in this study. The reason for this is unclear, but may suggest an important role of MLH1 in PCF *T. brucei* in response to MNNG methylation. Whether it may also reflect the different phenotypes of *MSH2* and *MLH1* mutants in response to oxidative damage is unclear (see below). The *T. brucei* PCF MMR mutants were also tested for genetic instability using a JS-2 microsatellite. This analysis showed that at least 3 out of 10 clones of both *msh2-/-* and *mlh1-/-* cells showed MSI in this locus, but no examples were seen for the heterozygous mutants, a strikingly similar phenotype to that seen previously in BSF MMR mutants (Bell 2004).

Once it was confirmed that *MSH2* and *MLH1* mutants had impaired MMR activity, their role in the *T. brucei* response to oxidative stress was examined. For all the experiments, $H_2O_2$ was used as a source of oxidative stress and we have not attempted other agents or treatments. Survival of the PCF MMR mutants in the presence of $H_2O_2$ was considered important to analyse for two reasons. Firstly, PCF wild type *T. brucei* Lister 427 cells have been shown to be 10-30 times more sensitive to $H_2O_2$ oxidative damage than BSF wild type Lister 427 ((Barnes 2006); and this study). Several reasons might explain this increased sensitivity. One of the characteristic features of PCF *T. brucei* parasites is increased mitochondrial metabolism relative to BSF cells, which results in increased intracellular redox activity and thus increased biological and intracellular oxidative stress (Colasante 2009;Vertommen 2008). This could mean that cells are nearly saturated with oxidative damage and thus have less capacity to entertain extracellular oxidative stress (Krauth-Siegel 2008). PCF *T. brucei* cells may also be more sensitive towards oxidative stress due to the media in which the parasites are cultured. Both the *in vitro* and *in vivo* environments of PCF and BSF *T. brucei* are very different, and a key element is the presence of metal ions, in particular in the culture media (Brun 1992;Hirumi & Hirumi 1994), and most prominently $Fe^{++}$. I*n vivo*, iron uptake in BSF cells occurs via the transferrin receptor (TF-R). TF-R is not expressed in PCF cells and how PCF *T. brucei* uptake iron is not well understood (Bitter 1998;Ligtenberg 1994;Steverding 1995). It might be that *in vivo* PCF do not need to uptake extracellular $Fe^{++}$, and it appears that they use metal ion that has been stored from their previous life stage, i.e. the BSF. When PCF cells

are cultured *in vitro*, heam is added into the culture media as a source of iron (Brun 1992), since prolonged passage will use up any store. $H_2O_2$ is a highly unstable compound and can be broken down to water molecules in the presence of catalase; in the presence of certain metal ions, such as iron and copper, $H_2O_2$ is more readily converted to hydroxyl radicals ($OH^-$) by the Fenton reaction (Loft and Poulsen 1996). Thus, *in vitro* more reactive molecules are likely present to induce oxidative stress in PCF cultures, causing the cells to be more sensitive to oxidative stress in the presence of smaller quantities of exogenous $H_2O_2$.

The second reason for examining survival of the PCF MMR mutants in $H_2O_2$, as we have discussed in Section 1.4.7.2, is that MMR is one of the most important cellular systems to repair DNA damage caused by oxidation (DeWeese 1998;Ni 1999). BSF *T. brucei* MMR mutant survival has already been analyzed in the presence of varying concentrations of $H_2O_2$ (Machado-Silva 2008). From that study we know that BSF *msh2-/-* mutants are sensitive towards oxidative stress as compared to wild type parasites, whereas *mlh1-/-* mutants were shown to have no impaired survival in the presence of $H_2O_2$. This was further validated in our repeat of the experiment, where BSF *msh2-/-* mutants have 10% survival as compared to 57% survival for wild type cells (Figure 3-25) when subjected to 100 μM $H_2O_2$ for 48 hours. This was the highest level of exposure used by Machado-Silva et al, and in the experiments here we examined survival at higher concentrations of $H_2O_2$. This suggested that *mlh1-/-* mutants are also sensitive to oxidative damage, though their sensitivity is less than that of *msh2-/-* null mutants. This would be compatible with a broad role for *T. brucei* MMR is the response to oxidative damage, as seen in other organisms (Colussi 2002;DeWeese 1998;Mazurek, Berardini, & Fishel 2002;Sanders et al. 2011), but reiterates the more pronounced role of MSH2 in response towards oxidative stress, for reasons that are unclear.

Analysis of the survival of MMR mutants in PCF *T. brucei* in the presence of $H_2O_2$has generated some striking and unexpected results. Firstly, we have found that PCF MMR mutants are resistant to oxidative damage, in contrast to BSF MMR mutants, which are sensitive to oxidative stress, when compared with wild type cells. Even after deleting one allele of either *MSH2* or *MLH1*, the parasites display increased resistance to the stress; this result that was seen even at the earliest time point (24 hours) and at the lowest concentration of $H_2O_2$ tested, and was seen throughout the repeated survival time courses. When the second allele of the two MMR genes was deleted, generating the null mutants, a differential response between MSH2 and MLH1 was revealed, consistent with the

dissociation between these factors seen in the BSF but taking a different from. The *msh2-/-* mutants are seen to be still resistant to $H_2O_2$ stress relative to wild type, albeit more sensitive than the *MSH2+/-* mutants. In contrast, when both *MLH1* genes are deleted, the *mlh1-/-* mutants have approximately the same degree of sensitivity to $H_2O_2$ as wild type (see below for further discussion). In fact, it is possible that the differential role of MSH2 and MLH1 is also seen when comparing the phenotypes of the *MLH1+/-* and *MSH2+/--* mutants, since the *MSH2+/-* cells appeared more resistant to $H_2O_2$ overall throughout the survival curves. These data are, however, less clear compared with the bigger difference in survival of the null mutants, since *msh2-/-* survival rates were approximately twice that of the *mlh1-/-* cells. As stated, the overall impression of this study is that when a null mutant is made in *MLH1*, the phenotype for $H_2O_2$ sensitivity is approximately the same as wild type cells. This phenotype was consistent throughout the survival curves, with the exception of the data at 24 hours, where the *mh1-/-* mutants were more resistant to oxidative stress than wild type. Also, at this time point, the *MLH1+/-* and *msh2-/-* cells were more resistant than the *MSH2+/-*, which different from the rest of the time points where *MSH2 +/-* is seen to be the more resistant of all the mutants analyzed. This effect has been observed before, where *T. cruzi* cells that are sensitive towards a specific stress, when exposed to non-cytotoxic levels of stress, tend to be more resistant to the damage than the cells which are more resistant to the damage. This phenotype is accounted for by the cells acting to boost repair/defence mechanisms (Finzi 2004). However, when the sensitive cells are exposed to higher drug concentrations of stress, or are exposed for longer periods of time, the repair/defence mechanisms cannot cope with the damage caused and cells display their sensitivity to the damage. This may account for the trends in this work.

The major finding of this work is that loss of MSH2 in *T. brucei* PCF cells leads not to the sensitivity to $H_2O_2$ seen in *msh2-/-* cells in BSF *T. brucei*, but to resistance to this oxidative stress. Thus, there is life cycle stage-dependent difference in the consequences of MMR mutation in *T. brucei*. However, this difference is not due to a shared function of MSH2 and MLH1 since, as seen in BSF mutants, the severity of the phenotype of *msh2-/-* and *mlh1-/-* PCF cells is not equivalent in $H_2O_2$ survival curves. These data are made complex by the observations that the generation of heterozygous mutants of either *MLH1* or *MSH2* renders PCF *T. brucei* parasites more resistant to oxidative damage, both compared with the null mutants and the wild type. We propose that the best explanation for these data is that MMR plays a role in the response of *T. brucei* to oxidative damage and that this role has greater importance in PCF cells, because of greater exposure to either exogenous or

endogenous oxidative stress. Indeed, this role is of sufficient importance in the PCF that loss of a single gene copy of *MSH2* or *MLH1* necessitates an adaptation in some aspect of cell function to cope with the increased damage. However, when both copies of the MMR genes are lost, MMR function is impaired and the cells display increased sensitivity. The data also suggest that MSH2 acts not simply in MMR during repair of oxidative damage, but provides a further role in the absence of MLH1; this is the reason that *MSH2* mutants have more severe phenotypes in the response to $H_2O_2$. In BSF cells, which show sensitivity to $H_2O_2$ treatment, and mainly only in *MSH2* mutants, it seems likely that either the MLH1-independent role of MSH2 assumes predominance or that the levels of oxidative stress are sufficiently low that MMR repair is not as significant as in the PCF parasites.

As has been mentioned earlier, the role of MMR in response to oxidative stress has been widely studied both in prokaryotes and eukaryotes (Campos 2011;Colussi 2002;Machado-Silva 2008;Mazurek 2002;Ni, Marsischky, & Kolodner 1999;Sanders 2011). The phenotypes are widely described as increased accumulation of ROS leading to increased mutagenesis in MMR deficient strains which directly relates to importance of MMR and its role in protection against oxidative damage. In mouse embryonic fibroblasts, it was observed that *MSH2* mutants display an increased level of 8oxoG (Colussi 2002;DeWeese 1998). A similar phenotype has also been observed in *T. cruzi*, which showed that strains with compromised MMR accumulate high levels of 8oxoG upon treatment with oxidative stress (Campos 2011). Differences in sensitivity/resistance towards oxidative stress with respect to impaired MMR activity has been studied in various organisms. It has been observed in *Pseudomonas aureginosa* that MutS deficient cells are hypersensitive as compared to wild type when grown in the presence of oxidative stress (Sanders 2011). It was also found that increased sensitivity of *P. aureginosa* MutS mutants was further accompanied by increased levels of $H_2O_2$ induced mutagenesis. The sensitivity of *mutS* mutants towards oxidative stress was reverted if *dinB* (a member of the Y family of DNA polymerases catalysing TLS) was impaired. *dinB mutS* double mutants cells accumulated less ROS and no increase in sensitivity to $H_2O_2$ was observed. Sensitivity towards oxidative stress has also been observed in *Thermus thermophilus* (Fukui 2011). It has been reported that MMR deficient strains, as compared to wild type, are insensitive to $H_2O_2$ when grown to a concentration of 30 mM; however, an increased $H_2O_2$ induced mutagenesis was observed at concentrations of 10 mM and higher. Sensitivity towards oxidative stress has also been observed in *T. cruzi* MSH2 heterozygous mutants (Campos 2011) and BSF *T. brucei msh2-/-* mutants (Machado-Silva 2008) where it has been

observed that loss of MSH2 resulted in impaired MMR and an increased sensitivity to $H_2O_2$ along with an increased accumulation of 8oxoG in nucleus and kinetoplast.

In contrast to the sensitivity of MSH2 mutants in response to oxidative stress, resistance to oxidative stress in *MSH2* mutants has also been reported in both prokaryotes and eukaryotes. In a study done in *E. coli* it was observed that sensitivity to $H_2O_2$ is reduced in MMR mutants (Wyrzykowski 2003). It was concluded from the study that that in the presence of functional MMR system, DNA breaks are introduced in an attempt to correct the oxidative lesion, which increases its sensitivity towards oxidative stress leading to cell death. However, in the absence of MMR activity, repair process is avoided and cellular processes continue until the cell accumulates mutagens and cell viability is compromised. A similar phenotype is documented in mammals where it was observed that loss of MMR reduces the sensitivity to $H_2O_2$ by 1.5 fold in human colon cancerous cells (Glaab 2001;Lin 2000). Resistance to oxidative stress has also been observed in mouse embryonic cells (DeWeese 1998). In the studies done in mammalian system it has been concluded that non cytotoxic levels of oxidative stress induces resistance to the damage even in the wild type cells as lower level of stress inactivated MMR, though an increased accumulation of oxidized bases in the genome was observed in all the cases (Chang 2002). Furthermore, non-cytotoxic levels of $H_2O_2$ induces apoptosis, which is hypothesized to be generated through MMR and is avoided in MMR-deficient cells (Lin 2000).

The $H_2O_2$ survival analysis of PCF MMR mutants suggested the possibility that the MMR mutants are resistant to oxidative damage due to an unspecified adaptation. To explore this, we considered whether this might be reflected in greater maintenance of genome integrity in the presence of oxidative stress. We analysed this by PCR-amplifying JS-2 microsatellite from the DNA of wild type and MMR mutants grown in the presence and absence of $H_2O_2$. We have previously observed that in wild type and heterozygous mutants there was no difference in stability of the JS-2 microsatellite in the absence of $H_2O_2$; growing the same cells in the presence of $H_2O_2$ does not result in instability of this locus. Subtle instability in the larger allele was detected in wild type and heterozygous mutants by Genescan; however, this putative instability was independent of oxidative stress and, in fact, was not seen by the gel analysis, so may simply reflect errors in the automated peak calling from the electropherograms (e.g. due to amplification errors made by Taq polymerase). A more pronounced effect of $H_2O_2$ was seen in the null mutants. In the *msh2*-/- mutants the larger allele of the JS-2 microsatellite appeared to be more stable in the presence of $H_2O_2$ compared with the *mlh1*-/- mutants. However, for the smaller allele, the

level of variation induced by $H_2O_2$ appeared equivalent in the two mutants. As a result, taken as a whole we can conclude that $H_2O_2$ affects the *msh2-/-* mutants in a positive way, inducing a backup system that provokes genetic stability, whereas in *mlh1-/-* clones genetic instability is increased in the presence of oxidative stress. However, this cannot be considered as definite as we have seen some MSI in the absence of $H_2O_2$ in both the mutants, so more number of clones would be needed to draw a final conclusion. However, since DNA slippage is not the only effect $H_2O_2$ causes on the cells, genetic instability cannot be the only reason directly attributed to the cell survival in the presence of oxidative stress.

Survival curves in the presence of $H_2O_2$ gave a clearer suggestion that an adaption that might have happened in the process of generating *MSH2* mutants. For this purpose, we made re-expressers in which MSH2 was re-introduced into the null mutant. Phenotypic analysis of both MNNG alkylation tolerance and MSI confirmed that a gene copy had been restored, with the re-expressers phenotypically indistinguishable from heterozygous mutants. In contrast, in measuring the responses towards oxidative stress we have observed that the MSH2 re-expressers show survival levels essentially like that of *msh2-/-* mutants, suggesting that the increased resistance to $H_2O_2$ was not reversed. This appears consistent with background alterations of, for instance defence/ repair systems or in intracellular metabolism, that have been irreversibly provoked by MSH2 mutation, but further analysis needs to be done to test the hypothesis.

# 4 Localisation and function of MMR proteins in response to oxidative damage

## 4.1 Introduction

For a better understanding of the role of MSH2 in MMR and the oxidative damage response, we need to know about the localization and expression of this protein. In this chapter, we will test the hypothesis that MSH2 localizes to the nucleus and kinetoplast in *T. brucei*. We further hypothesise that the kinetoplast localisation of MSH2 is not seen for MLH1, another central component of MMR. Our hypothesis is based on previous studies. Firstly, we now know that in *T. cruzi* 8-oxoG can be localized to the kinetoplast DNA (kDNA) and nuclear DNA, which increases in the presence of oxidative stress (Furtado 2012). Secondly, it has also been shown that MSH2 has a pronounced role in repairing the base mismatch lesion generated by 8oxoG, since the levels of this lesion increase in the kDNA and, to a lesser extent, in the nuclear DNA of *T. cruzi MSH2* heterozygous mutants after exposure to oxidative stress, and that mammalian stage (BSF) *T. brucei msh2*, but not *mlh1*, homozygous mutants display pronounced sensitivity to oxidative stress (Campos 2011;Machado-Silva 2008). Thirdly, it has been observed in BSF *T. brucei* that *msh2-/-* mutants show increased loss of kDNA in the presence of oxidative stress (Campos et al. 2011). This loss of kDNA in *msh2* mutants has been explained as an increase in oxidative lesions and inability of the MMR pathway to repair the damage, but the contrasting sensitivities of *msh2* and *mlh1* mutants suggests a differential role of the two MMR components. Furthermore, we now know that insect stage (PCF; procyclic form) and BSF *T. brucei* wild type parasites have different tolerance towards oxidative stress, with PCF being 10-30 times more sensitive than BSF (Barnes 2006;Machado-Silva 2008). In chapter 3 we have shown that *msh2* mutants in PCF have a contrasting phenotype in response to oxidative stress as compared to BSF (see Section 3.2.3), causing increased tolerance, which was not seen in *mlh1* mutants.

Based on these findings, we wanted to check if localization and expression of the MMR proteins MSH2 and MLH1 is life cycle dependent and/or subject to stress applied. We also aimed to ask if the proteins localize to a specific sub-cellular compartment, or are found in the nucleus and kinetoplast. Finally, if we see localisation to both the nucleus and kinetoplast, we wished to ask if the MMR proteins shuttle between different compartments depending on need, or if the two compartments have their own pool of MMR proteins that they recruit at the site of damage. Previously, anti-peptide antiserum was generated against *T. brucei* MSH2 (Machado-Silva 2008), but this was poorly reactive and displayed weak specificity in western blots of cell extracts. Therefore, we decided to use a C-terminal epitope tagging strategy, using a 12-myc tag, to localize the proteins. Both BSF and PCF

cells were tagged; in PCF cells, both wild type and heterozygous *MSH2* and *MLH1* mutants were used for the tagging, whereas in BSF parasites only *MSH2* and *MLH1* heterozygous mutants were tagged.

## 4.2 Results

### 4.2.1 Generation of *T. brucei* cells expressing MSH2 and MLH1 C-terminal 12 myc tagged variants

#### 4.2.1.1 Strategy for generation of tagged cell lines

A C-terminal tagging strategy was used for the detection of MSH2 and MLH1 proteins (Figure 4-1). Primers were designed specific to the C-terminal region of each ORF, excluding the stop codon. For *MSH2*, primers were designed to specifically PCR-amplify a 513 bp region, while an 887 bp region of the *MLH1* ORF was PCR-amplified. *Hin*dIII and *Xba*I sites were added to the 5' ends of the forward and reverse primers, respectively, to assist in cloning the PCR products into the vector pISRPIbsd-12myc obtained from C.Tiengwe (Tiengwe 2012). The regions of ORF to be PCR-amplified were selected to have a unique restriction site present in that part of the genome and not in the vector, allowing the cloned constructs to be linearized within the ORF, promoting integration into the genes following transformation of parasites. A *Bmg*BI site was present in both the *MSH2* and *MLH1* ORF fragments used for cloning and the tagging constructs were digested with this enzyme prior to transformation into *T. brucei*, with transformants then selected via the blasticidin resistance (*BSD*) gene, which should be integrated downstream of the targeted gene (Figure 4-1).

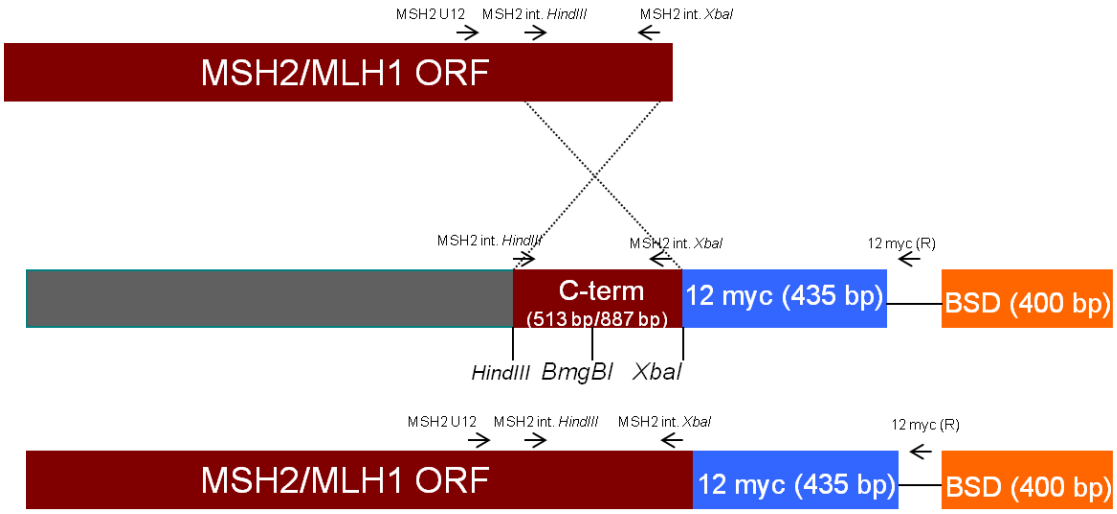


**Figure 4-1 Strategy for C-terminal 12 myc tagging of *MSH2* or *MLHI*.**

A 513 bp region of *MSH2* or an 887 bp region of *MLH1* were PCR-amplified from the C-terminal (indicated by C-term) coding region of the ORF of the respective gene, excluding the stop codon and flanking a *Bmg*BI site. The PCR-amplified regions of ORF were then cloned into a plasmid, generating an inframe fusion with an ORF encoding a 12myc epitope, using *Hin*dIII and *Xba*I sites in the plasmid and added to the primers. Both the constructs were linearized by *BmgBI* and used for transformation; the expected recombination with the genome is indicated by a cross and the resulting expected organisation of the targeted genes is then shown, including the blasticidin drug resistance gene (*BSD*) as used for selection of transformants.

#### 4.2.1.2 Transformation of BSF and PCF *T. brucei* with 12 myc tagged MSH2 and MLH1 constructs.

Wild type Lister 427 *T. brucei* were transformed with both 12 myc tagging constructs, while heterozygous *MSH2*+/- *(MSH2::PUR*) and *MLH1*+/- (*MLH1::PUR*) cells were transformed with the *MSH2* or *MLH1* constructs, respectively. Transformations were done both in BSF and PCF cells (refer to Section 2.1.4). Wildtype cells were tagged in case tagging should prove impossible in the heterozygous lines, for instance if the alteration proved lethal, in which case a non-tagged allele would be retained. Heterozygous mutants were grown in the presence of 1 $\mu g.ml^{-1}$ puromycin for 1 week and checked for any cross contamination by growing them on 10 $\mu g.ml^{-1}$ blasticidin. Approximately 5 μg of the constructs linearized by *Bmg*BI was used for the transformation and heterozygote mutant transformants were selected on media containing 0.5 $\mu g.ml^{-1}$ puromycin and 10 $\mu g.ml^{-1}$ blasticidin, whereas wildtype transformants were selected using only 10 $\mu g.ml^{-1}$ blasticidin. The efficiency of transformation was very low, for reasons that are unclear. In BSF cells, only one antibiotic resistant *MSH2*+/- clone was recovered, and only four *MLH1*+/- clones; no wild type transformants were recovered. In PCF cells, no clones were recovered from the *MSH2*+/- transformation, while five putative 12myc-tagged MSH2 clones were recovered in wild type cells (Figure 4-2); three putative *MLH1* tagged clones were recovered in wild type cells and four in the *MLH1*+/- heterozygous mutants. Clones collected were grown in the appropriate antibiotic for 1 week before they were analyzed. Transformants were first checked by PCR (Figure 4-2, Figure 4-3 and Figure 4-4) and then by western analysis (Figure 4-5). PCR was done as described in Section 2.2.5.

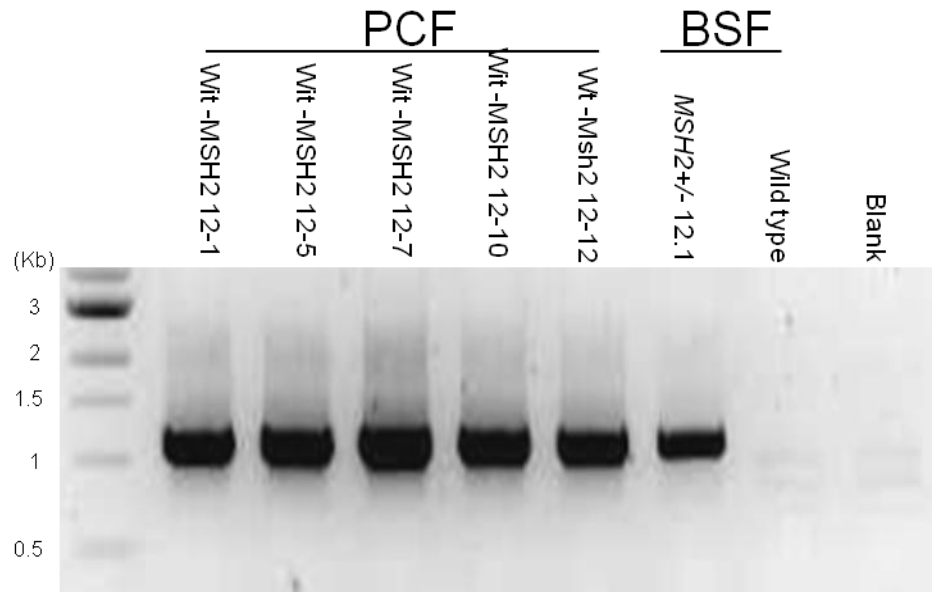


**Figure 4-2 PCR analysis putative *MSH2* C-terminal-12 myc tagged clones.**

A gel is shown of five putative wild type PCF C-terminally12 myc tagged MSH2 cells (Wildtype-msh2-12myc 1,5,7,10,12) and one *MSH2+/-PUR* BSF C-terminally 12 myc tagged MSH2 cell (*MSH2+/-PUR-12myc*) following PCR-amplification using forward primer MSH2-U12 and reverse primer 12myc(R), as detailed in Fig.4.1. Gel size markers are shown and sizes in Kb are labelled.

To test for the presence of the 12 myc tag at the C-terminus of *MSH2* in the five wild type PCF transformants and in the one *MSH2+/-* BSF transformant, primers were designed to PCR-amplify a region encompassing 513 bp of the *MSH2* ORF and 435 bp of 12 myc sequence, which would form after integration of the tagging construct. The forward primer (MSH2 U 12) was designed to bind just upstream of the recombining region, and the reverse primer (12 myc (R)) bound 16 bp downstream of the 12 myc epitope-encoding sequence. The PCR results showed a band of the expected size in each PCF wild type transformant and in the BSF *MSH2* heterozygous mutant transformant (Figure 4-2), suggesting that in each case the myc tagging construct had integrated as expected.

Since no blasticidin resistant clones were recovered from transformation of PCF *MSH2* heterozygous cells with the MSH2-12myc tagging construct, the *MSH2* tagged wild type clones 10 and 12 were transformed with an *MSH2* knockout construct with a *PUR* drug resistance gene, as described in Section 3.2.1. Transformation was conducted as previously described (Sections 3.2.1.2 and 2.1.4.1) and transformants were selected on 1 $\mu g.ml^{-1}$ puromycin and 10 $\mu g.ml^{-1}$ blasticidin. Four clones were recovered from the transformation and tagging analyzed by PCR, using the same primers as described above. Parental clone WT-MSH2-12MYC 10 was used as a positive control. Integration of the *MSH2::PUR* construct was assessed with PCR using the primers MSH2 (F) and PUR (R), as described in Section 3.2.1.2; Figure 3-2 C. The results of this analysis are shown in Figure 4-3.

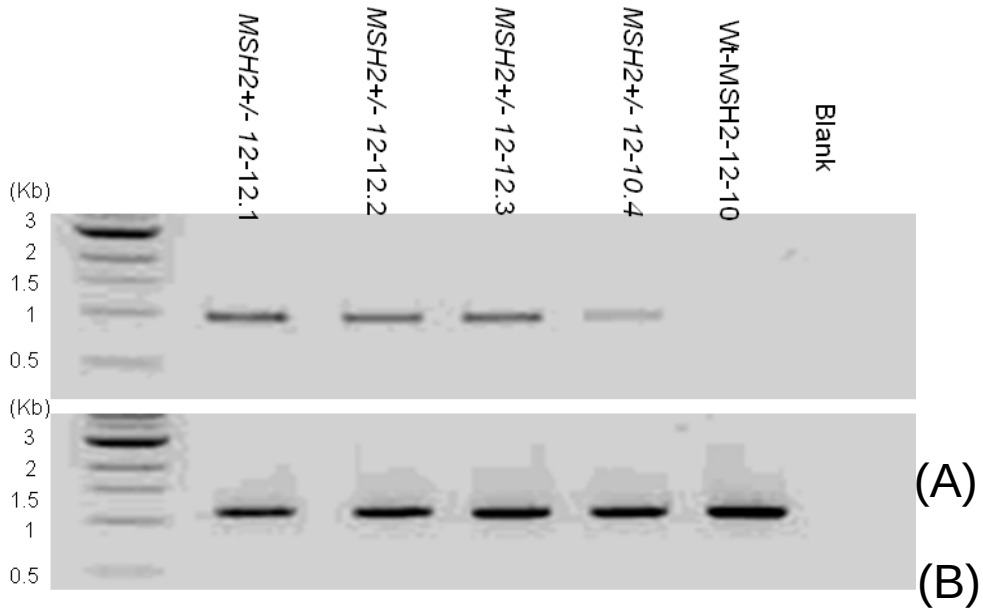


**Figure 4-3 PCR analysis of putative PCF *MSH2*+/- MSH2-12 myc tagged clones.**

The gel shows PCR analysis of four putative *MSH2+/-* PCF C-terminally12 myc tagged MSH2 cells ; wild type-MSH2-12myc10 was used as a control. (A) PCR with forward primer MSH2 (F) and reverse primer PUR (R). (B) PCR with forward primer MSH2-U12 and reverse primers 12 myc (R). Gel size markers are shown and sizes in Kb are labelled.

Figure 4-3 A shows that the *PUR* drug resistance cassette could be PCR-amplified from all the transformed clones and not from the wild type C-terminally tagged MSH2 cells that were the parent: a product of ~0.8 kb was observed, which was consistent with the expected product (856 bp). In all the clones, PCR to check if the myc-tagged *MSH2* gene is present showed a ~1 kb band, which is in relation to the expected product (1074 bp) (Figure 4-3 B). These data suggest that in all clones one allele with *MSH2* replaced by *PUR* is present and another allele that is myc-tagged, though we cannot say if an unaltered (wild type) allele is also present.

MLH1 was putatively tagged in both wild type and *MLH1* heterozygous *T. brucei* PCF cells, which were analysed by both PCR and western blotting. In BSF cells, MLH1 was tagged only in *MLH1* heterozygous mutants and these were examined only by Western analysis. The PCR analysis of the MLH1 tagged cells is shown in Figure 4-4.

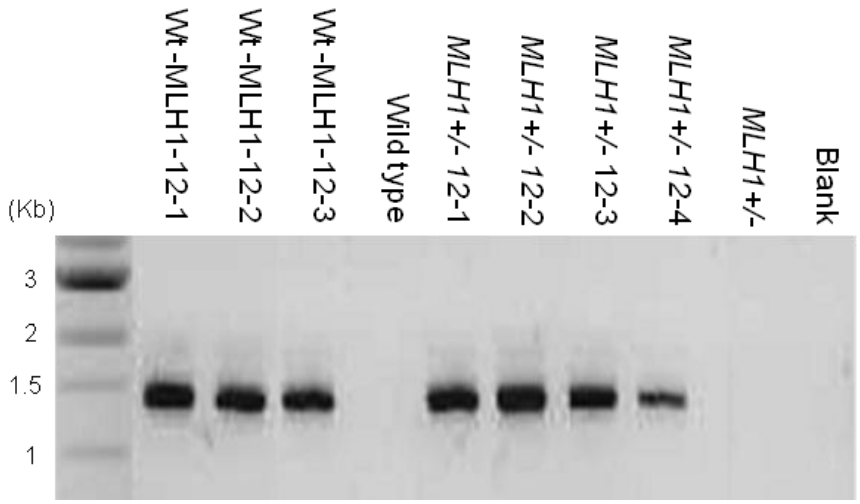


**Figure 4-4 PCR analysis putative PCF *MLH1+/-* -12 myc tagged clones.**

Gel shows PCR analysis of putative MLH1 C-terminally tagged in wild type and *MLH1+/- T. brucei*. Primers were designed to specifically amplify MLH1 ORF along with 12 myc gene sequence in *T. brucei* PCF wild type and *MLH1+/-*. MLH1 tagged clones in *MLH1+/- PUR* (MLH1+/-12myc (1-4)) and in wild type (Wild type-MLH1-12myc (1-3)) were PCR amplified using forward primer (MLH1-U12) reverse primers (12myc(R)). Gel size marker is shown and sizes in Kb are labelled.

To test for the correct integration of the 12 myc tag at C-terminus of *MLH1* in the different transformants, PCR analysis was done using primers designed to PCR-amplify a region of the *MLH1* ORF (887bp) and the 12 myc tagging sequence (435 bp) when they are fused. The forward primer (MLH1-U12) was designed 86 nucleotides upstream to the C-terminal region of the *MLH1* ORF used for recombination, and the downstream primer (12myc(R), was as described above. PCR amplification showed a single product of ~1.5 Kb in all cases; as the expected product size is 1523 bp, this suggests the integration has occurred as expected.

The putative 12myc tagged clones were next examined by western analysis, looking for the expression of proteins that react with antiserum against the 12myc epitope and of the size expected for MSH2 or MLH1. Western blotting was performed as described in Section 2.3.1. Briefly, 1 x$10^8$ cells were pelleted at 1000 *g* and cell pellet was resuspended in 100 µl protein loading buffer. Samples were resolved on a 10% SDS polyacrylamide gel and then transferred to a nitrocellulose membrane. The membrane was then probed with mouse anti-myc antiserum (1:7000 dilution) for a minimum of 1 hour. HRP-conjugated goat anti-mouse antibody (diluted at 1:5000) was used as secondary antibody, and bands were detected by incubating with enhanced chemiluminescence and exposing to X-ray film (KODAK). The results of this are shown in Figure 4-5.

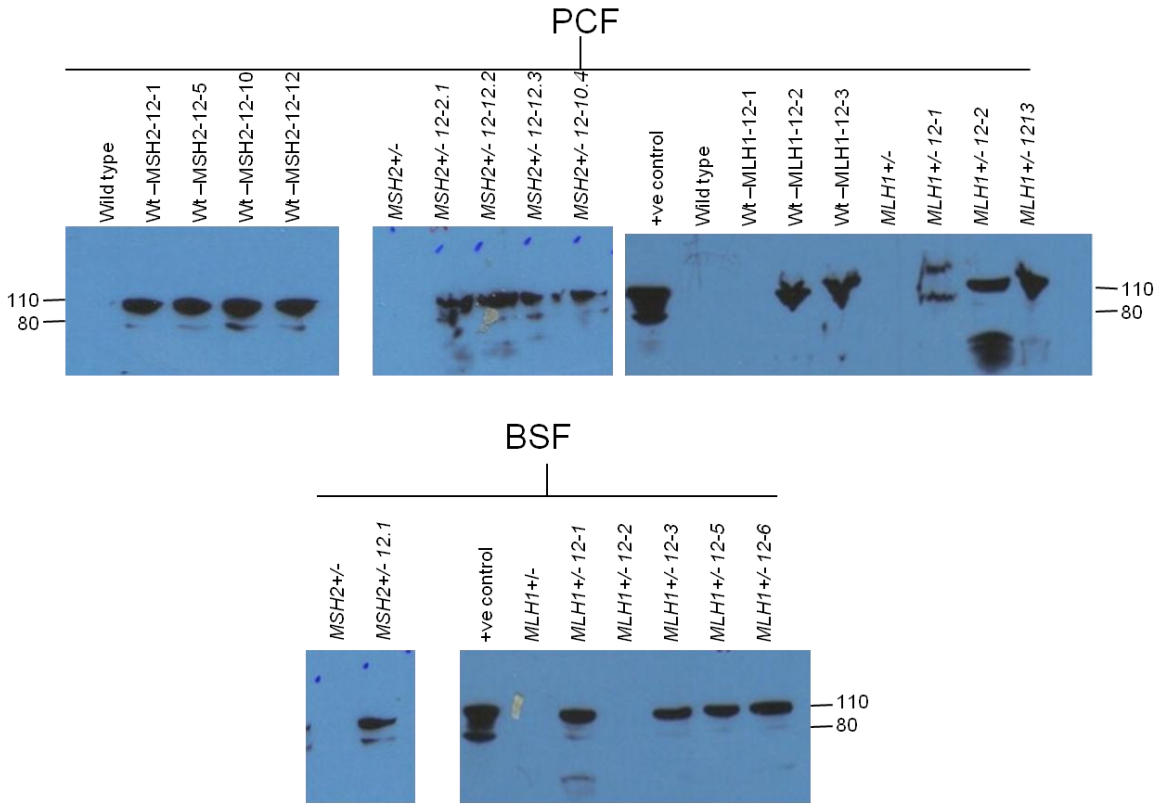


**Figure 4-5 Western analysis of MSH2 and MLH1 C-terminal 12 myc tagged clones.**

Two western blots are shown to check for the expression of 12 myc tagged MSH2 or MLH1 in PCF and BSF clones. PCF clones analysed in the study were Wt-MSH212-1, Wt-MSH212-5, Wt-MSH212-10, Wt-MSH212-12, *MSH2+/- 12-12.1, MSH2+/- 12-12.2, MSH2+/- 12-12.3, MSH2+/- 12-10.4, Wt-MLH1 12-.1, Wt-MLH1 12-2, Wt-MLH1 12-3, MLH1+/-12-1, MLH1+/-12-2, MLH1+/-12-3*. BSF clones analysed were *MSH2+/- 12.1, MLH1+/- 12-1-6.* Wild type and non tagged heterozygous (+/-) cells were used as negative controls, whereas Wt-MSH2 12-10 was used as positive control for the rest of the western analysis. ~2x$10^7$ cells were loaded per well. The membrane was probed with mouse anti- myc antiserum, diluted 1:7000, and detected with HRP-conjugated anti-mouse antiserum, diluted 1:5000.

The predicted sizes of 12 myc-tagged MSH2 and MLH1 are 116 kDa and 127 kDa, respectively. For most of the putative myc-tagged clones analysed a predominant band of the expected size was seen by western blotting (Figure 4-5). The two exceptions to this were clones WT-MLH1.1 (PCF) and *MLH1*+/-12.2 (BSF), where there was no reaction. These clones were discarded. However, besides the predominant bands of appropriate size, a smaller band of ~80 kDa was also seen, and in some cases in the putative MLH1 tagged cells a further band of ~60 kDa was also seen. From experiment to experiment, the extent of the detection of these bands varied and, though they normally appeared less abundant than the expected bands, sometimes they showed pronounced reactions (data not shown). Since the bands were only present in tagged lines, and were not seen in non-tagged controls, these may represent breakdown products of the MSH2 or MLH1 proteins, though they may also be modified forms of the protein. However, no evidence of modified MMR proteins has been reported to my knowledge. Of the different clones analysed, one clone

was randomly selected for further analysis. For PCF cells, the tagged lines *MSH2*+/- 12-12.2 and *MLH1*+/- 12.2 were used , while BSF *MSH2*+/-12.1 and *MLH1*+/-12.1 were used. Thus, only the cells in which MSH2 and MLH1 had been 12myc tagged in a heterozygous mutant background were examined further. Henceforth, the clones are referred to as *MSH2*-12 myc or *MLH*-12 myc.

## 4.2.2 Assessing the functionality of C-terminally 12myc tagged MSH2 and MLH1

The tagged clones were phenotypically characterised to ask if the addition of a C-terminal 12Myc tag affects the functionality of the MLH1 and MSH2 proteins. To do this, the BSF heterozygous tagged lines were analysed for their MMR proficiency. We assume that in these cells the only *MSH2* or *MLH1* gene present has been tagged, with the other allele deleted, and thus we can ask if tagging has affected the functionality of the proteins by asking if they display phenotypes more comparable with null (-/-) or heterozygous (+/-) mutants. MMR efficiency of the tagged clones was thus analyzed by tolerance to methylation (MNNG) damage and oxidative stress, as performed previously: see Sections 3.2.2.2 and 3.2.3, respectively. Wild type, +/- and -/- cells for MSH2 and MLH1 were compared with the tagged clones. For both the analyses, the cells were grown on their respective antibiotics for at least three days prior to the experiments. Heterozygous mutants were grown on 1 $\mu g.ml^{-1}$ puromycin and homozygous and tagged mutants were grown on 1 $\mu g.ml^{-1}$ puromycin and 10 $\mu g.ml^{-1}$ blasticidin.

### 4.2.2.1 MNNG Tolerance

MNNG tolerance was checked by the Alamar blue assay, which was conducted as described in Sections 3.2.2.2 and 2.5.1.2.2. Briefly, BSF cells were used at a starting density of 1 x $10^5$ $cells.ml^{-1}$. Cultures were grown in medium containing doubling dilutions of MNNG from 400 μM to 0.39 μM, in 96-well polystyrene plates (200 μl of cell culture per well). Each experiment was carried out in triplicate. The results of these experiments are shown in Figure 4-6.

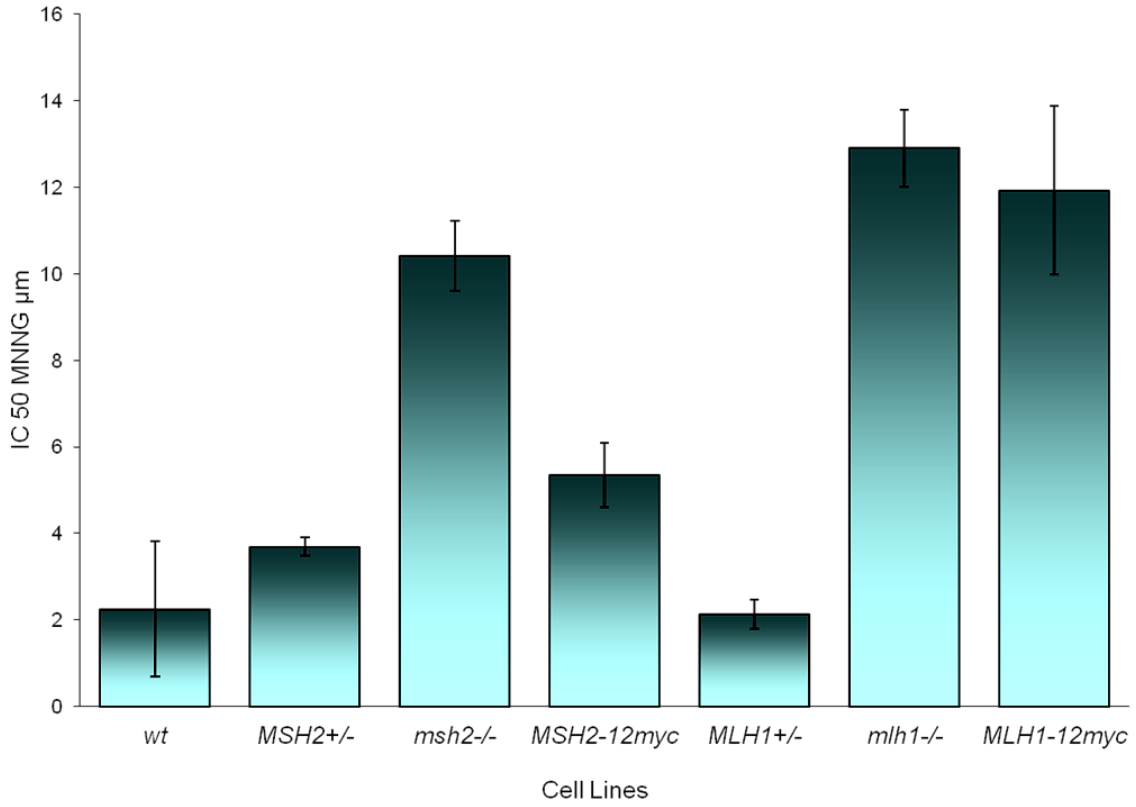


**Figure 4-6 MNNG tolerance of *T. brucei* bloodstream form *MSH2* and *MLH1* tagged clones assayed by Alamar Blue.**

The conversion of Alamar blue to fluorescent Resazurin was used to determine the sensitivity of the BSF *T. brucei* wild type (WT) cells, MMR mutants and C-terminally 12 myc tagged mutants towards MNNG. IC50 values of Lister 427 WT, *MSH2+/-*, *msh2-/-*, *MSH2-12myc*, *MLH1+/-*, *mlh1-/-* and *MLH1-12myc* cells are shown. IC50 values are the mean of three experiments and vertical bars indicate standard deviation. Cells were grown at a starting density of 1 x $10^5$ cells.$ml^{-1}$ n the presence of doubling dilutions of MNNG (from 0.39 µM-400 µM) in fluorscence- readable 96 well plates. After 48 hrs Alamar Blue was added to each well and fluorescence measured after a further 24 hours of growth.

The MNNG tolerance assay suggests that the C-terminal 12 myc has affected the functionality of the MLH1 protein, but not MSH2. This is indicated by the IC50 value (drug concentration causing the death of 50% of cells) of *MLH1-12myc* (11.93) cells, which was closer to *mlh1-/-* cells (12.91) and detectably more resistant to methylation when compared with *MLH1+/-* cells (2.12). In contrast, *MSH2-12myc* cells had approximately the same IC50 as *MSH2+/-* cells (5.351 and 3.684, respectively), and were clearly less tolerant than the *msh2-/-* mutants (10.41). These data suggest that the modification impairs the ability of MLH1 to act in MMR, and must be taken into consideration in localisation studies (see below). This impairment could reflect the fact that the C-terminus of MLH1 contains a CTH motif. Although no function has so far been attributed to this region, it has been shown that mutations here result in loss of MMR activity (Pang 1997).

### 4.2.2.2 Response to $H_2O_2$

The BSF MSH2 and MLH1 tagged cells were also examined for their sensitivity towards $H_2O_2$, as described in Section 3.2.6, in order to understand how the 12 myc tagging might affect the activity of the MMR proteins in response to oxidative damage. 20 ml of cells were cultured at a density of 1 x $10^5$cells.ml$^{-1}$. $H_2O_2$ was added to final concentrations of 0, 100, 200 and 300 µM and cells were counted after 48 hours of further growth, using a haemocytometer. The data are shown in Figure 4-7.

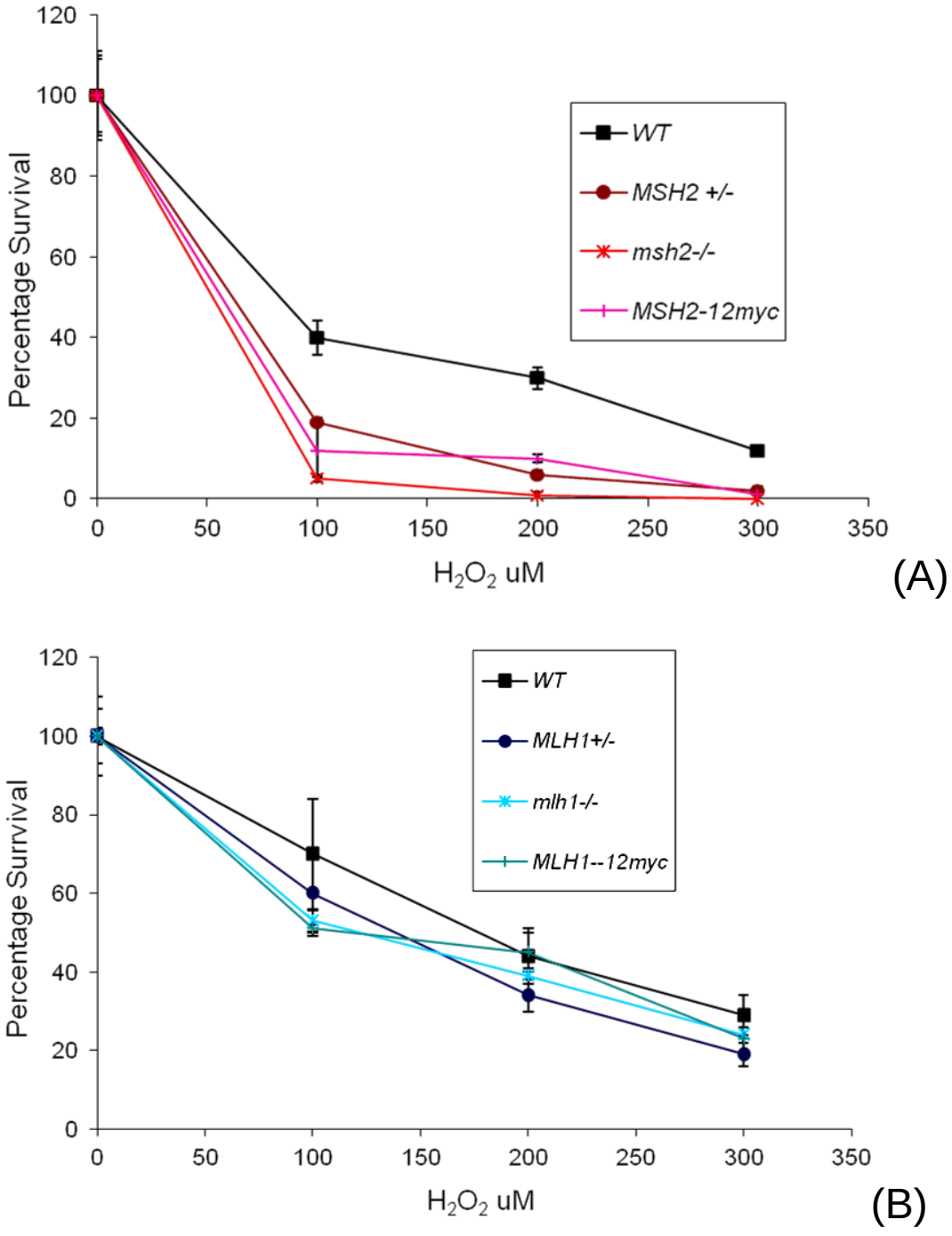


**Figure 4-7 Survival of bloodstream form *T. brucei* (A) MSH2-12myc and (B) MLH1-12myc tagged cells after 48 hours growth in $H_2O_2$.**

Wild type, *MSH2+/-*, *MSH2-12myc*, *msh2-/-, MLH1+/-, MLH1-12myc* and *mlh1-/- T. brucei* BSF cells were diluted to 1 x $10^5$ cells.$ml^{-1}$ in HMI-9 culture media containing 0, 100 µM, 200 µM or 300 µM $H_2O_2$. Two independent experiments were setup and cell densities were measured after 48 hours. Cell counts are shown as a percentage of the density of each cell line in the absence of $H_2O_2$ (taken as 100%). Each value is the mean of the two experiments, and vertical bars depict standard deviation.

As was seen for the MNNG assay, which suggested that *MSH2*-12 myc is functional and has the same MNNG tolerance as *MSH2*+/- (Figure 4-6), the response towards $H_2O_2$ suggests the same: survival of the *MSH2*-tagged cells most closely parallels the *MSH2*+/- cells, being more sensitive than wild type cells and more resistant than *msh2*-/- mutants (Figure 4-7 A). In contrast, it appears that we cannot evaluate the functionality of MLH1-12myc in response to $H_2O_2$. From the survival curves, and distinct from *msh2*-/- cells, *mlh1-/- and MLH1+/-* mutants did not show a pronounced phenotype after $H_2O_2$ treatment when compared with wild type cells (Figure 4-7 B, consistent with previous work: Machado-Silva 2008), and nor did the MLH1-12myc cells.

PCF tagged lines were not analysed for their functionality. Since the same construct was used for the transformation of both life cycle forms, we assume that tagged lines in PCF would have the same phenotype as BSF. Though the MLH1 tagged cells seemed to be non-functional for their MMR activity, we nonetheless localized and measured the expression of protein, since the 12myc tagged variant was detected by Western analysis (Figure 4-5).

### 4.2.3 Localization of MMR proteins

No studies have been done previously to localize MMR proteins in kinetoplastid organisms. In mammals, MSH2 is found both in the cytoplasm and in the nucleus (Christmann 2000). It was observed in the same study that, upon alkylation damage, the total quantity of the MMR protein does not alter in the cells. However, trafficking of MSH2 protein was seen following damage: it was observed that when cells are treated with MNNG, most of the cellular MSH2 protein relocates from the cytoplasm to nucleus, which again stressed the role of MMR in protection against methylation damage. As discussed in Section 1.4.1, alkylated bases are also repaired by alkyl guanine transferase (AGT). During the study carried out by Christmann and Kaina (2000), it was observed that in the presence of methyl guanine methyl transferase (MGMT), a mammalian homologue of AGT, higher concentrations of MNNG were required for the trafficking of MSH2 from cytoplasm to nucleus. However, in the absence of MGMT, MSH2 shuttles to the nucleus in the presence of smaller concentrations of MNNG.

MSH2 has not been localized in the presence of oxidative damage. However, recent studies in *T. cruzi* have shown that 8oxoG, a modified base formed due to oxidative damage (see Section 1.4.7.1), localizes to the nucleus and kinetoplast. It was observed that levels of 8oxoG increase in the presence of oxidative stress (Campos et al. 2011; Furtado et al. 2012). It is thus valuable to ask about the localization of MSH2, both before and after oxidative and alkylation damage. To date, no data is available regarding the localization of MLH1 and, with the caveat that the 12myc variant used here appears non-functional; we attempted to examine localisation of this MMR component also. Two approaches were taken to localize the tagged proteins: visual localization by immunofluorescence assays (IFA) and by Western blot analysis of sub-cellular fractions of the cells.

### 4.2.3.1 Immunofluorescence detection of *T. brucei* MSH2 and MLH1

IFA was performed as described in Section 2.4.2. BSF and PCF cells were grown for 48 hours in the presence or absence of MNNG or $H_2O_2$. Cells analysed in the study were wild type Lister 427, MSH2-12myc and MLH1-12myc. For the BSF, 20 ml of cells at a concentration of 1 x $10^5$cells.ml$^{-1}$ were incubated in the presence of 100 μM $H_2O_2$ (see Section 3.2.6) or 5 μM MNNG (see Section 3.2.2.2) and incubated at 37 $^0$C for 48 hours. For PCF cells, 10 ml cultures at 5 x $10^5$cells.ml$^{-1}$ were incubated for 48 hours in the presence of 20 μM $H_2O_2$ (see Section 3.2.3) or 5 μM MNNG (see Section 3.2.2.2). After 48 hours the cells were pelleted and 1 x$10^6$ cells were used for IFA, as described in Section 2.4. Cells were probed with mouse anti-myc antiserum as primary antibody, at a dilution of 1:7000, and incubated for 1 hour. Alexaflour-conjugated anti-mouse IgG was used as secondary antibody (1μg.ml$^{-1}$) and the slides were incubated in the dark. Slides were counter stained with mounting medium containing DAPI and visualized with a Zeiss Axioplan microscope. Images were captured using Hamamatsu ORCA-ER digital camera and analyzed by Openlab Software. Representative images are shown in Figure 4-8.

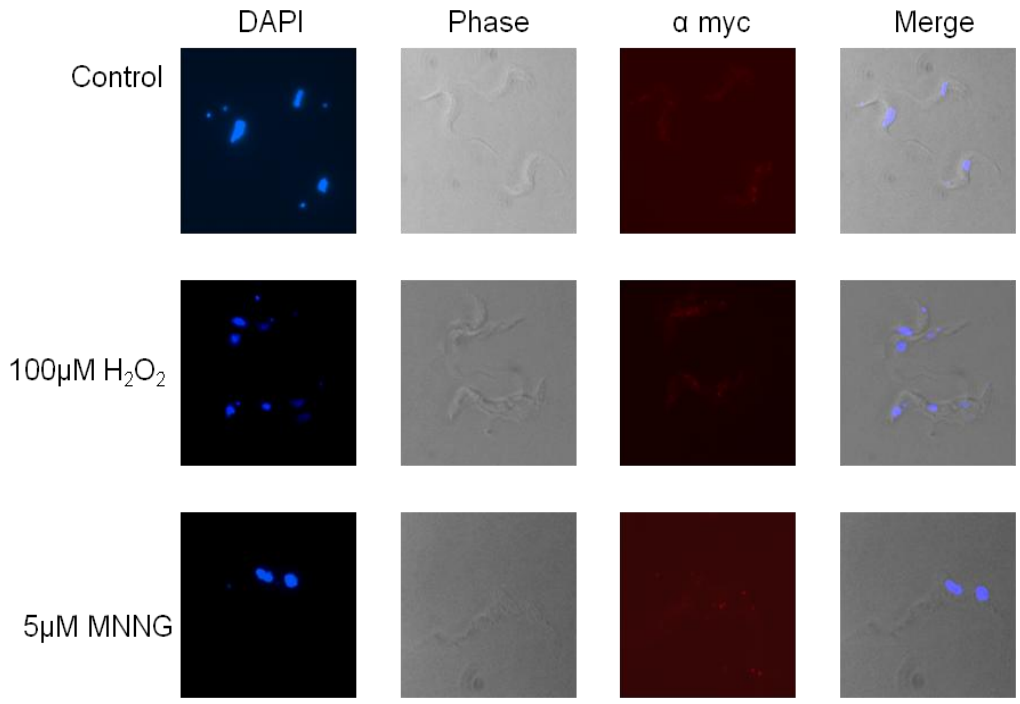
DAPI
Phase
α myc
Merge
Control
100μM $H_2O_2$
5μM MNNG

(A)

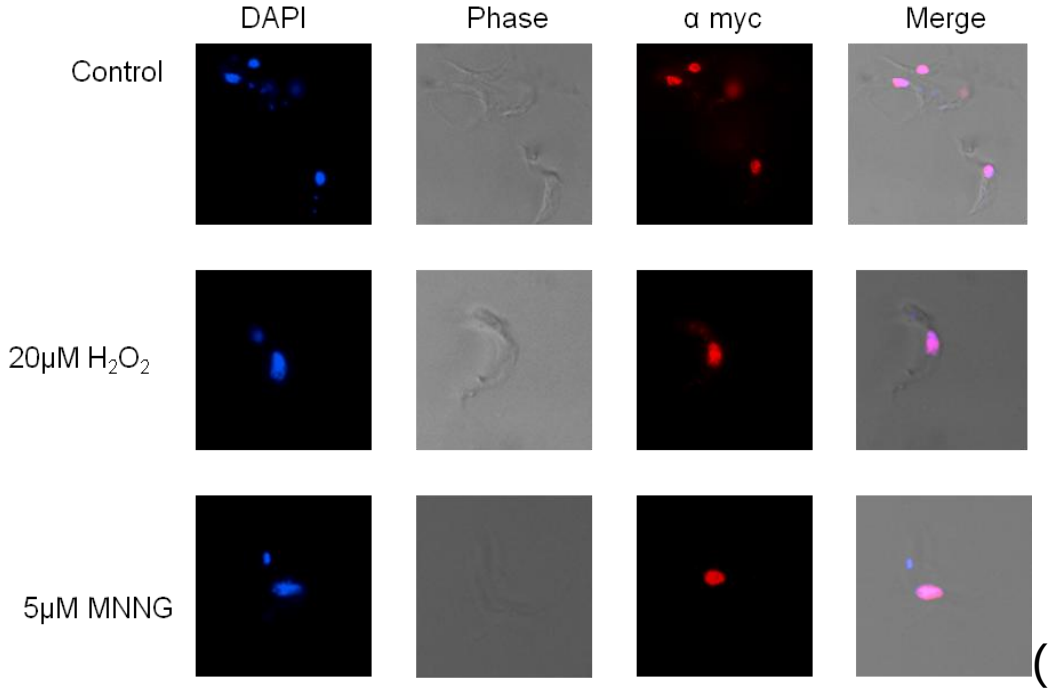
DAPI
Phase
α myc
Merge
Control
20μM $H_2O_2$
5μM MNNG

(B)

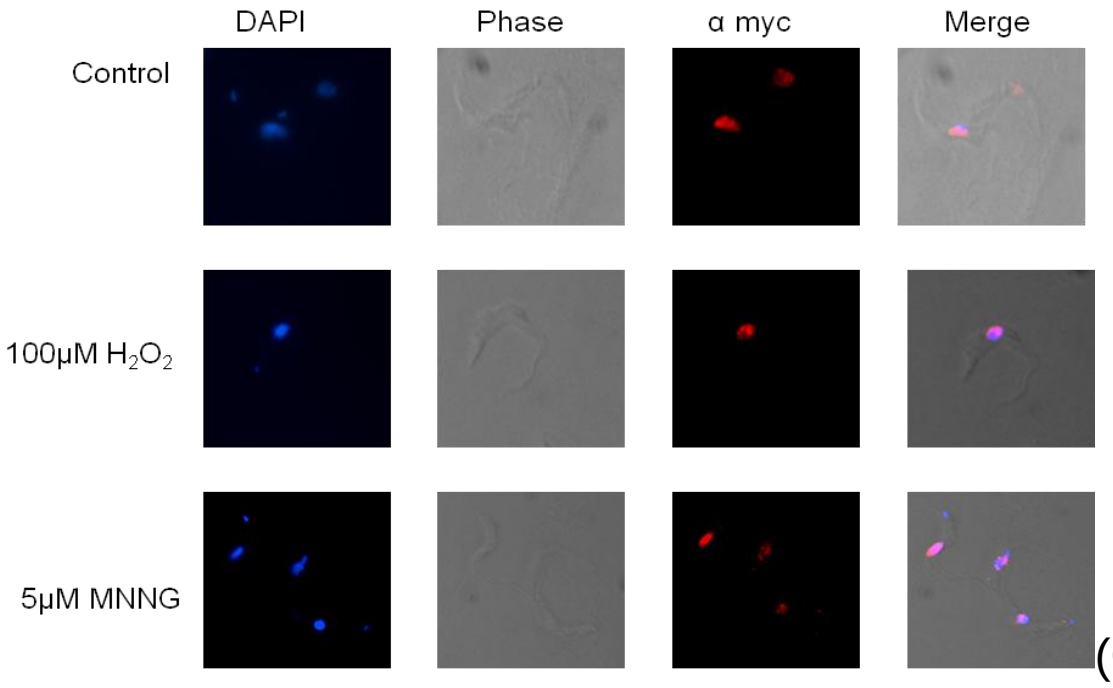
DAPI
Phase
α myc
Merge
Control
100μM $H_2O_2$
5μM MNNG

(C)

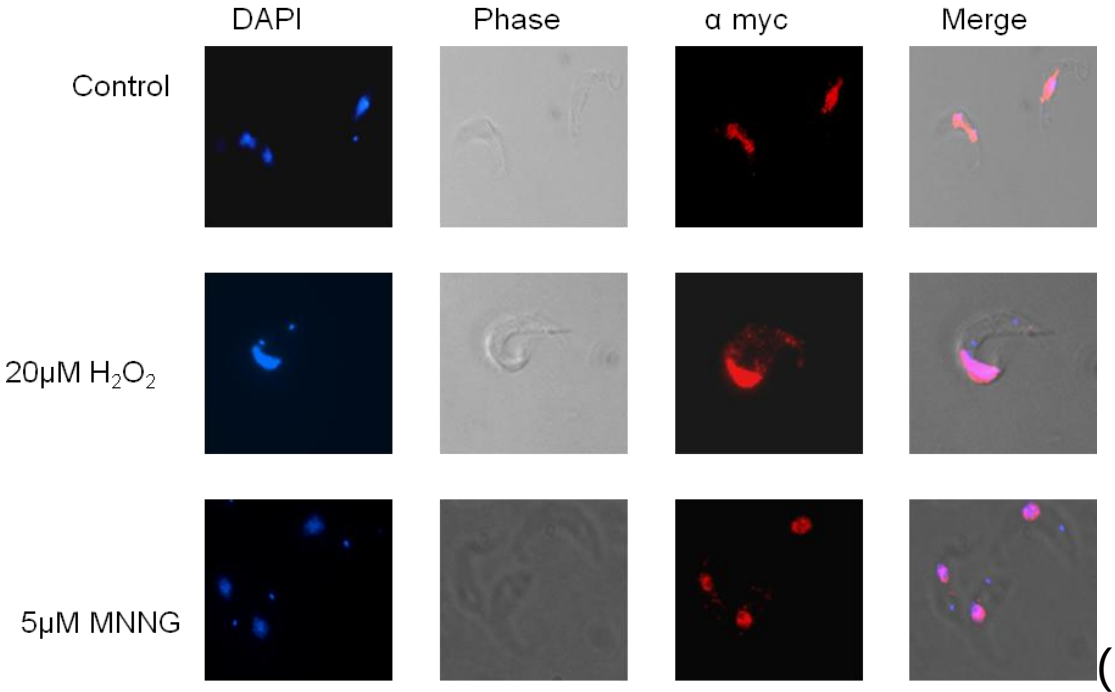
DAPI
Phase
α myc
Merge
Control
20μM $H_2O_2$
5μM MNNG

(D)

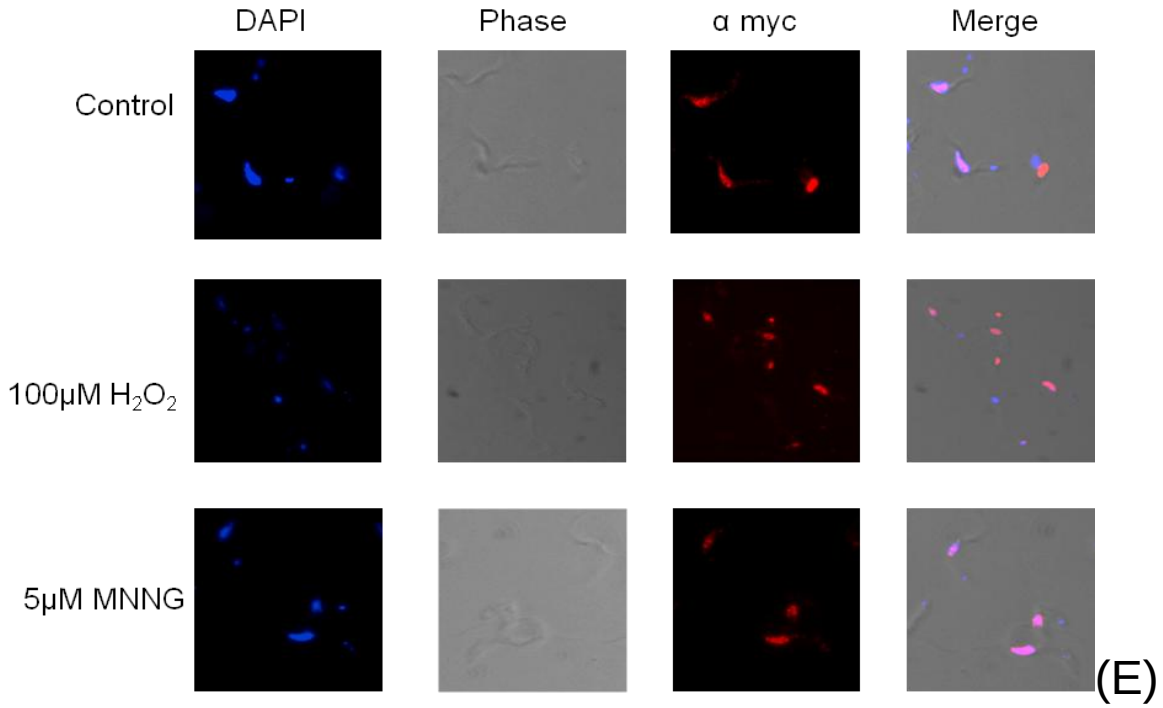


**Figure 4-8 Localization of *T. brucei* MMR proteins by IFA.**

(A) Wild type BSF Lister 427, (B) PCF MSH2-12myc, (C) BSF MSH2-12 myc , (D) PCF MLH1-12myc and (E) BSF MLH1-12 myc cells were grown to log phase and then grown for a further 48 hrs in media containing either MNNG or $H_2O_2$ at the concentrations indicated, or in media without these compounds (labelled control). Cells were probed with mouse anti-myc antiserum (1:5000 dilution) and visualised with Alexaflour-conjugated sheep anti-mouse antiserum (α myc). The cells are also shown counterstained with DAPI, as phase contrast images and as merged images.

IFA analysis suggests that both the myc tagged proteins are nuclear, since the only clear signal was seen in that compartment of the cell (Figure 4-8). Cells that were not treated with any mutagen do not show any signal, for either MSH2 12myc or MLH1 12myc, in around 10-30% of cells. When cells were treated with $H_2O_2$, approximately 50 % of cells did not show MSH2 or MLH1 localisation. Cells treated with MNNG showed clear nuclear signals from all the cells, for both MSH2 12myc and MLH1 12myc. In the wild type cells, no signal was seen in any cell with or without treatment. Thus, the signal that was seen is likely to derive from the tagged proteins, and that DNA damage used, at least in these conditions, does not cause detectable re-localisation of the proteins, or reorganisation of the nuclear-wide staining into discrete 'spots'.

### 4.2.3.2 Sub cellular fractionation

As an alternative approach to localize MSH2 and MLH1 in both the life cycle forms of *T. brucei*, sub cellular fractionation was done by a method described previously by Zeiner et al. (Zeiner, Sturm, & Campbell 2003), with certain modifications (refer to Section 2.3.2). For both BSF and PCF cells, wild type cells were used as a control, and were compared

with MLH1 12myc and MSH2 12 myc expressers. Four preparations were made from each cell: a whole cell extract, two cytoplasmic extracts, and a nuclear extract. Western analysis was performed for all the fractions, described in Section 2.3.1, using four separate gels for each sample that were probed with antiserum recognising four different proteins: Oligopepetidase B (OPB) is a cytoplasmic protein (Munday 2011) and was detected with sheep anti-OPB antiserum (gifted by Jeremy Mottram lab ; 1:2000 dilution); NOG, a nuclear protein associated with the nucleolus (Park 2001), was detected with rabbit anti-NOG (gifted by Marilyn Parsons; 1:5000 dilution); DNA Polymerase β is a mitochondrial protein and was detected with mouse anti-Polβ (gifted from Paul Englund; 1:5000 dilution (Saxowsky 2003); and MLH1 12myc and MSH2 12myc were detected with mouse antimyc antiserum (1:7000). Western analysis of fractionated samples is shown in Figure 4-9.

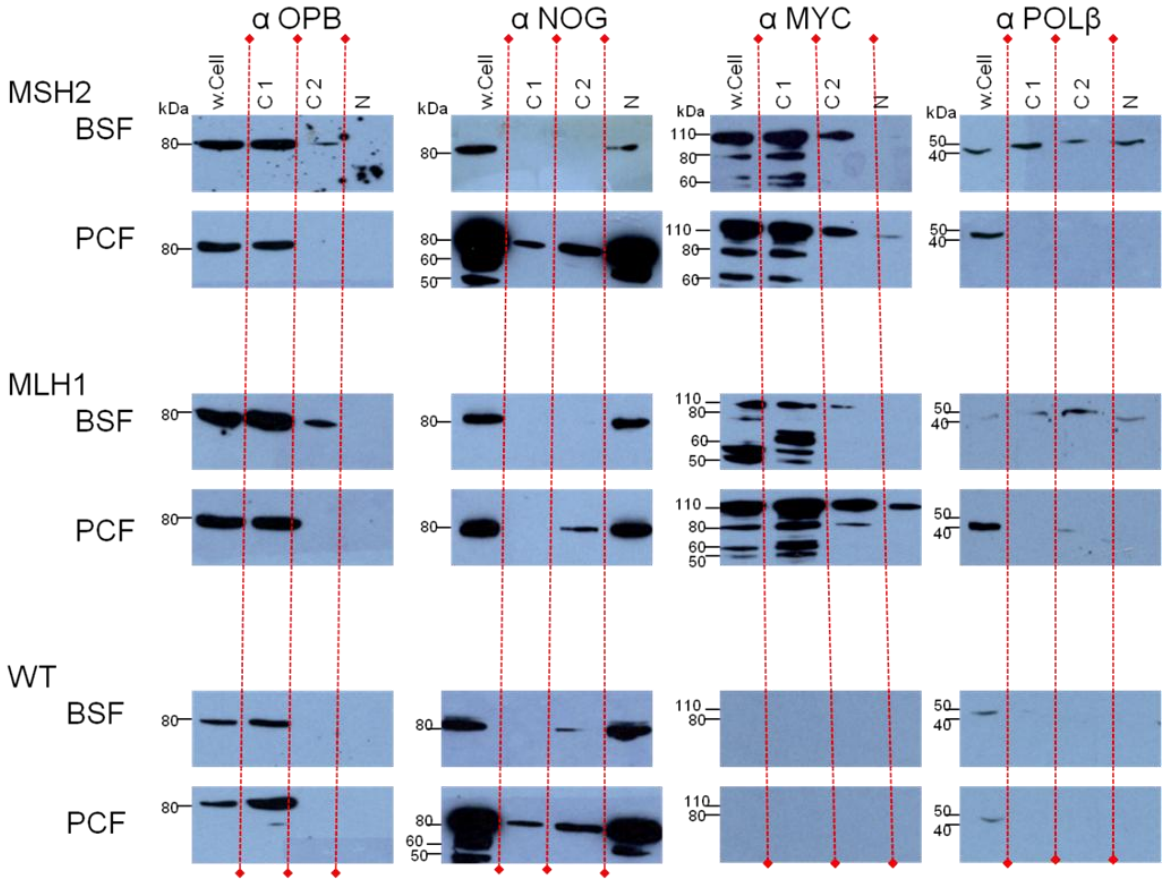


**Figure 4-9 Sub cellular fractionation of *T. brucei* bloodstream form (BSF) and procyclic form (PCF) wild type, *MSH2*-12myc and *MLH1*-12myc cells.**

Whole cell extracts (w.cell) are compared with two cytoplasmic fractions ( C1 and C2) and a nuclear fraction (N) prepared from BSF and PCF wild type, *MSH2*-12myc and *MLH1*-12myc cells. Fraction were resolved on a 10% SDS-PAGE gel and probed with sheep anti-OPB (1:2000 dilution), rabbit anti-NOG (1:5000), rat anti-POLβ (1:5000) or mouse anti-myc (1:7000).

The western blots detecting OPB (83 kDa) and NOG1 (81 kDa) suggest that the fractionation has substantially separated cytoplasmic and nuclear material from both PCF and BSF cells, since OPB signal was seen only in the former fractions (in addition to the whole cell extract) and NOG was strongly enriched in the latter. MSH2-12myc (116 kDa) and MLH1-12myc (127 kDa) were detected in samples from both life cycle forms in the whole cell extract and in the cytoplasmic fractions, though the antiserum did not detect a single band, but instead each protein was seen as a large band of the expected size and several smaller proteins, either due to degradation, processing or modification. Surprisingly, given the IFA (above), only a faint signal was detected in the nuclear fraction for both MLH1-12Myc and MSH2-12Myc, suggesting that both proteins are predominantly cytoplasmic. To ask whether mitochondrial proteins are found in a specific fraction, and thereby provide a clue as to whether the MMR proteins might localize in that organelle, the fractions were probed for Polβ (46 kDa) (Figure 4-9), but this gave only a faint signal that appeared both cytoplasmic and nuclear, so was somewhat inconclusive. The data suggest that PCF cells are more difficult to fractionate compared with BSF, since the cytoplasmic fractions were contaminated with nuclear proteins to a greater extent. From this subcellular fractionation, both MSH2 and MLH1 seem to be found in a substantial cytoplasmic pool.

### 4.2.4 Expression of *T. brucei* MSH2 and MLH1

We next attempted to ask if there are any changes in expression of the MMR proteins in the presence of oxidative stress. To do this, PCF and BSF cultures were set up as described in Sections 3.2.3 and 3.2.6, respectively. However, the cultures were scaled to collect enough samples for the Western blotting as described in Sections 4.2.1.2 and 2.3.1. Non-treated BSF were grown in 50 ml HMI-9 and treated cultures were grown in 500 ml HMI-9. Cultures were diluted to 1 $x10^5$cells.$ml^{-1}$ and incubated for 48 hours. Non-treated PCF cultures were grown in 15 ml SDM-79 and treated cultures were grown in 50 ml. PCF cells were diluted to 5 $x10^5$ cells.$ml^{-1}$ and incubated for 48 hours. Cells were spun at 600 g and pellets were washed in 5 ml sterile PBS. Cells were then counted and whole cell extracts from 3 $x10^7$ cells were loaded in each well. Samples were probed with mouse anti-myc antiserum (1:7000 dilution) and, in parallel, with mouse anti-EF1α (1:5000 dilution) as a loading control. HRP-conjugated goat anti-mouse antiserum was used as secondary antibody. These data are shown in Figure 4-10.

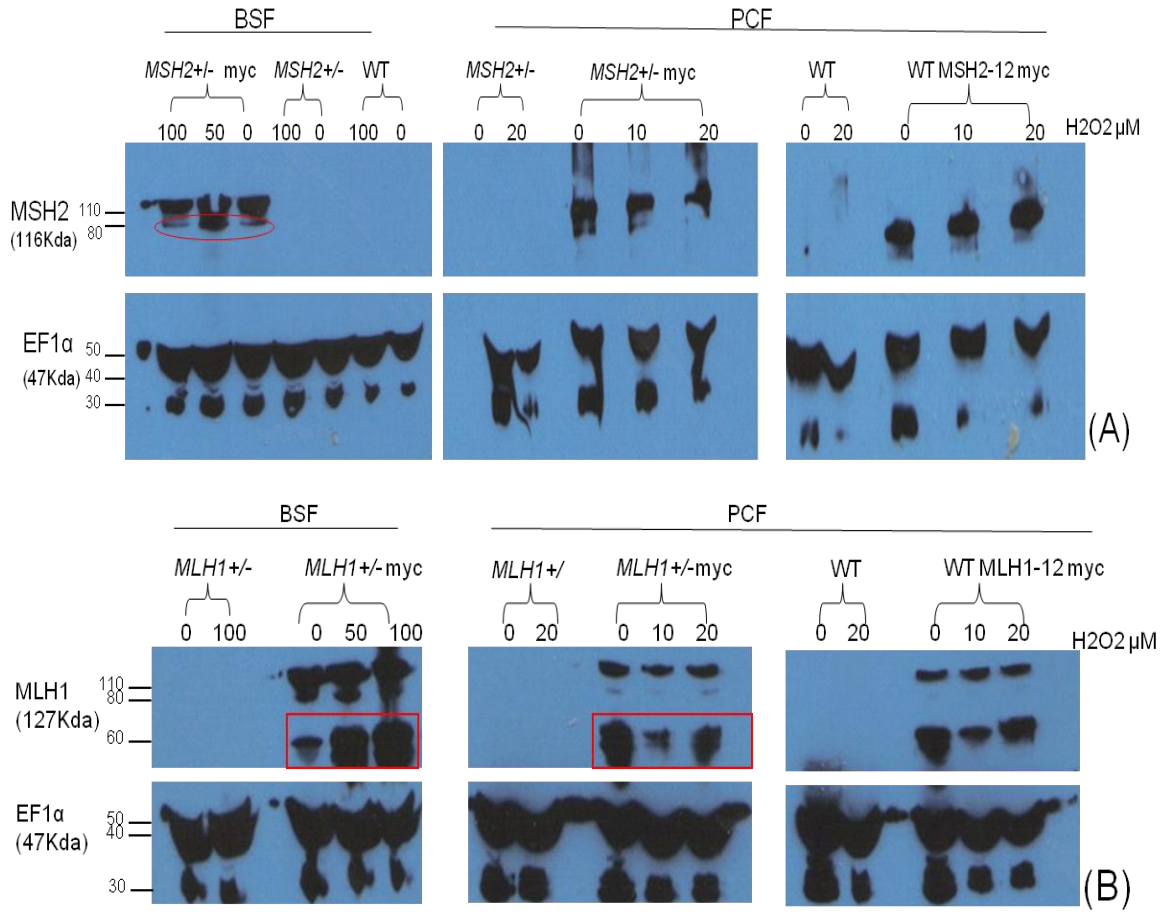


**Figure 4-10 Expression of MLH1-12Myc andMSH2-12Myc in the presence of varying concentration of $H_2O_2$.**

Bloodstream form (BSF) and procyclic form (PCF) *T. brucei* cells expressing 12 myc tagged MSH2 (A) or MLH1 are compared with untagged wild type and heterozygous (+/-) mutants after growth in the presence of increasing concentration of $H_2O_2$ (10 and 20 µM for PCF, and 50 and 100 µM for BSF), or in the absence of $H_2O_2$ (0) . Western blots are shown after samples were separated by SDS-PAGE probed with mouse anti-myc (1:7000) or mouse anti-EF1α (1:5000) antiserum and detected with HRP-conjugated goat anti-mouse antiserum.

The western blotting of both PCF and BSF *T. brucei* showed the presence of bands corresponding with the expected 116 kDa MSH2-12Myc and 127 kDa MLH1-12Myc. The abundance of these bands appeared not to change after oxidative stress, when compared with the EF1α signal, which was predominantly seen as a 50 kDa band, as well as a smaller 30 kDa species. Since the cells were counted prior to loading, it was clear that the percentage survival was as seen before, confirming that the $H_2O_2$ had been added (data not shown). For the MSH-12Myc cells, a smaller band was seen of ~ 80 kDa (as noted earlier in Figure 4-5). This was present at low abundance, which appeared not to change following treatment. In contrast, in the MLH1-12Myccells a more pronounced smaller band was seen of ~60 kDa, and the abundance of this appeared to increase after $H_2O_2$ treatment in the BSF. The same band was detected in PCF cells, but no such change in abundance was observed.

## 4.3 Discussion

MSH2 and MLH1 have been successfully tagged at their C-termini using a 12Myc epitope in two life cycle forms of *T. brucei*, as confirmed by both PCR and western blotting (Figure 4-2 - Figure 4-5). However, we have also demonstrated that tagging MLH1 in this way appears to render the protein non-functional in MMR, as judged by MNNG tolerance (Figure 4-6 and Figure 4-7 B). The tagged proteins were generated by endogenous manipulation in heterozygous mutants cells and we have shown (in Section 3.2.2) that such heterozygous PCF MMR mutants retain MMR activity; similarly, in BSF *T. brucei* it has been demonstrated that single gene knockout of these MMR proteins does not affect the MMR activity (Bell 2004). Though we could not demonstrate the reason for the tagged MLH1 protein being non-functional, we relate it to the fact that mutations in a carboxy terminal motif (CTH) present at the C-terminus of MLH1 proteins show that this part of the protein is important, though the exact function of this motif has not been determined (Bell, Harvey, Sims, & McCulloch 2004;Mohd 2006;Pang 1997). It is also possible that C-terminal tagging of MLH1 prevents dimerization of the protein, or prevents interaction with MSH proteins or downstream factors in the MMR reaction. However, since the 12Myc tagged variant was still expressed, we used it for localizing the MMR protein, since perturbation of function may not impair subcellular routing or interaction with mismatched in DNA. Furthermore, 12Myc tagged MSH2 appeared functional, and so it was possible to ask if the two proteins displayed similar of differing localisation in both BSF and PCF *T. brucei*.

We have localized the tagged proteins through two different strategies. Immunofluorescence microscopy showed the localization of the MMR proteins to be exclusively in the nucleus in both the life cycle forms (Figure 4-8). The cultures were grown on appropriate antibiotics for a week prior to analysis in order to avoid any contamination by non-tagged cell lines; nonetheless, not all the cells showed immunofluorescence. Although the exact number of cells was not counted, it was observed overall that in non-treated cultures approximately 10-30% of tagged cells do not show immunofluorescence, and this appeared to increase after treatment with $H_2O_2$ to 50% of cells. Indeed, the numbers of cells that did not show an immunofluorescent signal appeared greater in BSF *MSH2*-12myc cells (data not shown). In the Myc-tagged cells treated with MNNG, a greater proportion of cells displayed immunofluorescence of both proteins in both life cycle forms. In fact, this effect appeared more prominent in PCF MLH1-12myc cells, where not only the signals were stronger, but essentially all the cells showed nuclear

localisation. Despite this, no difference in the location of the subcellular localization was observed after either oxidative or methylation damage, in that we did not then see signal associated with the kDNA or in the cytoplasm. Taken from this work, it appears that most of the proteins are detected in the nucleus.

Localization by subcellular fractionation provided a contrasting result (Figure 4-9). Western blotting of fractionated samples suggested that the two MMR proteins are predominantly cytoplasmic, rather than nuclear. Though we observed that, for unknown reasons, PCF parasites were more challenging to fractionate (based on localisation of OPB and NOG, acting as cytoplasmic and nuclear markers, respectively) a substantial separation of the nuclear and cytoplasmic material had been achieved (Munday 2011; Park 2001). In PCF *T. brucei*, signals for both MSH2-12Myc and MLH1-12Myc could be seen in the nuclear fractions but the signal intensities were much fainter as compared with the cytoplasmic fractions. In the BSF cells, we failed to detect any significant nuclear signal for the MMR proteins. We predicted that MSH2, if not MLH1, might localize to the kinetoplast, as previous studies have demonstrated the accumulation of 8oxoG in the nucleus as well as kinetoplast of *T. cruzi* (Furtado 2012) and MMR has been shown to play an important role in protection against GC-TA transversion caused by 8oxoG (Slupphaug 2003). Western blotting of fractionated samples showed DNA Polβ, which is thought to be associated with kDNA replication (Li 2007;Saxowsky 2003), to be in all the fractions (though the signals were very weak), so we assume the kinetoplast is not discretely fractionated by the method used. Combining the results of the two methods used for the localization of MSH2 and MLH1, we cannot find any evidence for a kinetoplast localization of the MMR proteins in either of the life cycle forms examined.

By IFA it might be assumed that there is a change in expression of the MMR proteins when subject to stress, explaining the varying numbers and extent of signal detected. However, since precise cell counts were not made during the microscopy, the varying ratio of cells showing immunofluorescence may not be meaningful, and therefore we measured the levels of expression of the tagged proteins by Western analysis (Figure 4-10). Both BSF and PCF *T. brucei* were grown for 48 hours in the presence of $H_2O_2$ at concentrations known to cause effects, from previous survival curves (refer to Section 3.2.3). The maximum concentrations used in survival curves were not used in these experiments, as in these conditions the cells were almost dead. Western analysis did not show any differences in expression of the MMR proteins in either of the life cycle forms examined when subjected to oxidative stress. However, only visual quantification was done, and no

software was used to measure the band intensities. The western analysis suggested that additional bands, distinct from the expected 116 kDa and 127 kDa sizes of MSH2-12Myc and MLH1-12Myc, respectively, were detectable. In the MSH2-12Myc cells a smaller band of 80 kDa was routinely detected both BSF and PCF cells, while an 80 kDa and a further smaller band of 60 kDa were seen in the MLH1-12Myc cells. These small bands were mostly observed, and appeared more prominent, when western analysis was done with fresh samples; however, there was considerable variation in their levels. These bands were never seen in non-tagged lines, so they clearly associate with 12Myc tagging, but whether these bands reveal directed modification or alteration in the structures of MSH2 or MLH1, rather than sporadic degradation, we are not sure. Further analysis would need to be performed before any firm conclusions can be drawn.

# 5 Do other MMR or MMR-associated proteins function in *T. brucei* oxidative damage response?

## 5.1 Introduction

Eukaryotic MMR is initiated by either MutSα or MutSβ acting as the first protein complex to identify a base mismatch and initiate the process of repair. MutSα is activated to bind when the mismatch is 1-3 base pairs in size, whereas if the mismatch is 2-16 base pairs in size MutSβ is activated (Acharya 1996;Genschel 1998;Habraken 1997). MSH2 is the common protein in both these MSH heterodimers, and associates with MSH3 or MSH6, the MSH proteins that provide specificity for the different mismatches. In addition, it has been reported that MSH3 and MSH6 are responsible for anchoring the protein complexes onto the DNA via a specific PCNA interacting N-terminal domain, which is not present in MSH2. Mutation in this region of MSH3 or MSH6 greatly reduces the loading of MutS complex onto the DNA strand and thus MMR activity is impaired (Clark 2000). MSH6, also called the GT binding protein (GTBP) due to its high affinity towards G-T mismatches (Wu 2003), contains a conserved phenylalanine residue in its mismatch binding domain (MBD) present at N-terminal, which is required for the binding of the MSH2-MSH6 protein complex to the mismatch. MSH3 does not encode this residue and how the MSH2-MSH3 complex identifies and binds to a mismatch is currently unknown. In the absence of both MSH3 and MSH6, MSH2 binds unspecifically to DNA (Dowen 2010). Though MutSβ is said to have a more pronounced role in longer patches of mismatches and larger IDLs (2-16 base pairs), MSH3 also recognizes single base mismatches in the absence of MSH6, with a preference for weak hydrogen bonds (Dowen 2010). Thus it has been suggested that, though MSH6 and MSH3 are substrate-specific, they can work in place of each other, provided the other is missing. This was observed in human cells when, in the absence of MSH3, an MMR defect was not observed (Genschel 1998). Functional overlap of MutSα and MutSβ was more clearly observed in mismatches of 2-8 nucleotides (Genschel 1998;Ma 2000). Single base mismatches are though not to be repaired in the absence of MSH6 (Hinz 1999). *msh*3 null mutants, though impaired in MMR, have greater survival rates as compared with *msh2* and *msh6* null mutants in mouse cells, as larger mismatches are thought to form less frequently than single base mutations (Edelmann 2000). This is supported by the finding that expression levels of MutSα are higher than MutSβ: it appears that MSH6 and MSH3 compete with each other to bind to MSH2; since base mismatches are more frequent, MSH6 expression levels must be higher to maintain genome stability. In fact, over-expression of MSH3 results in decreased levels of MutSα and suppresses MMR activity (Marra 1998). Absence of both MSH3 and MSH6 results in total loss of MMR activity (Edelmann 2000).

Besides correcting base mismatches and IDLs, MMR is also involved in gene mutations resulting from the modified bases that arise from certain DNA damaging mutagens, such as $H_2O_2$ and MNNG (refer to Sections 3.2.3 and 3.2.2.2). It has been observed that mutations in *msh6*, but not in *msh3*, results in tolerance towards alkylation damage, as observed for *msh2* mutants (Christmann & Kaina 2000;Fordham 2010). No studies have been reported regarding the role of either MSH6 or MSH3 in response towards oxidative stress. The MMR machinery in *T. brucei* has already been detailed in Section 1.4.6.4. As discussed in that section, *T. brucei*, like most other eukaryotes, appears to encode two MutS complexes: MutSα (MSH2-MSH6) and MutSβ (MSH2-MSH3). *T. brucei* MutS proteins have been shown to be least conserved at their N-termini (see Section 1.4.6.4) (Bell 2004). *T. brucei MSH6* (Tb427.10.1640) is 2993 bp in length and positioned on chromosome 10. It was originally named as encoding a protein termed MSH8, because the predicted polypeptide is much smaller in size than MSH6 in other eukaryotes (e.g. 363 residues shorter than *H. sapiens* MSH6) (Bell 2004), due to an N-terminal truncation. However, at that time the genome had not been sequenced. Complete genome sequencing of *T. brucei* has failed to reveal a further MSH6-like protein that is not truncated at its N-terminus, and so MSH8 appears to be the *T. brucei* orthologue of eukaryotic Msh6; hence, it will be referred here as MSH6. Though less conserved at its N-terminus, *T. brucei* MSH6 has all the four residues conserved within the N terminal including mismatch binding domain and DNA anchoring domain (Bell 2004). *T. brucei MSH3* (Tb09.160.3760) is 2808 bp in length and positioned on chromosome 9. Like MSH6, MSH3 is also truncated at its N-terminus (Bell 2004). However, *T. brucei* MSH3 only encodes residues for anchoring the protein onto the DNA, and a clear mismatch recognition domain appears absent.

The roles of MSH2 and MLH1 have been well described in MMR (Bell 2004; Jiricny 2006) and in the response to oxidative stress (Bell, Harvey, Sims, & McCulloch 2004;Burgess 1999;Colussi 2002;DeWeese 1998)(also see Sections 3.2.3, 3.2.6 and 3.3). However, to have a detailed view of MMR, and the role of MMR components in oxidative damage repair, we needed to look for the functions of MSH3 and MSH6, which to date have not been functionally studied at all, in any kinetoplastid. Since we observed a different phenotype in BSF cells and PCF form cells with respect to $H_2O_2$ sensitivity and after mutation of MSH2 and MLH1, we wanted to expand this picture to provide a clearer understanding of the proteins, if any, that work with MSH2 in combating oxidative stress. To do this, this chapter describes the generation and analysis of knockout (KO) mutants of *MSH6* and *MSH3* in BSF *T. brucei*.

# 5.2 Results

## 5.2.1 Generation of *MSH6* and *MSH3* knockout mutants in BSF *T. brucei*

### 5.2.1.1 Strategy for the generation of knockout mutants

Plasmids were designed for homologous recombination-based gene integration based on the general strategy described in Section 3.2.1.1. Two independent plasmids were made, with either blasticidin (*BSD*) or puromycin (*PUR*) as drug resistance markers to replace the *MSH* genes. However, some minor changes were made in the design of the constructs relative to those used for *MSH2* and *MLH1* KO (Figure 5-1). The KO constructs designed for *MSH3* and *MSH6* had tubulin and actin intergenic regions as processing signals at the 5' and 3' ends of drug resistance genes, respectively. Primers were designed for the PCR amplification of the 5' and 3' UTRs of each gene, with specific restriction recognition sites added at the 5' end of the oligonucleotides. Initially, the *BSD* resistance cassette was made to generate gene-specific KO constructs in which the 5' and 3' UTRs of the genes flanked the *BSD* cassette. From these, the *PUR* drug resistance cassette was then inserted, replacing the *BSD* cassette, after digestion with *Pac*I and *Pst*I (*PstI* site is present in the βα tubulin region, immediately upstream of the *BSD* gene and *PacI* site is present downstream to actin region). For parasite transformation, the constructs were linearized with *Sac*I and *Xho*I. The 5' and 3' UTRs are used as regions of homology and, upon successful transformation and integration by recombination, the ORF of the targeted gene is replaced by drug resistance cassettes.

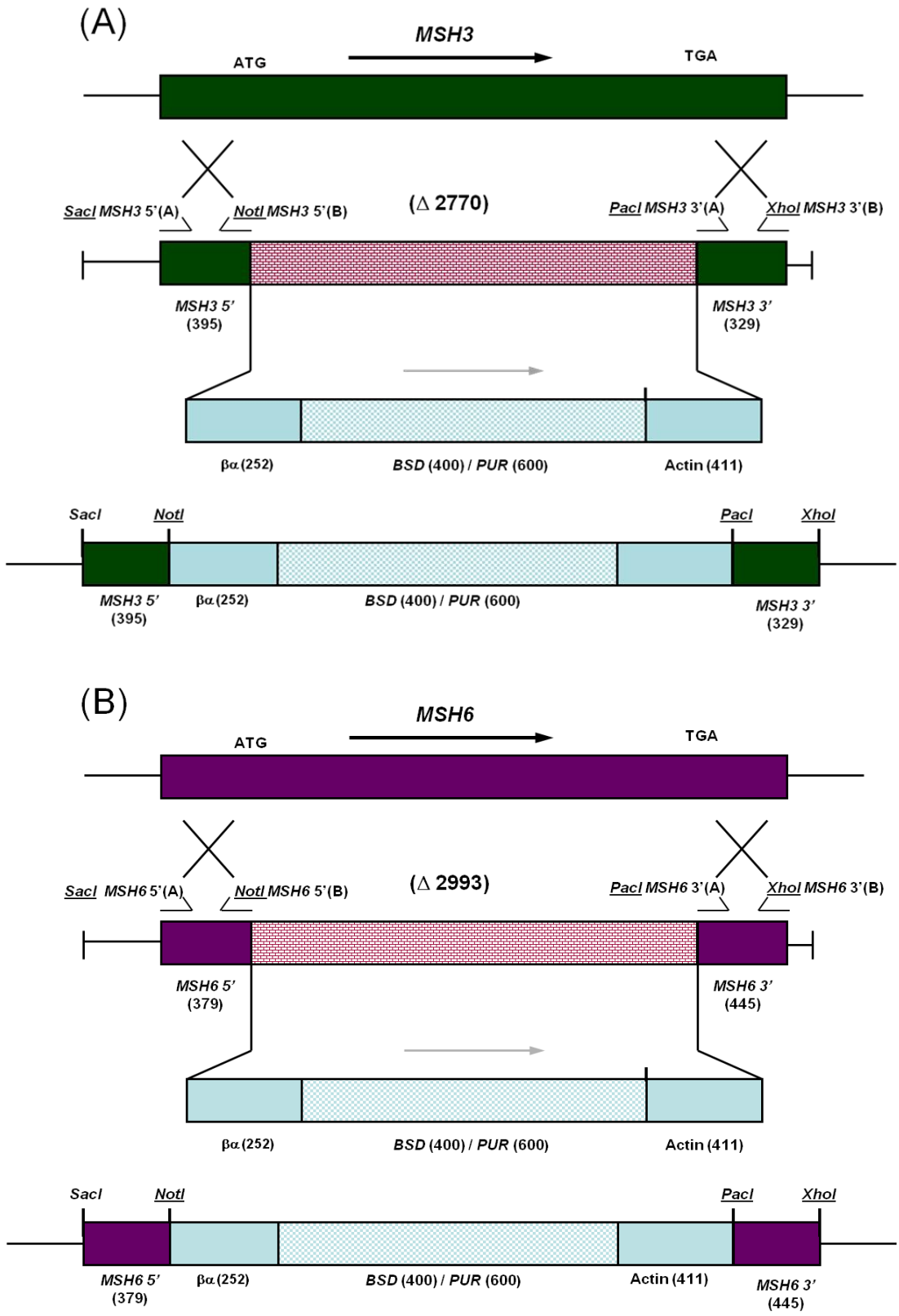


**Figure 5-1 Strategy for the generation of (A) *MSH3* and (B) *MSH6* knock out mutants.**

Gene sequences of (A) *MSH3* and (B) *MSH6*, along with their 5' and 3' UTRs, are shown as coloured boxes (green and purple, respectively). For both the genes, the open reading frame (ORF) is replaced by antibiotic resistance markers following transformation and recombination. The 5' and 3' UTRs are used as regions for homology to allow replacement of the ORFs (indicated as crosses). In each construct, the *MSH3/MSH6* ORF (indicated by checked boxes) is precisely replaced by resistance cassettes. Arrows represent the direction of transcription of the genes, numbers in brackets denote lengths in base-pairs, and half-arrows indicate the approximate positions of primers used in the analysis. Two constructs were generated for each gene to be

replaced with either blasticidin (*BSD*) or puromycin (*PUR*) resistance genes, each flanked by tubulin (Bα) and actin sequences to allow trans-splicing and polyadenylation.

#### 5.2.1.2 Transformation of bloodstream form Lister 427 *T. brucei* with the KO constructs.

BSF Lister 427 cells were transformed with the KO constructs as described in Section 2.1.4.2 . Briefly, ~20 µg of plasmid DNA was isolated from *E. coli* using the Qiagen plasmid miniprep kit (see Section 2.2.2) and linearized with *Sac*I and *Xho*I (refer to Figure 5-1 for respective positions of restriction sites). Digested DNA was then purified using the Qiagen PCR purification kit (Section 2.2.3). For transformation 3-4 x $10^7$ cells were used, with approximately 10 µg of linearized DNA. Cultures were then allowed to recover for 24 hours, and the respective drugs were then added and transformants recovered by limiting dilution. Blasticidin was added at a concentration of 5 $\mu g.ml^{-1}$ and puromycin was added at 0.5 $\mu g.ml^{-1}$. Independent transformations for heterozygous mutants were done to generate blasticidin and puromycin resistant clones. One clone was selected from every transformation, which was initially very sick, but recovered when transferred into media that did not contain any drug. All four heterozygous clones (*MSH3+/-BSD*, *MSH3+/-PUR*, *MSH6+/- BSD* and *MSH6+/- PUR*) were confirmed by PCR (see below). The *MSH3+/-BSD* and *MSH6+/- BSD* cells were then transformed with ~10 µg of the *PUR*-containing KO constructs and putative homozygous mutants selected with 5 $\mu g.ml^{-1}$ and 0.2 $\mu g.ml^{-1}$ blasticidin and puromycin, respectively. The transformation efficiencies were extremely low for this step of the *MSH6* and *MSH3* KOs and multiple clones were only recovered after several attempts at transformation. Indeed, the putative homozygous mutants were even sicker than the +/- mutants, and could only be grown in the presence of antibiotics if cultured at relatively high cell densities and after being grown in the absence of drugs for a number of passages. Initially, 10 clones from each transformation were collected after 3 days of transformation and grown on drug-free media for two days before they were cultured again on blasticidin and puromycin-containing media. Only two out of 10 clones continued to grow on the drugs, and these were grown on drug-free media for one week before genomic DNA was isolated using the Qiagen blood and tissue kit (see Section 2.2.2). Clones were tested for the genetic changes by PCR (Figure 5-2 and Figure 5-3), as described in Section 2.2.5, and by reverse transcriptase PCR (RT-PCR) (Section 2.2.11) (Figure 5-4).

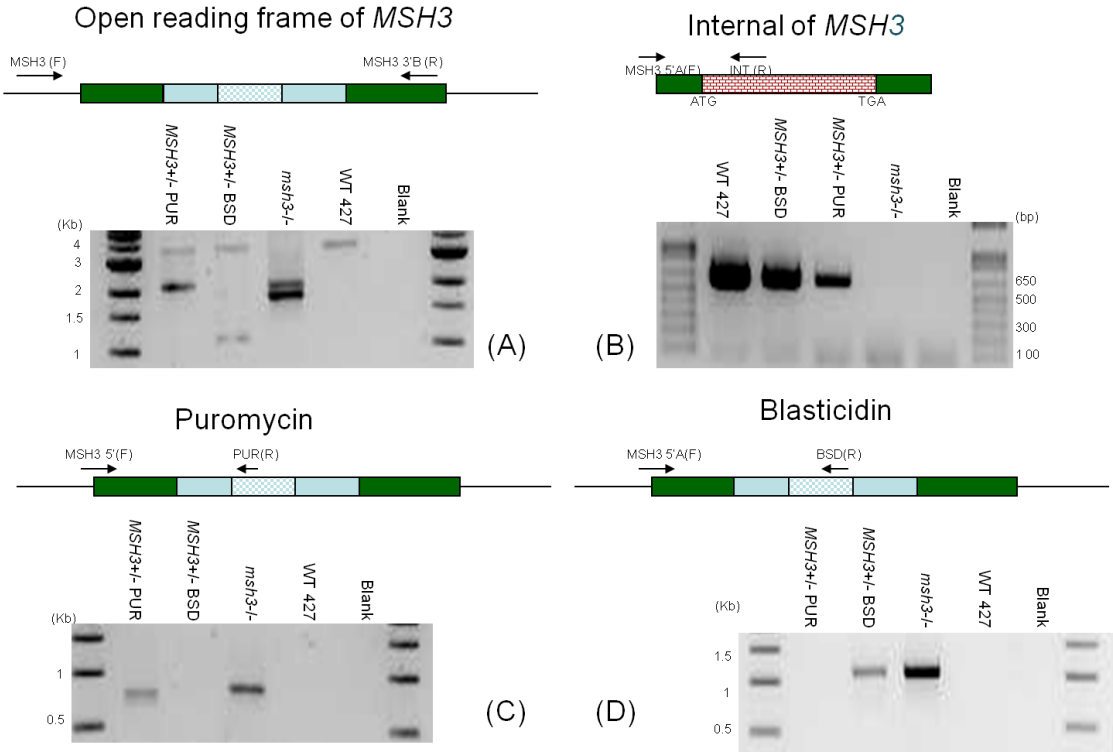


**Figure 5-2 PCR analysis for the confirmation of *MSH3* mutants.**

Different sets of primers (denoted by arrows and labelled) were designed to test the organisation of the *MSH3* locus in the wild type, *MSH3+/-BSD*, *MSH3+/-PUR* and *msh3-/-* cells: gels are shown of PCR with these primers on genomic DNA from the cells; blank denotes a reaction with no substrate DNA **(A)** Primers MSH3 (F),and MSH3 3'B (R) were used to PCR-amplify the ORF of *MSH3*; the forward primer is specific to the region upstream to the recombining 5' UTR, and the reverse primer is specific to the 3' UTR. **(B)** Primers used were to PCR-amplify a 639 bp region of ORF: MSH3 5'A(F) and MSH3 int (R). **(C)** In an attempt to confirm the presence of the puromycin (*PUR*) resistance cassette, PCR was performed using a forward primer (MSH3 5'A (F)) that was complementary to the 5' UTR and a reverse primer complementary to PUR (PUR (R)). **(D)** To test for the Blasticidin resistance cassette (*BSD*) PCR was performed was using MSH3 5'A (F) as the forward primer and a reverse primer complementary to *BSD* (BSD (R)).

The PCR results not only confirm the loss of each gene in the knockout mutants but also the correct integration of the drug resistance genes. Heterozygous (+/-) and homozygous (-/-) mutants were analysed along with wildtype Lister 427 (WT) parents, as a control. When the whole *MSH3* ORF was PCR-amplified (Figure 5-2 A) a single band of ~ 3.5 Kb (expected size of 3580 bp) was seen in the wild type cells and *MSH3*+/- mutants. In addition, in the *MSH3+/-PUR* mutants, the primers PCR-amplified the allele with the *PUR* drug resistance cassette (~2 Kb; 2063 bp expected size). In the *MSH3+/-BSD* cells, for reasons that are unclear, the allele mutated with the *BSD* resistance cassette (1863bp) was not PCR-amplified but instead a smaller band was seen in addition to the wild type copy. In the *msh3-/-* mutants, derived from the *MSH3+/- BSD* mutants, two bands of the expected sizes for both integrated drug resistance genes were PCR-amplified. Loss of the *MSH3* gene in the *msh3-/-* cells was further confirmed by PCR using primers specific to a

639 bp internal region of the ORF (Figure 5-2 B), which was PCR-amplified in wild type cells and both heterozygous mutants, but not in the null mutants. PCR of the *BSD* (Figure 5-2 D) and *PUR* (Figure 5-2 C) drug resistance genes yielded products of the expected sizes and in the expected mutants: ~1.1 Kb (1047 bp expected size) and ~0.8 Kb (754bp expected size), respectively, in the respective heterozygous mutants and in the *msh3*-/- null mutants, but not in wild type cells.

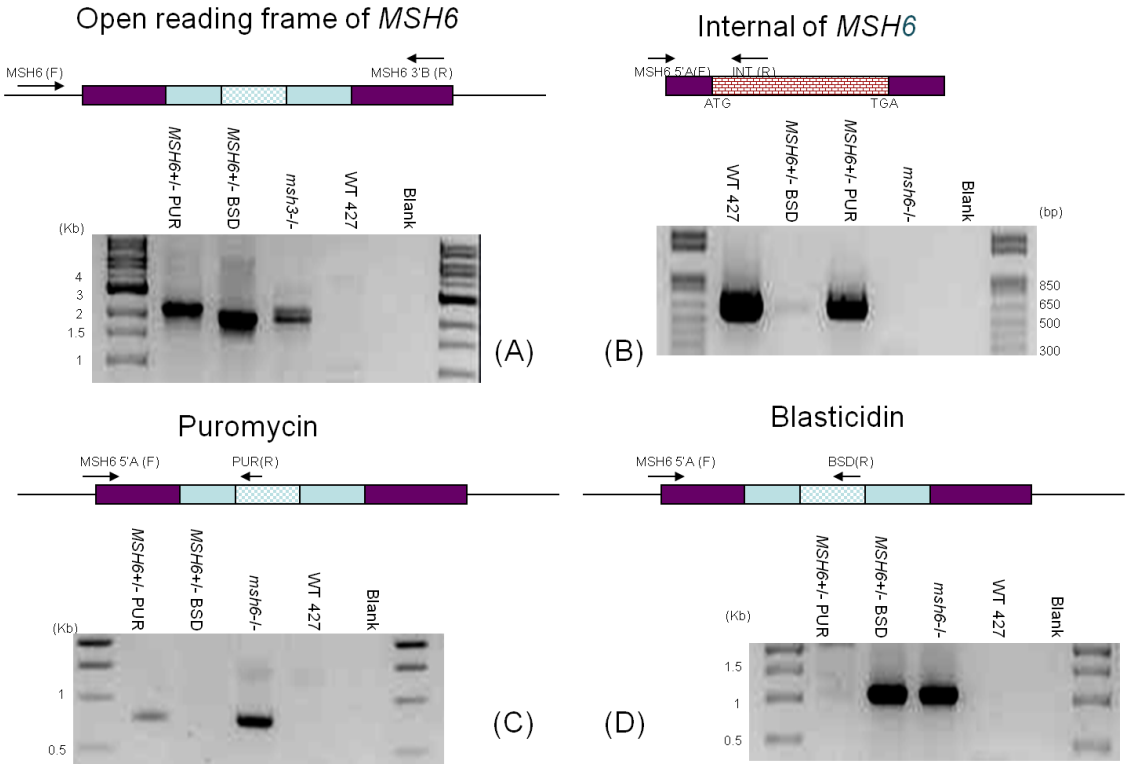


**Figure 5-3 PCR analysis for the confirmation of *MSH6* mutants.**

Different sets of primers (denoted by arrows and labelled) were designed to test the organisation of the *MSH6* locus in the wild type, *MSH6+/-BSD*, *MSH6+/-PUR* and *msh6-/-* cells: gels are shown of PCR with these primers on genomic DNA from the cells; blank denotes a reaction with no substrate DNA **(A)** Primers MSH6 (F),and MSH6 3'B (R) were used to PCR-amplify the ORF of *MSH3*; the forward primer is specific to the region upstream to the recombining 5' UTR, and the reverse primer is specific to the 3' UTR. **(B)** Primers used were to PCR-amplify a 678 bp region of ORF: MSH6 5'A(F) and MSH6 int (R). **(C)** In an attempt to confirm the presence of the puromycin (*PUR*) resistance cassette, PCR was performed using a forward primer (MSH6 5'A (F)) that was complementary to the 5' UTR and a reverse primer complementary to PUR (PUR (R)). **(D)** To test for the Blasticidin resistance cassette (*BSD*) PCR was performed was using MSH6 5'A (F) as the forward primer and a reverse primer complementary to *BSD* (BSD (R)).

For MSH6, the same type of PCR analysis also confirm the generation of heterozygous and homozygous mutants. Primers used to PCR-amplify the whole ORF (Figure 5-3 A) (3990 bp) did not generate a product in any cell line (presumably because the product is so large), whereas the *BSD* and *PUR* resistance gene-containing alleles were amplified: ~2 and 2.2 Kb, respectively, bands were seen in the respective heterozygous and homozygous

mutants, which are consistent with their expected product sizes (2060 bp and 2260 bp, respectively). An internal region of the *MSH6* ORF was PCR-amplified (Figure 5-3 B) to generate a ~650 bp band (expected product size 678 bp) in wild type cells and in the heterozygous mutants. No such amplification in the *msh6-/-* DNA sample confirms the loss of gene. Replacement of the ORF with the drug resistance cassettes (Figure 5-3 C and D) was confirmed by PCR-amplification of bands of the size expected for *BSD* (~1 Kb; expected product size, 1031bp) and *PUR* (~0.8 Kb; 738 bp expected product size) in the null mutants and their respective heterozygous mutants.

The above genomic DNA PCRs confirm the loss of ORF and replacement with respective resistance cassettes for both the two MMR genes. To further ensure that gene was not being expressed in the null mutants, RT- PCR was performed. Total RNA samples were prepared from wild type cells and from the +/- and -/- mutants and were first checked for the presence of any contaminating genomic DNA by performing PCR amplification with primers recognising *RAD51,* a gene that should be unaffected by the MMR mutation events; this is shown in Figure 5-4A. The RNA samples were then reverse transcribed to make cDNA using high capacity RNA-to-cDNA master mix (Applied Biosystems, see section 2.2.11) and the resulting cDNA was PCR-amplified with primers recognising *RAD51* as a control to check for the conversion of RNA to cDNA in all the samples; this is shown in Figure 5-4 B and in each case where PCR-amplification was expected to occur a band of the expected size (1122 bp) was seen. Having performed these controls, the cDNA samples were then PCR-amplified with primers binding specifically to the ORF of either *MSH3* or *MSH6,* as shown in Figure 5-4 C and Figure 5-4 D, respectively.

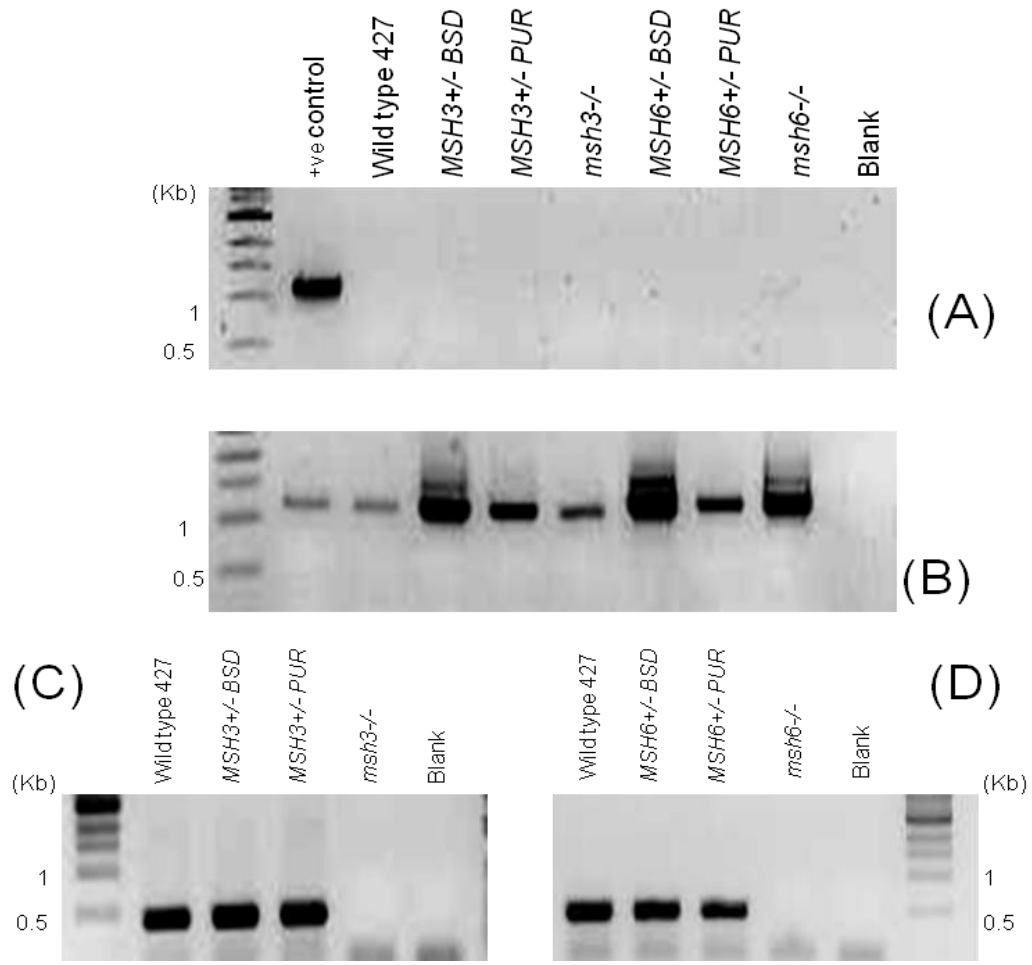


**Figure 5-4 RT-PCR analysis of BSF *MSH3* and *MSH6* mutants.**

Agarose gels are shown of reverse transcriptase (RT) PCRs to check for loss of mRNA in bloodstream form *T. brucei MSH3* and *MSH6* knockout mutants (labelled -/-), compared with wild type cells and heterozygous (+/-) mutants. (A) PCR is shown from RNA samples of wild type and mutants PCR-amplified with *RAD51* primers (RAD 51 (F) and RAD 51 (R); genomic DNA from wild type *T. brucei* was used as a positive control for the reaction, and blank is a control PCR with water as template. (B) *RAD51* PCR is shown from cDNA generated from the RNA used from the samples shown in A. (C) PCR is shown using cDNA from wild type and *MSH3* mutants and primers MSH3-D3 (F) and MSH3-U4 (R). (D) PCR is shown using cDNA from *MSH6* mutants and primers MSH6-D3 (F) and MSH6-U1 (R). In all gels markers are shown and selected sizes indicated.

This RT- PCR analysis demonstrates that both *MSH3* and *MSH6* null mutants have lost the expression of mRNA of the expected gene, while mRNA for both *MSH3* and *MSH6* could be detected from wild type cells and from heterozygous mutants that preceded the generation of the -/- mutants; for *MSH3* a PCR-product of 437 bp was expected and for *MSH6* a product of 502 bp.

### 5.2.2 Phenotypic analysis of mismatch repair activity in *MSH3* and *MSH6* mutants

In order to test for mismatch repair efficiency, the *MSH3* and *MSH6* mutants were analysed by the phenotypic assays as described for BSF as well as PCF *MSH2* and *MLH1* mutants (Bell 2004) (also refer to Chapter 3). Before any analysis, the -/- cells were cultured in the presence of 2 $\mu g.ml^{-1}$ blasticidin and 0.2 $\mu g.ml^{-1}$ puromycin for at least 3-5 days. These very low concentrations were used, since *MSH3* and *MSH6* mutants were found to be very sick in the presence of higher drug concentrations: for instance, though the *msh6*-/- cells were originally grown on 5 $\mu g.ml^{-1}$ blasticidin and 0.5 $\mu g.ml^{-1}$ puromycin, with the passage of time they grew more and more poorly at these dilutions. Cultures were never diluted below 2 $x10^5 cells.ml^{-1}$ when grown in the presence of drugs.

#### 5.2.2.1 *In vitro* growth analysis.

Population doubling times of the mutants were measured to ask if mutation of these genes causes any growth defect. This is also necessary so that any change can be taken into account when doing further analysis. Clones used in the study are wild type 427, *MSH3+/- (MSH3::BSD), msh3-/- (MSH3::BSD::PUR), MSH6+/- (MSH6::BSD)* and *msh6-/- (MSH6::BSD::PUR).* The cells were inoculated at a density of 1 x $10^5$ $cells.ml^{-1}$ in 15 ml of HMI-9, without any antibiotic and cell densities were counted 24, 48 and 72 hours later using a haemocytometer. Three replicates of this analysis were performed. These growth data are shown in Figure 5-5, and the doubling times of wild type cells and mutants then calculated and are presented in Table 5-1.

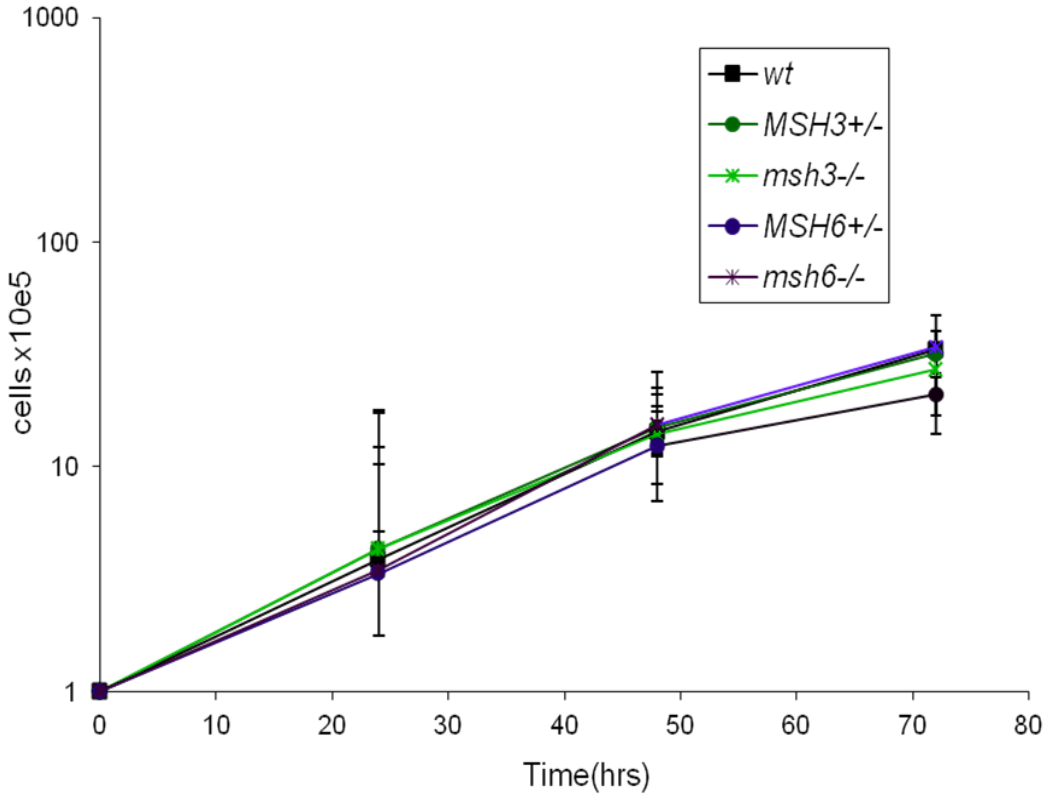


**Figure 5-5 *In vitro* growth analysis of *T. brucei* BSF *MSH3* and *MSH6* mutants.**

BSF wild type, *MSH3+/-, msh3-/-, MSH6+/-, msh6-/-* cells were inoculated at a density of $1x10^5$ cells.$ml^{-1}$ in 15 ml and counted each 24 hours up to 72 hours using haemocytometer. Three replicates were done for every clone and average values are plotted; vertical bars denote standard deviation .

**Table 5-1 Doubling times of wild type cells and MSH6 and MSH3 mutants**

| Cell line | | | | | |
|---|---|---|---|---|---|
| Doubline time | Wt | *MSH3+/-* | *msh3-/-* | *MSH6+/-* | *msh6-/-* |
| | 14.37 | 14.5 | 15.24 | 16.5 | 14.25 |

It is evident from the growth curve shown in Figure 5-5 and doubling times calculated in Table 5-1 that the deletion of these genes does not cause any growth defect. Although the *msh3-/-* and *MSH6+/-* cells appeared to grow slightly slower than the rest of the cells from the doubling times, this may be accounted for by growth of these cells reaching a more pronounced plateau at the end of the curves.

### 5.2.2.2 Tolerance to alkylation damage

Tolerance to alkylating damage was tested to see the role that MSH3 and MSH6 play in MMR. As discussed previously (see Section 3.2.2.2), MNNG is an alkylating agent that

causes G-T transition (Warren 2006) and MMR mutants are frequently found to more tolerant to this damage due inaccurate repair (Claij 2002;Karran 1994). MNNG induces a methyl group at 6$^{th}$ oxygen of guanine. This methylated guanine has an equal tendency to bind to cytosine and thymine. If this methylated guanine (6metG) is present in newly synthesized DNA it is not corrected, but if the altered base is in template strand it binds to T and also distorts the DNA conformation.

Tolerance to MNNG was measured by the Alamar blue assay, as described in Sections 2.5.1.2.2 and 3.2.2.2 (O'Brien 2000). The change in colour as Alamar blue is metabolised was measured by a luminescence spectrometer (LS 55, Perkin Elmer) at an emission wavelength of 590 nm. IC50 values (*i.e.*, drug concentrations causing death of 50% of the cells) were then calculated from the survival curves, using Prism (GraphPad). 1 x $10^5$cells.ml$^{-1}$ were added to the plates and MNNG was used in doubling dilutions from 0.39 to 400 µM in HMI-9. Each experiment was carried out in triplicate and the results are shown in Figure 5-6.

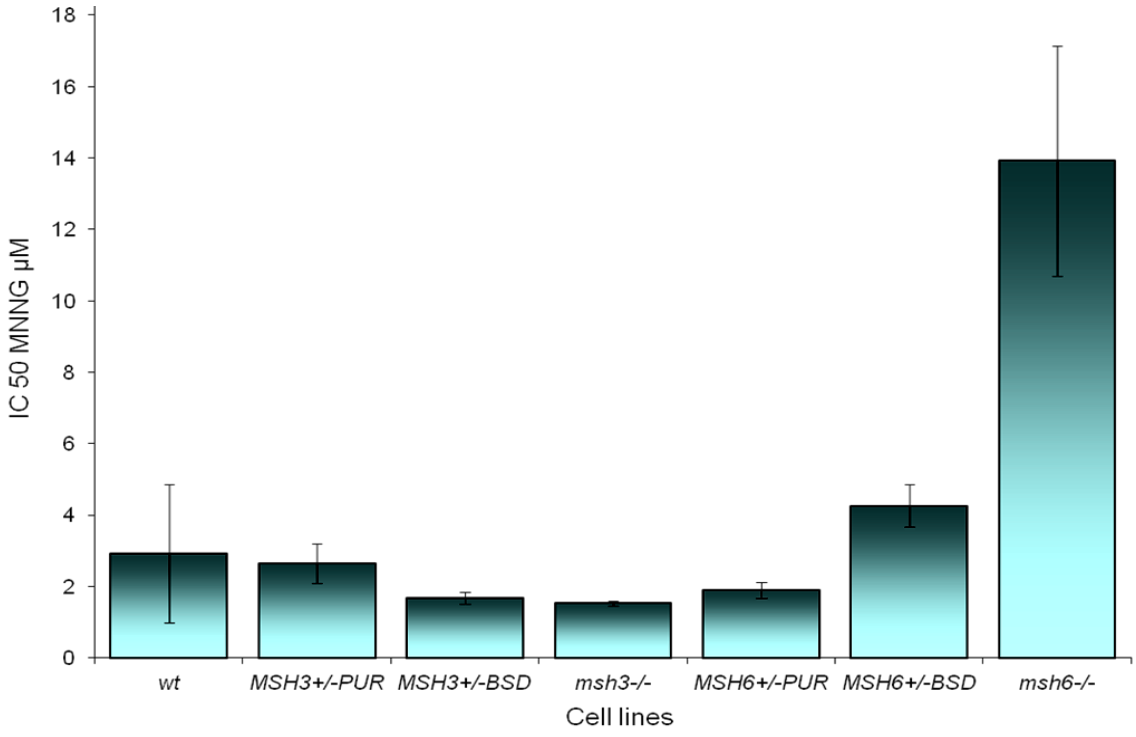


**Figure 5-6 IC50 values of *T. brucei* BSF *MSH3* and *MSH6* mutants in the presence of doubling dilutions of MNNG.**

The conversion of Alamar blue to fluorescent Resazurin was used to determine the sensitivity of BSF *T. brucei* wild type (WT) cells and *MSH3* and *MSH6* mutants towards MNNG. IC50 values of Lister 427 WT, *MSH3+/-, msh3-/-, MSH6+/-* and *msh6-/-* cells is shown. IC50 values are the mean of three experiments and vertical bars indicate standard deviation. Cells were grown from a starting density of 1 x $10^5$cells.ml$^{-1}$ n the presence of doubling dilutions of MNNG (from 0.39 -400 µM) in fluorescence- readable 96 well plates. After 48 hrs Alamar Blue was added to each well and fluorescence measured after a further 24 hours of growth.

These data on tolerance of *MSH3* and *MSH6* mutants towards MNNG damage suggests that the *msh6*-/- cells are most resistant, and significantly different from all the other cells examined. An approximately 2-fold difference was seen between the *MSH6+/- BSD* and *MSH6+/-PUR* cells. However, since both the values lie within the range of IC50 values of the wildtype cells, we conclude that *MSH6* heterozygous mutants have retained their MMR activity. In contrast with the *msh6*-/- mutants, there was no evidence that the *MSH3* mutants showed any effect of increased or decreased resistance to MNNG (Figure 5-6). These data indicate that the absence of MSH6 results in non-functional MMR in *T. brucei*, or at least a crucial role for MSH6 in MMR action against the damage caused by MNNG. MSH3 does not seem to be involved in the response to this alkylating damage, and thus we cannot say if this MSH protein contributes to *T. brucei* MMR.

#### 5.2.2.3 Testing for microsatellite instability

MSH3 and MSH6 mutants were next tested for microsatellite instability (MSI) by PCR-amplifying the JS2 microsatellite. Wild type cells and the mutants were sub-cloned as described in Sections 2.5.1.2.3 and 3.2.2.3 (Bell 2004) and 10 random clones were selected for each cell line. Cultures were then diluted in 15 ml HMI-9 grown for 10 generations. DNA was isolated using the Qiagen DNAse easy blood and tissue kit (see Section 2.2.2). As described in Section 3.2.2.3, JS2 is composed of repeating units of a GT dinucleotide and is positioned on chromosome 4 (Hope 1999). The JS-2 locus was amplified by PCR using the primers JS-2A and JS-2B from the DNA of each of the 10 sub clones of WT, *MSH3+/-, msh3-/-, MSH6+/-* and *msh6*-/- cells. PCR was performed using the protocol detailed in section 2.2.5 and the resulting PCR products were separated by electrophoresis on 3% low melting agarose gels (see Section 2.2.6 and 2.5.1.2.3); samples we were run at 100 V for 50 minutes. The results of this work are shown in Figure 5-7.

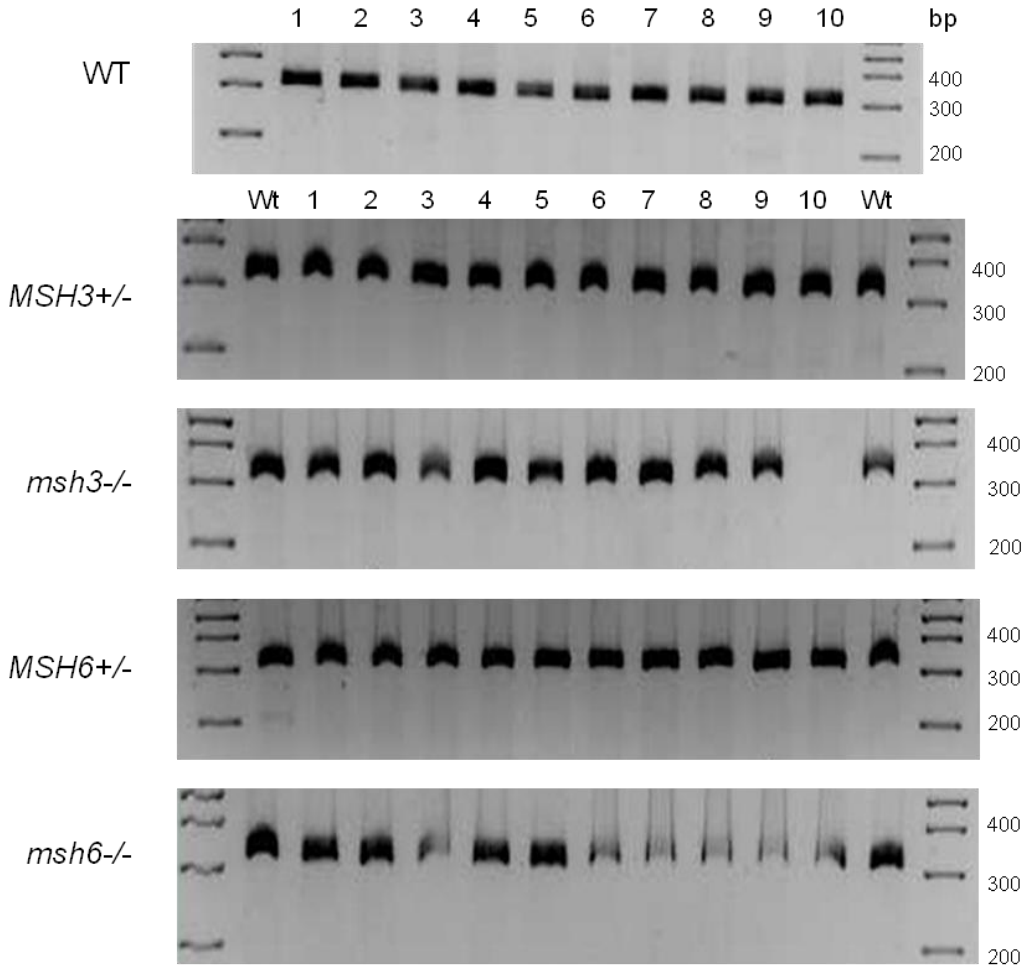


**Figure 5-7 Testing for MSI in bloodstream form wild type, *MSH3+/-*, *msh3-/-*, *MSH6+/-* and *msh6-/- T. brucei* cells**

The JS2 microsatellite locus was PCR-amplified from 10 clones each from WT, *MSH3+/-*, *msh3-/-*, *MSH6+/-* and *msh6-/-* cells using the primers JS2A and JS2B. PCR products were separated on 3% agarose gels at 100 V for 50 minutes. For a better comparison between wild type and mutants, PCR product from one of the wild type sub-clones was added in the first and last lane of the gel containing the 10 mutant clones, as indicted by WT. Different in size of wild type and mutants was compared. Marker lanes are shown and sizes indicated.

It is evident from the results in Figure 5-7 that neither the wild type cells, nor any of the mutants showed any evidence for MSI, in striking contrast to the BSF *msh2*-/- and *mlh1*-/- mutants (Bell 2004). All the clones from each cell showed a single PCR product of ~350 bp, which is consistent with the JS2 product size PCR-amplified previously from wildtype and *MSH2*+/- and *MLH1*+/- mutants examined (Bell 2004). This indicates that loss of either MSH3 or MSH6 does not result in alterations to the repeat lengths, for instance through replication slippage, in the JS2 locus. If *T. brucei* MSH6 and MSH3 act on mismatches as described in other eukaryotes, it might have been predicted that the *msh6*-/- cells would show MSI, since MSH3 acts on base mismatches larger than 2 nucleotides (and has a higher tendency to resolve IDLs of more than 4 nucleotides) (Haugen 2008), while MSH6 is more active in correcting mismatches and IDLs of 1-3 nucleotides

(Genschel 1998). The data here might then suggest the possibility of *T. brucei* MSH3 and MSH6 being able to work in place of each other in correcting the dinucleotide replication errors that may form at JS2. As discussed in the introduction, functional overlap between these two proteins has been described in other eukaryotes for mismatches and IDLs 2-8 nucleotides in length (Genschel, Littman, Drummond, & Modrich 1998;Ma et al. 2000), and thus this activity may be conserved in *T. brucei*. In contrast, MSH2 is common to all MutS-like dimers that form in eukaryotes (Acharya 1996;Genschel, Littman, Drummond, & Modrich 1998;Habraken 1996) and mutations in this gene would lead to less specific and more pronounced sequence changes associated with mismatches and IDLs, including the microsatellite tested here.

#### 5.2.2.4 Testing for a response towards $H_2O_2$.

Oxidative DNA lesions caused by $H_2O_2$, and the repair systems that tackle such lesions, have been discussed in detail in Section 1.4.7.2. *MSH2* mutants in BSF *T. brucei* cells have been shown to display a phenotype of sensitivity towards $H_2O_2$ (Machado-Silva et al. 2008). Whether MSH2 acts in this role on its own, or as part of a MutS-like complex, has not been tested: no role of MSH3 or MSH6 has been reported in the response towards any oxidative stress. To examine this, the wild type cells and all of the *MSH3* and *MSH6* mutants were grown in the presence of increasing concentrations of $H_2O_2$ as described in Sections 2.5.1.2.2 and 3.2.6. In brief, 1 x $10^5$ cells were inoculated in the 20 ml of HMI-9 with final $H_2O_2$ concentrations of 0, 50, 100 or 300 µM. Cell counts were then taken at 24, 48 and 72 hours, and the cell densities used to calculate percentage survival relative to the cell densities in the absence of $H_2O_2$. The experiment was done in triplicate, and the results are shown in Figure 5-8.

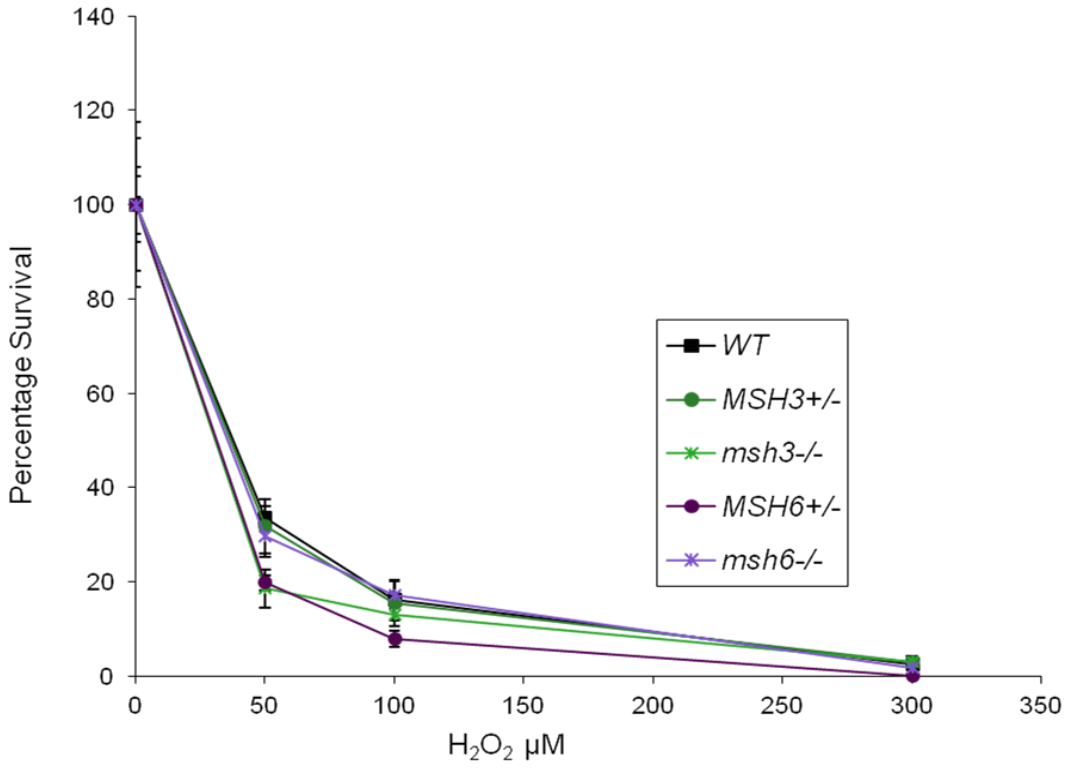
Percentage Survival
140
120
100
80
60
40
20
0
0
50
100
150
200
250
300
350
H2O2 µM
WT
MSH3+/-
msh3-/-
MSH6+/-
msh6-/-

(A)

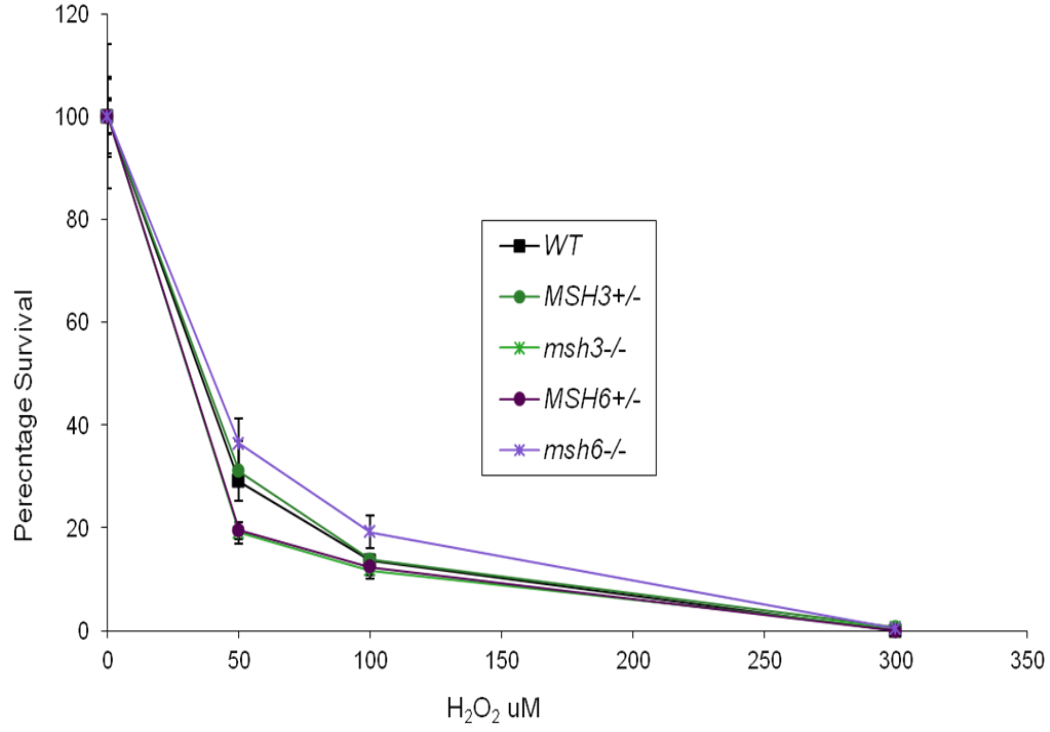
Perecntage Survival
120
100
80
60
40
20
0
0
50
100
150
200
250
300
350
H2O2 uM
WT
MSH3+/-
msh3-/-
MSH6+/-
msh6-/-

(B)

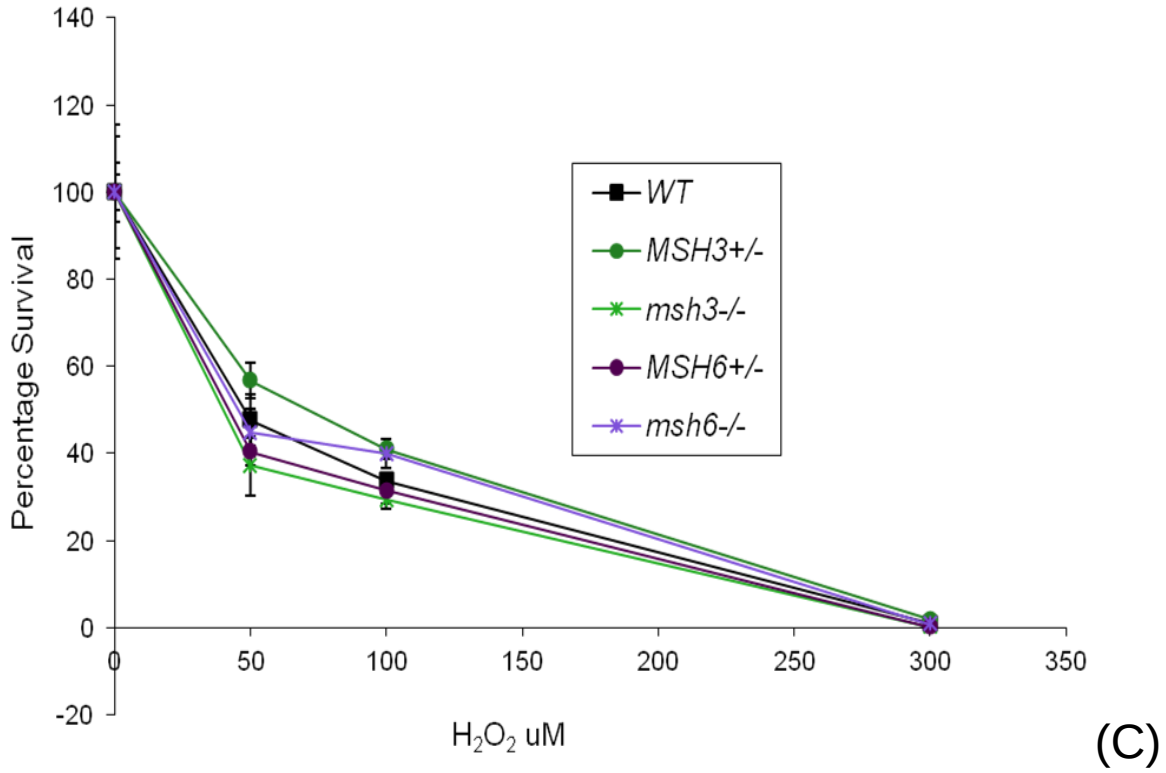


**Figure 5-8 Percentage survival of *T. brucei* BSF wild type, *MSH3* and *MSH6* mutants at various concentration of $H_2O_2$.**

Wild type, *MSH3+/-*, *msh3-/-*, *MSH6+/-* and *msh6-/- T. brucei* cells were diluted to $1x10^5$ cells.$ml^{-1}$ in HMI-9 culture media containing 0, 100, 200 or 300 µM $H_2O_2$. Cell densities were counted at (A) 24 hours, (B) 48 hours, and (C) 72 hours. Values are shown as percentage survival, which was calculated from the cell density of each cell type in the presence of $H_2O_2$ as a percentage of the same cells grown in the absence of damage (which was taken as 100%). Each value is the mean of three experiments, and vertical bars depict standard deviation.

These data suggest that there is no discernible difference in survival of the *MSH3* or *MSH6* mutants in the presence of $H_2O_2$ relative to wild type. At all concentrations of $H_2O_2$ used, and at each of the time points examined, there was strong overlap between the survival rate of the wild type cells and the +/- and -/- cells, of both genes. This suggests that there is no discrete role for one or other of these proteins in the response of *T. brucei* to oxidative damage, as has been seen for MSH2. However, given that the MSI analysis suggests the one protein may be able to act in place of the other in some circumstances, this result does not discount the possibility that MSH6 and MSH3 might act in this role.

## 5.2.3 Comparison between all the MMR mutants.

To test the results described in Section 5.2.2.4 and 3.2.6 above further, and to get a more complete picture of the relative importance of the *T. brucei* MMR factors in the response towards oxidative damage, growth of all available BSF null mutants were compared in the presence of $H_2O_2$ as described in Section 3.2.6. Again, the cells were inoculated at a

density of 1 x $10^5$ cells.ml$^{-1}$ in 20 ml of HMI-9. $H_2O_2$ was added to the medium at concentrations of 0, 100, 200, and 300 µM. Wild type cells were included in the experiment for comparison. Cells were counted after 48 and 72 hours of growth, in duplicate, and percentage survival determined, as shown in Figure 5-9.

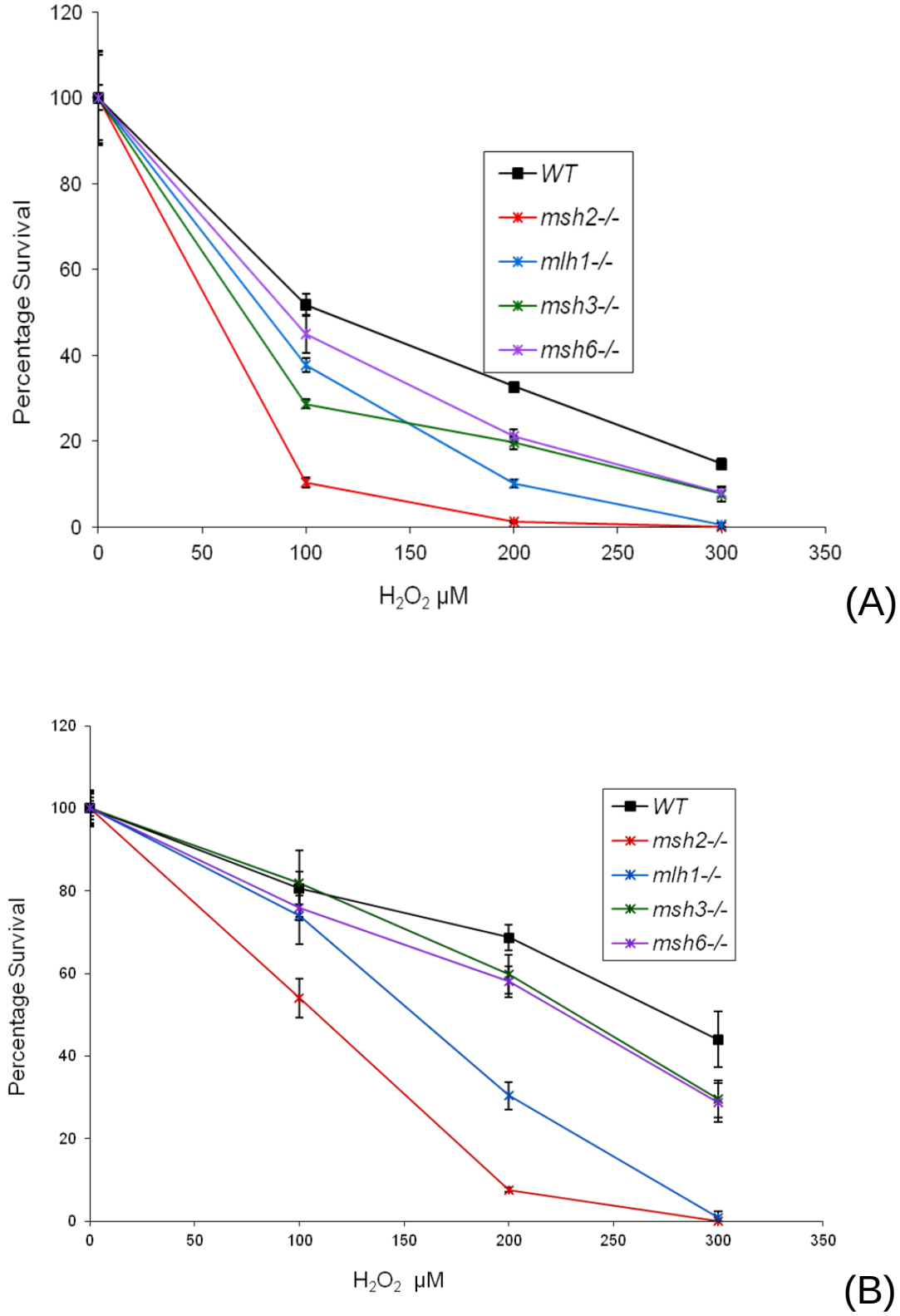


**Figure 5-9 Percentage survival of *T. brucei* BSF wild type and MMR mutants at various concentration of $H_2O_2$.**

Wild type, *msh2-/-* , *msh3-/-, mlh1-/-* and *msh6-/- T. brucei* BSF cells were diluted to $1x10^5$ cells.$ml^{-1}$ in HMI-9 culture media containing 0, 100, 200 or 300 µM $H_2O_2$. A control with no $H_2O_2$ was also set up in parallel. Wild type and mutants were counted at (A) 48 hours and (B) 72 hours. Percentage survival was counted accounting the cells grown in the absence of damage as 100%. Each value is the mean of two experiments, and vertical bars depict standard deviation. $H_2O_2$ concentrations in µM were plotted on x-axis and percentage survival was plotted on y-axis.

When comparing BSF form MMR homozygous mutants amongst each other, and with wild type, we can very clearly see the increased sensitivity of *msh2*-/- to $H_2O_2$ relative to wild type and to all other mutants (Figure 5-9). This experiment shows again that *mlh1-/-* mutants display a slightly different phenotype to what has been reported before (Machado-Silva 2008), when it was suggested that *MLH1* mutants do show a phenotype in response towards oxidative stress. However, in these previous studies the sensitivity of *mlh1*-/- mutants were only tested at concentrations of $H_2O_2$ up to 100 µM; Figure 5-9 suggests that increased sensitivity is observed in these null mutants relative to wild type cells when concentrations of more than 100 µM are used, and in particular when survival is measured at 72 hrs. This is a repeat of the experiment described in section 3.2.6 (Figure 3-25) and confirms that loss of *MLH1* causes some sensitivity towards oxidative stress, though still a less severe phenotype that in *msh2*-/- mutants. The data in Figure 5-9 confirms that *msh3-/-* and *msh6*-/- mutants do not increased sensitivity to $H_2O_2$ to the levels seen for *msh2*-/-, or indeed *mlh1*-/-, cells. Here, *msh3*-/- mutants may have shown slightly increased sensitivity to $H_2O_2$ relative to wild type at 48hrs (Figure 5-9 B), but this was less obvious at 72 hrs (Figure 5-9 B). The same trend was seen for *msh6-/-* mutants, though this is, is at best, a minor effect.

## 5.3 Discussion

In this chapter we have attempted to elaborate on the MMR machinery in *T. brucei* by testing for possible roles for MSH3 and MSH6 in genome maintenance, which has not so far been examined in any kinetoplastid. MSH2 and MLH1 functions have already been characterized in BSF and PCF cells, but here we have studied MSH3 and MSH6 only in the former. We show that it is possible to generate null mutants of both *MSH3* and *MSH6* and, in order to compare the phenotypes of these mutants with *MSH2* and *MLH1* mutants, assays were conducted as far as possible in the same way as done previously (Bell et al. 2004). Doubling time calculations suggest that the mutants grow at the same rate as wild type, suggesting that loss of no single MMR gene causes changes in fitness, at least *in vitro*. From the phenotypic analysis, the *msh6-/-* null mutants showed resistance towards methylation damage, whereas there was no evidence of this for *msh3*-/- mutants. The extent of the increased tolerance of the *msh6*-/- mutants relative to wild type cells (~5 fold)

was broadly comparable with *msh2*-/- and *mlh1*-/- mutants (~8-10 fold; see Figure 3-8, Chapter 3). These data appear consistent with the important role MSH6 has been proposed to play in repair of G-T mutations in other eukaryotes (Christmann & Kaina 2000; Fordham 2010). MNNG is a mutagen that modifies guanine (G) to $O^6$methyl guanine, which can cause GC-TA transition (Zhang 2000), and MSH6 mutants have been reported in human cells to be tolerant to alkylation damage (Fordham 2010). Indeed, in mammals MSH6 contains the nuclear localization signal that gets activated in the presence of alkylating agents and results in the increased translocation of the MutSα complex from the cytoplasm into the nucleus and thus can access the sites of damage (Christmann & Kaina 2000). MSH3 has never been reported to be involved in repair against methylation damage, and given the different mismatch spectrums of MutSα and MutSβ in other eukaryotes (Fordham 2010), it might be expected that in *T. brucei* that the single base mutations caused by MNNG are exclusively recognised by MutSα. In fact, *MSH3* mutants have not been reported to show effects against most mutagens, though they do shows a strong phenotype against 6-thioguanine (6gt) in mammalian cells (Hinz 1999). As we have been unable to confirm phenotypically that the *T. brucei msh3*-/- cells are mutant, it may be worth considering this agent for further analysis.

To analyze microsatellite instability (MSI) in the *MSH3* and *MSH6* mutants, the JS2 locus was examined. JS2 is a GT-dinucleotide repeat and, in contrast with *msh2*-/- and *mlh1*-/- mutants (Bell 2004), see section 3.2.2.3, Figure 3-10, we did not observe MSI in any clone of either of the *msh3*-/- or *msh6*-/- null mutants. Although *msh6*-/- cells might have been expected to show MSI, as MSH6 is involved in correcting mismatches of up to 3 nucleotides in other eukaryotes (Genschel 1998;Hinz 1999;Ma 2000), the protein is considered to be more active on mismatches or IDLs of 1 nucleotide (Genschel 1998). It may then be valuable to test for MSI in *T. brucei msh6*-/- mutants using loci with long runs of a single base-pair, if these could be identified. However, very little phenotype consequence is seen in the absence of either MSH3 or MSH6 alone in other eukaryotes, as it is generally considered that these two proteins can function in place of each other when one is absent (Hinz 1999). For instance, a missense mutation in *MSH6* has shown to cause MSI in *S. cerevisiae*, whereas deletion of the gene has no effect (Yang 2004). Double knockouts of these genes in human cells show a much stronger MSI phenotype, more comparable with *msh2*-/- mutants (Dowen 2010;Edelmann 2000). Given this, several attempts were made to make double knockout mutants of *MSH3* and *MSH6* in BSF *T. brucei*, after generating *MSH6* KO constructs carrying resistance markers for phleomycin and neomycin, but without success. Since the single null mutants were found to be sick

even in the presence of lowered antibiotic dilutions relative to what are used routinely in the lab, and to make double knockout mutants growth in the presence of yet further drugs was needed, the transformants did not survive the process of selection (despite using different strategies were used, including increasing the starting density of the cells and adding two antibiotics at a time) and no clones were recovered.

When the *T. brucei MSH3* and *MSH6* mutants were grown in the presence of increasing concentrations of $H_2O_2$, they did not show an altered survival phenotype compared with wild type cells, and did not show the pronounced increased sensitivity seen in BSF *msh2*-/- cells (Bell 2004) and the more limited increased sensitivity of *mlh1*-/- cells (this work, Figure 3-25 C, D). No supporting data is available regarding the sensitivity or resistance of *MSH3* and *MSH6* towards oxidative stress in other eukaryotes, so there are no precedents to aid our understanding of these findings in *T. brucei*. However, 8oxoG is a marker of oxidative stress damage to DNA and causes GC-TA transversion, which represents a single base mismatch and might then be expected to be target of MSH6. Indeed, studies in yeast have shown that MSH2-MSH6 can act to process adenine that has been misincorporated against 8oxoG (Ni 1999), though the significance of MMR in this repair has been questioned by other work (Larson 2003). MSH2-MSH6 has also been implicated in 8oxoG removal in mammalian cells, acting with the BER machinery (Colussi et al. 2002). Moreover, a recent study in mammalian cells has described an indirect role of MutSα in response to oxidative damage, where it was observed that in the presence of oxidative stress both MSH2 and MSH6 are responsible for the monoubiquitination of PCNA (mUb-PCNA), which induces translesion DNA synthesis (Zlatanou 2011). Absence of either of these two proteins effected the induction of DNA damage tolerance. Taken together, if these activities were conserved in *T. brucei*, these studies would suggest that MSH6, like MSH2, would have an important role in the response to oxidative damage, and the *msh6*-/- mutants might have been expected to show increased sensitivity. Why then they do not is unclear, though it is possible that MSH6 and MSH3 display redundancy in this role, or MSH2 plays a pronounced role that does require MSH6 in response to such damage.

For a better comparison of the role of the MMR proteins in the *T. brucei* oxidative damage response, all available MMR null mutants were analysed in a single set of experiments (Figure 5-9). The null mutants had been analysed previously, but in different experimental settings (Figure 3-25, and Figure 5-8) (Machado-Silva 2008). However, we frequently observed that, although the relative survival phenotypes of the mutants remain the same with respect to wild type, the absolute values of survival tend to vary in different repeats of

$H_2O_2$ exposure, making comparisons difficult. This is almost certainly because $H_2O_2$ is an unstable compound; for instance, since BSF cells are grown in culture dishes that allow air circulation, needed for their growth, the extent of conversion of $H_2O_2$ to $H_2O$ and $O_2$ will vary. In doing this, we observed that *msh2* null mutants are the most sensitive MMR mutants, but also that *mlh1* null mutants display sensitivity to $H_2O_2$ at high concentrations. What this means is unclear without further experiments. Loss of MSH2 has been inferred to primarily results in effects on the kDNA, as seen by increased accumulation of 8oxoG in this genome relative to the nucleus and elevated levels of *msh2*-/- cells lacking kDNA (Campos. 2011). However, it is very likely that $H_2O_2$ also causes damage to the nucleus, and these data may suggest that MMR in total, rather than MSH2 without MLH1, acts in this role and this activity is seen at higher concentrations of damage. This could be examined by localising 8oxoG in these conditions, as well as looking at DNA content by DAPI or FACS.

# 6 What other factors can be regulated in response to oxidative stress in the absence of MMR?

## 6.1 Introduction

In the previous chapters we have tried to dissect MMR in *T. brucei* and, in particular, have studied the importance of this DNA repair pathway towards the protection against oxidative DNA damage in two life cycle forms of the parasite. We provided evidence that following the mutation of *MSH2* in PCF *T. brucei* there was adaptation to this loss, rendering the cells more capable of survival in the presence of the oxidative damage agent hydrogen peroxide, which suggests the presence of a 'backup' or alternate system present in PCF *T. brucei* that can tackle oxidative damage or can reduce the cell's exposure to the damage. However, nothing could be said conclusively about what mechanism or process might account for this adaptation. In this chapter we have tried to take a targeted approach to study some systems, which are not a part of MMR, but might play a role in protection against oxidative DNA damage and could underlie the adaptation. The systems that are studied are not related to each other and are explained in turn, below.

## 6.2 Do *T. brucei* MSH4 and MSH5 co-localise with MSH2 and MLH1?

The MutS family of proteins, besides encoding for MSH2, MSH3 and MSH6 in *T. brucei* and other eukaryotes (related to MutS I in prokaryotes), which have a pronounced role in MMR (see section 1.4.6.3.1.1 and 1.4.6.3.2), also contains two further widely conserved proteins: Msh4 and Msh5 (MutS II in prokaryotes). Sequence alignments of these two proteins with rest of the MutS family members show that the proteins are conserved in the middle domain and C-terminal HTH motif. However, they do not encode for the N-terminal domain (Culligan & Hays 2000; Obmolova 2000), which is responsible for MMR activity (see Section 1.4.6.3.1.1). Absence of the N-terminal domain suggests that Msh4 and Msh5 are unlikely to be part of the MMR system (Snowden 2004) and, indeed, there is no evidence that organisms lacking either Msh4 or Msh5 show any defect in MMR. In contrast, each has been shown to play a pronounced role during meiotic recombination. It has been observed that *Msh4 or Msh5* mutant mice are infertile (de Vries 1999;Kneitz 2000), while in *S. cerevisiae* Msh4 and Msh5 are only expressed in meiotic cells (Rossmacdonald 1994). Mammalian Msh4 was initially thought to be specifically localized to reproductive tissues (PaquisFlucklinger 1997). However, recent studies have showed that both Msh4 and Msh5, though abundantly expressed in meiotic cells, are also expressed at low levels in non-reproductive tissues, including the lymph node, thymus, liver and placenta (Her 2003;Her 2007;Winand 1998). It has also been reported that in human non-

meiotic cells expression levels of Msh4 are significantly lower than Msh5 (Santucci-Darmanin 2000;Wu 2011).

Like other MutS proteins, Msh4 and Msh5 work in the form of dimers. They are thought only to be capable of forming a heterodimer with each other, since no evidence of either of them forming a homodimer or being paired with other MutS proteins has been reported so far (Bocher 1999;Pochart 1997;Winand 1998). However, a recent study in the bacterium *Thermus thermophilus* showed that MutS II (complementary to eukaryotic MSH4-MSH5) interacts with MutS I (complementary to eukaryotic MutSα and MutSβ) (Fukui 2011) *in vivo*, since when protein lysates were immunoprecipitated with antisera against either MutS I or MutL MutS II was also detected in the eluates. Although a role of MutS II in MMR was not demonstrated, mutation of *mutSI*, *mut*L or *mutSII* resulted in increased oxidative stress-induced mutagenesis and up-regulation of vitamin B1 biosynthesis genes, encoding a pathway that can scavenge ROS species. Indeed, MutS II has also been shown to repair oxidative DNA damage in *Helicobacter pylori*, in addition to the more commonly accepted role for this factor in suppressing recombination (Wang 2005). Such roles for MSH4 and MSH5 have not been detailed in eukaryotes, but these prokaryotic findings might suggest our knowledge of MutS II/MSH4-MSH5 function is limited, and that a potential for the putative eukaryotic meiotic MutS II-like factors to interact with the MMR machinery is worth considering.

MSH4 and MSH5 were identified in *T. brucei* during Blast searches for core meiotic machinery components (Berriman 2005; El Sayed 2000) and have been have been studied by a previous student in Glasgow (Barnes 2006). R. Barnes has demonstrated that both *MSH4* and *MSH5* mRNA is expressed in both BSF and PCF life forms of *T. brucei*, as confirmed by RT-PCR. *MSH5*, but not *MSH4*, mRNA was also detected by northern blot analysis, which might indicate that the decreased expression of Msh4 compared with Msh5 observed in human tissues is conserved in *T. brucei*. Several unsuccessful attempts were made to generate knockout mutants of both genes in BSF *T. brucei*, but not even heterozygous mutants could be recovered. Because of this, attempts were made to examine the putative functions of the factors by ectopic expression from the tubulin locus; though integrations of both genes were confirmed, increased mRNA levels was only observed for *MSH5*. This approach did not reveal evidence of a role for either of these proteins in MMR, as illustrated by unchanged IC50 values measured by the alamar blue assay in the presence of increasing concentrations of MNNG.

## 6.2.1 Generation of *T. brucei* cells expressing MSH4 and MSH5 C-terminal 6-HA tagged variants

### 6.2.1.1 Strategy for generation of tagged cell lines

Based on the study in *T. thermophilus*, which demonstrated that MutS II interacts with MMR proteins, we attempted to ask if MSH4 and MSH5 adopt such a role in *T. brucei*. To do this, constructs were made to allow MSH4 and MSH5 to be expressed C-terminally tagged with 6-HA epitopes. If successful, this would allow the proteins to be expressed in the 12 Myc-tagged MSH2 and MLH1 heterozygous cell lines generated in Section 4.2.1, and therefore allow interaction to be tested by immunoprecipitation with either anti-Myc or anti-HA antiserum.

The strategy used for C-terminal tagging MSH4 and MSH5 is essentially as described in Section 4.2.1.1. However, a construct was used in which coding sequence for 6-HA epitopes, rather than 12myc, was fused to a portion of the C-terminus of the genes' ORFs, and phleomycin was used as the drug resistance marker for selection of cells that had integrated the DNA after transformation. To do this, PCR was performed with primers designed to specifically recognise a short stretch of the C-terminal region of the ORF of each gene, flanking a unique restriction site, and cloned after digested with *Hin*dIII and *Xba*I into the HA tagging vector TbMCM-HA, gifted by C. Tiengwe (Tiengwe 2012).

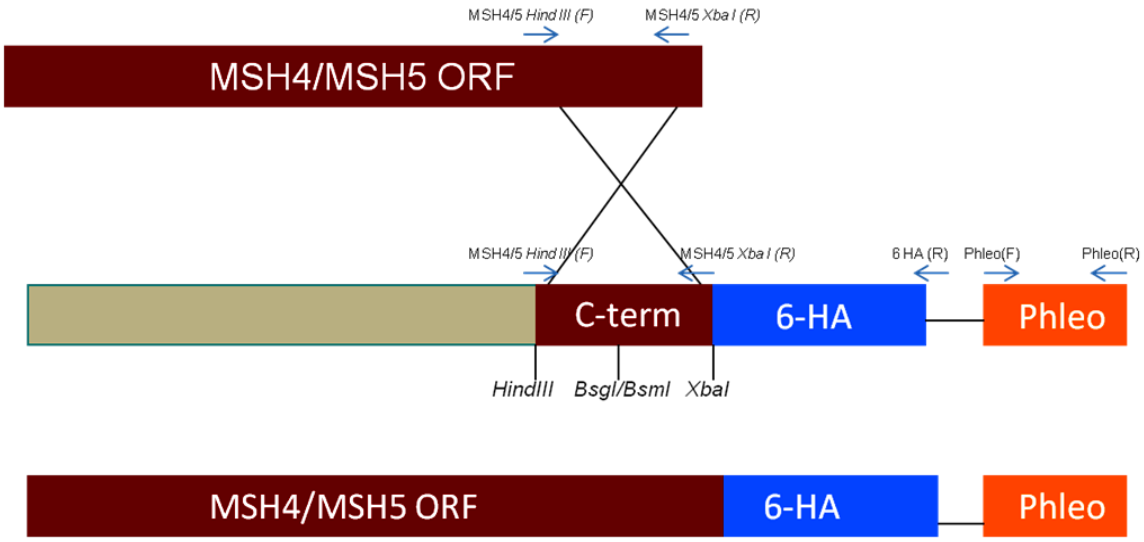


**Figure 6-1 Strategy for generation of 6-HA tagged *MSH4* and *MSH5.***

A 579 bp region of *MSH4* or an 877 bp region of *MSH5* was PCR-amplified from the C-terminus of the ORF of the respective genes, excluding the stop codon. Regions of the ORFs used for generation of plasmids are indicated by a cross and restriction sites used for cloning are labelled (*Hin*dIII and *Xba*I). The *MSH4* construct was linearized by *BsgI* I and *MSH5* was linearized by *Bsm*I prior to transformation. Upon successful integrations, the ORF of *MSH4* or *MLH5* will be C-terminally tagged in frame with a 6-HA epitope, and such transformants are selected using

phleomycin (Phleo) as a drug resistance gene. Primers used for generation of the constructs and checking the antibiotic resistant transformants are indicated.

#### 6.2.1.2 Transformation of BSF and PCF 12 myc tagged MSH2 and MLH1 heterozygous tagged lines with MSH4 and MSH5 6-HA tagging constructs.

Both PCF and BSF MSH2-12myc and MLH1-12myc tagged heterozygous cells (*MSH2+/- 12 myc*; *MLH1+/- 12 myc*) were grown to log phase in their respective media in the presence of 1 $\mu g.ml^{-1}$ puromycin and 10 $\mu g.ml^{-1}$ blasticidin. $3x10^7$ cells were used for transformation with *MSH4-6HA* or *MSH5-6HA* tagging constructs, previously linearized using *Bsg*I or *BsmI*, respectively. 5-10 μg of linearized DNA was used per transformation. Four independent transformations were performed in each BSF and PCF cell line, as described in Section 2.1.4.1 and 2.1.4.2, and transformants were selected on 2.5 $\mu g.ml^{-1}$ phleomycin , in order to generate the following double-tagged cell lines: *MSH4-HA: MSH2-12myc, MSH4-HA: MLH1-12myc, MSH5-HA: MSH2-12myc* and *MSH5-HA: MLH1-12myc*. Three antibiotic resistant clones were selected from each of the eight transformations and grown in the presence of 1 $\mu g.ml^{-1}$ puromycin, 10 $\mu g.ml^{-1}$ blasticidin and 2.5 $\mu g.ml^{-1}$ phleomycin for at least three days. DNA was then extracted and the clones were tested by PCR amplification of the *BLE* drug resistance gene using primers Phleo (A) and Phleo (B) (data not shown), showing that the gene was present in all. One out of the three clones was next selected from each cell line and tested for expression of epitope tagged proteins by western blotting as described in Section 2.3.1. Samples were independently probed with mouse anti-myc antiserum (1:7000) (Figure 6-2 A) and mouse anti-HA anti serum (1:10000) (Figure 6-2 B) for the presence of proteins linked to either tag. The only cells in which HA-tagged protein could be detected were the *MSH5-HA: MSH2-12myc* and *MSH5-HA: MLH1-12myc* cells in the PCF, and *MSH5-HA: MSH2-12myc* in the BSF. The size of the HA protein was consistent with the predicted size of HA-tagged MSH5 (93 kDa) in each case, and this band was not seen in the parental cells. In addition, bands consistent with 127 kDa MLH1-12myc and 116 kDa MSH2-12myc were seen with the anti-myc antiserum in both HA tagged and non-tagged 12 myc tagged lines (Figure 6-2 A), where no such band was observed in heterozygous cell that had not been tagged at all. Re-analysis of all transformants showed that none of the BSF *MSH5-HA:MLH1-12myc* clones collected were positive for HA-tagged protein by western analysis, and HA-tagged MSH4 could not be detected in any clone, either PCF or BSF.

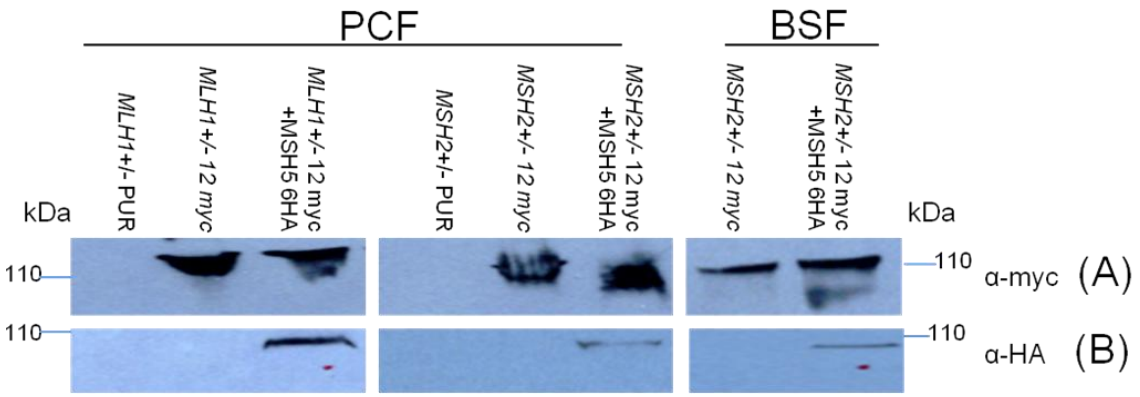


**Figure 6-2 Confirmation of MSH5-6HA tagged clones by western blotting**

Western analysis was performed to check for the expression of 6HA-tagged MSH5 (MSH5-6HA) in PCF and BSF clones that also express 12Myc tagged MSH2 or MLH1 (in each case, the tagging is in a heterozygous mutant background: *MLH1*-/- 12Myc, and *MSH2*+/- 12myc). For comparison, the double tagged clones are compared with untagged *MLH1*+/- and *MSH2*+/- cells (PCF clones only), or with the parental 12myc tagged cells (BSF and PCF). Whole cell extracts from ~ $2x10^7$ cells were loaded per well, the proteins were separated by SDS-PAGE and, after western blotting, the membrane was probed with mouse anti-myc (myc) antiserum diluted as 1:7000 (A) and mouse anti-HA (he) antiserum diluted as 1:10000; HRP-conjugated anti-mouse, used in 1:5000 dilutions, was used as secondary antibody for detection.

The above data confirm that MSH5 has been successfully HA-tagged in most MMR myc tagged cells, so why it was not successful in the putative *MSH5-HA: MLH1-12myc* BSF cells is unclear. Whether the clones selected had incorrectly inserted the tagging construct, or whether MSH5 expression was too low to be detected specifically in these cells is unclear. For MSH4, no HA-tagged protein was seen, and the same arguments apply. However, as all the transformant clones collected had been growing on phleomycin and the presence of the resistance gene was confirmed by PCR-amplification, the uniform lack of MSH4 detection may suggest that MSH4 is expressed at too low a level to be detected in these conditions. Indeed, this may be consistent with the previously detected lower levels of *MSH4* mRNA relative to *MSH5* (Barnes 2006).

### 6.2.1.3 Testing for co-immunoprecipitation (Co-IP) of MSH5 with MSH2 and/or MLH1

To test for the potential interaction of MSH5 with MSH2 or MLH1, the cells described above were grown in the presence of their respective drugs for at least 1 week and immunoprecipitation (IP) performed as described in section 2.3.3. Briefly, $1x10^9$ cells were used per cell line analysed. Cell pellets were resuspended in whole cell extract buffer (WCE) to lyse the cells and then incubated with pre myc/HA coated magnetic beads. A small aliquot was kept back and used as input sample (I). After incubation for two hours on ice, magnetic beads were collected using a magnetic rack and proteins that were not

associated with the mouse anti myc/HA antiserum collected from the supernatant, and referred to as flow through (F). The beads were washed using wash buffer (WB) to remove weakly associated protein and then antibodies and antibody-bound protein was eluted (E) from the beads using elution buffer. Two independent experiments were performed. In one, the IP was performed using anti-myc antiserum (CoIP α-myc) and in the other the IP was performed with anti-HA antiserum (CoIP α-HA); in all cases the I, F and E fractions were probed with anti-myc and anti-HA antiserum to check for the expected recovery by IP and for CoIP between MSH5 and MSH2 or MLH1. Western blotting of the samples was performed as described in Section 2.3.1 and results are shown in Figure 6-3.

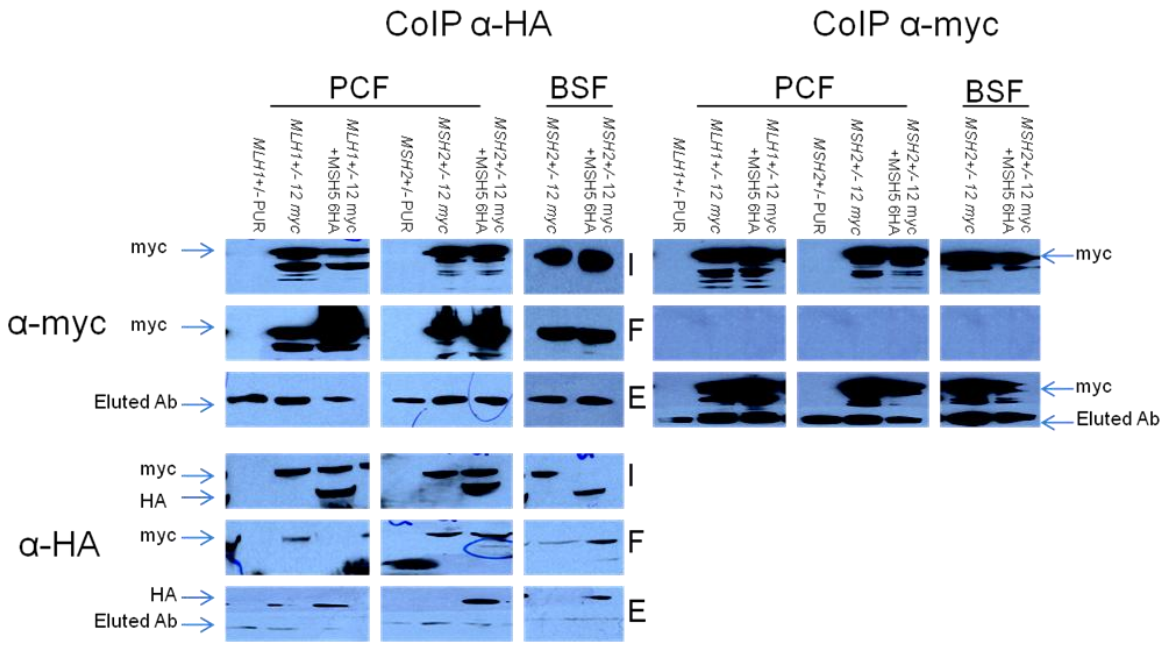


**Figure 6-3 Testing for interaction between MSH5-HA and MSH2-12myc or MLH1-12myc in *T. brucei.***

The experiment shows western blot analysis of immunoprecipitation (IP) from *T. brucei* cells. PCF cells analysed in the study were *MSH2+/-, MSH2+/- 12myc, MSH2+/-12myc-MSH5-6HA, MLH1+/-, MLH1+/-12myc, MLH1+/-12myc-MSH5-6HA.* BSF cells analysed were *MSH2+/- 12myc, MSH2+/- 12myc-MSH5-6HA.*Two independent experiments were setup for each cell; in the first experiment IP was performed anti-HA antiserum (CoIP α-HA) and fractions were probed with anti-myc (α-myc) and anti- HA (α-HA) antiserum; in the second experiment IP was performed with anti-myc antiserum (CoIP α-myc) and samples probed with anti-myc antiserum and anti-HA (not shown). In all cases (I) refers to input, which represents proteins present in whole cell extracts, (F) is flow-through collected from the magnetic beads, and represents non-IP proteins, and (E) refers to the eluted fraction, which represents proteins that were recovered by the IP. Bands corresponding to epitope tagged proteins have been labelled, as have eluted antibody (Ab).

In the first IP performed, anti-HA antiserum (CoIP α-HA) was used to IP HA-tagged proteins from the samples and the western was first probed with anti-myc antiserum (1:7000). Myc-specific bands of sizes consistent with MLH1-12myc (127 kDa) and MSH2-12myc (116 kDa) were seen in all Myc-tagged cells, including those co-tagged with

6HA, but not in the control, untagged cells in the I (input/whole cell lysate) and F (flow through/unbound) fractions. However, in the E (eluted/bound) fractions only a band corresponding with the released antibody was seen, and no bands of the size expected for the Myc-tagged MSH2 or MLH1. To confirm the presence of HA-tagged protein in the same samples, and to determine whether these proteins had been eluted from the beads, the anti-myc probed membranes were stripped (Thermo Scientific western blot stripping buffer, Catalogue number 21059) and the membrane was then re-blocked with 5% block and immunoblotted with anti-HA antiserum (1:10000). This showed that relatively weak HA-specific bands of a size consistent with MSH5-6HA (93 kDa) were seen in MSH5-HA clones in I and E fractions, suggesting that the IP had worked. Note that Myc-specific bands of sizes expected for MSH2-12myc and MLH1-12myc, which appear to be abundant (as suggested by the intensities of the Myc bands in the first blot) were also still seen in the I and F fractions, which is most likely because the blot was not completely stripped. These data indicate that while MSH5-6HA can be recovered by IP with anti-HA antiserum, it does not result in CoIP of MSH2-12Myc or MLH1-12Myc. To ask if this same result would be seen if IP was performed to recover the Myc tagged proteins, the experiment was next performed by IP with anti-myc antiserum (CoIP α-myc). Westerns of the samples probed with anti-myc antiserum clearly showed myc-specific bands in I and E fractions in all the Myc-tagged cells, but not in the controls, indicating that MSH2-12Myc and MLH1-12Myc were recovered. However, when the membrane was stripped and reprobed with anti-HA antiserum, no bands were seen (and hence the blots are not shown). Since this was also true of the input (I) samples, it is not clear if this experiment worked or MSH5-6HA were expressed too low to be detected by western blot , but time did not allow it to be repeated.

## 6.3 Role of Trypanosome Alternate Oxidase (TAO) in protection against oxidative stress

Uncoupling proteins (UCP) are a set of proteins that are present in the mitochondrial matrix of eukaryotes, including mammals, plants and protozoa. They play a key role in maintaining a proton influx into the mitochondrial matrix and also to serve as a protection against oxidative stress (Colasante 2009). Besides UCP, certain eukaryotes, such as plants, fungi and some protozoa, further encode alternate oxidase (AOX) and cytochrome *c* oxidase (COX), each of which can act as a terminal oxidase that serves to reduce oxidative stress by transferring the reducing equivalents to oxygen and catalyzing the reduction of molecular oxygen to water (Colasante 2009). *T. brucei* and related kinetoplastids lack UCP

but code for AOX and COX homologues to regulate cellular redox balance. A role of AOX in kinetoplastids have been proposed by Fang *et al* in defence against ROS (Fang & Beattie 2003). AOX in *T. brucei* is termed trypanosome alternative oxidase (TAO; further discussed in Section 1.4.8). TAO in *T. brucei* has been characterized by Chaudhuri *et al* (Chaudhuri, Ajayi, Temple, & Hill 1995;Chaudhuri et al. 2002;Chaudhuri et al. 2006), who showed that in BSF cells, where mitochondrial activity is reduced, TAO serves as a sole terminal oxidase that is expressed. In contrast, mitochondrially active PCF *T. brucei* express both TAO and COX. BSF *T. brucei* appear unique in limiting terminal oxidase expression to TAO, and it has been suggested that the absence of AOX in mammals makes TAO a potential drug target. TOA is a single di-iron polypeptide and has been identified as a 33 kDa mitochondrial protein with its expression level being 100-fold higher in BSF cells than PCF. It was observed that inhibition of TAO by SHAM (salicylhydroxamic acid) results in increased production of ROS followed by increased production of Fe-SOD, an iron dependent superoxide dismutase which plays an important role in protection against oxidative damage (see Section 1.4.8). Furthermore, it was observed that when parasites are grown in the presence of $H_2O_2$ increased production of TAO is also seen (Fang & Beattie 2003). Taken together, these findings suggested a potential role of TAO in defence against oxidative damage by preventing ROS production, and that the expression of the protein can be modulated. Given this, we considered it possible that changes in TAO expression might underlie the proposed adaptation to oxidative damage we observed after MMR mutation in PCF *T. brucei*. To test this, we attempted to measure the expression levels of TAO in wild type (WT) and MMR mutants in both PCF and BSF *T. brucei.*

## 6.3.1 Expression of TAO in BSF and PCF

Expression of TAO was initially monitored to check for the presence of detectable protein, and to monitor those levels. To do this, wild type (WT), *MSH2::BSD* (*MSH2+/-)*, *MSH2::BSD::PUR ( msh2-/-), MLH1::BSD* (*MLH1+/-)* and *MLH1::BSD::PUR* (*mlh1-/-)* cells, both PCF and BSF, were grown to their log phase and subjected to western blotting as described in Section 2.3.1. Several attempts were made at this experiment as the protein was not identifiable initially unless cell extracts were freshly prepared and at least $5x10^7$ PCF cells and $2 \times 10^7$ BSF cells were used per lane. Also, it was important that a fresh dilution of the anti-TAO antiserum was used at 1:100 dilution (mouse anti-TAO antiserum was generously gifted by Minu Chaudhuri) (Chaudhuri 1995). The results of the most successful western blots are shown in Figure 6-4.

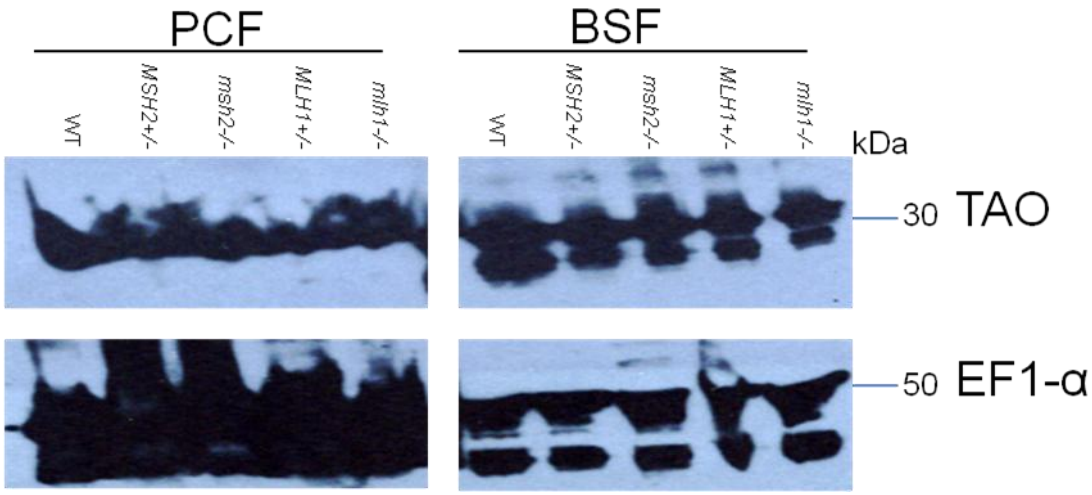


**Figure 6-4 Expression of TAO in wildtype and MMR mutants in *T. brucei***

Bloodstream form (BSF) and procyclic form (PCF) *T. brucei* wildtype(WT), *MSH2+/-*, *msh2-/-*, *MLH1+/-* and *mlh1-/-* cells were used for western analysis after whole cell extracts from 2 and 5 x$10^7$ cells, respectively, per lane were separated by SDS PAGE and probed with mouse anti-TAO antiserum (1:100). Mouse anti-EF1α antiserum (1:10000) was used as loading control. HRP-conjugated goat anti-mouse was used at a 1:5000 dilution for detection.

This western analysis confirmed that 33 kDa TAO is expressed in both PCF and BSF *T. brucei* wild type and MMR mutants (Figure 6-4), and the relatively greater amount of TAO in the latter life cycle stage could be seen relative to the EF1α (47.5 kDa) loading control. Figure 6-4 further suggests that the levels of TAO are not altered in any of the MMR mutants when compared with wild type, suggesting that mutation has not resulted in detectable changes in TAO expression.

## 6.3.2 Expression levels of TAO in the presence of $H_2O_2$

Since we could see no detectable change in expression levels of TAO in wild type *T. brucei* cells relative to the MMR knockout mutants, we next attempted to ask if any change in expression of TAO was seen when the cells are subjected to oxidative stress. To do this, PCF and BSF wild type cells and *msh2*-/- and *mlh1*-/- null mutants were grown to log phase. BSF wild type and mutant cells were then diluted to 1 x $10^5$cells.ml$^{-1}$ and further grown in the absence or presence of 50 μM $H_2O_2$ for 48 hours (see Section 4.2.4). Cultures grown in the absence of damage were grown in a 100 ml volume, and the cultures grown in $H_2O_2$ were in 500 ml in order to allow for sufficient numbers of cells to be recovered for western blotting. PCF wild type cells and MMR null mutants were diluted to 5 x $10^5$cells.ml$^{-1}$ and then grown in the absence or presence of 20 μM $H_2O_2$ for 48 hours. Non-treated cells were grown in 15 ml cultures whereas cells subjected to $H_2O_2$ were cultured in 100 ml (refer to Section 4.2.4). In all cases after 48 hours the cultures were centrifuged at

600 *g* for 20 minutes at 4 $^{0}$C and the cell pellets were resuspended at a concentration of 1x10$^{8}$ cells/50µl in protein loading buffer and the extracts prepared as described in Section 2.3.1.1. Extracts equivalent to 2 x 10$^{7}$ cells were then used per lane and the samples were resolved in 10% SDS-polyacrylamide gels and immune blotted with mouse anti-TAO antiserum (1:100) as described in Section 2.3.1. Sheep anti-OPB antiserum was used as loading control (1:2000 dilution). The western blots are shown in Figure 6-5.

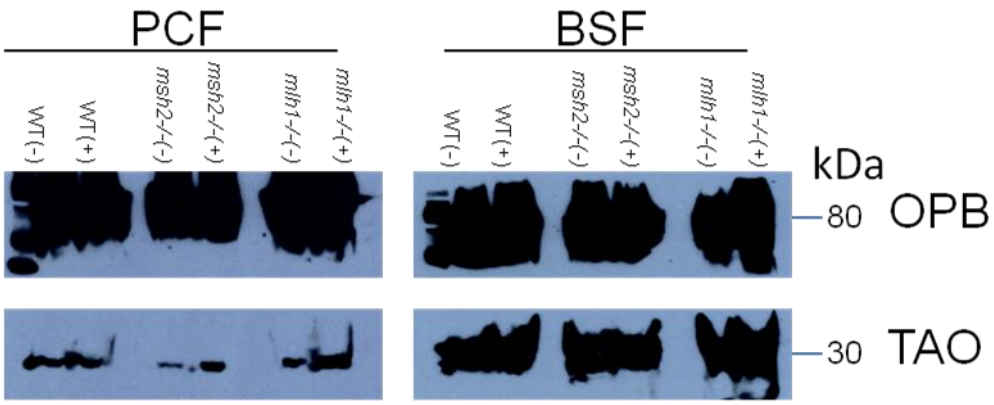


**Figure 6-5 Expression of TAO in the presence of oxidative stress.**

Blood stream form (BSF) and procyclic form (PCF) *T. brucei* wild type (WT), *msh2-/-* and *mlh1-/-* cells were grown in the absence (-) or presence (+) of $H_2O_2$. PCF and BSF cells were subjected to 20 or 50 µM $H_2O_2$, respectively for, 48 hours. Whole cell extracts were then separated by SDS-PAGE, blotted and probed with mouse anti-TAO antiserum (1:100 dilution). Sheep anti-OPB antiserum (1:2000) was used as loading control.

This western analysis again confirmed the decreased expression of TAO in PCF *T. brucei* relative to BSF. In BSF *T. brucei*, induction of oxidative stress by addition of $H_2O_2$ did not appear to result in altered TAO levels in either wild type or mutants. In contrast, when PCF parasites were treated with 20 µM $H_2O_2$, the levels of TAO appeared to be greater than in non-treated cells. The high intensities of the OPB band in treated and non-treated cultures, which was used as a loading control, make evaluation of the relative loadings difficult, but if we assume that these are equal, then the band intensities of TAO appear greater in each MMR mutant in the presence of oxidative stress. This was less clear in the wild type, where previous work has suggested that treatment with 50 µM $H_2O_2$, as used here, causes an ~2-fold increase in PCF TAO levels (Fang & Beattie 2003). These data may hint that the up regulation response of TAO to oxidative damage may be increased when either *MSH2* or *MLH1* is mutated. However, this cannot bet concluded with confidence, as the experiment could not be repeated due to limited amount of TAO antibody.

## 6.4 RNA interference of *MSH2* and *MLH1* in bloodstream form and procyclic form *T. brucei*

From the analysis of MMR mutants in PCF *T. brucei* described in Chapter 3, we have suggested there might have been an adaptation during the course of selection of knock out mutants. Since we only select for clones that survive the process of transformation and antibiotic selection, we cannot say if any such change was pre-existing prior to transformation or is capable of emerging in response to the mutation. Indeed, since we select for mutants that have lost a specific gene, we cannot conclude if the non-essential nature of that gene is only true if further changes are also selected for in the course of making the desired, directed mutation. For instance, it has been reported that RNAi of metacaspases such as MCA4 result in pronounced retardation of growth in BSF *T. brucei*, and yet it is possible to make null mutants in these genes in the same life cycle stage (Proto 2011).

To explore this for the MMR mutants in *T. brucei*, and to ask if loss of the genes can have a more severe phenotype than was revealed by targeted disruption, an RNAi strategy was used. This used an RNAi vector which contains two opposing tetracycline-inducible T7 promoters that drive the expression double-stranded RNA derived from any gene. To use this system, a fragment of the gene to be tested is cloned between the promoters. Upon transformation, the RNAi vector integrates into the ribosomal locus of a strain in which the tetracycline repressor and T7 RNA Polymerase are expressed and, upon addition of tetracycline, repressor blockage of the T7 promoters is lifted and the vector produces dsRNA. This dsRNA is targeted by the RNAi machinery of the parasite and the expression of the targeted gene is reduced (LaCount 2000;Ngo 1998).

### 6.4.1 Generation of *MSH2* and *MLH1* RNAi in BSF and PCF *T. brucei*.

#### 6.4.1.1 Strategy for the generation of *MSH2* and *MLH1* RNAi constructs

To generate RNAi constructs for *MSH2* and *MLH1*, 513 and 887 bp regions, respectively, of the genes were PCR-amplified from wild type Lister 427 genomic DNA using the same primers used for the generation of 12 myc tagging constructs as described in Section 4.2.1.1. The amplified products were digested with *Hin*dIII and *Xba*I and cloned into the vector pZJM, obtained from L.Marcello (WTCMP, University of Glasgow)

#### 6.4.1.2 Transformation of PCF and BSF *T. brucei* with MSH2 and MLH1 RNAi constructs

The *MSH2* and *MLH1* RNAi plasmids were linearized with *Not*I and purified using PCR purification kit (see Section 2.2.3). *T. brucei* Lister 427 29.13 BSF cells and *T. brucei* Lister 427 90.13 PCF cells were transformed as described in Section 2.1.4 with 5 μg of each DNA and clones were selected on 2.5 $\mu g.ml^{-1}$ phleomycin. The PCF parasites were grown on 50 $\mu g.ml^{-1}$ hygromycin and 15 $\mu g.ml^{-1}$ neomycin, whereas the BSF cells were grown on 10 $\mu g.ml^{-1}$ hygromycin and 5 $\mu g.ml^{-1}$ neomycin for at least 1 week prior to transformation. After transformation, two antibiotic resistant clones from each of the four transformations were selected and used for the study. BSF clones were grown on 10 $\mu g.ml^{-1}$ hygromycin, 5 $\mu g.ml^{-1}$ neomycin and 2.5 $\mu g.ml^{-1}$ phleomycin, and PCF clones were grown on 50 $\mu g.ml^{-1}$ hygromycin, 15 $\mu g.ml^{-1}$ neomycin and 2.5 $\mu g.ml^{-1}$phleomycin for 1 week before the effect of *MSH2* or *MLH1* RNAi induction on growth was tested.

### 6.4.2 Effect of RNAi knockdown of *MSH2* and *MLH1* on BSF and PCF *T. brucei*.

#### 6.4.2.1 *In vitro* growth analysis after RNAi

2 clones of each BSF RNAi cell line targeting *MSH2* (MSH2.1, MSH2.2) or *MLH1* (MLH1.1, MLH1.2) were grown to log phase and diluted to a starting density of 1 x $10^5$ $cells.ml^{-1}$ in 20 ml. 2 clones of each PCFF RNAi cell line targeting MSH2 (MSH2.1, MSH2.2) or MLH1 (MLH1.1, MLH1.2) were grown to log phase and diluted to a starting density of 5 x $10^5$ $cells.ml^{-1}$ in 10 ml. Each culture was then split and grown in the absence of tetracycline or after the addition of tetracycline to 2 $\mu g.ml^{-1}$. Cell density was counted every 24 hours up to 72 hours and then the cultures were diluted back to their starting density, tetracycline was again added to the RNAi-induced cells, and the cultures were further counted every 24 hours for a further 72 hrs (144 hours from the start) before being again diluted back to starting densities. The same process was then repeated again and the cultures were counted at 168 hours, 196 hours and 216 hour time points. The experiment was repeated twice for each clone and the average cell densities of the two clones analysed in the two repeats was plotted, as shown in Figure 6-6.

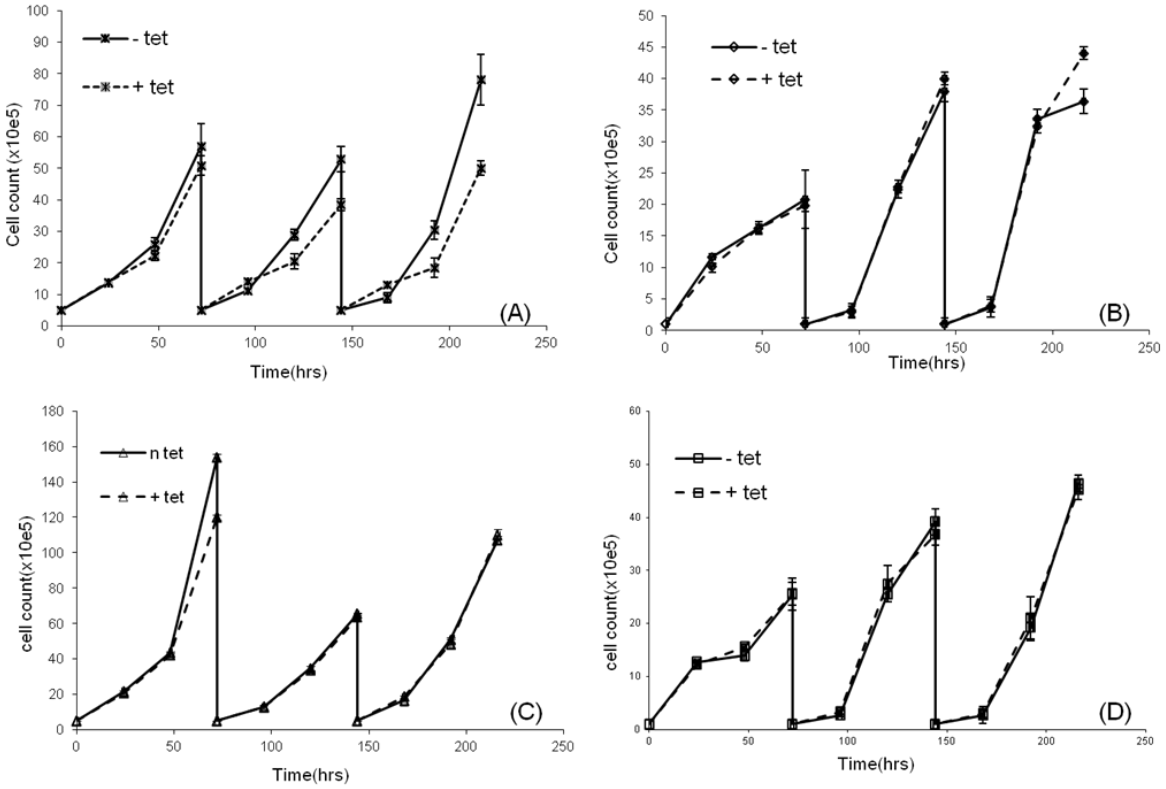


**Figure 6-6 *In vitro* growth analyses of *T. brucei* following RNAi of *MSH2* or *MLH1***

Growth is shown of *T. brucei* cells in which RNAi is induced by the presence (+tet) of 2 μg.ml$^{-1}$ tetracycline relative to uninduced cells grown in the absence (-tet) of tetracycline. **(A)** shows PCF RNAi against MSH2, **(B)** shows BSF MSH2 RNAi, **(C)** shows PCF MLH1 RNAi, and **(D)** shows BSF MLH1 RNAi. In each case cell density is shown every 24 hrs over a period of 216 hours for every 24 hours; the cultures were diluted to their starting density every 72 hours. Each graph shows the average cell density of two independent clones, repeated twice; vertical lines indicate standard deviation.

The results of the cell growth analysis showed no evidence for an alteration in growth rate when *MSH2* or *MLH1* RNAi knockdown was induced in BSF *T. brucei* (Figure 6-6 B and D). This is consistent with the observation that null mutants of either of these genes in this life cycle stage are unaltered in growth relative to wild type (Bell 2004). In PCF *T. brucei*, RNAi knockdown of *MLH1*also had no effect on the growth of the parasite (Figure 6-6 C), again consistent with growth comparisons of PCF *mlh1-/-* mutant and wild type cells (Section 3.2.2.1). In contrast, MSH2 RNAi in PCF *T. brucei* resulted in detectable growth defects that were visible 72 hours after RNAi induction and appeared to increase with time (Figure 6-6 A). This suggests a difference in the putative response to the loss of MSH2 after RNAi and after the generation of null mutants, which grew as wild type (Section 3.2.2.1).

### 6.4.2.2 Expression levels of *MSH2* and *MLH1* after RNAi

We have observed that in none of the RNAi cultures, except that targeting *MSH2* in PCF *T. brucei*, shows growth defect upon tetracycline induction (Figure 6-6 C). To evaluate the effectiveness of the RNAi, we next sought to measure the abundance of *MSH2* and *MLH1* transcripts. To do this, the RNAi cell lines were diluted to the starting density described previously in Section 6.4.2.1 and cultured in the absence or presence of 2 $\mu g.ml^{-1}$ tetracycline for 120 hours, including being diluted back to their starting density at 72 hours. At 120 hours, cell pellets were collected and total RNA was extracted using Qiagen mRNA isolation kit (see Section 2.2.11). RNA was tested for any genomic DNA contamination by PCR-amplifying (using Taq polymerase) *RAD51* as described in Section 3.2.1.2, Figure 3-4; no PCR product was seen for any sample (data not shown). 1 μg of RNA from each sample was then used to make cDNA as described in Section 2.2.11 and to check the quality of cDNA present in each sample by PCR-amplifying a fragment RAD51 gene using primers RAD51 (F) and RAD51 (R) as described in section 3.2.1.2 Figure 3-4 (data not shown).

To quantify mRNA levels in tetracycline-induced and uninduced samples, quantitative real time PCR (QRT-PCR) was used. Primers were designed using Primer Express software (Applied Biosystems) and QRT-PCR was performed using a Prism7500 real time PCR machine (Applied Biosystems). cDNA prepared from 1 μg of all the RNA samples collected 120 hours post RNAi induction and from the control, uninduced cells were amplified as described in Sections 2.2.11 and 2.2.12. *Glycosylphosphotidylinositol-8* (*GPI8*) was used as endogenous control. PCR was performed in quadruplicate and data was analysed using ABS 7500 system software. The levels of *MSH2* and *MLH1* RNA measured in the absence or presence of tetracycline induction of RNAi in BSF and PCF cells, and relative to *GPI8*, are shown in Figure 6-7.

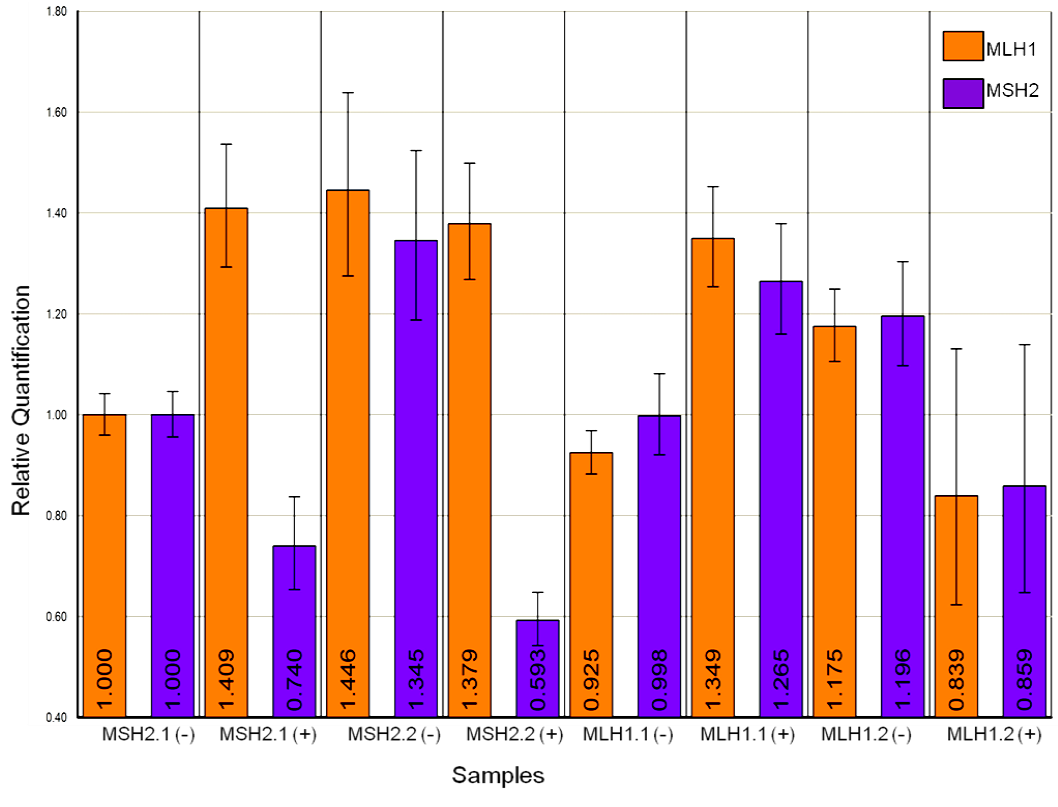


(A)

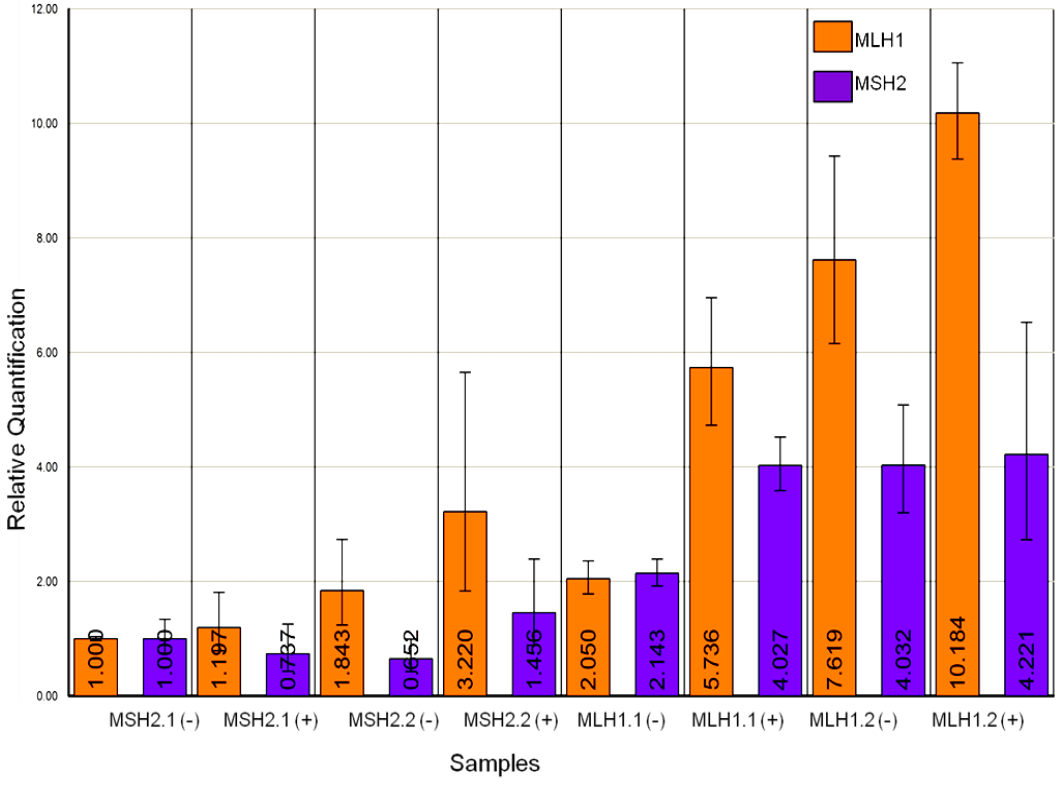


(B)

**Figure 6-7 mRNA levels of *MSH2* and *MLH1* in (A) PCF and (B) BSF *T. brucei* before and after RNAi induction**

QRT-PCR analysis of *MSH2* and *MLH1* RNA abundance is shown in RNAi-induced (+) and non-induced (-) *T. brucei* cells by relative quantification using *GPI8* as an endogenous control Transcript levels for both *MSH2* (purple) and *MLH1* (orange) were analysed in both MSH2 targeting (MSH2.1 and MSH2.2) and MLH1 targeting (MLH1.1 and MLH1.2) RNAi cell lines. Concentrations of PCR product in MSH2.1 RNAi (-) were normalised to 1 and *MSH2* and *MLH1* abundances are then shown relative to that; quantification was performed using ABS7500 prism software. Relative quantities are representatives of 4 repeats, and vertical lines denote standard deviation.

Figure 6-7A shows that in both the PCF MSH2 RNAi clones examined the abundance of *MSH2* transcript decreased after addition of tetracycline. In the same cells, the levels of *MLH1* were not reduced, as expected. In contrast, in the two PCF MLH1 RNAi lines, the levels of neither *MSH2* nor *MLH1* reduced after RNAi induction, suggesting that the RNAi of MLH1 has not occurred. Similarly, for the BSF RNAi lines, Figure 6-7 B, targeting both genes, the levels of *MLH1* or *MSH2* did not decrease upon tetracycline induction. Again, therefore, we cannot conclude that the RNAi has had the expected knockdown. Given these findings, the difference in growth of PCF *T. brucei* after RNAi against *MSH2* appears to be due to loss of that gene function, but the lack of growth changes in the PCF after attempted RNAi of *MLH1* and in the BSF after attempted RNAi of both MMR genes is due to unsuccessful RNAi, for reasons that are unclear.

## 6.5 Tryparedoxin peroxidise

As discussed in Section 1.4.8, trypanosomatids possess certain peroxiredoxins to maintain the redox potential of the parasites. Three peroxiredoxins have been found in *T. brucei*, which are localized in both the cytoplasm and mitochondrion and have a great affinity towards $H_2O_2$, thymine peroxide and lineolic peroxide. Of the peroxiredoxins found in *T. brucei*, cytoplasmic TXNPxs are crucial for cell survival and RNAi against TbCPX results in increased sensitivity to $H_2O_2$. In contrast, mitochondrial TXNPxs (TbMPX) has shown to be non-essential and reduced expression of the protein does not result in $H_2O_2$ sensitivity (Flohe 2004;Schlecker 2005;Tetaud 2001;Wilkinson 2003). However, this phenotype has only been tested in BSF *T. brucei* and the results might represent reduced mitochondrial activity and minimal requirement of the protein.

$H_2O_2$ sensitivity has been tested in MMR mutants in both BSF and PCF *T. brucei* parasites. It is evident from the results that PCF MMR mutants are resistant to oxidative damage (Section 3.2.3), while BSF MMR mutants are sensitive (Section 3.2.6) (Machado-Silva et al. 2008). We therefore attempted to check if there is any difference in the expression of TXNPxs in the two life cycle forms and if their expression level alters in the MMR mutants or in presence of oxidative stress. For this purpose, cultures were grown in the absence or presence of $H_2O_2$ (BSF and PCF cells in of 100 μM or 20 μM, respectively) as described in Section 6.3.2, the cells were collected at 48 hours, total RNA was extracted and cDNA was prepared as explained in Section 2.2.11. Primers were designed against the

ORF of *TbCPX* (Tb09.160.4250) using primer express software and QRT-PCR was performed as described in Section 2.2.12. Primers against *GPI8* were used as endogenous control PCR to normalise any differences in cDNA concentration. Levels of *TbCPX* transcript are shown in Figure 6-8.

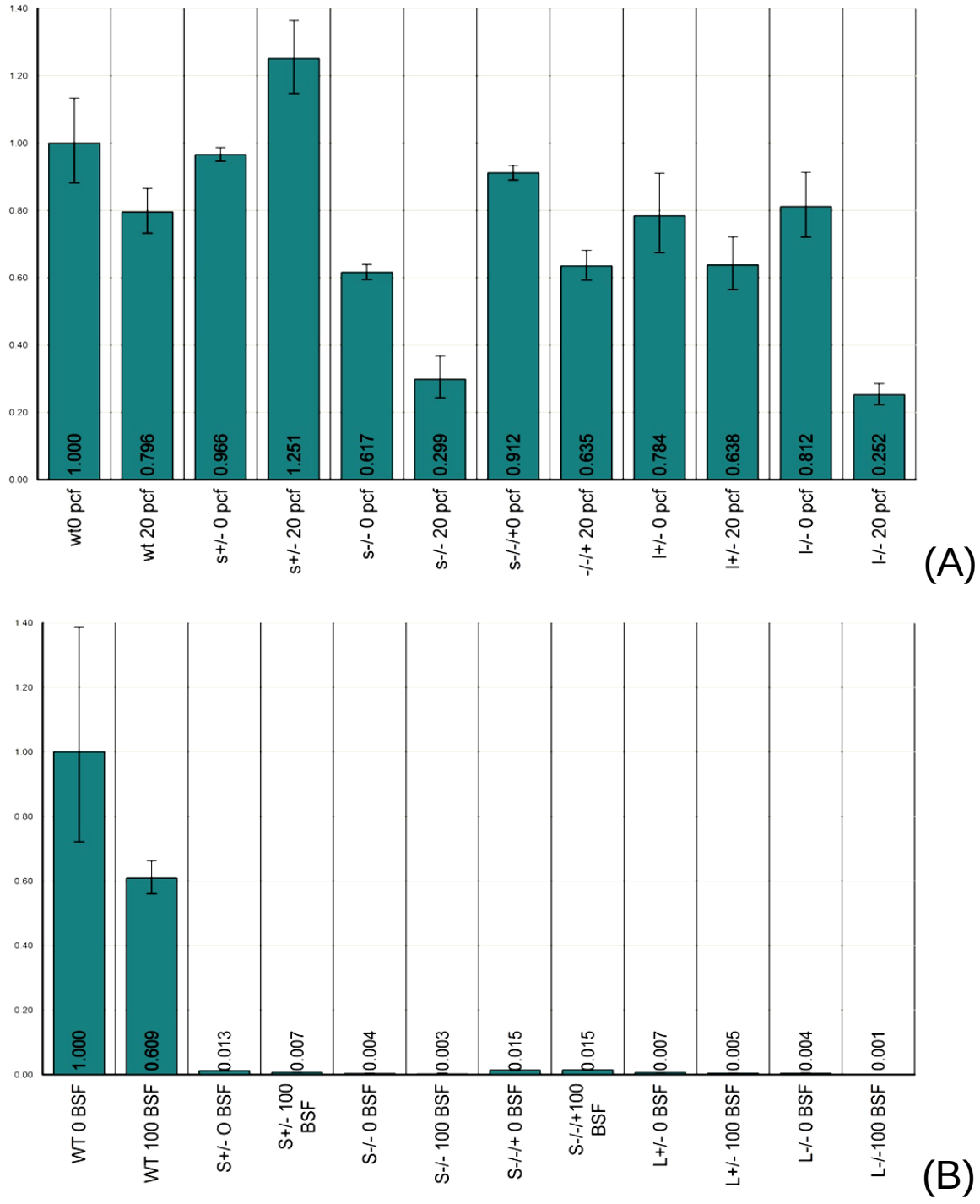


**Figure 6-8 Levels of *TbCPX* transcript in *T. brucei* (A) PCF and (B) BSF wild type cells and MMR mutants.**

QRT-PCR analysis of *TbCPX* transcript abundance is shown wild type (WT), *MSH2+/- (s+/-), msh2-/- (s-/-), MSH2-/-/+ (s-/-/+), MLH1+/- (l+/-), mlh1-/- (l-/-)* cells grown in the absence (0) or presence of $H_2O_2$. PCF cultures were grown on 20μM $H_2O_2$ (20) and BSF cultures were grown on 100 μM $H_2O_2$ (100) for 48 hours before *TbCPX* RNA abundance was analysed using primers TbCPX (F) and TbCPX (R) relative to *GPI8*For each cell line, QRT-PCR was performed in

quadruplicate in two independent experiments; the results are shown as relative abundance of the transcript in each cell relative to GPI8 and relative to non-treated wild type cells, which were normalised to 1; values of the mean of all repeats and vertical lines denote standard deviation.

The first findings suggested by these data is a huge difference in the level of *TbCPX* transcript between in BSF and PCF *T. brucei* MMR mutants, since it appears that former lost expression of the peroxiredoxin gene (Figure 6-8 B). This was not limited to the null mutants, since it was seen also in the +/- cells and in the *MSH2*-/-/+ re-expressers, and this striking loss was common to both MSH2 and MLH1 mutant BSF cells. This was not seen for one other gene analysed (DYN, below), so cannot be accounted for by lack of cDNA in these samples. Since the *TbCPX* transcript levels were much reduced it cannot be determined if the oxidative stress induced by $H_2O_2$ has any effect on the expression in these cells, though in wild type BSF, *TbCPX* transcript levels appeared to decrease in the presence of $H_2O_2$.

In PCF *T. brucei TbCPX* levels appeared essentially the same when wildtype cells and MMR mutants were compared in the absence of $H_2O_2$, with the exception of *msh2-/-* mutants, whose *TbCPX* levels were reduced ~40% ( Figure 6-8 A). When the cultures were grown in the presence of 20 μM $H_2O_2$, the levels of *TbCPX* reduced in the wild type cells and in each of the MMR mutants, with the exception of *MSH2+/-* cells, which were the only clones where *TbCPX* expression levels increased in the presence of $H_2O_2$.

## 6.6 OGG1

*OGG1* is a DNA glycosylase that are works as a part of base excision repair (BER) (Furtado 2012). *OGG1*, as described in Sections 1.4.2 and 1.4.7.2, are the functional homologues of MutM in prokaryotes that function to repair the oxidative lesion which results in 8oxoG-C base pairing. In trypanosomatids, *OGG1* has been widely studied in *T. cruzi* and it was found that lack of this gene results in increased accumulation of ROS in the cell. Also was also observed that cells over-expressing *TcOGG1* are more sensitive to oxidative damage (Furtado 2012). Given this, we used the same samples described above analysed the expression of OGG1 in MMR mutants to determine if any changes in OGG1 was responsible for the contrasting phenotype of BSF and PCF MMR phenotypes. Primers were designed against *TbOGG1* using primer express software provided by ABS and transcript levels were analysed by QRT-PCR as described above. These data are shown in Figure 6-9.

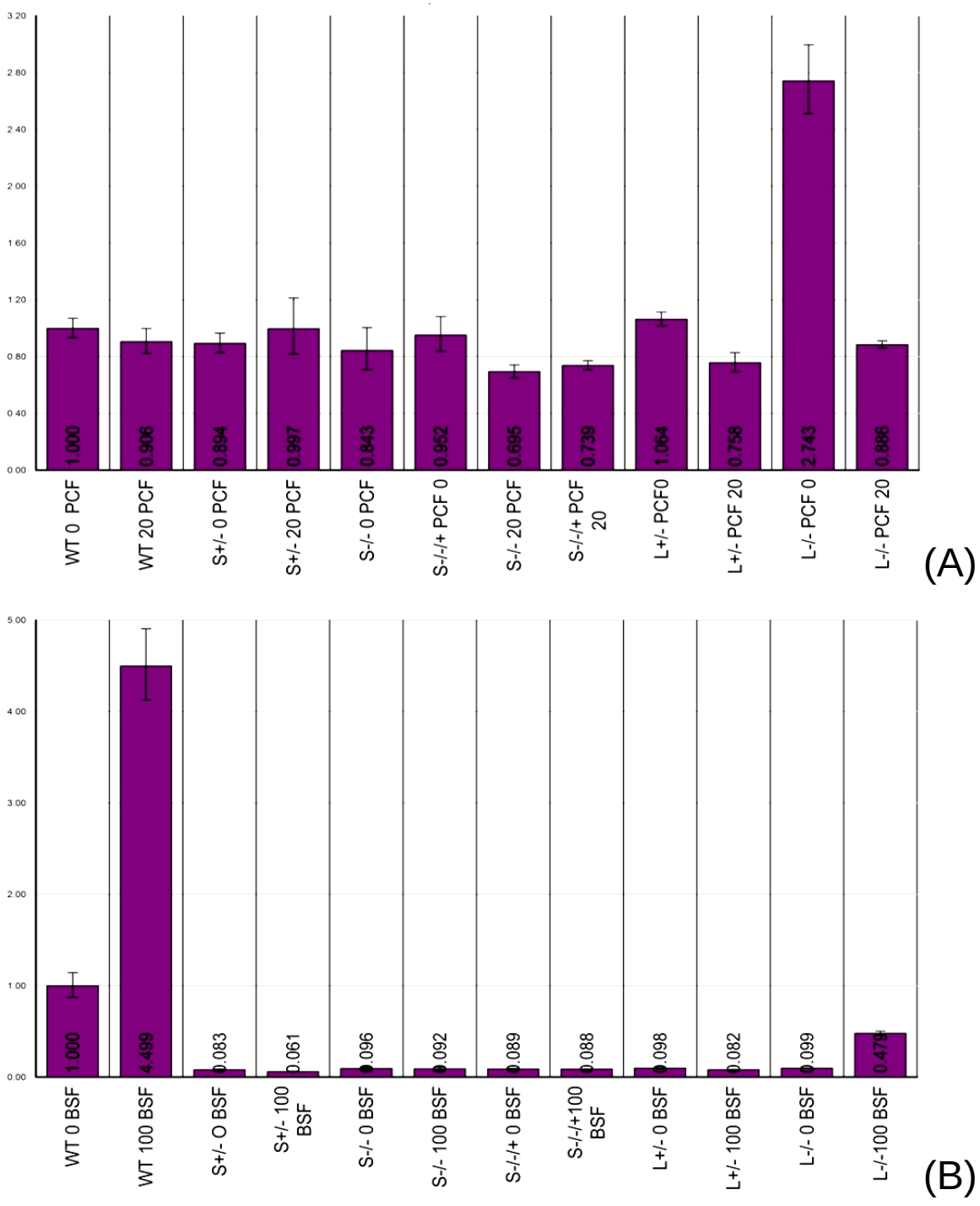


**Figure 6-9 Levels of *TbOGG1* transcript in *T. brucei* (A) PCF and (B) BSF wild type cells and MMR mutants.**

QRT-PCR analysis of *TbOGG1* transcript abundance is shown wild type (WT), *MSH2+/- (s+/-), msh2-/- (s-/-), MSH2-/-/+ (s-/-/+), MLH1+/- (l+/-), mlh1-/- (l-/-)* cells grown in the absence (0) or presence of $H_2O_2$. PCF cultures were grown on 20μM $H_2O_2$ (20) and BSF cultures were grown on 100 μM $H_2O_2$ (100) for 48 hours before *TbOGG1* RNA abundance was analysed using primers TbOGG1 (F) and TbOGG1 (R) relative to *GPI8* for each cell line, QRT-PCR was performed in quadruplicate in two independent experiments; the results are shown as relative abundance of the transcript in each cell relative to GPI8 and relative to non-treated wild type cells, which were normalised to 1; values of the mean of all repeats and vertical lines denote standard deviation.

From these results we can deduce that expression of *OGG1* appeared to be not altered in PCF *T. brucei* wild type cells and MMR mutants (Figure 6-9 A), with the exception of

*mlh1-/-* mutants, which seemed to have increased levels, for reasons that are unclear. Treatment with $H_2O_2$ had little marked effect, again with the exception of *mlh1-/-* cells, where the levels reduced substantially. In contrast, BSF MMR mutants showed highly reduced levels of *OGG1* transcript (Figure 6-9 B) in all the MMR mutants, closely mirroring the *TbCPX* data. In contrast, in BSF wild type cells the levels of *OGG1* increased in the presence of oxidative stress, the opposite of *TbCPX*.

Since the same samples were used to PCR-amplify *OGG1* and *TbCPX*, both of which showed a near undetectable transcript in BSF MMR mutants, a control QRT-PCR was performed, again from the same samples, using primers against a gene found within a polycistronic region to confirm the presence of amplifiable quality of cDNA present on all the samples. Primers (TbDinB (F) and TbDinB (R) were designed against putative dynein heavy chain-encoding gene (*DynB*) (Tb427.08.3250) and PCR- performed as before and as primers as described in Section 2.2.12. Expression of *DynB* in BSF and PCF wild type cells and MMR mutants is shown in Figure 6-10.

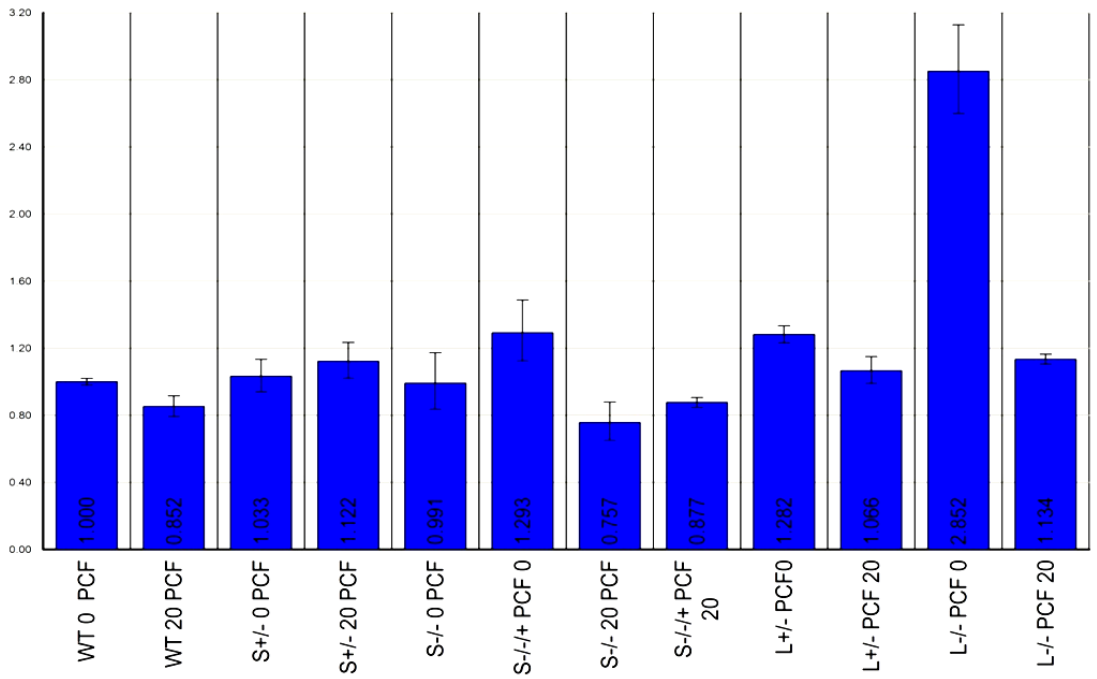


(A)

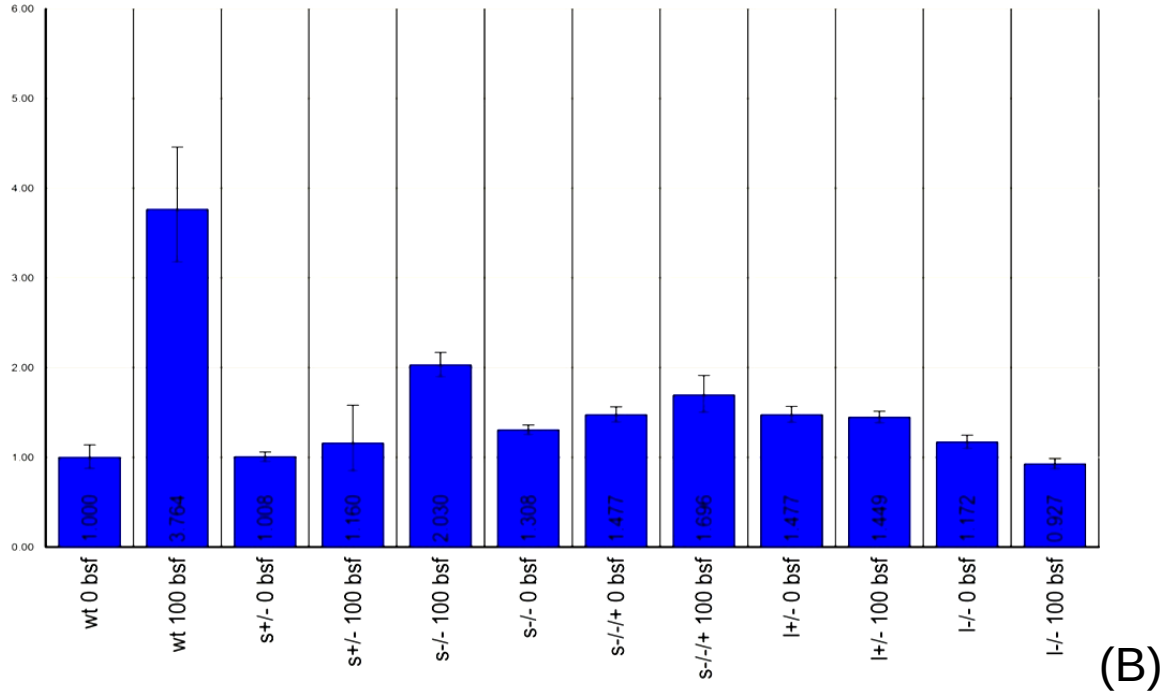


**Figure 6-10 Levels of *TbDynB* transcript in *T. brucei* (A) PCF and (B) BSF wild type cells and MMR mutants.**

QRT-PCR analysis of *TbDynB* transcript abundance is shown wild type (WT), *MSH2+/- (s+/-), msh2-/- (s-/-), MSH2-/-/+ (s-/-/+), MLH1+/- (l+/-), mlh1-/- (l-/-)* cells grown in the absence (0) or presence of $H_2O_2$. PCF cultures were grown on 20μM $H_2O_2$ (20) and BSF cultures were grown on 100 μM $H_2O_2$ (100) for 48 hours before *TbDyB* RNA abundance was analysed using primers TbDinB (F) and TbDinB (R) relative to *GPI8.* For each cell line, QRT-PCR was performed in quadruplicate in two independent experiments; the results are shown as relative abundance of the transcript in each cell relative to *GPI8* and relative to non-treated wild type cells, which were normalised to 1; values of the mean of all repeats and vertical lines denote standard deviation.

The much reduced expression of *OGG1* and *TbCPX* in BSF MMR mutants, when compared with wild type cells was not observed for *DynB*: all the BSF MMR mutants PCR-amplified *DynB* to levels similar to wild type, which was the only cell that showed altered levels after $H_2O_2$ treatment, for reasons that are unclear (Figure 6-10 B). The results also shows that PCF MMR mutants have approximately similar expression of *DYNB*, except for *mlh1-/-* mutants, which showed a much increased expression and may then suggest that the increase also observed for *OGG1* may be artefactual.

## 6.7 Discussion

In this chapter a number of distinct and independent experiments were performed in order to try to expand our understanding of MMR in *T. brucei*. In previous chapters we have analysed the phenotypes of BSF and PCF MMR mutants and have found a contrast in the

response to oxidative stress between BSF and PCF MMR mutants (see Sections 3.2.3 and 3.2.6). We hypothesized that since oxidative stress damages a range of macromolecules, including DNA, further uncharacterised defence and repair systems may act in parallel with MMR and might be further activated in response to the stress. If one or more of these systems were further activated in the absence of the MMR system this could be responsible for the observed contrast in phenotypes of BSF and PCF MMR mutants.

The roles of Msh4 and Msh5 have been widely studied, as described in Sections 1.4.6.3.1.1 and 6.2. Studies primarily conducted in mammals and yeast have demonstrated convincingly a role for the MutS-like factors in meiotic recombination (de Vries 1999;Kneitz 2000), although low expression levels of Msh4 and Msh5 have also been found in non-meiotic cells such as the heart, brain and liver (Her et al. 2003;Her et al. 2007). It has also been shown that in eukaryotes Msh4 interacts with Mlh1 through its amino terminus during crossing over in meiosis (Santucci-Darmanin 2000). Furthermore it has also been observed in bacterial systems that MutS II (equivalent to MSH4-MSH5 complex) interacts with MutS I (equivalent to MutSα and MutSβ) (Fukui 2011). Although no role for either Msh4 or Msh5 has been demonstrated in MMR, due to their presence in mitotic cells it is postulated that they might have a role in DNA repair. As been suggested by Her *et al* (2007), Msh4 and Msh5 can work independently of each other during mitotic DSB repair as the two proteins are not necessarily expressed in concert with each other (Her 2007). Furthermore, both Msh4 and Msh5 have been shown to interact with other repair proteins, such as Rad51 and MRE11, which might suggest their role in DNA repair (Her 2007). We intended to check if in *T. brucei* MSH4 and /or MSH5 work in concert with the reported MMR system. For this purpose we generated both BSF and PCF cells expressing MSH4 and MSH5 that are C-terminally 6-HA tagged, and in which MSH2 or MLH1 were C-terminally 12Myc tagged. Clones were confirmed by western analysis for MSH5-6HA , but no clones were selected for MSH4-6HA that were positive by western analysis. It is possible that the clones were not correctly tagged due to an undetected error in the construct, or the expression of MSH4 could be too low to be detected by western analysis, or even absent. Indeed, it has been reported that *T. brucei MSH4* mRNA has a reduced expression as compared with MSH5 (Barnes 2006), which may correlate with other eukaryotes, but the functional significance of this in *T. brucei* would require further analysis. Co-immunoprecipitation using the 12 myc and 6-HA epitopes failed to reveal evidence that MSH5 interacts with either MSH2 or MLH1 (Figure 6-3), so we cannot conclude that MSH5 plays a role in MMR. Indeed, its function in *T. brucei* remains unclear, though it would be of interest to ask if it interacts with MSH4 and whether the

expression of the latter protein is limited to recently described tsetse fly parasite life cycle stages in which mating is thought to occur (Peacock 2011).

TAO is an alternative oxidase that appears unique to African trypanosomes and belongs to the group of proteins called UCP, which work as a defence system to maintain the homeostasis of the mitochondrial matrix and also to prevent damage induced by oxidative stress. As described in Section 6.3, TAO is a di-iron protein and is expressed in both the life forms. Furthermore, in comparison to BSF *T. brucei*, TAO is expressed 100 times less in PCF cells (Chaudhuri 1995;Chaudhuri 2006;Chaudhuri 1998). The western analysis of BSF and PCF wild type cells and MMR mutants that was performed here (Figure 6-4) confirms this expression level variation. It has also been suggested that when cells are exposed to oxidative damage, the level of TAO is increased in PCF cells (Fang & Beattie 2003). To ask if this might explain the difference in sensitivity to oxidative damage in BSF and PCF *T. brucei*, and might contribute to differing phenotypes when MMR genes are mutated in these life cycle stages, western analysis was performed of the cells grown in the presence of $H_2O_2$. Our data found little evidence that TAO protein levels are altered upon oxidative stress (Figure 6-5) in wild type PCF cells. However, in *MSH2* and *MLH1* PCF null mutants we found greater evidence that expression of TAO increased in the presence of $H_2O_2$. However, due to the limited amount of antibody we could not repeat the experiments to confirm the results, and therefore further work will be required to validate this and to ask about the potential relationship between TAO and MMR functions.

RNAi was attempted as an alternative strategy to the MMR knock out (KO) mutants made in Section 3.2.1.2 in PCF cells and previously in the BSF (Bell 2004). This strategy has been widely used in several organisms, including *T. bruce*i, for the study of various genes (LaCount 2000;Wilkinson 2003) and used this to rapidly reduce the expression of MSH2 or MLH1 in both BSF and PCF cells in order to have a better understanding of if any adaptation occurs during the selection of MMR gene KO mutants. We have observed that MMR null mutants do not show a growth phenotype in either BSF or PCF *T. brucei* when compared with wild type (Bell 2004) (see Sections 3.2.3 and 3.2.6). If MMR is an important repair system required to maintain the genome integrity in the face of oxidative stress, we considered that a growth defect in the MMR mutants may be seen predominantly in PCF cells, compared with BSF, for instance because they are more exposed to oxidative damage due to mitochondrial metabolism. In our analysis MSH2 and MLH1 RNAi specific lines were generated in both BSF and PCF *T. brucei*. Cultures were induced by tetracycline and growth was compared to non-induced cultures (Figure 6-6; section 6.4.2.1). We have

observed that only the MSH2-specific RNAi PCF cells showed a growth defect after tetracycline induction (Figure 6-6 A). This phenotype appeared to be accumulative over 72 hours growth post induction, and was maintained, and perhaps even became more pronounced over the time frames 72-144 and 144-216 hrs post-RNAi induction. Although the cell counts of induced and non-induced cells were clearly different from each other, RNAi against MSH2 did not result in death of PCF *T. brucei*, but instead growth impairment. Whether this would be sufficient to require further selection for changes during the generation of KO mutants is unclear. No such growth defect was seen in the PCF MLH1-specific RNAi cells (Figure 6-6 C) or in either of the MMR RNAi lines in the BSF (Figure 6-6 B and D). However, quantitative RT-PCR suggested that the levels of *MLH1* mRNA in the PCF, and both *MSH2* and *MLH1* in BSF, were not reduced after tetracycline induction of RNAi. This would appear to mean that the RNAi did not take effect in these cell lines, and thus expression of the genes was not affected, meaning that further work will be needed to ask if loss of MMR genes by this route uniformly results in growth impairment.

As discussed in Section 1.4.7.2 tryparedoxin peroxidises (TXNPxs) are enzymes that localize in both the cytoplasm and mitochondrion and maintain the redox potential of the parasite cells. RNAi has confirmed that cytoplasmic tryparedoxin (TbCPX) is essential for BSF *T. brucei*, whereas mitochondrial tryparedoxin (TbMPX) is found to be non-essential for *T. brucei* survival (Schlecker 2005;Wilkinson, Horn, Prathalingam, & Kelly 2003). They enzymes work by reducing reactive oxygen species like $H_2O_2$ into molecular oxygen ($O_2$) and water ($H_2O$). It has been observed that BER null mutants in *T. brucei* display an increased expression of TXNPxs when subjected to oxidative stress (personnel communication, Fernando Aguilar; Institute of Parasitology and Biomedicine, CSIC, Spain). Furthermore, it has been observed that when *T. cruzi* is grown in sub-lethal doses of $H_2O_2$, this results in resistance to oxidative damage and it was hypothesized that such resistance develops by increasing the expression of genes, including TXNPx (Finzi et al. 2004). We attempted to ask if the expression of TXNPx is altered in presence of oxidative stress and in MMR mutants in *T. brucei*. BSF and PCF wild type and MMR mutants were grown in the presence of $H_2O_2$ and QRT-PCR was carried using TXNPx-specific primers (Figure 6-8). QRT-PCR results suggested, remarkably, that all BSF MMR mutants had almost lost the expression of TXNPx, even in the non-treated cultures, so we cannot compare if oxidative stress has any effect in the expression (Figure 6-8 B). The basis and significance of this putative change in expression is unclear, and may be surprising given that the gene is considered to be essential in the BSF. In PCF cells *MSH2*+/- were the only

mutants that showed an increased expression of TXNPx in the presence of $H_2O_2$ (Figure 6-8 A), and this might be very interesting, since the cells are the most resistant to oxidative damage, as compared with wild type cells and rest of the MMR mutants analysed for survival (Section 3.2.3) . When wild type cells and MMR mutants were tested for OGG1 expression, it was observed that BSF MMR mutants had almost lost the expression of *OGG1*, whereas in PCF wild type cells and MMR mutants OGG1 expression was not noticeably different from each other. Since OGG1 and TXNPx are enzymes that work independently of each other, and no studies have been done to show that either of these proteins work in concert with MMR, further work is required to understand and validate these findings. However, all the three systems have an important role in protection against oxidative damage, and decreased expression of OGG1 and TXNPx might have a role in increased sensitivity of MMR mutants in response to oxidative stress.

# 7 Conclusions

DNA repair mechanisms have been proven to be vital for maintaining efficient cellular mechanisms and in ensuring the genome integrity. Both prokaryotic and eukaryotic cells acquire certain conserved yet tailored repair mechanisms. These have been widely studied and the participating factors have been characterized, as discussed in Section 1.4. Although each of the repair systems are specific towards the DNA damage that they recognize and the mechanisms that they use to repair the damage differ from each other, they have been shown to work in synchronization with each other (Bell 2003;DeWeese 1998;Mazon 2010;Scharer 2003;Slupphaug 2003;Swanson 1999).

Cells are continuously exposed to oxidative damage which arises from both exogenous sources such as UV radiations or chemical mutagens as well as endogenous sources such as mitochondrial respiration (see section 1.3)(De Bont 2004). Oxidative mutagens generate a range of reactive oxygen species (ROS) which can affect several macromolecules in the cell including proteins, lipids and DNA (De Bont & van Larebeke 2004). Although cells possess a line of defence system that neutralize the ROS before they are able to cause any damage (see section 1.4.7.2)(Slupphaug 2003), certain oxidative molecules manage to escape the defence system and cause damage to the cell. Oxidative DNA damage is one of the major threats to genome fidelity as ROS have the tendency to modify nucleotide bases (Fraga 1990). These base modifications, if left unrepaired, might result in either DNA breaks or base mismatches, which lead to genomic instability or even cell death. Two primary pathways involved in the repair of oxidative damage are Base Excision Repair (BER) and Mismatch repair (MMR) see Section 1.4.7.2 (De Bont & van Larebeke 2004;Lu et al. 2001;Slupphaug, Kavli, & Krokan 2003). The ‘‘*Go system’’* of BER, composed of MutM, MutY, MutT in bacteria and related proteins in eukaryotes, which serves to prevent oxidative DNA damage (Bjoras 1997;Fujii 1999;Jansson 2010;Lu 2001;Michaels 1992;Ohtsubo 2000;Tchou 1991;Tsaiwu 1992). Further oxidative lesions are repaired by a specific player of BER, termed as OGG1 (Lu, Li, Gu, Wright, & Chang 2001;Slupphaug, Kavli, & Krokan 2003). OGG1 is a DNA glycosylase that primarily repairs 7,8 dihydro-8-oxoguanine (8-oxo-G) lesion. Of the different kinds of base modifications, 8-oxo-G represents one of the most abundant and thus widely studied base modifications (Slupphaug, Kavli, & Krokan 2003). This modified guanine can still pair with C following Watson and Crick base pairing (Moriya 1993;Shibutani 1991;Wood 1990). However, if left unrepaired, it can base pair with either A or C and cause GC-TA transversion. Apart from BER, base mismatches that occur due to 8-oxo-G:A pairing are also repaired by post-replicative MMR (see Section 1.4.7.2)(DeWeese 1998;Mazurek 2002). MMR is a repair process that is conserved in both prokaryotes and eukaryotes and serves to correct the

replication errors left behind by the proof reading activity of DNA polymerase. Along with the replication errors, it also recognises the base mismatches generated due to base modifications which are sometimes not recognized by the proof reading activity of DNA polymerase. However, MMR is specific towards the recognition of base mismatch and due to the way the reaction initiates and is executed, it can only repair lesions present in the daughter strand (see section 1.4.6)(Jiricny 2006;Kunkel 2005;Modrich 2006).

The MMR machinery of kinetoplastids is conserved throughout evolution (see Section 1.4.6.4; Figure 1-12) and posses all the major proteins required in the process. Five MutS homologues have been identified so far including MSH2, MSH3, MSH6, MSH4 and MSH5, whereas two MutL homologues yet identified in kinetoplastids are MLH1 and PMS1 (Bell 2004). Of these MSH2, MSH3 and MSH6 of MutS family and both MLH1 and PMS1 of MutL family have been implicated in kinetoplastid MMR, based on sequence homology. In *T. brucei*, *MSH2* and *MLH1* have been previously characterized and it was confirmed that both of these genes are vital for MMR in the BSF of *T. brucei* (Bell 2004). In the study it was observed that loss of either of these genes results in increased microsatellite instability (MSI) and tolerance to alkylation damage. Both of these phenotypes are considered markers for impaired MMR (Bell et al. 2004). Further it was shown that loss of *MSH2* results in increased sensitivity to oxidative damage whereas loss of *MLH1* showed no such effect at least at the dose of $H_2O_2$ tested during the study (Machado-Silva 2008). Loss of *MSH2* was also attributed to the loss of kDNA in BSF *T. brucei* (Campos 2011). Furthermore, a role of *T. brucei* MMR in recombination has also been studied. It was observed that in BSF *T. brucei*, homologous recombination is more efficient in *MSH2* deficient BSF cells (Barnes & McCulloch 2007;Bell & McCulloch 2003). An increase in recombination was observed in *msh2-/-* cells as compared to wildtype, particularly in recombination between longer stretches of non-homologous DNA (Barnes & McCulloch 2007;Datta et al. 1996;Selva et al. 1995). Although MSH3 and MSH6 have been annotated in *T. brucei*, their roles have not been studied at all in any kinetoplastids.

In this study we have attempted to generate *MSH2* and *MLH1* mutants in the PCF *T. brucei* and, in particular, document their role, if any, in response towards oxidative stress. We had hypothesized that it might not be possible to generate MMR mutants in PCF *T. brucei* based on studies in *T. cruzi* where all the attempts to generate *MSH2* null mutants have so far failed (Campos et al. 2011) and where heterozygous mutants display MMR defect. Our hypothesis was proved to be wrong since *MSH2* and *MLH1* mutants were made in PCF.

Although generation of the null mutants took a couple of attempts and the clones selected were initially very sick (see Section 3.2.1.2). However, both PCR and RT-PCR analysis confirms that the MMR mutants have been successfully made in the PCF (Figure 3-2, Figure 3-3, Figure 3-4). Once verified by genotypic analysis, clones were examined for the loss of MMR activity by testing for alkylation tolerance and MSI, the phenotypes associated with impaired MMR. Survival curves in the presence of MNNG, an alkylating agent, confirm that MMR mutants are resistant to methylation damage as compared with wild type (Figure 3-9). Also, it was observed that *mlh1-/-* mutants were clearly the most resistant of all the clones analyzed , which was not observed in BSF *MLH1* mutants ((Bell 2004); Figure 3-8 this study). Although we could not specify a reason for the phenotype, this suggests that MLH1 might provide a substantial role in the response to methylating damage.

MSI in PCF MMR mutants was tested by sub cloning wild type and MMR mutants and PCR amplifying the JS-2 microsatellite. PCR products, resolved in 3% agarose, showed that 3 out of 10 clones of both *msh2* and *mlh1* null mutants show MSI and not in wild type and heterozygous mutants (Figure 3-10). Similar phenotype was also observed BSF MMR mutants (Bell 2004).

To examine the role of MMR in the response to oxidative stress, the MMR mutants were also analysed in the presence of increasing concentration of $H_2O_2$ as a means of inducing oxidative stress. This was particularly important as role for MSH2 has been widely studied in response towards oxidative stress in various organisms including prokaruties sucas E. coli, P. aureginosa, protozoa such as T. cruzi and higher eukaryotes including mouse and mammalian cells (Campos et al. 2011;Colussi et al. 2002;DeWeese 1998;Glaab et al. 2001;Sanders et al. 2011; Wyrzykowski 2003)(see section 3.3). Furthermore, in *T. brucei* BSF cells *msh2-/-* mutants are very sensitive when grown in the presence of $H_2O_2$, although no phenotype was observed in *mlh1-/-* mutants when compared with wild type (Machado-Silva 2008). The phenotype was only observed in the presence of maximum concentration of 100 μM $H_2O_2$. In this study this experiment was repeated with higher concentrations of $H_2O_2$ and a sensitive phenotype of *mlh1-/-* mutants was observed, though the sensitivity towards oxidative stress was not as pronounced as *msh2-/-* mutants (Figure 3-25). Also in a study performed previously, it was showed that wild type PCF cells are 10-30 times more sensitive to oxidative stress as compared with BSF (Barnes 2006). Several reasons for this increased sensitivity have been discussed in Section 3.3, which include increased endogenous oxidative stress due to mitochondrial respiration in PCF and the presence of

$Fe^{++}$ in culture medium. When the MMR mutants were analysed in the PCF, a contrasting phenotype was observed as compared to BSF MMR mutants. We have observed that PCF MMR mutants are resistant to oxidative damage as compared to wild type (Figure 3-14). This phenotype was pronounced even in heterozygous mutants at the earliest time points and at the lowest concentrations of $H_2O_2$ tested during the study. However, as a further contrast to BSF MMR mutants where $H_2O_2$ sensitivity was more exaggerated in null mutants as compared with heterozygous mutants, PCF MMR null mutants reverted the resistance and displayed great sensitivity as compared with heterozygous mutants. PCF *mlh1-/-* mutants showed the same percentage survival as wild type whereas *msh2-/-*, though being more sensitive than *MSH2+/-*, were still resistant to oxidative damage as compared with wild type and *mlh1-/-*. These data reveal a life cycle dependent difference in the response towards oxidative stress in *T. brucei*, and may suggest a more important role of MMR against oxidative stress in PCF *T. brucei*. This follows for the fact that PCF are exposed to increased endogenous oxidative stress and therefore might require more active repair mechanisms to deal with oxidative lesions. Increased resistance of heterozygous mutants as compared with null mutants and wild type may be due to an adaptation that the cell undergo in order to cope with the increased oxidative lesions where a single copy of *MSH2* or *MLH1* is lost. When MSI was analysed in the presence and absence of $H_2O_2$, *msh2 -/-* cells display some genome stability as compared to MSI analysed in *msh2-/-* grown in the absence of $H_2O_2$. This phenotype was different from *mlh1 -/-* mutants, which showed an increased MSI in the presence of oxidative stress.

The importance of *MSH2* in PCF *T. brucei* was further re-iterated when re-expressing the gene in *msh2-/-* mutants. I was found that such re-expression reverted the phenotypes of alkylation tolerance (Figure 3-22) and MSI (Figure 3-24) to levels comparable with *MSH2+/-* but this was not the case in response to oxidative damage. Survival curves showed that PCF *MSH2-/-/+* re-expressers had the same levels of resistance as *msh2-/-* cells, at least at most time points analysed (Figure 3-23). In contrast to this, re-expression of MSH2 in BSF *msh2-/-* did not revert the phenotype of sensitivity to oxidative damage. This further re-enforces the hypothesis that MMR is particularly important in the PCF *T. brucei* and that the cells might have gone through an adaptation process during the course of selection of mutants.

For a better understanding of the function of MSH2 and MLH1, to determine if they are predominantly present in either of the genome containing compartments (nucleus or mitochondrion), and if there was any change in the expression or localization of MMR

proteins after genotoxic damage, two proteins were epitope tagged. Since previous attempts to generate antibodies against TbMSH2 and TbMLH1 had failed (Machado-Silva 2008), we generated C-terminal 12 myc tagged variants for both the proteins in heterozygous cell lines generated previously in the two life forms of *T. brucei*. Tagged transformants were confirmed by both PCR and western analysis (Figure 4-2,Figure 4-3, Figure 4-4 and Figure 4-5). We demonstrated by MNNG tolerance and response towards $H_2O_2$ that MSH2 tagged variants retained their MMR activity (Figure 4-6 and Figure 4-7 A) though it was observed that for unknown reason C-terminal tagging has made MLH1 non functional. The proteins were localized by two alternate strategies; immune fluorescence (IF) and sub-cellular fractionation. IF demonstrated that the two proteins are nuclear and that the localization did not seem to be effected by the stress applied (Figure 4-8). However, it was observed that approximately 50% of the cells do not show fluorescence when the cells were subjected to oxidative stress. This is contrary to the western analysis which showed that expression level of the proteins is not influenced by the stress applied. IF further showed an increase in in nuclear localization when the cells were cultured in the presence of MNNG, though, this cannot be definite as exactly the same number of cells were not counted for each slide and no statistics were performed. In contrast to this, localization by sub-cellular fractionation showed the MMR proteins to be cytoplasmic (Figure 4-9). The reason for this difference relative to IF are unclear , and we cannot conclude if the proteins are either cytoplasmic or nuclear, though we could not find any evidence of kinetoplastid localization of either of MSH2 or MLH1, even though we had hypothesized that the MMR machinery, or specifically MSH2, might be localized to the kinetoplastid, as studies done in *T. cruzi* have demonstrated an accumulation of 8oxoG in the nucleus and kinetoplast (Furtado 2012) and it is known that MMR plays a vital role in repairing the lesions generated by this adduct (Lu 2001;Slupphaug 2003).

To have a further understanding of the MMR machinery, we also characterized *MSH3* and *MSH6* in BSF *T. brucei*. Although these proteins have been well documented for their role in MMR in other eukaryotes, their importance in kinetoplastid MMR have not been studied so far. We generated the gene knockout mutants for both genes and have confirmed the loss of both the alleles by PCR and RT-PCR analysis (Figure 5-2, Figure 5-3, Figure 5-4). In order to determine their importance in kinetoplastid MMR, we performed the assays that were used to analyse the phenotypes of *MSH2* and *MLH1* mutants in the BSF (Bell et al. 2004). We have observed that only *MSH6* null mutants show tolerance towards alkylation damage, a phenotype characteristic of impaired MMR (Figure 5-6). Indeed alkylation tolerance of *msh6-/-* were shown to be comparable to *msh2-/-* and *mlh1-/-* . In contrast

*MSH3* mutants did not show any growth. These results are consistent with previous finding which suggest an important role of MSH6 in protection against methylation damage (Christmann & Kaina 2000;Fordham et al. 2010). However, no role of MSH3 has been displayed in response to alkylating mutagens (Fordham et al. 2010). When *MSH3* and *MSH6* gene knock out mutants were tested for MSI by PCR amplifying the JS2 locus, none of these mutants displayed any MSI (Figure 5-7). Since JS2 is a GT-dinucleotide repeat, and MSH3 and MSH6 have been shown to work in place of each other for base mismatch that is 2-8 nucleotides long, functional redundancy could be the reason that we did not see any MSI in the JS2 locus. No studies have been done so far to elucidate the role of either MSH3 or MSH6 in protection against oxidative damage. In our study, when *MSH3* and *MSH6* mutants were grown in the presence of increasing concentrations of $H_2O_2$, none of the mutants showed a phenotype distinct from wild type *T. brucei*. We expected to see an increased sensitivity of *msh6-/-* mutants in response towards oxidative stress, that was more comparable to *msh2-/-* mutants as damage caused by $H_2O_2$ causes GC-TA transversions that are primarily repaired by the MSH2-MSH6 complex (Colussi et al. 2002;Ni, Marsischky, & Kolodner 1999).

To further understand the potential players involved in defence and repair against oxidative damage in *T. brucei*, we have selectively analysed certain proteins that might have a role against oxidative damage. Experiments were done in both BSF and PCF *T. brucei* where we attempted to check if MSH4 and MSH5 work in concert with MSH2 and MLH1. We attempted to generate C-terminally 6-HA tagged variants for both MSH4 and MSH5 in BSF and PCF cells, in cell lines in which MSH2 and MLH1 were C-terminally 12myc tagged. However, when the clones were analysed by western analysis, it showed that MSH4 was not tagged in any of the cell lines transformed. Positive clones for MSH5 C-terminally 6-HA tag were confirmed by western analysis (Figure 6-2) in both PCF 12myc tagged MSH2 and MLH1 and BSF 12 myc tagged MSH2. Co-IP, using both 12myc and 6-HA epitopes, of the tagged lines has shown that MSH5 does not interact with either MSH2 or MLH1 (Figure 6-3), and we cannot conclude if MSH5 plays a role in MMR.

The role of trypanosome alternate oxidase (TAO), which has a function in protection against oxidative stress (Chaudhuri et al. 2006;Fang and Beattie 2003), was also analysed in this study. Expression levels of TAO were analysed in both PCF and BSF wild type and MMR mutants in the absence and presence of $H_2O_2$ and the results showed that in PCF wild type cells, TAO expression was unaltered, in contrast to MMR mutants, which show an increase in expression of TAO in the presence of $H_2O_2$ (Figure 6-5). No alteration in

TAO expression was observed in BSF wild type and MMR mutants. However, the results cannot be reported in confidence as experiments could not be repeated due to the limited amount of antibody.

RNAi was attempted as an alternative strategy to MMR knock out (KO) mutants generated in section 3.2.1.2. We used a conditionally tetracycline-inducible system for RNAi to reduced the expression of *MSH2* or *MLH1* in both PCF and BSF. Our results of MMR KO show that both *MSH2* and *MLH1* null mutants do not show any growth defect compared with wild type. In contrast, RNAi against *MSH2* in PCF *T. brucei* showed that an impaired growth phenotype. This response was not seen following MLH1 specific RNAi PCF cells, or for either MMR genes in BSF.

Tryparedoxin peroxidises (TXNPxs) are the enzymes that serve to maintain the redox homeostasis of the cell (Tetaud 2001). Previous studies done in *T. brucei* have localized TXNPxs in both the cytoplasm and mitochondrion (Schlecker 2005) and it has displayed a role in *T. cruzi* BER mutants (personnel communication, Fernando Aguilar; Institute of Parasitology and Biomedicine, CSIC, Spain). We attempted to analyse the expression levels of *TXNPx* mRNA in wild type and MMR mutants by QRT-PCR and our results showed that in PCF cells *MSH2*+/- were the only mutants that showed an increased expression of TXNPx in the presence of $H_2O_2$ ( Figure 6-8A). Interestingly this was the cell line which has shown the highest resistance to oxidative stress. In contrast, BSF MMR mutants seemed to have almost lost the expression of TXNPx (Figure 6-8B). Similar phenotype was observed when BSF MMR mutants were PCR amplified for OGG1 mRNA, which show a much reduced expression (Figure 6-9B). PCF wild type and MMR mutants, on the other hand, do not show any variation in expression of *OGG1* (Figure 6-9A). Although MMR, TXNPx and OGG1 work independent of each other and no studies, to my knowledge, have been done to show that these might work in concert with each other, our studies are still in progress and further analysis are required to validate these findings.

# Appendix 1 - Percentage survival cell counts of PCF MMR mutants.

**Percentage Survival - 24hrs**

| Strain | Repeats | $H_2O_2$ conc. µM | Cell count $X10^5$ | Average | %survival | %average | sd |
|---|---|---|---|---|---|---|---|
| WT | 1 | 0 | 30.4 | 29.33333 | 103.6364 | 100 | 3.149183 |
| | 2 | 0 | 28.8 | | 98.18182 | | |
| | 3 | 0 | 28.8 | | 98.18182 | | |
| | 1 | 10 | 18.3 | 16.36667 | 62.38636 | 55.79545 | 5.868523 |
| | 2 | 10 | 15 | | 51.13636 | | |
| | 3 | 10 | 15.8 | | 53.86364 | | |
| | 1 | 20 | 6.7 | 6.933333 | 22.84091 | 23.63636 | 1.997545 |
| | 2 | 20 | 7.6 | | 25.90909 | | |
| | 3 | 20 | 6.5 | | 22.15909 | | |
| | 1 | 40 | 2.9 | 3 | 9.886364 | 10.22727 | 0.340909 |
| | 2 | 40 | 3 | | 10.22727 | | |
| | 3 | 40 | 3.1 | | 10.56818 | | |
| *MSH2+/-* | 1 | 0 | 27.6 | 28.93333 | 95.39171 | 100 | 4.223572 |
| | 2 | 0 | 29.2 | | 100.9217 | | |
| | 3 | 0 | 30 | | 103.6866 | | |
| | 1 | 10 | 17.2 | 19.86667 | 59.447 | 68.66359 | 9.71028 |
| | 2 | 10 | 19.6 | | 67.74194 | | |
| | 3 | 10 | 22.8 | | 78.80184 | | |
| | 1 | 20 | 13.6 | 14.26667 | 47.00461 | 49.30876 | 2.111786 |
| | 2 | 20 | 14.4 | | 49.76959 | | |
| | 3 | 20 | 14.8 | | 51.15207 | | |
| | 1 | 40 | 3.1 | 3.866667 | 10.71429 | 13.36406 | 2.45205 |
| | 2 | 40 | 4 | | 13.82488 | | |
| | 3 | 40 | 4.5 | | 15.553 | | |
| *msh2-/-* | 1 | 0 | 24.6 | 25.26667 | 97.36148 | 100 | 8.238784 |
| | 2 | 0 | 23.6 | | 93.40369 | | |
| | 3 | 0 | 27.6 | | 109.2348 | | |
| | 1 | 10 | 20.8 | 19.2 | 82.3219 | 75.98945 | 5.707997 |
| | 2 | 10 | 18 | | 71.24011 | | |
| | 3 | 10 | 18.8 | | 74.40633 | | |
| | 1 | 20 | 15.6 | 15.6 | 61.74142 | 61.74142 | 4.74934 |
| | 2 | 20 | 14.4 | | 56.99208 | | |

| | | | | | | | |
|---|---|---|---|---|---|---|---|
| | 3 | 20 | 16.8 | | 66.49077 | | |
| | 1 | 40 | 4.7 | 4.933333 | 18.60158 | 19.52507 | 0.823878 |
| | 2 | 40 | 5.1 | | 20.1847 | | |
| | 3 | 40 | 5 | | 19.78892 | | |
| *MSH2-/-/+* | 1 | 0 | 25.2 | 26.74667 | 94.21735 | 100 | 6.527935 |
| | 2 | 0 | 26.4 | | 98.70389 | | |
| | 3 | 0 | 28.64 | | 107.0788 | | |
| | 1 | 10 | 18.21 | 18.65 | 68.08325 | 69.72832 | 8.09004 |
| | 2 | 10 | 21 | | 78.51446 | | |
| | 3 | 10 | 16.74 | | 62.58724 | | |
| | 1 | 20 | 14 | 15.4 | 52.34297 | 57.57727 | 5.125816 |
| | 2 | 20 | 16.74 | | 62.58724 | | |
| | 3 | 20 | 15.46 | | 57.8016 | | |
| | 1 | 40 | 5.84 | 5.966667 | 21.8345 | 22.30808 | 0.63596 |
| | 2 | 40 | 5.9 | | 22.05882 | | |
| | 3 | 40 | 6.16 | | 23.03091 | | |
| *MLH1+/-* | 1 | 0 | 25.2 | 27.33333 | 92.19512 | 100 | 9.961257 |
| | 2 | 0 | 26.4 | | 96.58537 | | |
| | 3 | 0 | 30.4 | | 111.2195 | | |
| | 1 | 10 | 22 | 22.13333 | 80.4878 | 80.97561 | 2.235403 |
| | 2 | 10 | 22.8 | | 83.41463 | | |
| | 3 | 10 | 21.6 | | 79.02439 | | |
| | 1 | 20 | 12.8 | 13.06667 | 46.82927 | 47.80488 | 1.689806 |
| | 2 | 20 | 12.8 | | 46.82927 | | |
| | 3 | 20 | 13.6 | | 49.7561 | | |
| | 1 | 40 | 3.8 | 4.133333 | 13.90244 | 15.12195 | 3.457914 |
| | 2 | 40 | 5.2 | | 19.02439 | | |
| | 3 | 40 | 3.4 | | 12.43902 | | |
| *mlh1-/-* | 1 | 0 | 24.6 | 25.06667 | 98.1383 | 100 | 2.564801 |
| | 2 | 0 | 25.8 | | 102.9255 | | |
| | 3 | 0 | 24.8 | | 98.93617 | | |
| | 1 | 10 | 14.4 | 14.6 | 57.44681 | 58.24468 | 0.797872 |
| | 2 | 10 | 14.6 | | 58.24468 | | |
| | 3 | 10 | 14.8 | | 59.04255 | | |
| | 1 | 20 | 9 | 8.933333 | 35.90426 | 35.6383 | 1.21877 |
| | 2 | 20 | 8.6 | | 34.30851 | | |
| | 3 | 20 | 9.2 | | 36.70213 | | |
| | 1 | 40 | 4.7 | 3.9 | 18.75 | 15.55851 | 2.87677 |

| | | | |
|---|---|---|---|
| 2 | 40 | 3.3 | 13.16489 |
| 3 | 40 | 3.7 | 14.76064 |

**Percentage Survival - 48hrs**

| Strain | Repeats | $H_2O_2$ conc. µM | Cell count x$10^5$ | average | %survival | %average | sd |
|---|---|---|---|---|---|---|---|
| WT | 1 | 0 | 83 | 89.66667 | 92.56506 | 100 | 7.8332 |
| | 2 | 0 | 89 | | 99.25651 | | |
| | 3 | 0 | 97 | | 108.1784 | | |
| | 1 | 10 | 60 | 54.66667 | 66.9145 | 60.96654 | 5.61326 |
| | 2 | 10 | 50 | | 55.76208 | | |
| | 3 | 10 | 54 | | 60.22305 | | |
| | 1 | 20 | 6 | 7.766667 | 6.69145 | 8.66171 | 1.778569 |
| | 2 | 20 | 8.2 | | 9.144981 | | |
| | 3 | 20 | 9.1 | | 10.1487 | | |
| | 1 | 40 | 0 | 0 | 0 | 0 | 0 |
| | 2 | 40 | 0 | | 0 | | |
| | 3 | 40 | 0 | | 0 | | |
| *MSH2+/-* | 1 | 0 | 133 | 134 | 99.25373 | 100 | 6.376122 |
| | 2 | 0 | 143 | | 106.7164 | | |
| | 3 | 0 | 126 | | 94.02985 | | |
| | 1 | 10 | 106 | 109.6667 | 79.10448 | 81.8408 | 4.110127 |
| | 2 | 10 | 116 | | 86.56716 | | |
| | 3 | 10 | 107 | | 79.85075 | | |
| | 1 | 20 | 65 | 66 | 48.50746 | 49.25373 | 0.746269 |
| | 2 | 20 | 67 | | 50 | | |
| | 3 | 20 | 66 | | 49.25373 | | |
| | 1 | 40 | 0.2 | 0.266667 | 0.149254 | 0.199005 | 0.043086 |
| | 2 | 40 | 0.3 | | 0.223881 | | |
| | 3 | 40 | 0.3 | | 0.223881 | | |
| *msh2-/-* | 1 | 0 | 114 | 114.3333 | 99.70845 | 100 | 8.312873 |
| | 2 | 0 | 105 | | 91.83673 | | |
| | 3 | 0 | 124 | | 108.4548 | | |
| | 1 | 10 | 99 | 88.66667 | 86.58892 | 77.55102 | 8.404394 |
| | 2 | 10 | 87 | | 76.09329 | | |
| | 3 | 10 | 80 | | 69.97085 | | |
| | 1 | 20 | 28.8 | 33.6 | 25.1895 | 29.38776 | 8.670811 |
| | 2 | 20 | 27 | | 23.61516 | | |
| | 3 | 20 | 45 | | 39.3586 | | |

| | | | | | | | |
|---|---|---|---|---|---|---|---|
| | 1 | 40 | 0.4 | 0.3 | 0.349854 | 0.262391 | 0.087464 |
| | 2 | 40 | 0.3 | | 0.262391 | | |
| | 3 | 40 | 0.2 | | 0.174927 | | |
| *MSH2-/-+* | 1 | 0 | 114 | 118 | 96.61017 | 100 | 7.387964 |
| | 2 | 0 | 112 | | 94.91525 | | |
| | 3 | 0 | 128 | | 108.4746 | | |
| | 1 | 10 | 94 | 88.45667 | 79.66102 | 74.96328 | 5.684643 |
| | 2 | 10 | 90.37 | | 76.58475 | | |
| | 3 | 10 | 81 | | 68.64407 | | |
| | 1 | 20 | 48.3 | 47.07667 | 40.9322 | 39.89548 | 1.143168 |
| | 2 | 20 | 47.3 | | 40.08475 | | |
| | 3 | 20 | 45.63 | | 38.66949 | | |
| | 1 | 40 | 1.3 | 0.805333 | 1.101695 | 0.682486 | 0.386951 |
| | 2 | 40 | 0.716 | | 0.60678 | | |
| | 3 | 40 | 0.4 | | 0.338983 | | |
| *MLH1+/-* | 1 | 0 | 114 | 116.3333 | 97.99427 | 100 | 9.191413 |
| | 2 | 0 | 107 | | 91.97708 | | |
| | 3 | 0 | 128 | | 110.0287 | | |
| | 1 | 10 | 100 | 87.66667 | 85.95989 | 75.35817 | 9.191413 |
| | 2 | 10 | 82 | | 70.48711 | | |
| | 3 | 10 | 81 | | 69.62751 | | |
| | 1 | 20 | 23.6 | 23.4 | 20.28653 | 20.11461 | 2.325688 |
| | 2 | 20 | 26 | | 22.34957 | | |
| | 3 | 20 | 20.6 | | 17.70774 | | |
| | 1 | 40 | 0.1 | 0.133333 | 0.08596 | 0.114613 | 0.049629 |
| | 2 | 40 | 0.1 | | 0.08596 | | |
| | 3 | 40 | 0.2 | | 0.17192 | | |
| *mlh1-/-* | 1 | 0 | 65.6 | 63.46667 | 103.3613 | 100 | 2.91101 |
| | 2 | 0 | 62.4 | | 98.31933 | | |
| | 3 | 0 | 62.4 | | 98.31933 | | |
| | 1 | 10 | 34 | 36.53333 | 53.57143 | 57.56303 | 7.466116 |
| | 2 | 10 | 42 | | 66.17647 | | |
| | 3 | 10 | 33.6 | | 52.94118 | | |
| | 1 | 20 | 8.2 | 7.833333 | 12.92017 | 12.34244 | 1.139839 |
| | 2 | 20 | 7 | | 11.02941 | | |
| | 3 | 20 | 8.3 | | 13.07773 | | |
| | 1 | 40 | 0 | 0 | 0 | 0 | 0 |
| | 2 | 40 | 0 | | 0 | | |

| | | | | | | | |
|---|---|---|---|---|---|---|---|
| | 3 | 40 | 0 | | 0 | | |

**Percentage Survival -72hrs**

| Strain | Repeats | $H_2O_2$ conc. µM | Cell count $x10^5$ | average | %survival | %average | sd |
|---|---|---|---|---|---|---|---|
| WT | 1 | 0 | 174 | 166.3333 | 104.6092 | 100 | 11.25282 |
| | 2 | 0 | 145 | | 87.17435 | | |
| | 3 | 0 | 180 | | 108.2164 | | |
| | 1 | 10 | 64 | 61.33333 | 38.47695 | 36.87375 | 1.469363 |
| | 2 | 10 | 59.2 | | 35.59118 | | |
| | 3 | 10 | 60.8 | | 36.55311 | | |
| | 1 | 20 | 1.3 | 1.766667 | 0.781563 | 1.062124 | 0.250301 |
| | 2 | 20 | 2.1 | | 1.262525 | | |
| | 3 | 20 | 1.9 | | 1.142285 | | |
| | 1 | 40 | 0 | 0 | 0 | 0 | 0 |
| | 2 | 40 | 0 | | 0 | | |
| | 3 | 40 | 0 | | 0 | | |
| *MSH2+/-* | 1 | 0 | 232 | 224 | 103.5714 | 100 | 9.449112 |
| | 2 | 0 | 200 | | 89.28571 | | |
| | 3 | 0 | 240 | | 107.1429 | | |
| | 1 | 10 | 184 | 177.3333 | 82.14286 | 79.16667 | 3.717261 |
| | 2 | 10 | 180 | | 80.35714 | | |
| | 3 | 10 | 168 | | 75 | | |
| | 1 | 20 | 100 | 109.3333 | 44.64286 | 48.80952 | 5.740268 |
| | 2 | 20 | 104 | | 46.42857 | | |
| | 3 | 20 | 124 | | 55.35714 | | |
| | 1 | 40 | 0 | 0 | 0 | 0 | 0 |
| | 2 | 40 | 0 | | 0 | | |
| | 3 | 40 | 0 | | 0 | | |
| | | | | | | | |
| *msh2-/-* | 1 | 0 | 280 | 257.3333 | 108.8083 | 100 | 15.25641 |
| | 2 | 0 | 212 | | 82.38342 | | |
| | 3 | 0 | 280 | | 108.8083 | | |
| | 1 | 10 | 180 | 181.3333 | 69.94819 | 70.46632 | 3.911831 |
| | 2 | 10 | 192 | | 74.6114 | | |
| | 3 | 10 | 172 | | 66.83938 | | |
| | 1 | 20 | 112 | 113.3333 | 43.52332 | 44.04145 | 1.617875 |
| | 2 | 20 | 118 | | 45.85492 | | |

| | | | | | | | |
|---|---|---|---|---|---|---|---|
| | 3 | 20 | 110 | | 42.74611 | | |
| | 1 | 40 | 0 | 0 | 0 | 0 | 0 |
| | 2 | 40 | 0 | | 0 | | |
| | 3 | 40 | 0 | | 0 | | |
| *MSH2-/-+* | 1 | 0 | 248 | 253.3333 | 97.89474 | 100 | 1.823211 |
| | 2 | 0 | 256 | | 101.0526 | | |
| | 3 | 0 | 256 | | 101.0526 | | |
| | 1 | 10 | 157.39 | 157.7967 | 62.12763 | 62.28816 | 0.80162 |
| | 2 | 10 | 160 | | 63.15789 | | |
| | 3 | 10 | 156 | | 61.57895 | | |
| | 1 | 20 | 97.89 | 97.07667 | 38.64079 | 38.31974 | 0.715447 |
| | 2 | 20 | 95 | | 37.5 | | |
| | 3 | 20 | 98.34 | | 38.81842 | | |
| | 1 | 40 | 4.07 | 3.28 | 1.606579 | 1.294737 | 0.270934 |
| | 2 | 40 | 2.83 | | 1.117105 | | |
| | 3 | 40 | 2.94 | | 1.160526 | | |
| *MLH1+/-* | 1 | 0 | 248 | 253.3333 | 97.89474 | 100 | 1.823211 |
| | 2 | 0 | 256 | | 101.0526 | | |
| | 3 | 0 | 256 | | 101.0526 | | |
| | 1 | 10 | 152 | 162.6667 | 60 | 64.21053 | 3.973597 |
| | 2 | 10 | 172 | | 67.89474 | | |
| | 3 | 10 | 164 | | 64.73684 | | |
| | 1 | 20 | 106 | 110 | 41.84211 | 43.42105 | 3.441236 |
| | 2 | 20 | 104 | | 41.05263 | | |
| | 3 | 20 | 120 | | 47.36842 | | |
| | 1 | 40 | 0 | 0 | 0 | 0 | 0 |
| | 2 | 40 | 0 | | 0 | | |
| | 3 | 40 | 0 | | 0 | | |
| *mlh1-/-* | 1 | 0 | 148 | 156 | 94.87179 | 100 | 6.783978 |
| | 2 | 0 | 152 | | 97.4359 | | |
| | 3 | 0 | 168 | | 107.6923 | | |
| | 1 | 10 | 87 | 84.66667 | 55.76923 | 54.2735 | 1.334401 |
| | 2 | 10 | 83 | | 53.20513 | | |
| | 3 | 10 | 84 | | 53.84615 | | |
| | 1 | 20 | 2.4 | 3.3 | 1.538462 | 2.115385 | 0.65057 |
| | 2 | 20 | 3.1 | | 1.987179 | | |
| | 3 | 20 | 4.4 | | 2.820513 | | |
| | 1 | 40 | 0 | 0 | 0 | 0 | 0 |

| | | | |
|---|---|---|---|
| 2 | 40 | 0 | 0 |
| 3 | 40 | 0 | 0 |

# References

Abdelnoor, R.V. 2006. Mitochondrial genome dynamics in plants and animals: Convergent gene fusions of a MutS homologue.

Acharya, S. 1996. hMSH2 forms specific mispair-binding complexes with hMSH3 and hMSH6.

Alani, E. 1997. Genetic and biochemical analysis of Msh2p-Msh6p: Role of ATP hydrolysis and Msh2p-Msh6p subunit interactions in mismatch base pair recognition.

Aline, R. 1985. (Taa)N Within Sequences Flanking Several Intrachromosomal Variant Surface Glycoprotein Genes in Trypanosoma-Brucei.

Allen, D.J. 1997. MutS mediates heteroduplex loop formation by a translocation mechanism.

Antony, E. 2003. Mismatch recognitioh-coupled stabilization of Msh2-Msh6 in an ATP-bound state at the initiation of DNA repair.

Aquilina, G. 1998. N-(2-chloroethyl)-N '-cyclohexyl-N-nitrosourea sensitivity in mismatch repair-defective human cells.

Aquilina, G. 1999. Mismatch repair, G(2)/M cell cycle arrest and lethality after DNA damage.

Aramini, J.M. 2010. Structural Basis of O-6-Alkylguanine Recognition by a Bacterial Alkyltransferase-like DNA Repair Protein.

Aravind, L. 2001. The DNA-repair protein AlkB, EGL-9, and leprecan define new families of 2-oxoglutarate- and iron-dependent dioxygenases.

Asagoshi, K. 2000. Comparison of substrate specificities of Escherichia coli endonuclease III and its mouse homologue (mNTH1) using defined oligonucleotide substrates.

Aslett, M. 2010. TriTrypDB: a functional genomic resource for the Trypanosomatidae.

Atrih, A. 2005. Trypanosoma brucei glycoproteins contain novel giant poly-N-acetyllactosamine carbohydrate chains.

Augusto-Pinto, L. 2003. Single-nucleotide Polymorphisms of the Trypanosoma cruzi MSH2 gene support the existence of three phylogenetic lineages presenting differences in mismatch-repair efficiency.

Avidor-Reiss, T. 2004. Decoding cilia function: Defining specialized genes required for compartmentalized cilia biogenesis.

Avila, H.A. 1991. Polymerase Chain-Reaction Amplification of Trypanosoma-Cruzi Kinetoplast Minicircle Dna Isolated from Whole-Blood Lysates - Diagnosis of Chronic Chagas-Disease.

Ban, C. 1998. Structural basis for MutH activation in E-coli mismatch repair and relationship of MutH to restriction endonucleases.

Ban, C. 1999. Transformation of MutL by ATP binding and hydrolysis: A switch in DNA mismatch repair.

Barnes, R. 2006. *Mismatch repair, Recombination and Genetic Variability in T.BRUCEI.*

Barnes, R.L. 2007. Trypanosoma brucei homologous recombination is dependent on substrate length and homology, though displays a differential dependence on mismatch repair as substrate length decreases.

Barrett, M.P. 2003. The trypanosomiases.

Barry, J.D. 1979. Capping of Variable Antigen on Trypanosoma-Brucei, and Its Immunological and Biological Significance.

Barry, J.D. 1998. VSG gene control and infectivity strategy of metacyclic stage Trypanosoma brucei.

Barry, J.D. 2001. Antigenic variation in trypanosomes: Enhanced phenotypic variation in a eukaryotic parasite.

Bastin, P. 1998. Paraflagellar rod is vital for trypanosome motility.

Beckmann, J.S. 1992. Survey of Human and Rat Microsatellites.

Bell, J.S. 2002. *Mismatch Repair in DNA Recombination and Antigenic Variation in T.brucei.*

Bell, J.S. 2003. Mismatch repair regulates homologous recombination, but has little influence on antigenic variation, in Trypanosoma brucei.

Bell, J.S., Harvey, T.I., Sims, A.M., & McCulloch, R. 2004. Characterization of components of the mismatch repair machinery in Trypanosoma brucei. *Molecular Microbiology*, 51, (1) 159-173 available from: ISI:000186974100015

Berriman, M. 2005. The genome of the African trypanosome Trypanosoma brucei.

Bertrand, P. 1998. Physical interaction between components of DNA mismatch repair and nucleotide excision repair.

Bhagwat, A.S. 2002. Cooperation and competition in mismatch repair: very short-patch repair and methyl-directed mismatch repair in Escherichia coli.

biosci. (2001. *parasite.*

Biswas, I. 2001. Disruption of the helix-u-turn-helix motif of MutS protein: Loss of subunit dimerization, mismatch binding and ATP hydrolysis.

Bitter, W. 1998. The role of transferrin-receptor variation in the host range of Trypanosoma brucei.

Bjoras, M. 1997. Opposite base-dependent reactions of a human base excision repair enzyme on DNA containing 7,8-dihydro-8-oxoguanine and abasic sites.

Bjornson, K.P. 2003. Differential and simultaneous adenosine di- and triphosphate binding by MutS.

Blackwell, L.J. 1998. Nucleotide-promoted release of hMutS alpha from heteroduplex DNA is consistent with an ATP-dependent translocation Mechanism.

Blum, B. 1990. A Model for Rna Editing in Kinetoplastid Mitochondria - Guide Rna Molecules Transcribed from Maxicircle Dna Provide the Edited Information.

Bocher, T. 1999. hMSH5: A human MutS homologue that forms a novel heterodimer with hMSH4 and is expressed during spermatogenesis.

Borst, P. 2002. Antigenic variation and allelic exclusion.

Bourn, R.L. 2009. E-coli mismatch repair acts downstream of replication fork stalling to stabilize the expanded (GAA.TTC)(n) sequence.

Bowers, J. 2001. MSH-MLH complexes formed at a DNA mismatch are disrupted by the PCNA sliding clamp.

Breidbach, T. 2002. Trypanosoma brucei: in vitro slender-to-stumpy differentiation of culture-adapted, monomorphic bloodstream forms.

Brun, R. 1981. Stimulating Effect of Citrate and Cis-Aconitate on the Transformation of Trypanosoma-Brucei Blood-Stream Forms to Procyclic Forms Invitro.

Brun, R. 1992. Cultivation of Human Pathogenic Blood Protozoa - A Citation-Classic Commentary on Cultivation and Invitro Cloning of Procyclic Culture Forms of Trypanosoma-Brucei in A Semi-Defined Medium by Brun,R., and Schonenberger,M. *Current Contents/Agriculture Biology & Environmental Sciences* (20) 8 available from: ISI:A1992HQ90500001

Buermeyer, A.B. 1999. Mammalian DNA mismatch repair.

Bugreev, D.V. 2006. Rad54 protein promotes branch migration of Holliday junctions.

Burdett, V. 2001. In vivo requirement for RecJ, ExoVII, ExoI, and ExoX in methyl-directed mismatch repair.

Burgess, S.M. 1999. Collisions between yeast chromosomal loci in vivo are governed by three layers of organization.

Burton, P. 2007. Ku heterodimer-independent end joining in Trypanosoma brucei cell extracts relies upon sequence microhomology.

Bush, A. O. & Fernández, J. C. 2001, "Immunological, pathological and biochemical aspects of parasitism," *In Parasitism: the diversity and ecology of animal parasites*, A. O. Bush & J. C. Fernández, eds., Cambridge University Press, pp. 13-41.

Campos, P.C. 2011. Trypanosoma cruzi MSH2: Functional analyses on different parasite strains provide evidences for a role on the oxidative stress response.

Cannavo, E. 2007. Characterization of the interactome of the human MutL homologues MLH1, PMS1, and PMS2.

Chahwan, R. 2011. Mismatch-mediated error prone repair at the immunoglobulin genes.

Chang, C.L. 2002. Oxidative stress inactivates the human DNA mismatch repair system.

Chang, D.J. 2009. DNA damage tolerance: when it's OK to make mistakes.

Chaudhuri, M., Ajayi, W., Temple, S., & Hill, G.C. 1995. Identification and Partial-Purification of A Stage-Specific 33 Kda Mitochondrial Protein As the Alternative Oxidase of the Trypanosoma-Brucei-Brucei Blood-Stream Trypomastigotes. *Journal of Eukaryotic Microbiology*, 42, (5) 467-472 available from: ISI:A1995RY38500005

Chaudhuri, M., Ott, R.D., & Hill, G.C. 2006. Trypanosome alternative oxidase: from molecule to function. *Trends in Parasitology*, 22, (10) 484-491 available from: ISI:000241254500010

Chaudhuri, M., Sharan, R., & Hill, G.C. 2002. Trypanosome alternative oxidase is regulated post-transcriptionally at the level of RNA stability. *Journal of Eukaryotic Microbiology*, 49, (4) 263-269 available from: ISI:000177457800001

Chaudhuri, M. 1998. Biochemical and molecular properties of the Trypanosoma brucei alternative oxidase.

Chen, P.C. 2005. Contributions by MutL homologues MLH3 and PMS2 to DNA mismatch repair and tumor suppression in the mouse.

Christmann, M. 2000. Nuclear translocation of mismatch repair proteins MSH2 and MSH6 as a response of cells to alkylating agents.

Claij, N. 2002. Methylation tolerance in mismatch repair proficient cells with low MSH2 protein level.

Clark, A.B. 2000. Functional interaction of proliferating cell nuclear antigen with MSH2-MSH6 and MSH2-MSH3 complexes.

Clayton, C.E. 2002. Life without transcriptional control? From fly to man and back again (vol 21, pg 1881, 2002).

Colasante, C. 2009. Mitochondrial carrier family inventory of Trypanosoma brucei brucei: Identification, expression and subcellular localisation.

Colussi, C. 2002. The mammalian mismatch repair pathway removes DNA 8-oxodGMP incorporated from the oxidized dNTP pool.

Conway, C. 2002. Ku is important for telomere maintenance, but not for differential expression of telomeric VSG genes, in African trypanosomes.

Cooper, G. 2000, "DNA Repair,".

Culligan, K.M. 2000. Arabidopsis MutS homologs-AtMSH2, AtMSH3, AtMSH6, and a novel AtMSH7-form three distinct protein heterodimers with different specificities for mismatched DNA.

Cunningham, R.P. 1997. DNA glycosylases.

D'Atri, S. 1998. Involvement of the mismatch repair system in temozolomide-induced apoptosis.

Daniels, D.S. 2004. DNA binding and nucleotide flipping by the human DNA repair protein AGT.

Dao, V. 1998. Mismatch-, MutS-, MutL-, and helicase II-dependent unwinding from the single-strand break of an incised heteroduplex.

Datta, A. 1996. Mitotic crossovers between diverged sequences are regulated by mismatch repair proteins in Saccharomyces cerevisiae.

De Bont, R. 2004. Endogenous DNA damage in humans: a review of quantitative data.

de Vries, S.S. 1999. Mouse MutS-like protein Msh5 is required for proper chromosome synapsis in male and female meiosis.

Delange, T. 1983. Telomere Conversion in Trypanosomes.

DeWeese, T.L. 1998. Mouse embryonic stem cells carrying one or two defective Msh2 alleles respond abnormally to oxidative stress inflicted by low-level radiation.

Dewind, N. 1995. Inactivation of the Mouse Msh2 Gene Results in Mismatch Repair Deficiency, Methylation Tolerance, Hyperrecombination, and Predisposition to Cancer.

Dobson, R. 2011. Interactions among Trypanosoma brucei RAD51 paralogues in DNA repair and antigenic variation.

Dowen, J.M. 2010. Functional Studies and Homology Modeling of Msh2-Msh3 Predict that Mispair Recognition Involves DNA Bending and Strand Separation.

Downs, J.A. 2007. Chromatin dynamics and the preservation of genetic information.

Drummond, J.T. 1997. DHFR/MSH3 amplification in methotrexate-resistant cells alters the hMutS alpha/hMutS beta ratio and reduces the efficiency of base-base mismatch repair.

Duckett, D.R. 1996. Human MutS alpha recognizes damaged DNA base pairs containing O-6-methylguanine, O-4-methylthymine, or the cisplatin-d(GpG) adduct.

Dutta, R. 2000. GHKL, an emergent ATPase/kinase superfamily.

Dzantiev, L. 2004. Defined human system that supports bidirectional mismatch-provoked excision.

Edelmann, W. 2000. The DNA mismatch repair genes Msh3 and Msh6 cooperate in intestinal tumor suppression.

Egashira, A. 2002. Mutational specificity of mice defective in the MTH1 and/or the MSH2 genes.

Ehrlich, M. 1981. 5-Methylcytosine in Eukaryotic Dna.

Eisen, J.A. 1998. A phylogenomic study of the MutS family of proteins.

El Sayed, N.M. 2000. The African trypanosome genome.

Ellegren, H. 2000. Microsatellite mutations in the germline: implications for evolutionary inference.

Englster, M. 2007, "Intracellular transport systems in Trypanosomes: Function Evolution and Virulence,".

Ersfeld, K. 1999. Nuclear and genome organization of Trypanosoma brucei.

Esterbauer, H. 1990. Possible Mutagens Derived from Lipids and Lipid Precursors.

Estevez, A.M. 1999. Uridine insertion/deletion RNA editing in trypanosome mitochondria - a review.

Evans, E. 1997. Mechanism of open complex and dual incision formation by human nucleotide excision repair factors.

Fang, J. & Beattie, D.S. 2003. Alternative oxidase present in procyclic Trypanosoma brucei may act to lower the mitochondrial production of superoxide. *Archives of Biochemistry and Biophysics*, 414, (2) 294-302 available from: ISI:000183498000020

Fang, W.H. 1993. Human Strand-Specific Mismatch Repair Occurs by A Bidirectional Mechanism Similar to That of the Bacterial Reaction.

Ferguson, M.A.J. 1988. Glycosyl-Phosphatidylinositol Moiety That Anchors Trypanosoma-Brucei Variant Surface Glycoprotein to the Membrane.

Filippo, J.S. 2008. Mechanism of eukaryotic homologous recombination.

Finzi, J.K. 2004. Trypanosoma cruzi response to the oxidative stress generated by hydrogen peroxide.

Fishel, R. 1998. Mismatch repair, molecular switches, and signal transduction.

Flohe, L. 2004. The trypanothione system.

Foster, D.N. 1976. Nuclear Location of Mammalian Dna-Polymerase Activities.

Fraga, C.G. 1990. Oxidative Damage to Dna During Aging - 8-Hydroxy-2'-Deoxyguanosine in Rat Organ Dna and Urine.

Friedberg, E.C. 2001. How nucleotide excision repair protects against cancer.

Friedberg, E.C. 2005. Suffering in silence: The tolerance of DNA damage.

Fromme, J.C. 2004. DNA glycosylase recognition and catalysis.

Fujii, Y. 1999. Functional significance of the conserved residues for the 23-residue module among MTH1 and MutT family proteins.

Fukui, K. 2008a. Bound nucleotide controls the endonuclease activity of mismatch repair enzyme MutL.

Fukui, K. 2011. Inactivation of the DNA Repair Genes mutS, mutL or the Anti-Recombination Gene mutS2 Leads to Activation of Vitamin B-1 Biosynthesis Genes.

Furtado, C. 2012. Functional Characterization of 8-Oxoguanine DNA Glycosylase of <italic>Trypanosoma cruzi</italic>.

Garcia-Ortiz, M.V. 2001. An OGG1 orthologue encoding a functional 8-oxoguanine DNA glycosylase/lyase in Arabidopsis thaliana.

Garrison, E.M. 2009. Disruption of a mitochondrial MutS DNA repair enzyme homologue confers drug resistance in the parasite Toxoplasma gondii.

Gates, K.S. 2009. An Overview of Chemical Processes That Damage Cellular DNA: Spontaneous Hydrolysis, Alkylation, and Reactions with Radicals.

Genschel, J. 1998. Isolation of MutS beta from human cells and comparison of the mismatch repair specificities of MutS beta and MutS alpha.

Genschel, J. 2002. Human exonuclease I is required for 5 ' and 3 ' mismatch repair.

Genschel, J. 2003. Mechanism of 5 '-directed excision in human mismatch repair.

Genschel, J. 2006. Analysis of the excision step in human DNA mismatch repair.

Genschel, J. 2009. Functions of MutL alpha, Replication Protein A (RPA), and HMGB1 in 5 '-Directed Mismatch Repair.

Gilinger, G. 2001. Trypanosome spliced leader RNA genes contain the first identified RNA polymerase II gene promoter in these organisms.

Ginger, M.L. 2002. Ex vivo and in vitro identification of a consensus promoter for VSG genes expressed by metacyclic-stage trypanosomes in the tsetse fly.

Glaab, W.E. 2001. Suppression of spontaneous and hydrogen peroxide-induced mutagenesis by the antioxidant ascorbate mismatch repair-deficient human colon cancer cells.

Gradia, S. 1997. The human mismatch recognition complex hMSH2-hMSH6 functions as a novel molecular switch.

Gradia, S. 1999. hMSH2-hMSH6 forms a hydrolysis-independent sliding clamp on mismatched DNA.

Griffin, S. 1994. Dna Mismatch Binding and Incision at Modified Guanine Bases by Extracts of Mammalian-Cells - Implications for Tolerance to Dna Methylation Damage.

Groisman, R. 2006. CSA-dependent degradation of CSB by the ubiquitin-proteasome pathway establishes a link between complementation factors of the Cockayne syndrome.

Grunfelder, C.G. 2003. Endocytosis of a glycosylphosphatidylinositol-anchored protein via clathrin-coated vesicles, sorting by default in endosomes, and exocytosis via RAB11-positive carriers.

Grunfelder, C.G., Engstler, M., Weise, F., Schwarz, H., Stierhof, Y.D., Boshart, M., & Overath, P. 2002. Accumulation of a GPI-anchored protein at the cell surface requires sorting at multiple intracellular levels. *Traffic*, 3, (8) 547-559 available from: ISI:000176905600005

Gu, Y.S. 2002. Human MutY homolog, a DNA glycosylase involved in base excision repair, physically and functionally interacts with mismatch repair proteins human MutS homolog 2/human MutS homolog 6.

Guarne, A. 2004. Structure of the MutL C-terminal domain: a model of intact MutL and its roles in mismatch repair.

Gull, K. 2004, "Basal bodies and microtubule organization in pathogenic protozoa,".

Gunzl, A. 2003. RNA polymerase I transcribes procyclin genes and variant surface glycoprotein gene expression sites in Trypanosoma brucei.

Guo, S.L. 2004. Differential requirement for proliferating cell nuclear antigen in 5 ' and 3 ' nick-directed excision in human mismatch repair.

Habraken, Y. 1996. Binding of insertion/deletion DNA mismatches by the heterodimer of yeast mismatch repair proteins MSH2 and MSH3.

Habraken, Y. 1997. Enhancement of MSH2-MSH3-mediated mismatch recognition by the yeast MLH1-PMS1 complex.

Hanawalt, P.C. 2002. Subpathways of nucleotide excision repair and their regulation.

Harfe, B.D. 2000a. Discrete in vivo roles for the MutL homologs Mlh2p and Mlh3p in the removal of frameshift intermediates in budding yeast.

Harfe, B.D. 2000b. DNA mismatch repair and genetic instability.

Hartley, C.L. 2008. Trypanosoma brucei BRCA2 acts in antigenic variation and has undergone a recent expansion in BRC repeat number that is important during homologous recombination.

Haugen, A.C. 2008. Genetic Instability Caused by Loss of MutS Homologue 3 in Human Colorectal Cancer.

Her, C. 2003. Human MutS homologue MSH4 physically interacts with von Hippel-Lindau tumor suppressor-binding protein 1.

Her, C. 2007. MutS homologues hMSH4 and hMSH5: Diverse functional implications in humans.

Hertz-Fowler, C. 2007, "The Genome of Trypanosoma brucei,".

Hertz-Fowler, C. 2008. Telomeric Expression Sites Are Highly Conserved in Trypanosoma brucei.

Heynaman, D. 2007, "Medical Prasitology,".

Hinz, J.M. 1999. MSH3 deficiency is not sufficient for a mutator phenotype in Chinese hamster ovary cells.

Hirumi, H. & Hirumi, K. 1994. Axenic Culture of African Trypanosome Blood-Stream Forms. *Parasitology Today*, 10, (2) 80-84 available from: ISI:A1994MV15200014

Holland, I.B. 1999. ABC-ATPases, adaptable energy generators fuelling transmembrane movement of a variety of molecules organisms from bacteria to humans.

Hollingsworth, N.M. 1995. Msh5, A Novel Muts Homolog, Facilitates Meiotic Reciprocal Recombination Between Homologs in Saccharomyces-Cerevisiae But Not Mismatch Repair.

Honigberg, B. M. 1963, "A contribution to systematics of the non-pigmented flagellates,".

Hope, M. 1999. Analysis of ploidy (in megabase chromosomes) in Trypanosoma brucei after genetic exchange.

Hsu, G.W. 2004. Error-prone replication of oxidatively damaged DNA by a high-fidelity DNA polymerase.

Iaccarino, I. 1998. hMSH2 and hMSH6 play distinct roles in mismatch binding and contribute differently to the ATPase activity of hMutS alpha.

Iaccarino, I. 2000. Mutation in the magnesium binding site of hMSH6 disables the hMutS alpha sliding clamp from translocating along DNA.

Imboden, M.A. 1987. Transcription of the Intergenic Regions of the Tubulin Gene-Cluster of Trypanosoma-Brucei - Evidence for A Polycistronic Transcription Unit in A Eukaryote.

Ismail, S.O. 1997. Molecular cloning and characterization of two iron superoxide dismutase cDNAs from Trypanosoma cruzi.

Iyer, R.R. 2006. DNA mismatch repair: Functions and mechanisms.

Iyer, R.R. 2010. MutL alpha and Proliferating Cell Nuclear Antigen Share Binding Sites on MutS beta.

Jansson, K. 2010. **Evolutionary loss of 8-oxo-G repair components among eukaryotes**.

Janzen, C.J. 2004. Telomere length regulation and transcriptional silencing in KU80-deficient Trypanosoma brucei.

Jaruga, P. 1996. Repair of products of oxidative DNA base damage in human cells.

Jiang, J.J. 2005. Detection of high-affinity and sliding clamp modes for MSH2-MSH6 by single-molecule unzipping force analysis.

Jiricny, J. 2000. Mismatch repair: The praying hands of fidelity.

Jiricny, J. 2006. The multifaceted mismatch-repair system. *Nature Reviews Molecular Cell Biology*, 7, (5) 335-346 available from: ISI:000237057500013

Johnson, R.E. 1996. Requirement of the yeast MSH3 and MSH6 genes for MSH2-dependent genomic stability.

Jonsson, Z.O. 1997. Proliferating cell nuclear antigen: more than a clamp for DNA polymerases.

Joseph, N. 2006. Prokaryotic DNA mismatch repair.

Junop, M.S. 2001. Composite active site of an ABC ATPase: MutS uses ATP to verify mismatch recognition and authorize DNA repair.

Kadyrov, F.A. 2006. Endonucleolytic function of MutL alpha in human mismatch repair.

Kadyrov, F.A. 2007. Saccharomyces cerevisiae MutL alpha is a mismatch repair endonuclease.

Kaniak, A. 2009. Msh1p counteracts oxidative lesion-induced instability of mtDNA and stimulates mitochondrial recombination in Saccharomyces cerevisiae.

Karran, P. 1982. Mismatch Correction at O-6-Methylguanine Residues in Escherichia-Coli Dna.

Karran, P. 1994. Dna-Damage Tolerance, Mismatch Repair and Genome Instability.

Kelman, Z. 1997. PCNA: Structure, functions and interactions.

Kenji Fukui 2010. DNA Mismatch Repair in Eukaryotes and Bacteria.

Kipling, D. 1995, "Telomere structure,".

Klaunig, J.E. 1998. The role of oxidative stress in chemical carcinogenesis.

Kleczkowska, H.E. 2001. hMSH3 and hMSH6 interact with PCNA and colocalize with it to replication foci.

Klingbeil, M.M. & Englund, P.T. 2004. Closing the gaps in kinetoplast DNA network replication. *Proceedings of the National Academy of Sciences of the United States of America*, 101, (13) 4333-4334 available from: ISI:000220648700001

Klungland, A. 1999. Accumulation of premutagenic DNA lesions in mice defective in removal of oxidative base damage.

Kneitz, B. 2000. MutS homolog 4 localization to meiotic chromosomes is required for chromosome pairing during meiosis in male and female mice.

Kosinski, J. 2008. The PMS2 subunit of human MutL alpha contains a metal ion binding domain of the iron-dependent repressor protein family.

Krauth-Siegel, R.L. 2008. Redox control in trypanosomatids, parasitic protozoa with trypanothione-based thiol metabolism.

Kunkel, T.A. 2005. DNA mismatch repair.

LaCount, D.J. 2000. Double-stranded RNA interference in Trypanosoma brucei using head-to-head promoters.

Lamers, M.H. 2000. The crystal structure of DNA mismatch repair protein MutS binding to a G center dot T mismatch.

Langlerouault, F. 1987. Gatc Sequences, Dna Nicks and the Muth Function in Escherichia-Coli Mismatch Repair.

Larson, E.D. 2003. Strand-specific processing of 8-oxoguanine by the human mismatch repair pathway: inefficient removal of 8-oxoguanine paired with adenine or cytosine.

Lee, J.Y. 2005. MutH complexed with hemi- and unmethylated DNAs: Coupling base recognition and DNA cleavage.

Li, G.M. 2008a. Mechanisms and functions of DNA mismatch repair.

Li, X. 2008b. Homologous recombination in DNA repair and DNA damage tolerance.

Li, Y. 2007. Identification of new kinetoplast DNA replication proteins in trypanosomatids based on predicted S-Phase expression and mitochondrial targeting.

Ligtenberg, M.J.L. 1994. Reconstitution of A Surface Transferrin-Binding Complex in Insect Form Trypanosoma-Brucei.

Lin, X.J. 2000. p53 interacts with the DNA mismatch repair system to modulate the cytotoxicity and mutagenicity of hydrogen peroxide.

Lindahl, T. 1982. Suicide Inactivation of the Escherichia-Coli O-6-Methylguanine-Dna Methyltransferase.

Lipkin, S.M. 2000. MLH3: a DNA mismatch repair gene associated with mammalian microsatellite instability.

Liu, P.F. 2010. DNA Repair in Mammalian Mitochondria: Much More Than We Thought?

Loft, S. & Poulsen, H.E. 1996. Cancer risk and oxidative DNA damage in man. *Journal of Molecular Medicine-Jmm*, 74, (6) 297-312 available from: ISI:A1996UR14000003

Lopes, D.D. 2008. Biochemical studies with DNA polymerase beta and DNA polymerase beta-PAK of Trypanosoma cruzi suggest the involvement of these proteins in mitochondrial DNA maintenance.

Lu, A.L. 2001. Repair of oxidative DNA damage - Mechanisms and functions.

Lundkvist, G.B. 2004. Why trypanosomes cause sleeoing sickness.

Ma, A.H. 2000. Somatic mutation of hPMS2 as a possible cause of sporadic human colon cancer with microsatellite instability.

Machado-Silva, A. 2008. Mismatch repair in Trypanosoma brucei: Heterologous expression of MSH2 from Trypanosoma cruzi provides new insights into the response to oxidative damage.

MacLean, L., Chisi, J.E., Odiit, M., Gibson, W.C., Ferris, V., Picozzi, K., & Sternberg, J.M. 2004. Severity of human African trypanosomiasis in East Africa is associated with geographic location, parasite genotype, and host inflammatory cytokine response profile. *Infection and Immunity*, 72, (12) 7040-7044 available from: ISI:000225453900033

MacLeod, A. 2005. The genetic map and comparative analysis with the physical map of Trypanosoma brucei.

Madison-Antenucci, S. 2002. Editing machines: The complexities of trypanosome RNA editing.

Maga, G. 2003. Proliferating cell nuclear antigen (PCNA): a dancer with many partners.

Mair, G., Shi, H.F., Li, H.J., Djikeng, A., Aviles, H.O., Bishop, J.R., Falcone, F.H., Gavrilescu, C., Montgomery, J.L., Santori, M.I., Stern, L.S., Wang, Z.F., Ullu, E., & Tschudi, C. 2000. A new twist in trypanosome RNA metabolism: cis-splicing of pre-mRNA. *Rna-A Publication of the Rna Society*, 6, (2) 163-169 available from: ISI:000085267900001

Maki, H. 1992. Mutt Protein Specifically Hydrolyzes A Potent Mutagenic Substrate for Dna-Synthesis.

Malkov, V.A. 1997. Photocross-linking of the NH2-terminal region of Taq MutS protein to the major groove of a heteroduplex DNA.

Marcello, L. 2007. Analysis of the VSG gene silent archive in Trypanosoma brucei reveals that mosaic gene expression is prominent in antigenic variation and is favored by archive substructure.

Margison, G.P. 2007. Alkyltransferase-like proteins.

Marnett, L.J. 2001. Endogenous DNA damage and mutation.

Marra, G. 1998. Mismatch repair deficiency associated with overexpression of the MSH3 gene.

Marsischky, G.T. 1996. Redundancy of Saccharomyces cerevisiae MSH3 and MSH6 in MSH2-dependent mismatch repair.

Martik, D. 2004. Differential specificities and simultaneous occupancy of human MutS alpha nucleotide binding sites.

Matthews, K.R. 1999. Developments in the differentiation of Trypanosoma brucei.

Matthews, K.R. 2005. The developmental cell biology of Trypanosoma brucei.

Mauris, J. 2009. Adenosine Triphosphate Stimulates Aquifex aeolicus MutL Endonuclease Activity.

Maxwell, D.P. 1999. The alternative oxidase lowers mitochondrial reactive oxygen production in plant cells.

Mazon, G. 2010. Alkyltransferase-like protein (eATL) prevents mismatch repair-mediated toxicity induced by O-6-alkylguanine adducts in Escherichia coli.

Mazurek, A. 2002. Activation of human MutS homologs by 8-oxo-guanine DNA damage.

McCulloch, R. 1999. A role for RAD51 and homologous recombination in Trypanosoma brucei antigenic variation.

McCulloch, S.D. 2008. The fidelity of DNA synthesis by eukaryotic replicative and translesion synthesis polymerases.

Mechanic, L.E. 2000. Escherichia coli MutL loads DNA helicase II onto DNA.

Mendillo, M.L. 2010. Probing DNA- and ATP-mediated Conformational Changes in the MutS Family of Mispair Recognition Proteins Using Deuterium Exchange Mass Spectrometry.

Michaels, M.L. 1992. The Go System Protects Organisms from the Mutagenic Effect of the Spontaneous Lesion 8-Hydroxyguanine (7,8-Dihydro-8-Oxoguanine).

Miller, H. 2000. 8-OxodGTP incorporation by DNA polymerase beta is modified by active-site residue Asn279.

Modrich, P. 1989. Methyl-Directed Dna Mismatch Correction.

Modrich, P. 2006. Mechanisms in eukaryotic mismatch repair. *Journal of Biological Chemistry*, 281, (41) 30305-30309 available from: ISI:000241075900002

Mohd, A.B. 2006. Truncation of the C-terminus of human MLH1 blocks intracellular stabilization of PMS2 and disrupts DNA mismatch repair.

Moller, I.M. 2001. Plant mitochondria and oxidative stress: Electron transport, NADPH turnover, and metabolism of reactive oxygen species.

Morita, R. 2008. An O(6)-methylguanine-DNA methyltransferase-like protein from Thermus thermophilus interacts with a nucleotide excision repair protein.

Moriya, M. 1993. Single-Stranded Shuttle Phagemid for Mutagenesis Studies in Mammalian-Cells - 8-Oxoguanine in Dna Induces Targeted G.C -] T.A Transversions in Simian Kidney-Cells.

Munday, J.C. 2011. Oligopeptidase B deficient mutants of Leishmania major.

Natrajan, G. 2003. Structures of Escherichia coli DNA mismatch repair enzyme MutS in complex with different mismatches: a common recognition mode for diverse substrates.

Ngo, H. 1998. Double-stranded RNA induces mRNA degradation in Trypanosoma brucei.

Ni, T.T. 1999. MSH2 and MSH6 are required for removal of adenine misincorporated opposite 8-oxo-guanine in S-cerevisiae.

Nishant, K.T. 2008. A mutation in the putative MLH3 endonuclease domain confers a defect in both mismatch repair and meiosis in Saccharomyces cerevisiae.

O'Brien, J. 2000. Investigation of the Alamar Blue (resazurin) fluorescent dye for the assessment of mammalian cell cytotoxicity.

Obmolova, G. 2000. Crystal structures of mismatch repair protein MutS and its complex with a substrate DNA.

Ohtsubo, T. 2000. Identification of human MutY homolog (hMYH) as a repair enzyme for 2-hydroxyadenine in DNA and detection of multiple forms of hMYH located in nuclei and mitochondria.

Opperdoes, F.R., Borst, P., Bakker, S., & Leene, W. 1977. Localization of Glycerol-3-Phosphate Oxidase in Mitochondrion and Particulate Nad+-Linked Glycerol-3-Phosphate Dehydrogenase in

Microbodies of Blood-Stream Form of Trypanosoma-Brucei. *European Journal of Biochemistry*, 76, (1) 29-39 available from: ISI:A1977DK88000005

Overath, P. & Engstler, M. 2004. Endocytosis, membrane recycling and sorting of GPI-anchored proteins: Trypanosoma brucei as a model system. *Molecular Microbiology*, 53, (3) 735-744 available from: ISI:000222722000003

Oyola, S.O. 2009. A Kinetoplastid BRCA2 interacts with DNA replication protein CDC45.

Pang, Q.S. 1997. Functional domains of the Saccharomyces cerevisiae Mlh1p and Pms1p DNA mismatch repair proteins and their relevance to human hereditary nonpolyposis colorectal cancer-associated mutations.

PaquisFlucklinger, V. 1997. Cloning and expression analysis of a meiosis-specific MutS homolog: The human MSH4 gene.

Park, J.H. 2001. A novel nucleolar G-protein conserved in eukaryotes.

Parsons, M. 2004. Glycosomes: parasites and the divergence of peroxisomal purpose. *Molecular Microbiology*, 53, (3) 717-724 available from: ISI:000222722000001

Payne, G., Heelis, P.F., Rohrs, B.R., & Sancar, A. 1987. The Active Form of Escherichia-Coli Dna Photolyase Contains A Fully Reduced Flavin and Not A Flavin Radical, Both Invivo and Invitro. *Biochemistry*, 26, (22) 7121-7127 available from: ISI:A1987K785300038

Pays, E. 1994. Genetic-Controls for the Expression of Surface-Antigens in African Trypanosomes.

Pazour, G.J., Agrin, N., Leszyk, J., & Witman, G.B. 2005. Proteomic analysis of a eukaryotic cilium. *Journal of Cell Biology*, 170, (1) 103-113 available from: ISI:000230388700012

Peacock, L. 2011. Identification of the meiotic life cycle stage of Trypanosoma brucei in the tsetse fly.

Pearl, L.H. 2000. Structure and function in the uracil-DNA glycosylase superfamily.

Pena-Diaz, J. 2004. Trypanosoma cruzi contains a single detectable uracil-DNA glycosylase and repairs uracil exclusively via short patch base excision repair.

Pepin, J. & Meda, H.A. 2001. The epidemiology and control of human African trypanosomiasis. *Advances in Parasitology, Vol 49*, 49, 71-132 available from: ISI:000170185800002

Perez, J. 1999. Apurinic/apyrimidinic endonuclease genes from the Trypanosomatidae Leishmania major and Trypanosoma cruzi confer resistance to oxidizing agents in DNA repair-deficient Escherichia coli.

Pericone, C.D. 2003. Factors contributing to hydrogen peroxide resistance in Streptococcus pneumoniae include pyruvate oxidase (SpxB) and avoidance of the toxic effects of the Fenton reaction.

Plotz, G. 2006. Mutations in the MutS alpha interaction interface of MLH1 can abolish DNA mismatch repair.

Ploubidou, A., Robinson, D.R., Docherty, R.C., Ogbadoyi, E.O., & Gull, K. 1999. Evidence for novel cell cycle checkpoints in trypanosomes: kinetoplast segregation and cytokinesis in the absence of mitosis. *Journal of Cell Science*, 112, (24) 4641-4650 available from: ISI:000084711500016

Pluciennik, A. 2010. PCNA function in the activation and strand direction of MutL alpha endonuclease in mismatch repair.

Pochart, P. 1997. Conserved properties between functionally distinct MutS homologs in yeast.

Podlipaev, S. 2001. The more insect trypanosomatids under study-the more diverse Trypanosomatidae appears. *International Journal for Parasitology*, 31, (5-6) 648-652 available from: ISI:000169101300034

Proto, W.R. 2011. Trypanosoma brucei Metacaspase 4 Is a Pseudopeptidase and a Virulence Factor.

Proudfoot, C. 2006. Trypanosoma brucei DMC1 does not act in DNA recombination, repair or antigenic variation in bloodstream stage cells.

R+ñz, B., Iten, M., Grether-B++hler, Y., Kaminsky, R., & Brun, R. 1997. The Alamar Blue-« assay to determine drug sensitivity of African trypanosomes (T.b. rhodesiense and T.b. gambiense) in vitro. *Acta Tropica*, 68, (2) 139-147 available from: http://www.sciencedirect.com/science/article/pii/S0001706X9700079X

Raschle, M. 1999. Identification of hMutL beta, a heterodimer of hMLH1 and hPMS1.

Reenan, R.A.G. 1992a. Characterization of Insertion Mutations in the Saccharomyces-Cerevisiae Msh1 and Msh2 Genes - Evidence for Separate Mitochondrial and Nuclear Functions.

Reenan, R.A.G. 1992b. Isolation and Characterization of 2 Saccharomyces-Cerevisiae Genes Encoding Homologs of the Bacterial Hexa and Muts Mismatch Repair Proteins.

Riou, G. 1969. Nuclear and Kinetoplastic Dna from Trypanosomes.

Robertson, A.B. 2009. DNA Repair in Mammalian Cells.

Robinson, N.P. 1999. Predominance of duplicative VSG gene conversion in antigenic variation in African trypanosomes.

Robinson, N.P. 2002. Inactivation of Mre11 does not affect VSG gene duplication mediated by homologous recombination in Trypanosoma brucei.

Roditi, I. 1998. Unravelling the procyclin coat of Trypanosoma brucei.

Rossmacdonald, P. 1994. Mutation of A Meiosis-Specific Muts Homolog Decreases Crossing-Over But Not Mismatch Correction.

Sancar, A. 2008. Structure and Function of Photolyase and in Vivo Enzymology: 50th Anniversary.

Sanders, L.H. 2011. Epistatic Roles for Pseudomonas aeruginosa MutS and DinB (DNA Pol IV) in Coping with Reactive Oxygen Species-Induced DNA Damage.

Sant'Anna, C., Campanati, L., Gadelha, C., Lourenco, D., Labati-Terra, L., Bittencourt-Silvestre, J., Benchimol, M., Cunha-e-Silva, & De Souza, W. 2005. Improvement on the visualization of cytoskeletal structures of protozoan parasites using high-resolution field emission scanning electron microscopy (FESEM). *Histochemistry and Cell Biology*, 124, (1) 87-95 available from: ISI:000231649500009

Santucci-Darmanin, S. 2000. MSH4 acts in conjunction with MLH1 during mammalian meiosis.

Saxowsky, T.T. 2003. Trypanosoma brucei has two distinct mitochondrial DNA polymerase beta enzymes.

Schaaper, R.M. 1993. Base Selection, Proofreading, and Mismatch Repair During Dna-Replication in Escherichia-Coli. *Journal of Biological Chemistry*, 268, (32) 23762-23765 available from: ISI:A1993MF29400008

Scharer, O.D. 2003. Chemistry and biology of DNA repair.

Schlecker, T. 2005. Substrate specificity, localization, and essential role of the glutathione peroxidase-type tryparedoxin peroxidases in Trypanosoma brucei.

Schnaufer, A., Domingo, G.J., & Stuart, K. 2002. Natural and induced dyskinetoplastic trypanosomatids: how to live without mitochondrial DNA. *International Journal for Parasitology*, 32, (9) 1071-1084 available from: ISI:000177414600001

Schofield, M.J. 2001. The Phe-X-Glu DNA binding motif of MutS - The role of hydrogen bonding in mismatch recognition.

Schuelke, M. 2000. An economic method for the fluorescent labeling of PCR fragments.

Selby, C.P. 1993. Molecular Mechanism of Transcription-Repair Coupling.

Selva, E.M. 1995. Mismatch Correction Acts As A Barrier to Homeologous Recombination in Saccharomyces-Cerevisiae.

Shapiro, T.A. & Englund, P.T. 1995. The Structure and Replication of Kinetoplast Dna. *Annual Review of Microbiology*, 49, 117-143 available from: ISI:A1995TB31900006

Sherwin, T. 1989. Visualization of Detyrosination Along Single Microtubules Reveals Novel Mechanisms of Assembly During Cytoskeletal Duplication in Trypanosomes.

Shibutani, S. 1991. Insertion of Specific Bases During Dna-Synthesis Past the Oxidation-Damaged Base 8-Oxodg.

Shimada, A. 2010. A novel single-stranded DNA-specific 3'-5' exonuclease, Thermus thermophilus exonuclease I, is involved in several DNA repair pathways.

Sia, E.A. 1997. Genetic control of microsatellite stability.

Simpson, A.G.B., Stevens, J.R., & Lukes, J. 2006. The evolution and diversity of kinetoplastid flagellates. *Trends in Parasitology*, 22, (4) 168-174 available from: ISI:000236873000008

Sinicrope, F.A. 2012. Molecular Pathways: Microsatellite Instability in Colorectal Cancer: Prognostic, Predictive, and Therapeutic Implications.

Sixma, T.K. 2001. DNA mismatch repair: MutS structures bound to mismatches.

Sloof, P., Dehaan, A., Eier, W., Vaniersel, M., Boel, E., Vansteeg, H., & Benne, R. 1992. The Nucleotide-Sequence of the Variable Region in Trypanosoma-Brucei Completes the Sequence-Analysis of the Maxicircle Component of Mitochondrial Kinetoplast Dna. *Molecular and Biochemical Parasitology*, 56, (2) 289-299 available from: ISI:A1992KE27400011

Slupphaug, G. 2003. The interacting pathways for prevention and repair of oxidative DNA damage.

Smith, G.C.M. 1999. The DNA-dependent protein kinase.

Smith, J. 2003. Impact of DNA ligase IV on the fidelity of end joining in human cells.

Snowden, T. 2004. hMSH4-hMSH5 recognizes Holliday junctions and forms a meiosis-specific sliding clamp that embraces homologous chromosomes.

Song, L.M. 2010. Does a Helicase Activity Help Mismatch Repair in Eukaryotes?

Steverding, D. 1995. Transferrin-Binding Protein Complex Is the Receptor for Transferrin Uptake in Trypanosoma-Brucei.

Strauss, B.S. 1999. Frameshift mutation, microsatellites and mismatch repair.

Su, T.T. 2006. Cellular responses to DNA damage: One signal, multiple choices.

Sung, P., Krejci, L., Van Komen, S., & Sehorn, M.G. 2003. Rad51 recombinase and recombination mediators. *Journal of Biological Chemistry*, 278, (44) 42729-42732 available from: ISI:000186157000001

Svrcek, M. 2010. Methylation Tolerance Due to O6-Methylguanine Dna Methyltransferase (Mgmt) Field Defect in the Colonic Mucosa: An Initiating Step in the Development of Mismatch Repair Deficient Colorectal Cancers.

Swanson, R.L. 1999. Overlapping specificities of base excision repair, nucleotide excision repair, recombination, and translesion synthesis pathways for DNA base damage in Saccharomyces cerevisiae.

Tachiki, H. 2000. DNA binding and protein-protein interaction sites in MutS, a mismatched DNA recognition protein from Thermus thermophilus HB8.

Tajiri, T. 1995. Functional Cooperation of Mutt, Mutm and Muty Proteins in Preventing Mutations Caused by Spontaneous Oxidation of Guanine-Nucleotide in Escherichia-Coli.

Takamatsu, S. 1996. Mismatch DNA recognition protein from an extremely thermophilic bacterium, Thermus thermophilus HB8.

Tan, K.S.W. 2002. Trypanosoma brucei MRE11 is non-essential but influences growth, homologous recombination and DNA double-strand break repair.

Taylor, J.E. & Rudenko, G. 2006. Switching trypanosome coats: what's in the wardrobe? *Trends in Genetics*, 22, (11) 614-620 available from: ISI:000242196300008

Tchou, J. 1991. 8-Oxoguanine (8-Hydroxyguanine) Dna Glycosylase and Its Substrate-Specificity.

Tetaud, E. 2001. Molecular characterisation of mitochondrial and cytosolic trypanothione-dependent tryparedoxin peroxidases in Trypanosoma brucei.

Tetley, L. 1985. Differentiation in Trypanosoma-Brucei - Host-Parasite Cell-Junctions and Their Persistence During Acquisition of the Variable Antigen Coat.

Tetley, L. 1987. Onset of Expression of the Variant Surface Glycoproteins of Trypanosoma-Brucei in the Tsetse-Fly Studied Using Immunoelectron Microscopy.

Thacker, J. 2005. The RAD51 gene family, genetic instability and cancer. *Cancer Letters*, 219, (2) 125-135 available from: ISI:000227766700001

Tiengwe, C. 2012. Identification of ORC1/CDC6-Interacting Factors in Trypanosoma brucei Reveals Critical Features of Origin Recognition Complex Architecture.

Toft, N.J. 1999. Msh2 status modulates both apoptosis and mutation frequency in the murine small intestine.

Torizawa, T. 2004. Investigation of the cyclobutane pyrimidine dimer (CPD) photolyase DNA recognition mechanism by NMR analyses.

Torri, A.F. 1988. Posttranscriptional Regulation of Cytochrome-C Expression During the Developmental Cycle of Trypanosoma-Brucei.

Truglio, J.J., Croteau, D.L., Van Houten, B., & Kisker, C. 2006. Prokaryotic nucleotide excision repair: The UvrABC system. *Chemical Reviews*, 106, (2) 233-252 available from: ISI:000235347300003

Tsaiwu, J.J. 1992. Escherichia-Coli Muty Protein Has Both N-Glycosylase and Apurinic Apyrimidinic Endonuclease Activities on A-Circle-C and A-Circle-G Mispairs.

Tsuzuki, T. 2007. Significance of error-avoiding mechanisms for oxidative DNA damage in carcinogenesis.

Tubbs, J.L. 2009. Flipping of alkylated DNA damage bridges base and nucleotide excision repair.

Tunc-Ozdemir, M. 2009. Thiamin Confers Enhanced Tolerance to Oxidative Stress in Arabidopsis.

Tuo, J.S. 2003. Primary fibroblasts of Cockayne syndrome patients are defective in cellular repair of 8-hydroxyguanine and 8-hydroxyadenine resulting from oxidative stress.

Turner, C.M.R. 1989. High-Frequency of Antigenic Variation in Trypanosoma-Brucei-Rhodesiense Infections.

Turner, C.M.R. 1995. Replication, Differentiation, Growth and the Virulence of Trypanosoma-Brucei Infections.

Umbach, A.L. 2005. Characterization of transformed Arabidopsis with altered alternative oxidase levels and analysis of effects on reactive oxygen species in tissue.

van der Horst, G.T.J. 1999. Mammalian Cry1 and Cry2 are essential for maintenance of circadian rhythms.

Vanderploeg, L.H.T., Cornelissen, A.W.C.A., Barry, J.D., & Borst, P. 1984. Chromosomes of Kinetoplastida. *Embo Journal*, 3, (13) 3109-3115 available from: ISI:A1984TX37100012

Vanhamme, L. 2001. An update on antigenic variation in African trypanosomes.

Vanhamme, L., Paturiaux-Hanocq, F., Poelvoorde, P., Nolan, D.P., Lins, L., Van den Abbeele, J., Pays, A., Tebabi, P., Van Xong, H., Jacquet, A., Moguilevsky, N., Dieu, M., & Pays, E. 2003. Apolipoprotein L-I is the trypanosome lytic factor of human serum. *Nature*, 422, (6927) 83-87 available from: ISI:000181343100042

Vanhouten, B. 1990. Nucleotide Excision Repair in Escherichia-Coli. *Microbiological Reviews*, 54, (1) 18-51 available from: ISI:A1990CQ91600002

Vaughan, S. & Gull, K. 2003. The trypanosome flagellum. *Journal of Cell Science*, 116, (5) 757-759 available from: ISI:000181529600001

Verhoeven, E.E.A. 2000. Catalytic sites for 3 ' and 5 ' incision of Escherichia coli nucleotide excision repair are both located in UvrC.

Vertommen, D. 2008. Differential expression of glycosomal and mitochondrial proteins in the two major life-cycle stages of Trypanosoma brucei.

Vickerman, K. 1985. Developmental Cycles and Biology of Pathogenic Trypanosomes.

Vickerman, K. & Coombs, G.H. 1999. Protozoan paradigms for cell biology. *Journal of Cell Science*, 112, (17) 2797-2798 available from: ISI:000082613400001

Wang, G. 2005. The Helicobacter pylori MutS protein confers protection from oxidative DNA damage.

Wang, H. 2003. DNA bending and unbending by MutS govern mismatch recognition and specificity.

Wang, T.F. 1999. Functional specificity of MutL homologs in yeast: Evidence for three Mlh1-based heterocomplexes with distinct roles during meiosis in recombination and mismatch correction.

Warbrick, E. 2000. The puzzle of PCNA's many partners.

Warren, J.J. 2006. The structural basis for the mutagenicity of O-6-methyl-guanine lesions.

Warren, J.J. 2007. Structure of the human MutS alpha DNA lesion recognition complex.

Weiden, M., Osheim, Y.N., Beyer, A.L., & Vanderploeg, L.H.T. 1991. Chromosome Structure - Dna Nucleotide-Sequence Elements of A Subset of the Minichromosomes of the Protozoan Trypanosoma-Brucei. *Molecular and Cellular Biology*, 11, (8) 3823-3834 available from: ISI:A1991FX72300001

Weterings, E. & van Gent, D.C. 2004. The mechanism of non-homologous end-joining: a synopsis of synapsis. *Dna Repair*, 3, (11) 1425-1435 available from: ISI:000224225400003

who vector. (2009. *vector.*

Wickstead, B., Ersfeld, K., & Gull, K. 2004. The small chromosomes of Trypanosoma brucei involved in antigenic variation are constructed around repetitive palindromes. *Genome Research*, 14, (6) 1014-1024 available from: ISI:000221852400003

Wiestler, O. 1984. O-6-Alkylguanine-Dna Alkyltransferase Activity in Human-Brain and Brain-Tumors.

Wilkinson, S.R. 2000. Biochemical characterization of a trypanosome enzyme with glutathione-dependent peroxidase activity.

Wilkinson, S.R. 2003. RNA interference identifies two hydroperoxide metabolizing enzymes that are essential to the bloodstream form of the African trypanosome.

Winand, N.J. 1998. Cloning and characterization of the human and Caenorhabditis elegans homologs of the Saccharomyces cerevisiae MSH5 gene.

Wiseman, H. 1996. Damage to DNA by reactive oxygen and nitrogen species: Role in inflammatory disease and progression to cancer.

Wood, M.L. 1990. Mechanistic Studies of Ionizing-Radiation and Oxidative Mutagenesis - Genetic-Effects of A Single 8-Hydroxyguanine (7-Hydro-8-Oxoguanine) Residue Inserted at A Unique Site in A Viral Genome.

Wu, S.Y. 2003. Dissimilar mispair-recognition spectra of Arabidopsis DNA-mismatch-repair proteins MSH2.MSH6 (MutS alpha) and MSH2.MSH7 (MutS gamma).

Wu, T.H. 1994. Dominant-Negative Mutator Mutations in the Muts Gene of Escherichia-Coli.

Wu, X. 2011, "The Role of MutS Homologues MSH4 and MSH5 in DNA Metabolism and Damage Response,".

Wyrzykowski, J. 2003. The Escherichia coli methyl-directed mismatch repair system repairs base pairs containing oxidative lesions.

Yagi, Y. 2005. DNA polymerases eta and kappa are responsible for error-free translesion DNA synthesis activity over a cis-syn thymine dimer in Xenopus laevis oocyte extracts.

Yamagata, A. 2001. Overexpression, purification and characterization of RecJ protein from Thermus thermophilus HB8 and its core domain.

Yang, G.Z. 2004. Dominant effects of an Msh6 missense mutation on DNA repair and cancer susceptibility.

You, H.J. 1999. Saccharomyces cerevisiae Ntg1p and Ntg2p: Broad specificity N-glycosylases for the repair of oxidative DNA damage in the nucleus and mitochondria.

Zeiner, G.M., Sturm, N.R., & Campbell, D.A. 2003. Exportin 1 mediates nuclear export of the kinetoplastid spliced leader RNA. *Eukaryotic Cell*, 2, (2) 222-230 available from: ISI:000182188700004

Zhang, H. 2000. Mismatch repair is required for O-6-methylguanine-induced homologous recombination in human fibroblasts.

Zharkov, D.O. 2008. Base excision DNA repair.

Zlatanou, A. 2011. The hMsh2-hMsh6 Complex Acts in Concert with Monoubiquitinated PCNA and Pol eta in Response to Oxidative DNA Damage in Human Cells.